AD-A046 012 COLORADO UNIV BOULDER SYSTEMS ENGINEERING LAB F/G 12/2
REDUCTION OF THE COST OF FEEDBACK IN SYSTEMS WITH LARGE PARAMET--ETC(U)
AUG 77 P ROSENBAUM, I HOROWITZ AFOSR-76-2946

UNCLASSIFIED AFOSR-TR-77-1224 NL

1 OF 3
AD
A046012

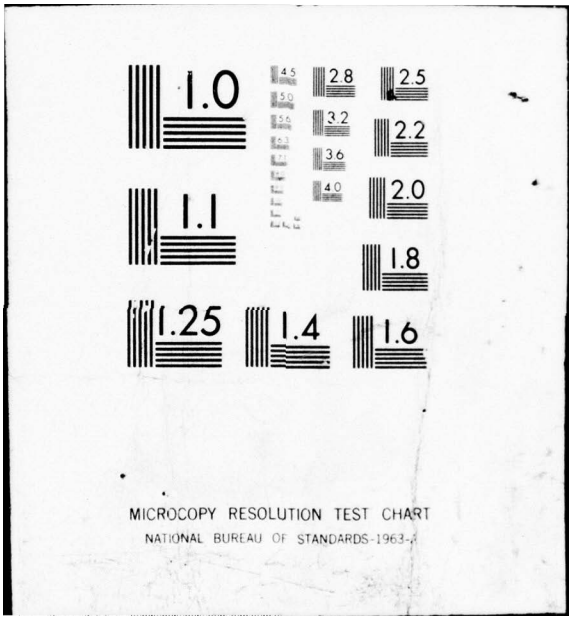
1.0
1.1
1.25
1.4
1.6
1.8
2.0
2.2
2.5
2.8
3.2
3.6
4.0
4.5
5.0
5.6
6.3
MICROCOPY RESOLUTION TEST CHART
NATIONAL BUREAU OF STANDARDS-1963-A

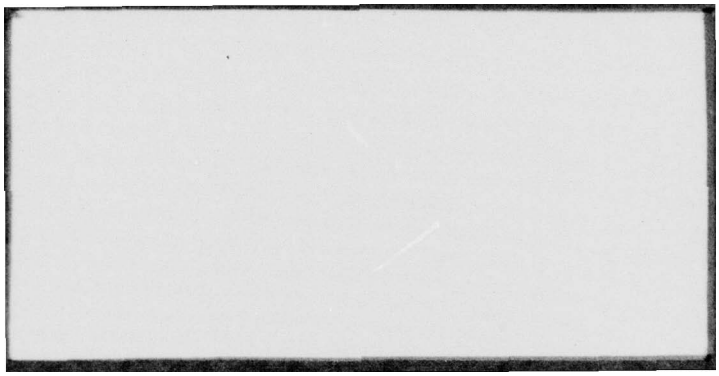

(2)

(6) REDUCTION OF THE COST OF FEEDBACK IN SYSTEMS WITH LARGE PARAMETER UNCERTAINTIES.

(10) Patrick/Rosenbaum
Isaac/Horowitz

Systems Engineering Laboratory
Department of Electrical Engineering
UNIVERSITY OF COLORADO
Boulder, Colorado 80309

(9) Interim rept.

This research was supported by the
AIR FORCE OFFICE OF SCIENTIFIC RESEARCH
under Research Grant AFOSR-76-2946
(15)

(12) 205p.

(11) 1 August 1977

(16) 2304

(17) A1

(18) AFOSR

(19) TR-77-1224

410 446

LB

ABSTRACT

This work deals with the synthesis of feedback systems to achieve specified performance tolerances, despite large uncertainty in a constrained part of the system, denoted as the 'plant'. Part of this work deals with linear time-invariant (lti) plants where the 'cost of feedback', if lti compensation is used, is primarily in the bandwidth of the feedback loop being much larger than that of the system as a whole - making the system very sensitive to sensor noise. Here, the objective is to reduce the loop bandwidth by means of non-lti compensation. A nonlinear first-order reset element (FORE) is introduced and with it, a quantitative synthesis procedure which permits design to specifications despite large but bounded plant uncertainty. The result is a very significant reduction in loop bandwidth and with it, system sensitivity to sensor noise. Stability criteria are included which helps generalize the useful inputs classes.

Another method of non-lti synthesis is by means of linear time-varying compensation, applicable to a certain problem class. The solution is not in general available analytically, but is found for certain cases and exhibits in these reduced 'cost of feedback'. In the final part of this work, the plant can be nonlinear with large uncertainty giving a set of nonlinear plants W. The concept is use of a lti set P which is precisely equivalent to W providing the output is, in both cases, a member of an acceptable output set A. A synthesis procedure is presented, based on this concept, for achieving time-domain specifications of a specified nonlinear character. All of the methods are illustrated by detailed design examples.

TABLE OF CONTENTS

CHAPTER I. INTRODUCTION.

I.1 Generalities

An important problem area in systems theory is to satisfy quantitative specifications despite parameter uncertainty. It is assumed here that there is a single-input-single-output constrained part denoted as the 'plant' and described by a linear differential equation with fixed coefficients. (Fig. I.1)

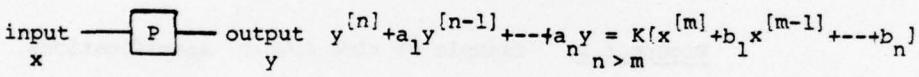

Figure I.1. Plant characterization

There exists a finite set of parameters $\{k_1,k_2,\ldots,k_\ell\}$ such that each coefficient is a function of those parameters, i.e. $a_i = \mathcal{A}_i(k_1,k_2,\ldots,k_\ell)$ for $i=1,n$, $b_j = \mathcal{B}_j(K_1,k_2,\ldots,k_\ell)$ for $j=1,m$ and $K = \mathcal{K}(k_1,k_2,\ldots,k_\ell)$. Furthermore, it is assumed that each parameter k_i , $i=1, \ell$, is associated with a known range of uncertainty $[k_{i_{min}},k_{i_{max}}]$ which can be small or large. We want to guarantee time domain specifications (T.D.S.), for example unit step response of the type shown in Fig. I.2, despite the uncertainty of the plant parameters. This means that for any plant parameter combination P_j belonging to the set $\mathcal{P}$ of possible combinations, the system output $c_j(t)$ is to lie within some prescribed time-domain bounds defining the region $\mathcal{R}^*$ (Fig.I.2) $\subset \mathcal{R}$.

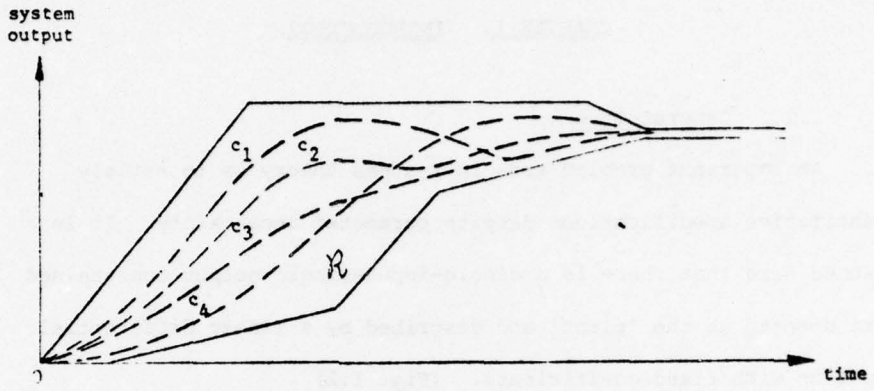

Figure I.2. Example of time-domain specifications.

It should be noted at this point that it is implicitly assumed that we restrict $\mathcal{R}^*$ to "reasonable" signals $c_j(t) \in \mathcal{R}$. Mathematically this means that the designer restricts himself to signals $c_j(t)$ such that $\left|\frac{d^i c_j(t)}{dt^i}\right| < \gamma_i(t)$ for $i = 1,2,\ldots,\rho$ for some given functions $\gamma_i(t)$. Although the synthesis technique uses frequency domain specifications, it was shown[H1] that frequency domain specifications suffice for T.D.S. of even more general type.

It is assumed possible to measure the command input $r(t)$ and the plant output $c(t)$ and therefore the most general structure is that with two-degrees-of-freedom, of which one is shown in Fig. I.3, where F and G must be chosen by the designer.

It should be underlined that because of large plant uncertainty that is assumed here, it is impossible in general to use an open-loop system and therefore feedback is definitely needed. This necessitates use of a sensor, which in turn introduces sensor noise N (Fig. I.3).

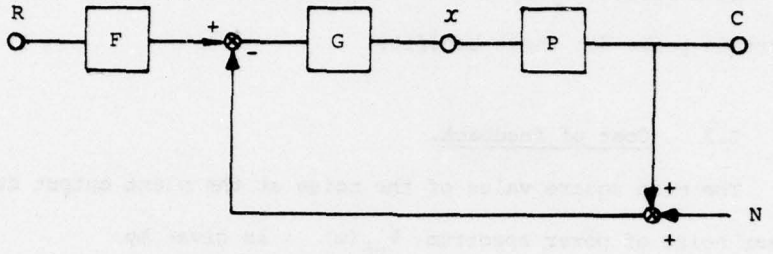

Figure I.3. A two-degree of freedom structure

I.2 Linear time invariant design.

If the plant is minimum-phase there exists [H1] an infinite set $\mathcal{A}$ of (F_i, G_i) which satisfies the T.D.S., despite plant-uncertainty. The restrictions on the range of uncertainty have been discussed [H7], [H8]. Furthermore, given a region $\mathcal{R}$ (Fig. I.4) of width at most ε where $\varepsilon > 0$ is arbitrarily small, it is possible to show [H1] that the set $\mathcal{A}_\varepsilon$ of $(F_i, G_i)_\varepsilon$ which satisfy those T.D.S. is not empty.

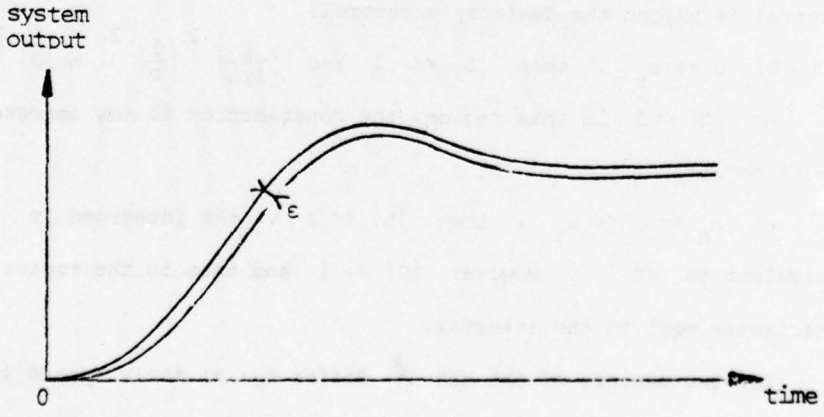

Figure I.4. Example of time domain specifications.

If a feedback loop gives us such benefits we should expect to pay a certain price for these benefits.

I.3 Cost of feedback.

The mean square value of the noise at the plant output due to the sensor noise of power spectrum $\Phi_{nn}(\omega)$, is given by

$$\sigma^2_{P.I.} = \frac{1}{2\pi} \int_{-\infty}^{+\infty} \left| \frac{L(j\omega)}{1+L(j\omega)} \right|^2 \frac{\Phi_{nn}(\omega)}{|P(j\omega)|^2} d\omega \quad . \qquad (I.1)$$

Assuming white sensor noise of strength σ_N^2 and following the general procedure for the synthesis of linear time invariant systems (L.T.I.) derived by Horowitz and Sidi [H2] we get results of the form shown in Fig. I.5. We can divide the domain of integration in three regions.

a) $\omega << \omega_c$, $|L| >> 1$ and the integrand $\doteq \frac{\sigma_N^2}{|P|^2}$ which tends to be small over that range, and the range itself (on an arithmetic scale) is a small part of the range in which the noise effects are significant. In any case, in this range the contribution to the integral is beyond the designer's control.

b) $\omega >> \omega_t$, then $|L| << 1$ and $\left|\frac{L}{1+L}\right|^2 \left|\frac{1}{P}\right|^2 \approx |G|^2$.

As $|G| << 1$ in this region, the contribution to the integral can be neglected.

c) $\omega_c << \omega << \omega_t$, then $|L| << 1$, the integrand is equivalent to $|G|^2$. However $|G| >> 1$ and this is the region which contributes most to the integral.

So, two members of the set $\mathcal{A}$ differ by: a) their spread in the time domain system-responses to a command-input or by: b) their respective level of sensor's noise rejection at the plant-input, or by:

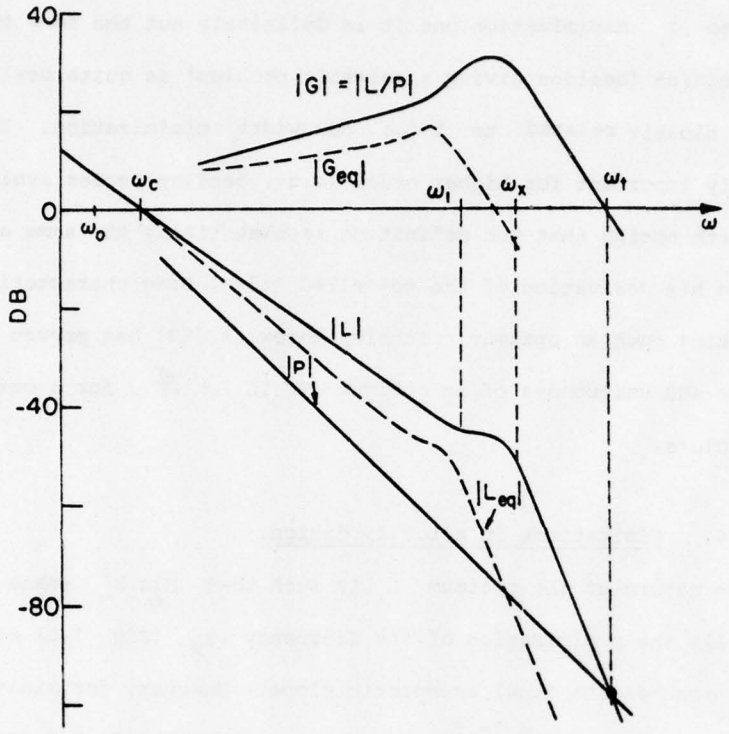

Figure I.5. Typical linear time invariant design.

both a) and b).

Therefore in a general sense, the less sensitive we want the output system to be to plant-parameters uncertainty, the bigger will be the sensor noise effect at the plant input, and vice-versa, and this is the real trade-off in any feedback system design. So a reasonable definition of optimum is to select $(F,G) \in \mathcal{A}$ with minimum $\sigma_p = \underset{P}{E} \int_0^\infty \left|\frac{G}{1+L}\right|^2 \Phi_{nn} d\omega$ where $\Phi_{nn}(\omega)$ is the power spectrum of the sensor noise. However, this is a very difficult problem, as yet unsolved. Our definition for optimum $(F_i,G_i)_{opt} \in \mathcal{A}$ is one for which: $\underset{\mathcal{A}}{\text{Min}}\ k^i_\infty$ where as $s \to \infty$, $G_i(s) \to \frac{k^i_\infty}{s^e}$ for a-priori chosen value of the integer e. Obviously, this definition is closely

related to σ_p minimization but it is definitely not the same thing. Our definition (besides giving a solvable problem) is quite realistic as it is closely related to $L(j\omega)$ bandwidth minimization. This is especially important for higher order (e.g., bending) modes avoidance. It is worth noting that our definition is essentially the same as Bode's in his derivation of the so-called 'ideal Bode characteristics' [B1]. Using such an optimum criterion, Horowitz [H3] has proven the existence and uniqueness of an optimum $(F_0, G_0) \in \mathcal{A}$, for a certain problem class.

I.4. *Limitations in a L.T.I. design.*

The nature of the optimum L is such that $\underset{\mathcal{A}}{\text{Min}}\, k_\infty^i$ means essentially the minimization of the frequency ω_x (Fig. I.5) at which $|L(j\omega)|$ reaches its final asymptotic slope. However, for minimum-phase L.T.I. networks $\frac{d \ln|L|}{d\omega}$ is related through Bode Integrals to $\angle L$.

If $\ln L(j\omega) \triangleq A(\omega) + j\, B(\omega)$ with A in nepers and B in radians and if $u \triangleq \ln \omega/\omega_x$ then [B1]

$$\pi B(\omega_x) = \int_{-\infty}^{+\infty} \frac{dA}{du} \ln \coth \frac{|u|}{2}\, du$$

$$\pi [A(\omega_x) - A(\infty)] = -\frac{1}{\omega_x} \int_{-\infty}^{+\infty} \frac{d(\omega B)}{du} \ln \coth \frac{|u|}{2}\, du \ .$$

As stability requires $\angle L(j\omega_c) > -180°$ for $|L(j\omega_c)| = 1$, then, because of large uncertainty, the maximum rate of decrease of L is -40 db/decade over some frequency range. It will be shown (section II.1), however, that the disturbance specifications are translatable into a certain phase margin θ_M for $L(j\omega)$ to satisfy over some frequency

range $[\omega_a, \omega_b]$ (Fig. I.6), thus increasing the cost of feedback. Indeed, over that frequency range $\frac{d\ell n|L|}{d\omega}$ is then at most $-(2 - \frac{\theta_M}{90}) \times 40$ db/decade and recalling (I.1) and Fig. I.5, the level of noise at the plant input is then accordingly increased. This can be visualized as follows (Fig. I.7):

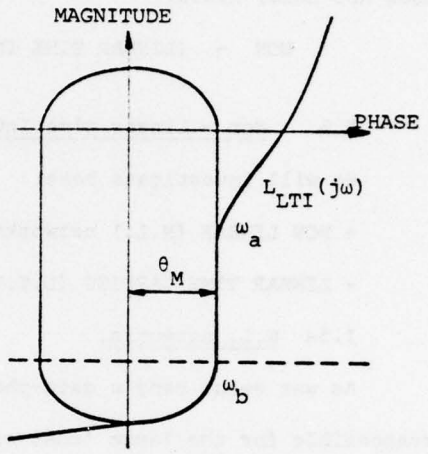

Figure I.6. Typical L.T.I. design.

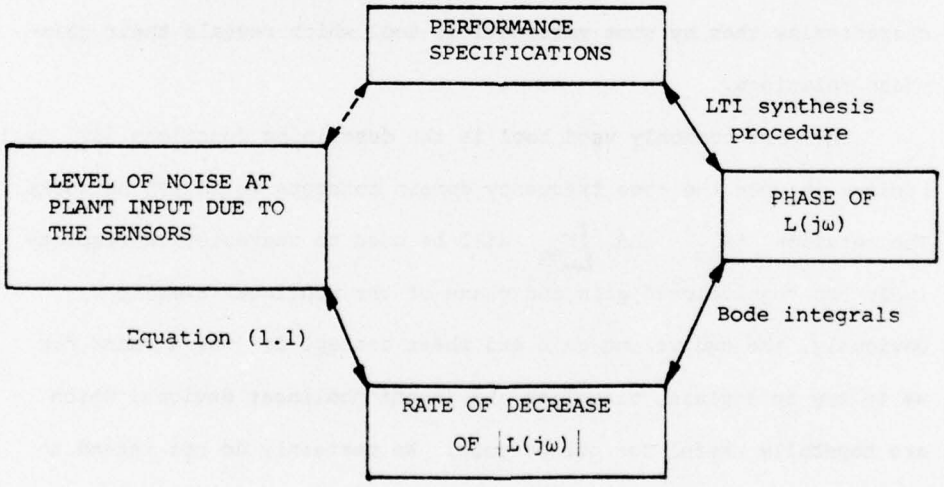

Figure I.7. Trade-off in a L.T.I. design.

One possible way to break this vicious circle is to concentrate on devices for which the Bode relationship relating phase lag to $\frac{d\ell n|L|}{d\omega}$

does not hold, namely:

NON - (LINEAR TIME INVARIANT) networks.

I.5 Non - Linear Time Invariant compensation.

We will investigate here:

- NON LINEAR (N.L.) networks
- LINEAR TIME VARYING (L.T.V.) networks.

I.5a N.L. networks.

As was seen, Bode's gain-phase relationship for LTI networks is responsible for the large 'cost of feedback' in the synthesis of systems with large uncertainty.

It is therefore logical to seek nonlinear networks for which that relationship does not exist, and for the purpose of comparison, to characterize them by some mathematical tool which reveals their gain-phase relations.

The most commonly used tool is the describing functions [G2],[M1] because it uses the same frequency domain concepts as in LTI networks. The notation $|N_{eq}|$ and $\angle N_{eq}$ will be used to characterize respectively the "equivalent" gain and phase of the nonlinear element N. Obviously, the equivalent gain and phase concept is just a means for us to try to explain, visualize and invent nonlinear devices, which are hopefully useful for our purpose. We certainly do not intend to rely on Describing Functions to give a quantitative sythesis procedure. Using the above notation we are then looking for N.L. devices such that:

$$\frac{d|N_{eq}|}{d\omega} = -m \text{ db/decade with } \angle N_{eq} > -\frac{m}{20} \times 90°$$

(recall that for a L.T.I. system a rate of decrease of -m db/decade is associated with an average phase lag of $-m \times 90/20°$) . This would then lead to some open loop transfer function $L_{eq}(s)$ for which:

$$\frac{d|L|_{eq}}{d\omega} = -k \text{ db/decade with } \angle L_{eq} > -\frac{k}{20} \times 90°$$

which then implies

$$\frac{d|L_{eq}|}{d\omega} < \frac{d|L|}{d\omega}_{L.T.I} \text{ with } \angle L_{eq} = \angle L_{L.T.I.}$$

and therefore $|L_{eq}(s)|$ would be as shown in dashed lines in Fig. I.5. The improvement to expect in terms of sensor noise rejection is then obvious by inspection of Fig. I.5.

I.5b Linear time varying networks.

It is well known that time-invariant filters are optimum for stationary processes, i.e., if all signals are stationary [P1] . The fact that we concentrate on specific command inputs starting at time $t = 0$, implies non-stationary processes. Therefore we are induced to think that L.T.V. filters (F, G) can give better performances than L.T.I. (F,G) . Physically it means that the feedback properties are tuned to follow the time-varying sensitivity needs, rather than be time-invariant.

I.6 Previous work.

The above topics constitute a very broad area of investigation. Long ago Holzmann [H10] mentioned that "control engineers in the chemical process industries have long recognized the possibility of achieving superior responses by means of nonlinear control". And Chesnut [C2] quoted John Mocre "that for any linear control, he could

always build a nonlinear control which would be better". Clegg [C1] and others have noted that N.L. compensation can give better gain-phase relations than LTI networks (from the describing function viewpoint). But no quantitative synthesis techniques exploiting this idea were reported. Recently, however, Krishnan and Horowitz [H4] proposed a quantitative design procedure using a N.L. element.

On the other hand, it was shown that "variable structure systems" have adaptive properties (see for example, [E1], [U1], [U2], [K1]). In these systems the LTI compensation changes when system state crosses a switching surface. However, no quantitative synthesis technique for satisfying assigned specifications over a given range of uncertainty has appeared for this class. A search of the literature reveals that besides [H4] no quantitative synthesis procedure using N.L. compensation has ever been given for uncertainty plants and which is quantitatively related to the performance specifications and to the range of uncertainty.

Much work has been done on the filter problem in both stationary and non-stationary processes (see, for example, [W1], [B2], [S1], [K2]). Very little has been done in this area for uncertain plants. Fleisher [F1] did consider the problem of stochastic plant-parameters and gave a synthesis procedure that uses lti compensation. However, because of the linearization that he made in order to obtain a solvable problem, his synthesis technique is approximately valid, at best, for relatively small parameter uncertainty.

In summary we can say that the field of quantitative synthesis of feedback systems using N.L. or L.T.V. networks has hardly been investigated as of now.

CHAPTER II. BASIC PRELIMINARIES

The work presented in this dissertation rests on the following foundations:

a) The synthesis procedure for L.T.I. systems to satisfy T.D.S. despite large plant ignorance, devised by Horowitz and Sidi [H2].

b) The derivation of optimum linear time varying filters for non-stationary processes due to Booton [B2].

c) The concept of set-Equivalent-Plant-Linear Time Invariant (E.P.L.T.I.) used to characterize a large class of non-linear-time-varying plants, introduced by Horowitz [H1].

We shall now briefly review those topics:

II.1 Synthesis procedure for L.T.I. systems.

The method presented in [H2] is restricted to minimum phase plants, but has recently been extended to non-minimum phase plants (Horowitz and Sidi, [H9]). In a first step, the T.D.S. are translated into frequency domain specifications (F.D.S.). Although no general rigorous translation between the two domains is known, there is, in practice, little difficulty in effecting one which is satisfactory for practical engineering purposes. Thus, for example [S2], the T.D.S. of Fig. I.2 are translated in the F.D.S. of Fig. II.1 and therefore at each frequency $\omega \in \Omega = [0,\infty]$, the maximum tolerable variation $\Delta \ln|T(j\omega)|$ on the system overall transfer function $T \triangleq \frac{C}{R}$ (see Fig. I.3) is defined. The synthesis technique is mathematically rigorous for such ω-domain specifications.

Secondly, at each $\omega_\ell \in \Omega$, $P_i(j\omega_\ell)$ denotes a point in the

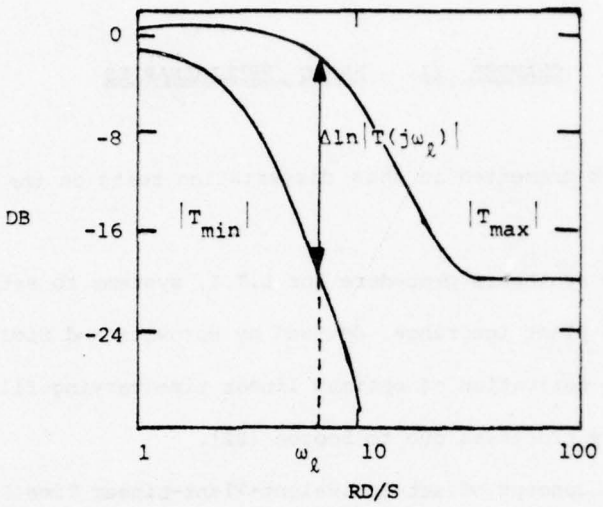

Figure II.1. Bounds on $\ln |T(j\omega)|$.

complex plane which is associated with the plant-parameter condition i . As i ranges over the uncertainty range the point $P_i(j\omega_\ell)$ describes a region in the complex plane denoted as the "template" $P(j\omega_\ell)$ of the plant $P(j\omega)$ at frequency ω_ℓ .

Using steps 1 and 2, (3rd step) for each $\omega_\ell \in \Omega$, a bound $\Gamma(\omega_\ell)$ (Fig. II.2) on the nominal open loop transfer function $L_n(j\omega)$ associated with the nominal plant condition $P_n(j\omega)$ (i.e., $L_n(j\omega) = GP_n(j\omega)$, Fig. I.3) is derived such that:

$$\Delta \ln \left| \frac{L_n(j\omega_\ell)}{1+L_n(j\omega_\ell)} \right| \leq \Delta \ln |T(j\omega_\ell)| \quad \text{permitted} \tag{2.1}$$

when $\Delta \ln L_n(j\omega_\ell) = \Delta \ln P_n(j\omega)$ (2.2)

Sooner or later there must exist a frequency range in which sensitivity increases rather than decreases, because in any practical feedback system [B1]

$$\int_0^\infty \ln |S| \, d\omega = 0 \text{ , where } S = \frac{dT|T}{dP|P} \tag{2.3}$$

is the sensitivity of $T(j\omega)$ to uncertainty in P. This is sometimes denoted as the 'equality of positive and negative feedback areas'. Hence, if $|S| < 1$ over some range (the primary objective in a feedback system), it must be balanced by another in which $|S| > 1$. It is easy to live with this constraint in the two-degree-of-freedom system, because at sufficiently large ω, $|T|$ is negligibly small, so that large relative changes in $|T|$ are inconsequential. This means that at large ω, it is essential that the response tolerances $\Delta \ln|T(j\omega)|$ exceed the range of the $P(j\omega)$ template in order that $L(j\omega)$ may go to zero as $\omega \to \infty$. $|S| >> 1$ is tolerable in this high-frequency range, as far as its effect on $T(j\omega)$ is concerned, because the prefilter F in Fig. I.3 attenuates the resulting high peaking in $L/(1+L)$. However, the disturbance response $T_d = C/D = (1+L)^{-1} = S$ of (2.3), is then also very large, which is generally not tolerable because there is no equivalent filter available. Although the parameter ignorance problem is assumed to dominate, it is necessary to consider the disturbance response, at least to the extent of adding the constraint

$$\exists \gamma > 0, \ \ni |T_d| \triangleq \left|\frac{C}{D}\right| = |(1+L)^{-1}| \leq \gamma, \ \forall \omega \qquad (2.4)$$

The value of γ may be related to the damping factor ζ of a second-order response function by the relation

$$\gamma = \max_{\omega} \left| \frac{1}{1-\omega^2+j2\zeta\omega} \right| = \left| \frac{1}{2\zeta\sqrt{(1-\zeta^2)}} \right|$$

The above leads to the boundary Γ_ℓ of Fig. II.2 with θ_m a function of γ, e.g. $\theta_m = 50°$ if $\gamma = 2{\cdot}3$ dB. At low frequencies the parameter factor dominates for $\omega < \omega_b$ in Fig. II.2, so these boundaries contain no part of Γ_ℓ. There is an intermediate frequency region in

which part of the boundary contains a portion of Γ_ℓ , e.g. $\Gamma(\omega_4)$ in Fig. II.2. At sufficiently large ω $(\omega>\omega_b)$, Γ_ℓ becomes the complete boundary.

In a fourth step, using the optimum criteria of I.3, i.e., Min k_∞^i , where as $s\to\infty$, $G_i(s) \to \frac{k_\infty^i}{s^e}$ for some given integer e , the optimum $L_n(j\omega)$ was proven to be the one which lies exactly on its bound $\Gamma(\omega_\ell)$ at each $\omega_\ell \in \Omega$. (see [H2], [H3] and [H9]).

$G(j\omega)$ only guarantees that $\Delta \ln|T(j\omega)|$ is satisfied. The pre-filter F is needed in order for $\left|\frac{FL}{1+L}\right|$ to lie in between $|T_{Min}|$ and $|T_{Max}|$.

F is thus derived, for example, by matching $|F| \cdot \left|\frac{L}{1+L}\right|_{Max}$ with the specified $|T_{Max}(j\omega)|$ for all $\omega \in \Omega$.

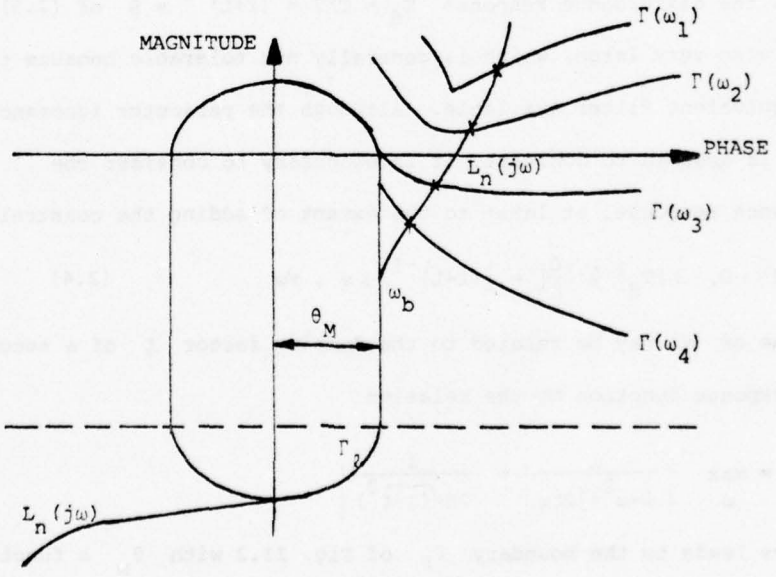

Figure II.2. Typical bounds on $L_n(j\omega)$ at different frequencies.

II.2 Design example.

The plant is $P(s) = \dfrac{k}{s^2+2\zeta_p\omega_p s+\omega_p^2}$ with $k \in [1,1000]$

$\zeta_p\omega_p \in [-5,3]$, $\omega_p\sqrt{1-\zeta_p^2} \in [2,10]$

the parameter being independant. It is required that the system step response lie within given T.D. bounds over the entire range of plant parameter values. This problem was solved by Horowitz and Sidi [H2] and [S2] and the resulting F.D.S. are shown on Fig. II.1. A peaking $\gamma = 2$ dB was tolerated which corresponds (Appendix A1) to $\zeta = .44$ and to a tolerable overshoot of 21% in the step-disturbance response. Using the procedure described above,

$$L_\ell(s) = \frac{47.1910^{15}(s+.905)(s+.92)(s+17.3)(s+26.1)(s+200)(s+2220)}{s(s+512)(s+5.28)(s+6.1)(s+37.8)(s+50)(s+1000)(s^2+10500s+(15000)^2)^2}$$

associated with the nominal plant $P_{nom}(s) = \dfrac{5}{s(s^2+2s+5)}$.

$L_\ell(s)$ is plotted in both Figs. III.13 and III.14. The prefilter is then calculated to be $F(s) = \dfrac{9\,(s+.94)(s+2.4)}{(s+1.5)^2(s^2+4.2s+9)}$. Corresponding command outputs and step-disturbance responses are plotted in Fig. III.18 and Fig. III.19 respectively for different plant parameter values.

II.3 Optimum L.T.V. filter for non-stationary inputs.

Given $\{x_I\}$ a set of input signals that are to be applied to a system characterized by its impulse response $h(t,\tau)$, i.e. (Fig. II.3):

$$x_R(t) = \int_0^t h(t,\zeta)\, x_I(\zeta)\, d\zeta$$

Furthermore let us assume that any input signal $x_I(t) \in \{x_I\}$ is the

sum of a signal component $x_s(t)$ and a noise component $x_N(t)$,

$x_I(t) = x_s(t) + x_N(t)$ with $\{x_s\}$, $\{x_N\}$ given.

Let:

$$\gamma_{II}(t_1,t_2) \triangleq \overline{x_I(t_1)\, x_I(t_2)}$$
$$\gamma_{Is}(t_1,t_2) \triangleq \overline{x_I(t_1)\, x_s(t_2)}$$

where the bar denotes the average over the ensemble of input functions.

Note that $\gamma_{Is}(t_1,t_2) = \gamma_{sI}(t_2,t_1)$. γ_{ss} , γ_{sN} , γ_{NN} are defined similarly. It can be shown that:

$$\gamma_{II} = \gamma_{ss} + \gamma_{sN} + \gamma_{Ns} + \gamma_{NN} \ .$$

Let $g(t,\tau)$ be a given ideal system impulse response which, operating on the signal component $x_s(t)$, gives the desired ideal output signal:

$$x_D(t) = \int_0^t g(t,\zeta)\ x_s(\zeta)\ d\zeta$$

If $e(t) \triangleq x_D(t) - x_R(t)$, how should $h(t,\tau)$ be chosen so as to minimize $\overline{e^2(t)}$ for all t ? It can be shown [B2] that:

$$\overline{e^2(t)} = \gamma_{DD}(t,t) - 2\int_0^t h(t,\zeta)\ \gamma_{ID}(\zeta,\tau)\ d\zeta + \int_0^t\int_0^t h(t,\tau_1)\ h(t,\tau_2)\ \gamma_{II}(\tau_1,\tau_2)\, d\tau_1 d\tau_2$$

A variational argument leads to the optimum $h(t,\tau)$ to be the solution

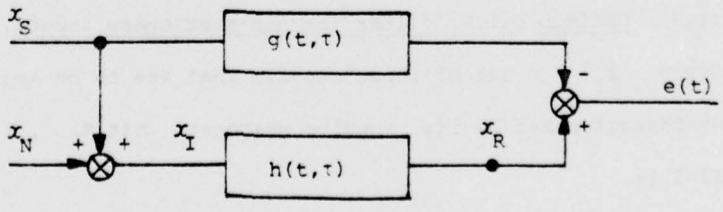

Figure II.3. Linear time varying optimum filter.

of the integral equation:

$$\gamma_{ID}(t,\tau) = \int_0^t h(t,\zeta)\ \gamma_{II}(\zeta,\tau)\ d\zeta \quad \text{for} \quad t > \tau \qquad (2.5)$$

Given the deterministic signal $s(t)$, how can one approximate the autocorrelation function $\gamma_{ss}(t_1,t_2)$ for practical purposes? We first note that $\gamma_{ss}(t_1,t_2)$ is a symmetric function, continuous if x_s is continuous. Let us consider signals existing on $[0,T]$ where T can be as large as desired. We can consider $\gamma_{ss}(t_1,t_2)$ as a definite symmetric kernel and by application of Mercer's theorem [C3], [C4]

$$\gamma_{II}(t_1,t_2) = \sum_{r=1}^{\infty} \frac{\varphi_r(t_1)\varphi_r(t_2)}{\lambda_r} \qquad (2.6) \quad \text{for all} \quad t_1,t_2 \in [0,T]$$

where λ_r and $\varphi_r(\cdot)$ are respectively eigenvalues and corresponding eigenfunctions of γ_{II}, i.e., non trivial solutions of:

$$\frac{1}{\lambda_r}\varphi_r(s) = \int_0^T \gamma_{II}(s,\zeta)\ \varphi_r(\zeta)\ d\zeta \qquad (2.7)$$

For practical purposes, we can certainly approximate (2.6) by:

$$\gamma_{II}(t_1,t_2) = \sum_{r=1}^{N} \frac{\varphi_r(t_1)\varphi_r(t_2)}{\lambda_r} \qquad (2.8) \quad \text{for all} \quad t_1,t_2 \in [0,T]$$

where N is such that the norm on the space $L_2[0,T]$ of the error is less than a given tolerated error ε, i.e.,

$$\int_0^T\int_0^T \left| \gamma_{II}(t_1,t_2) - \sum_{1}^{N} \frac{\varphi_r(t_1)\varphi_r(t_2)}{\lambda_r} \right|^2 dt_1\,dt_2 = \sum_{r=N+1}^{\infty} \left|\frac{1}{\lambda_r}\right|^2 < \varepsilon \qquad (2.9)$$

II.4 Concept of set-Equivalent-plant-linear time invariant.

It was suggested long ago to replace non-linear or linear time varying networks by an approximate equivalent linear time invariant ones, for convenience in analysis and synthesis. The Describing function [G2] is a well known example of such a substitution. However, it was

definitely not used as a tool for quantitative synthesis in uncertain systems. The concept of Equivalent Plant Linear Time Invariant (E.P.L.T.I.) set which can be properly used for quantitative synthesis was recently introduced by Horowitz [H1, H6]. This concept is now briefly reviewed. Given (Fig. II.4) $R=\{r\}$ and $D=\{d\}$ - two finite sets of deterministic command and disturbance inputs.

Let $I = \{i^{\alpha}(t), \alpha=1,\ldots N\}$ be the given set of system inputs for which the design is to be executed, where i^{α} may consist of a command, a disturbance, or a combination of any two of these. Given the set $C^{\alpha}[t] = \{c^{\alpha}(t)\}$ of acceptable system output signals associated with $i^{\alpha}(t)$, it is possible to find the corresponding set $Z^{\alpha}[t] = \{z^{\alpha}(t)\}$ of acceptable plant output signals and thus the set $Z^{\alpha}[s] = \{\mathcal{L}(z^{\alpha}(t))\}$. Let the plant be characterized by a set $W = \{w\}$ (because of plant uncertainty) of nonlinear time invariant (the latter for the sake of simplicity - the extension to nonlinear time varying is straighforward) continuous mappings $w : x(t) \to z(t)$, with <u>unique continuous inverse w^{-1} (B1)</u>. Then for any plant $w_i \in W$ there exists a plant input signal $x_{\nu i}^{\alpha}(t)$ which produces the plant output signal $z_{\nu}^{\alpha}(t) \in Z^{\alpha}[t]$ and we can define:

$$P_{i\nu}^{\alpha}(s) = \frac{\mathcal{L}[z_{\nu}^{\alpha}(t)]}{\mathcal{L}[x_{\nu i}^{\alpha}(t)]} = \frac{z_{\nu}^{\alpha}(s)}{x_{\nu i}^{\alpha}(s)}$$

as the $\alpha_{i\nu}$ - equivalent plant linear time invariant (E.P.L.T.I.) transfer function, in the sense that the input $x_{\nu i}^{\alpha}(t)$ into the linear $P_{i\nu}^{\alpha}(s)$ gives the same output as the input $x_{\nu i}^{\alpha}(t)$ into the non-linear plant w_i. Thus the method is restricted to nonlinear w for which the set X is Laplace transformable. Restriction is made in the meantime to design procedure for w such that $P_{i\nu}^{\alpha}(s)$ is minimum phase

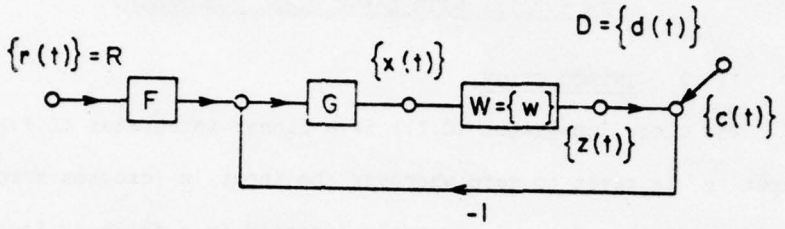

Figure II.4. Feedback structure with nonlinear uncertain plant set W .

(B2) for all α, i, ν .

As i ranges over all $w_i \in W$ and ν ranges over all $z_\nu^\alpha(t) \in Z^\alpha[t]$, $P_{i\nu}^\alpha(s)$ describes the set:

$$P^\alpha[s] = \{P_{i\nu}^\alpha(s) \ , \ z_\nu^\alpha(t) \in Z^\alpha[t] \ , \ w_i \in W\}$$

which is defined as the α -E.P.L.T.I. transfer function set associated with the input signal $i^\alpha(t)$ over the output set $C^\alpha[t]$ and the nonlinear plant set W .

Once this is done, the quantitative design procedure used for L.T.I. systems [H2] can be applied to the E.P.L.T.I. problem where the specifications on the acceptable output are those assigned to the nonlinear problem. $P^\alpha[s]$ becomes the uncertain L.T.I. plant set in this equivalent L.T.I. problem. Schauder's fixed point theorem is used to prove that the solution to the latter problem is valid for the nonlinear plant set. The synthesis procedure of Paragraph II.1 can be easily extended to nonlinear time varying plants.

CHAPTER III. NONLINEAR DESIGN FOR COST OF FEEDBACK REDUCTION IN SYSTEMS WITH LARGE PLANT IGNORANCE.

III.1 INTRODUCTION.

The Clegg Integrator (C.I.) is a linear integrator (L.I.) whose output y is reset to zero whenever the input x crosses zero ([Cl], see Fig. III.1). If it is properly inserted in a feedback loop system, it can reduce considerably the system step response overshoot.

The C.I. response y(t) to a sinusoidal excitation x(t) is shown on Fig. III.2 and its describing function N for sinusoidal inputs is plotted on Fig. III.3. It is seen that the rate of decrease of $|N|$ and of the L.I. are the same. However, $\angle N = -38°$ compared to $-90°$ for the L.I. Therefore the phase margin θ_M associated with the "non-linear" open loop transfer function $L_{eq}(s)$ containing a C.I. is bigger (by 52°) than the one associated with $L_{LTI}(s)$ containing a L.I. in place of the C.I. As we know phase margin is closely related to the overshoot in the system step response. This explains qualitatively the differences mentioned earlier noted by Clegg. However, quantitative synthesis can not rely on Describing Function Theory (as already stated) and in any realistic design one has to overcome a big instability problem if one wants to use a C.I. (see Chapter IV). To a large extent the 'First order reset element' (FORE) (which is the linear element 1/s+b whose output y is reset to zero whenever the input x crosses zero (Fig. III.4)) overcomes the instability problem mentioned before, and this will be explained in detail in Chapter IV.

It is worth noting (Figs.III.3, III.2, III.5), that FORE appears

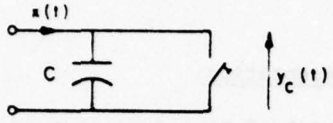

Figure III.1. C.I.

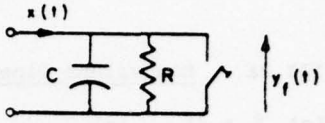

Figure III.4. FORE.

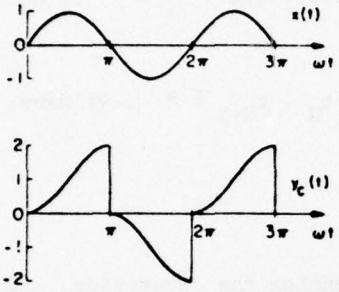

Figure III.2. C.I. response to a sine wave.

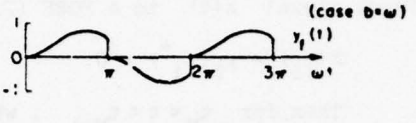

b/ω	.01	.1	1.	2.	3.	7.
Normalized reset value (% of the CI reset value)	.98	.86	.26	.10	.05	.01

Figure III.5. FORE response to a sine wave.

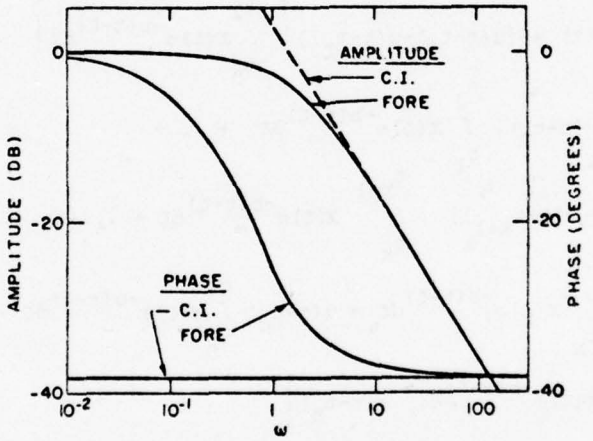

Figure III.3. Normalized describing functions of C.I. & FORE.

as a linear element to slow-varying signal and as a non-linear element to fast-varying signals, because the value of the reset (Fig. III.5) is definitely a function of the input signal frequency. This gives a flexibility, not available in the C.I.

Furthermore the frontier between the two characters can be adjusted to a particular design.

III.2 Analysis: Characterization of 'FORE'.

Some tools are first derived that are used to solve the synthesis problem.

III.2a. Equivalent linear representation.

Let $\theta = \{t_i , i=1,2...\}$ be the set of zero-crossings of the input signal $x(t)$ to a FORE (Fig. III.4), i.e. $t_i \in \theta$ is such that:

$$x(t_i) = y_f(t_i^+) = 0$$

Then for $t_N \leq t < t_{N+1}$, where $t_N , t_{N+1} \in \theta$, we have:

$$y_f(t) = \int_{t_N}^{t} x(\zeta) e^{-b(t-\zeta)} \, d\zeta \quad .$$

If $u(t-t_K) = \begin{cases} 1 & \text{for } t \geq t_K \\ 0 & \text{for } t < t_K \end{cases}$ denotes the Heaviside function

then: $y_f(t) = [u(t-t_0)-u(t-t_1)] \left[\int_{t_0}^{t_1} x(\zeta) e^{-b(t-\zeta)} d\zeta \right] +$

$$[u(t-t_1)-u(t-t_2)] \int_{t_1}^{t_2} x(\zeta) e^{-b(t-\zeta)} d\zeta + .. +$$

$$[u(t-t_K) - u(t-t_{K+1})] \int_{t_K}^{t_{K+1}} x(\zeta) e^{-b(t-\zeta)} d\zeta + .. +$$

$$u(t-t_N) \int_{t_N}^{t} x(\zeta) e^{-b(t-\zeta)} d\zeta = u(t-t_0) \int_{t_0}^{t} x(\zeta) e^{-b(t-\zeta)} d\zeta -$$

$$\sum_{K=1}^{N} \left[\int_{t_{K-1}}^{t_K} x(\zeta) e^{-b(t-\zeta)} d\zeta \;\; u(t-t_K) \right] \qquad (3.0a)$$

Let $x_K^* \triangleq \int_{t_{K-1}}^{t_K} x(\zeta) e^{-b(t_K-\zeta)} d\zeta$ (3.0) and notice that

$y_\ell(t) = \int_{t_0}^{t} x(\zeta) e^{-b(t-\zeta)} d\zeta$ is the output signal of the linear element $1/s+b$ for the same input $x(t)$.

Then $y_f(t) = y_\ell(t) - \sum_{K=1}^{N} \left[\int_{t_0}^{t} e^{-b(t-\tau)} \delta(\tau-t_K) d\tau \; x_K^* \right] u(t-t_k)$ (3.1)

where $\delta(t)$ is the unit impulse function.

At this stage several comments are necessary.

α). Note that x_K^* represents the reset value that occurs at time $t=t_K$. Thus the nonlinear aspect of FORE is represented (3.1) by a train of impulses of value $-x_K^*$ at $t_K \in \theta$, added to the input, i.e. FORE can be replaced (Fig. III.6) by $1/s+b$ and adding to the input the train of impulses $-\sum_1^N x_K^* \delta(t-t_K)$ for $t_N \leq t < t_{N+1}$. β). We also learn from (3.1) that if $x(t)$ produces $y_f(t)$, then $k \cdot x(t)$ (where k is some real constant) gives the output $k \cdot y_f(t)$ and therefore the linear character is preserved in the multiplication by a constant. This is quite an important feature because it is then sufficient to characterize FORE for unit signal, command or disturbance, in order to know its behaviour for the non unit one. γ). From (3.1) one notes that FORE is nonlinear from the additive point of view. If $x_1(t)$, $y_f^1(t)$, and $x_2(t)$, $y_f^2(t)$ are respectively paired, then in general, $x_3(t) = x_1(t) + x_2(t)$ gives rise to an output signal $y_f^3(t) \neq y_f^1(t) + y_f^2(t)$. The equality $y_f^3(t) = y_f^1(t) + y_f^2(t)$ occurs if and only if the sets of reset instants θ_1 and θ_2 associated with $x_1(t)$ and $x_2(t)$ are equal. Thus FORE is a linear element over the class X of input-signals $x(t)$ that have the same zero-crossings. However, even when FORE acts on X, it has not the commutativity property with linear elements, i.e. FORE $*$ LTI $\neq$ LTI $*$ FORE. All these, then, legitimize <u>as a notation</u>, the use of $(\frac{1}{s+b})^*$ to characterize FORE. From now on, any FORE will be followed (even if not specifically mentioned) by the element $s+b$ (Fig. III.7) and we define

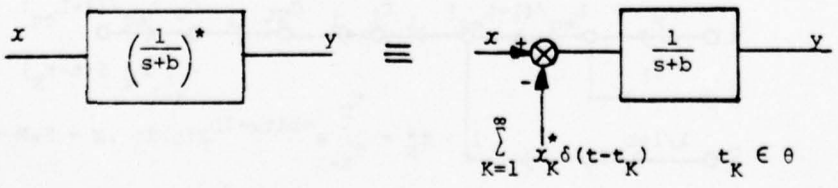

Figure III.6. Equivalent representation of FORE.

the equivalent open loop transfer function $L_{eq}(s) \triangleq G(s)\,P(s)$. Note that $L_{eq}(s) = L_{LTI}(s)$ when no reset occurs. In a similar manner the equivalent overall transfer function is defined as $T_{eq}(s) \triangleq F(s)\,L_{eq}(s)/(1+L_{eq}(s))$. By using the equivalent representation of FORE shown on Fig. III.6 and by application of the superposition theorem, Fig. III.7 becomes equivalent to Fig. III.8 from the output signals point of view. Thus the nonlinear output $C_{NL}(t)$ is the combination of the linear system output $C_\ell(t)$ and the train of impulse responses $C_T(t)$.

For example, in Fig. III.7, let $R(s) = 1/s$, $D = N = 0$, $F(s) = 1$, $L_{eq}(s) = \omega_N^2/(s(s+2\zeta\omega_N))$ with $\zeta < 1$. $T_{eq}(s) = \omega_N^2/(s^2+2\zeta\omega_N s+\omega_N^2)$. So, $C_\ell(t) = 1 - e^{-\zeta\omega_N t}\sin(\omega_0 t+\cos^{-1}\zeta)/\sqrt{1-\zeta^2}$ with $\omega_0 = \omega_N\sqrt{1-\zeta^2}$. The first reset instant t_1 is such that $C_\ell(t_1) = 1$ (because $x(t_1) = 0$) giving $t_1 = (\pi-\cos^{-1}\zeta)/\omega_0$. Using (3.0), $x_1^* = e^{-\zeta(\pi-\cos^{-1}\zeta)/\sqrt{1-\zeta^2}/\omega_N}$ and for $t_1 \le t < t_2$: $C_\ell(t) = -x_1^*\,\dot{C}_\ell(t-t_1) = e^{-\zeta\omega_N t}\sin(\omega_0 t+\cos^{-1}\zeta)/\sqrt{1-\zeta^2}$. Therefore for $t_1 \le t < t_2$ the nonlinear system output $C_{NL}(t) = C_\ell(t) + C_T(t) = 1$.

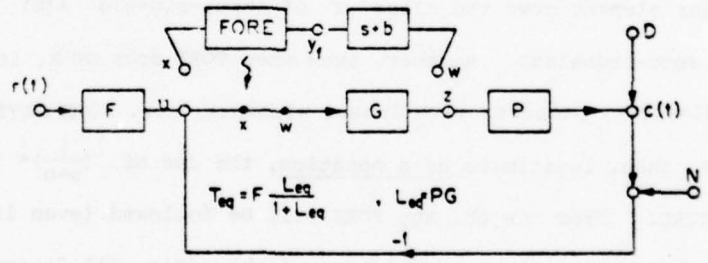

Figure III.7. System block diagram.

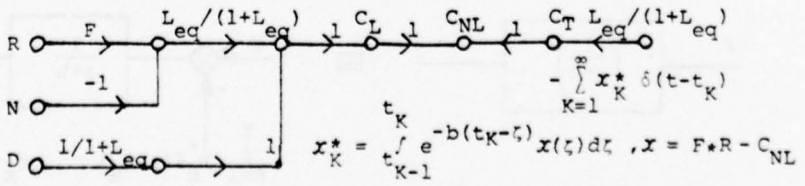

Figure III.8. Equivalent system block diagram.

In summary:

$$C_{NL}(t) = \begin{cases} C_{\ell}(t) & \text{for} \quad t \leq t_1 \\ 1 & \text{for} \quad t \geq t_2 \end{cases}$$

This result is very interesting because the steady state is reached in a finite time t_1, which is impossible to acheive with L.T.I. systems and because the result (0% overshoot in the system step response) is independant of ζ and ω_N. However, it is of little practical use because of the pure 2nd order system considered here.

Physically the above is easily explained. After the first reset occured, the steady state ($x=0$, $y_f=0$, $c=1$) is reached which eliminates the dynamics for $t \geq t_1$, despite possible ignorance in ω_N.

III.2b. Non-linear step response overshoot.

Using some of the results of the previous section, it is possible to calculate the nonlinear overshoot that occurs in the step disturbance response of the system shown in Fig. III.7. For practical purposes because of the universal character of the 'optimum' L.T.I. open loop transfer function $L(j\omega)$ in problems with large parameter uncertainty, it is possible to approximate the resulting high order $L/(1+L)$ by a delayed second order function $T_{APP}(s) = \dfrac{\omega_N^2 e^{-t_d s}}{s^2+2\zeta\omega_N s+\omega_N^2}$.

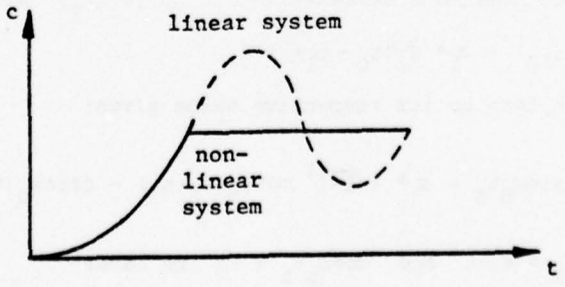

Figure III.9. Linear and nonlinear system step responses.

This approximation is justified in Appendix A1. In the second-order system the overshoot is related to ζ by $OV_{1in} = e^{-\zeta\pi/\sqrt{1-\zeta^2}}$ (3.1b) and to the magnitude peaking by $\left|\frac{L}{1+L}(j\omega)\right|_{max} = \frac{1}{2\zeta\sqrt{1-\zeta^2}}$. For the remaining of this paragraph, t_d is assumed to be zero. Therefore the following results will only be applied to those systems for which the time delay can be neglected (see Appendix 1).

Consider the system of Fig. III.7, where $r = n = 0$ and $d(t)$ is a step. Then in Fig. III.8 : $C_\ell(t) = \frac{e^{-\zeta\omega_N t}}{\sqrt{1-\zeta^2}} \sin(\omega_0 t + \cos^{-1}\zeta)$ with $\omega_0 = \sqrt{1-\zeta^2}\cdot\omega_N$.

The first reset instant occurs at $t_1 = \frac{\pi - \cos^{-1}\zeta}{\omega_0}$ and therefore the first reset value is: ($x_\ell = -C_\ell$)

$$x_1^* = -\int_0^{t_1} C_\ell(\zeta) e^{-b(t_1-\zeta)} d\zeta = +\frac{1}{b} e^{-bt_1} + \frac{e^{-bt_1}}{b} \int_0^{t_1} e^{b\zeta}\, \dot{C}_\ell(\zeta) d\zeta$$ after integrating by parts. As $\dot{C}_\ell(t) = \frac{\omega_N e^{-\zeta\omega_N t}}{\sqrt{1-\zeta^2}} \sin\omega_0 t$, we have

$$x_1^* = +\frac{e^{-bt_1}}{b} - \frac{\omega_N}{b^2} \quad \frac{1}{1-2\zeta\frac{\omega N}{b} + (\frac{\omega N}{b})^2} \left(e^{-\zeta\omega_N t_1} + \frac{\omega_N}{b} e^{-bt_1} \right) \quad (3.2)$$

The nonlinear system step disturbance response is therefore:

$$C_{NL}(t) = \begin{cases} C_\ell(t) & \text{for } t \leq t_1 \\ C_\ell(t) - x_1^* \dot{C}_\ell(t-t_1) & \text{for } t_1 \leq t \leq t_2 \end{cases} \quad (3.3)$$

with $t_1 , t_2 \in \theta$.

There exists at least one extremum at $t_0 \in [t_1, t_2]$ at which,

$$\dot{C}_{NL}(t_0) = \dot{C}_\ell(t_0) - x_1^* \dot{C}_\ell(t_0 - t_1) = 0 \quad (3.3a)$$

Replacing each term by its respective value gives:

$$\frac{\omega_N e^{-\zeta\omega_N t_0}}{\sqrt{1-\zeta^2}} \left[\sin\omega_0 t_0 - x_1^* \left(\sqrt{1-\zeta^2}\cos\omega_0(t_0-t_1) - \zeta\sin\omega_0(t_0-t_1)\right) e^{\zeta\omega_N t_1} \right] = 0$$

Using $\sin\omega_0 t_1 = \sqrt{1-\zeta^2}$ and $\cos\omega_0 t_1 = -\zeta$ we have:

$$\frac{\omega_N e^{-\zeta\omega_N t_0}}{\sqrt{1-\zeta^2}} \left(1 - x_1^* e^{\zeta\omega_N t_1}\omega_N\right) \sin\omega_0 t_0 = 0 \qquad (3.4a)$$

As $t_0 \in [t_1, t_2]$, there is only one extremum at $t_0 = \frac{\pi}{\omega_0}$ (3.4b) which corresponds to the instant at which $C_\ell(t)$ has its first minimum.

The value of the extremum is:

$$OV_{NL} = |C_{NL}(t_0)| = |C_\ell(t_0) - x_1^* \dot{C}_\ell(t_0 - t_1)| \triangleq OV_{LIN} - \Delta \qquad (3.5)$$

with $$\Delta = \frac{R}{1-2\zeta M_1 + M_1^2} \left(M_1^2 e^{-\zeta\mu} - M_1(1-2\zeta M_1)\, e^{-\mu/M_1}\right) \qquad (3.6)$$

$$R = e^{-\zeta \cos^{-1}\zeta/\sqrt{1-\zeta^2}} \qquad (3.7)$$

$$M_1 = \frac{\omega_c}{b}\sqrt{2\zeta^2 + \sqrt{4\zeta^4+1}} \qquad (3.8)$$

$$\mu = \frac{\pi - \cos^{-1}\zeta}{\sqrt{1-\zeta^2}} \qquad (3.9)$$

and ω_c denoting the crossover frequency of $L_{eq}(s)$, i.e., ω_c such that $|L_{eq}(j\omega_c)| = 1$.

Using (3.5) and (3.6), charts are presented in Fig. III.10, giving the net overshoot or undershoot in the step disturbance response, for the non-linear design, with $M = \frac{\omega_c}{b}$ as a parameter.

It is reasonable to hypothesize that for values of t_d very small relative to t_1 and t_0, Fig. III.10 can be used with good accuracy. Experimental results support this and will be given later.

III.2.c <u>When is it possible to consider FORE as a linear element?</u>

Assume FORE is located as shown in Fig. III.7. and let $d(t)$ be a step-disturbance and $r = 0$. Let $C_\ell(t)$ (Fig. III.8) be as shown in in Fig. III.11, then for $t < t_1$ we have:

$x(t) = x_\ell(t) = -C_\ell(t)$. Also $x_1^* = -\int_0^{t_1} C_\ell(t) e^{-b(t-t_1)} dt$. (3.10)

If $b = 0$ (C.I. case), x_1^* is the area under C_ℓ from $t = 0$ to t_1 in Fig. III.11. With $b \neq 0$, x_1^* is the area under curve $B = C_\ell(t) e^{-b(t_1 - t)}$. If $bt_1 > 1$ by a factor of 3 or more, B is very

small over $(0,t_1)$, so $C \doteq C_\ell$ for all t . Using previous results we have: $t_1 \approx \frac{\pi - \cos^{-1}\zeta}{\omega_N\sqrt{1-\zeta^2}}$ so $(t_1 > \frac{\pi}{2\omega_N})$ if $b > 3\omega_N$ (3.11) is

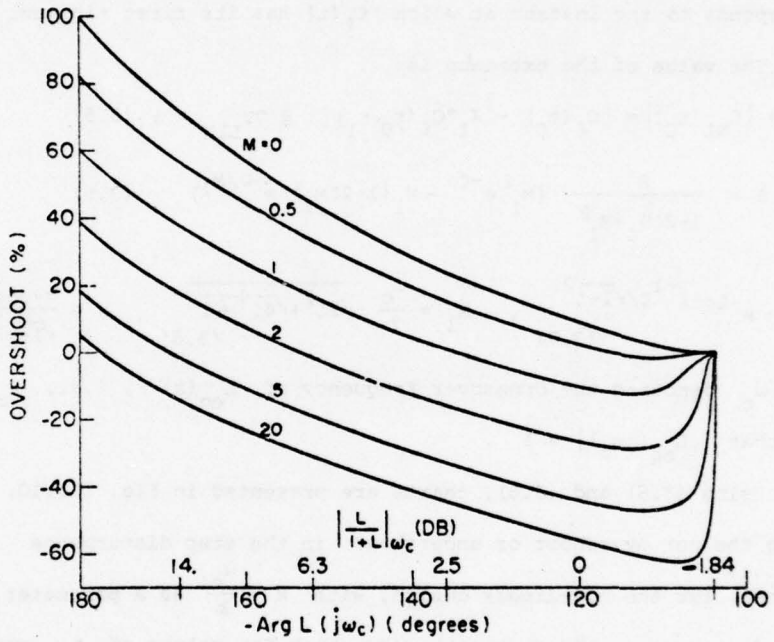

Figure III.10. Net overshoot in nonlinear design with $M = \omega_c/b$ as parameter.

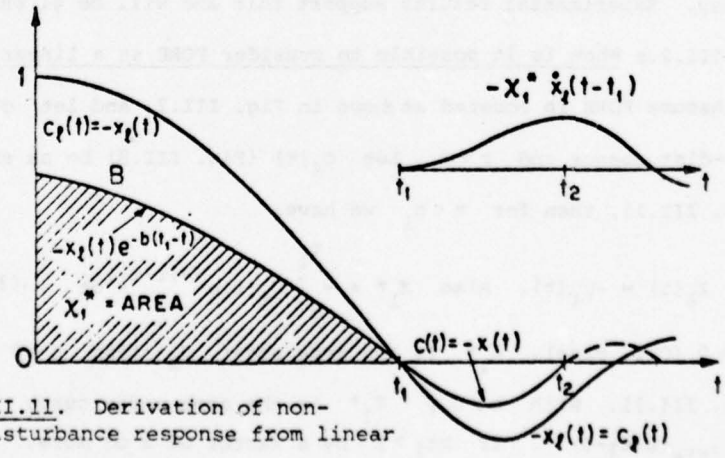

Figure III.11. Derivation of nonlinear disturbance response from linear response.

satisfied it implies that 'FORE' can be considered as behaving like 1/s+b from a practical point of view.

III.3. Synthesis.

III.3a. Philosophy of the design procedure.

We use the two degree of freedom structure of Fig. III.7. The open loop transfer function $L_{LTI}(s)$ has to satisfy bounds [H2] at each frequency $\omega \in [0,\infty]$ (Fig. III.12). In general in the low-frequency range $(\omega < \omega_b)$ $L_{LTI}(j\omega)$ lies on bounds due to the specifications on the command input responses and in $\omega > \omega_b$ $L_{LTI}(s)$ is determined by the maximum tolerable overshoot in the step disturbance response. This merely means that for $\omega_2 > \omega > \omega_b$, the bound Γ_ℓ imposes a certain phase margin θ_M for $L_{LTI}(j\omega)$.

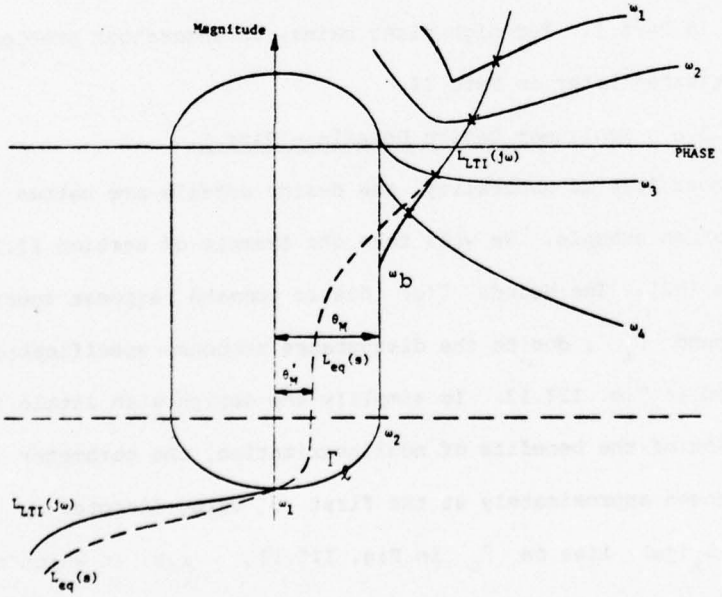

Figure III.12. Typical linear and nonlinear designs.

Recall that the smaller the phase margin, the bigger is the tendency to instability characterized by a larger overshoot. The N.L. character of the FORE in this higher frequency range $(\omega > \omega_b)$, will permit a smaller phase margin θ'_M on $L_{eq}(s)$ for acheiving the same specified maximum tolerable overshoot in the step disturbance response. This allows a faster decrease of $|L_{eq}(j\omega)|$ (Fig. III.12) and is accompanied by the reduction of the sensor noise effect at the plant input. We can adjust the value "b" of FORE such that in the lower frequency range $(\omega < \omega_b)$ FORE acts like a linear element, so that the bounds on $L_{eq}(s)$ due to the command input are unchanged. Consequently the prefilter F remains L.T.I. which is certainly an interesting feature and one of the important advantages of FORE over the C.I. Therefore a new set of bounds on $L_{eq}(s)$ has only to be derived in the higher frequency range $(\omega > \omega_b)$. This is done by using Chart III.10 as will be explained in Part I. For high plant gains, an undershoot problem arises which is treated later in Part II.

III.3.b. Nonlinear Design Details - Part I.

Without loss of generality, the design details are better presented by means of an example. We will take the example of section II.2 treated in [H2]. The bounds $\Gamma(\omega)$ due to command response specifications and the bound Γ_ℓ, due to the disturbance response specifications, are plotted in Fig. III.13. To simplify the design with little loss in exploitation of the benefits of nonlinearization, the parameter b of FORE is chosen approximately at the first ω value (denoted by ω_b) at which $L_\ell(j\omega)$ lies on Γ_ℓ in Fig. III.13, i.e. at which the disturbance response dominates, in the present case at 60 rps (Fig.III.13.). This definitely assures that the (nonlinear response to r) $\doteq$ (linear

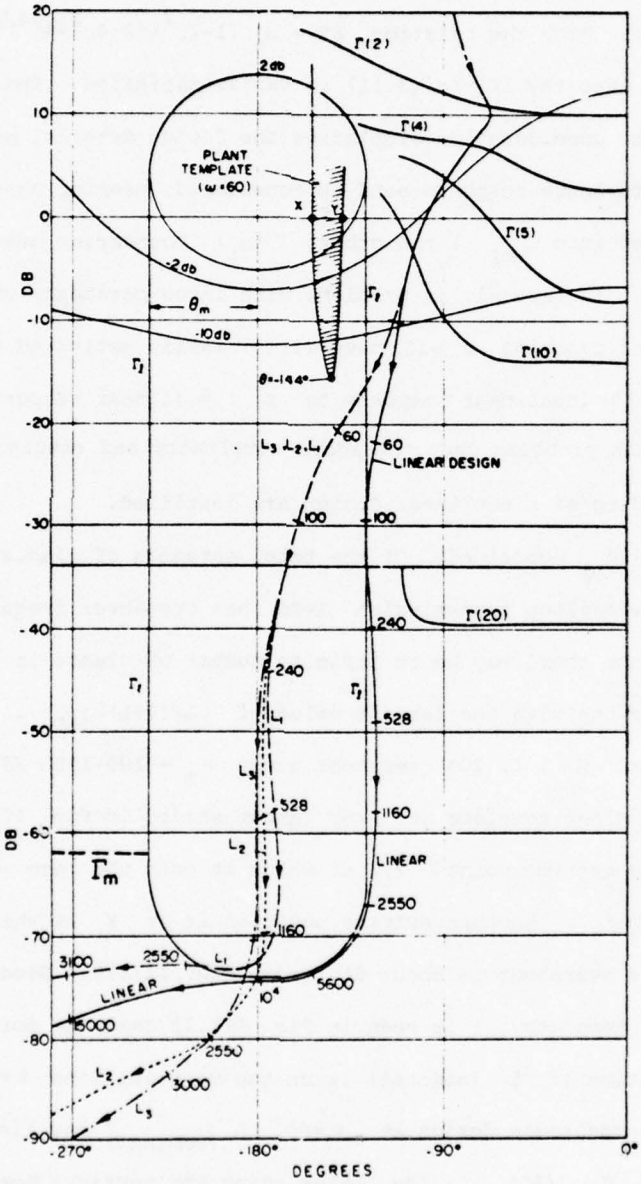

Figure III.13. Linear and nonlinear designs on Nichols chart (at K = 1).

response to r) . From Fig. II.1. the maximum bandwidth of $T(j\omega) \approx 7$ rps. From the relation $BW = \omega_n [1-2\zeta^2+(2-4\zeta^2+4\zeta^4)^{\frac{1}{2}}]^{\frac{1}{2}}$, ω_n is certainly less than 14, so (3.11) is easily satisfied. The above choice for b considerably simplifies the design details, because only the disturbance response need be considered, meaning that only Γ_ℓ is changed into $\Gamma_{n\ell}$; the other $\Gamma(\omega_i)$ boundaries need not be recalculated. In general, in problems with large parameter uncertainty, this method of choosing b will have (3.11) easily satisfied which then assures that the (nonlinear response to r) $\doteq$ (linear response to r). It is for such problems that the added complexity and resulting bandwidth saving of a nonlinear design are justified.

How is $\Gamma_{n\ell}$ obtained? Of the total ensemble of plants, consider that subset whose loop transmission $L=PG$ has crossover frequency $\omega_c=60$. Since there may be an infinite number of plants in this subset, pick the one with the largest value of $|L/(1+L)|_{j60}$. From Fig. III.10 at $M=1$, 20% overshoot gives $\theta_m = 180-155 = 25°$. We position the plant template at $\omega=60$ (shown shaded in Fig. III.13), such that one extreme point (χ) at which it cuts the zero db line is at $\theta_m = 25°$. Another extreme position is at Y at which $\theta=-138°$, for which the overshoot is about 3%, from Fig. III.10. Because of the shape of the template, it is seen in Fig. III.13 that the corresponding extreme position of L (nominal) is on the vertical line $\theta=-144°$, i.e., in the nonlinear design at $\omega=60$, $L_{(\text{nominal})}$ may lie on or to the right of $\Gamma_{n\ell}$ (60) , the latter being the vertical line $\theta=-144°$. The procedure is illustrated again, at $\omega=100$. Consider that plant value whose loop transmission has $\omega_c = 100$ and gives the largest value of $|L/(1+L)|_{j100}$. From Fig. III.10, at $M = 100/60$, 20% overshoot gives $\theta_m = 180-165.5 = 14.5°$. We position the $\omega=100$ plant

template such that the extreme point at which it cuts the zero db line is at $\theta_m = 14.5$. The corresponding positions of L (nominal) is on the vertical line $\theta = -160°$, which becomes $\Gamma_{n\ell}$ (100) .

Some of the experimental results are given in Figs. III.14, III.15 at this point to support the above. Fig. III.14 presents Bode plots of three nonlinear designs whose differences, significant only for $\omega > 1000$, will be explained later. Consider the response for $k = 10$ in Fig. III.15. In Figs. III.13, III.14, the corresponding ω_c is obtained by raising the nonlinear $L_{n\ell}(j\omega)$ by 20 log 10=20 db , or alternatively by lowering the zero db line by -20db , which cuts $L_{n\ell}(j\omega)$ very close to 60 rps and $-140°$. Hence $M = 1$ and from Fig. III.10 at 140° on the $M = 1$ curve, the net overshoot predicted is 5%, almost precisely that obtained. Similarly, consider $k = 25$ in Figs. III.13, III.14, III.15. The corresponding ω_c is obtained by examining the -20 log 25=-28 db line which cuts $L_{n\ell}(j\omega)$ close to $\omega = 1000$ at $-160°$. In Fig. III.10, on the curve M=100/60 (extrapolated from M=1,2) predicts 10% overshoot compared to 9.1% obtained. At $k = 100$, on the corresponding -40 db line: $\omega_c \doteq 200$, $\theta = -172°$ and in Fig. III.10 the corresponding extrapolated M=200/60 curve predicts about 12% overshoot, compared to 11.4% obtained in Fig. III.15.

III.3.c. Nonlinear design - Part II.

Suppose the above approach based on a second-order model, is pursued over the entire ω range, and the resulting nonlinear design implemented, as was in fact originally done in this research. It is found that the results are as predicted for command inputs r(t) for all plant conditions, and for disturbance inputs corresponding to the

smaller plant gain factor values, from $k = 1$ up to approximately $k = 100$. As the plant gain factor is further incresed, there is a transition from the second-order type response, in the manner indicated in Fig. III.15.

There are two important phenomena to be noted. One is the local maximum marked A in Fig. III.15, which gradually increases as k is increased, until $k>100$ approximately, it becomes the major maximum, as it clearly is for the case $k=1000$. The second phenomenon is the local minimum immediately following A, which eventually (at $k=100$) leads to an undershoot, growing by the time $k=1000$, to 31% undershoot; both phenomena not at all as predicted by the second-order model.

III.3.d. Explanation of divergence from second-order model.

The second-order model is satisfactory for all plant parameter combinations P_i such that the effective important part of L_i has relatively few poles and zeros, even though L has exactly the same number of poles and zeros over all P parameter combinations. Consider L_1 with say 7 zeros and 12 poles, such that most of the pole and zero corner frequencies occur at $|L_1(j\omega)|$ very small. Thus in Fig. III.14, the loop transmission at $k=25$ is obtained by letting the present -28 db line be the zero db line. $L_{k=25}(j\omega)$ can be reasonably approximated by a pure second order system for almost a decade beyond this point. The value of $L_{25}(j1000)$ is approximately $-70+28 = -44$ db and so is $|L_{25}/(1+L_{25})|_{j1000}$, since $1+L_{25}(j1000) \doteq 1$. Therefore, the large number of poles and zeros introduced in the $\omega=(1000,3000)$ range are comparitively far-off, and therefore the time delay t_d can be neglected in our approximation.

However, at larger k values these corner frequencies become

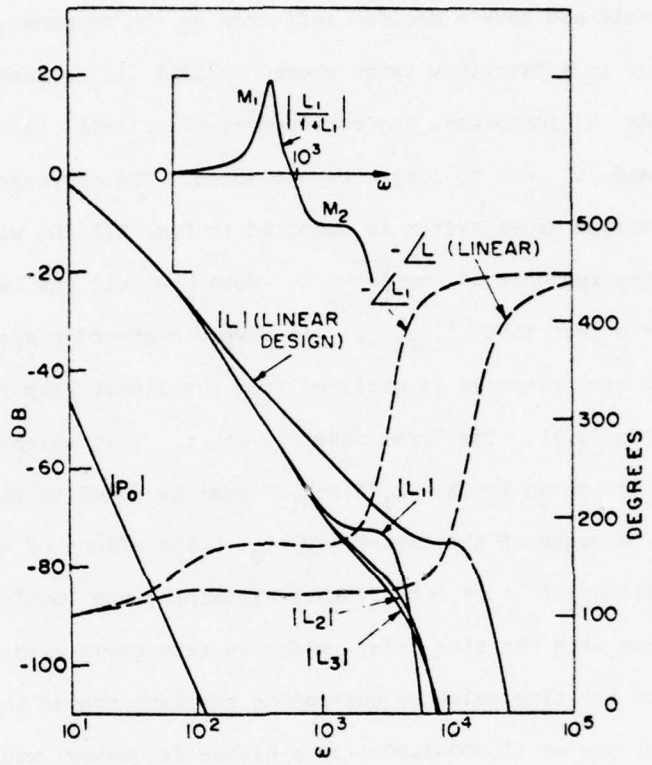

Figure III.14. Bode plots. Linear and nonlinear designs, at $k = 1$.

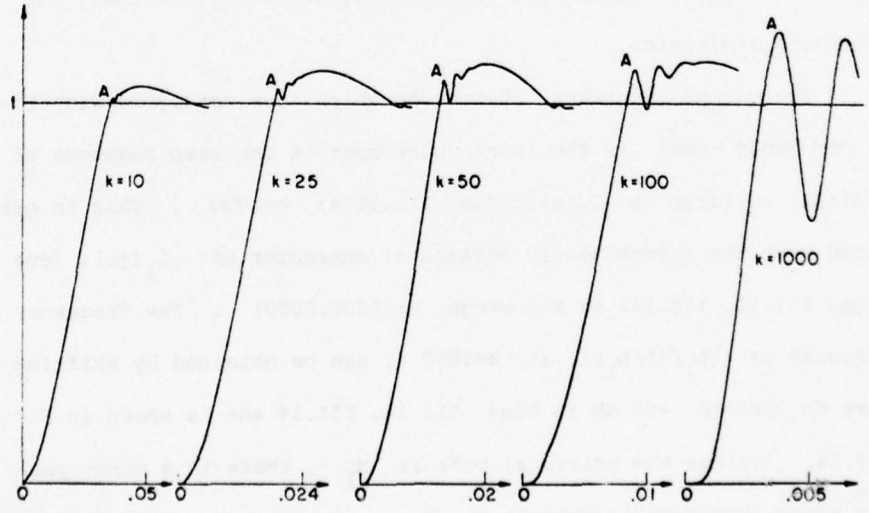

Figure III.15. Transition from second order type of responses as k increases.

less far-off and have a decided influence on the response, because they occur in a frequency range where $L/(1+L)$ is no longer very small. As k increases, the corresponding $L/(1+L)$ is a high-order system, and t_d can no longer be neglected. The response of a time-delayed second order system is compared in Fig. III.16a with the actual linear step response of $\frac{L_{1000}}{1+L_{1000}}$. Note how well the two agree, despite the fact that $L_{1000}(j\omega)$ is a very high-order system. The nonlinear step response is obtained from the linear step response, by means of Eq.(3.1). The first reset is at t_1, at which the impulse response due to an input $-x_1*\delta(t-t_1)$ must be added to find the effect of FORE. Because of the time-delay t_d, the effect of the impulse is not felt until $t > t_1 + t_d$, thus explaining the local maximum, which grows with the time delay, which in turn grows with k. Decrease of the time delay by postponing the fast change in L magnitude and phase, now at (1,000-3,000) to a higher frequency, would be very wasteful in terms of L bandwidth. Actually, it is found that a small increase of phase-margin by a few degrees, suffices to satisfy the overshoot limitation.

The second important phenomenon which does not agree with the second-order model, is the large undershoot in the step response of $L/(1+L)$ at large k, as in Fig. III.15 at $k=1000$. This is associated with the approximately horizontal character of $|L_1(j\omega)|$ (see Figs. III.13, III.14) in the range $\omega \sim (1500,3000)$. The frequency response of $|L_1/(1+L_1)|$ at $k=1000$, can be obtained by shifting the zero db line to -60 db in Figs. III.13, III.14 and is shown in Fig. III.14. Besides the principal peak at M_1, there is a minor peak (or almost horizontal segment) at M_2. It has been noted [S2] that

the inverse transform of $L_1/(1+L_1)$ can be approximately and qualitatively predicted from a sketch of $|L_1(j\omega)/(1+L_1(j\omega)|$ vs ω, by reflecting the latter about the vertical axis. The shape of $\left|\frac{L_1}{1+L_1}\right|$ at M_2 predicts an increase in the slope of the inverse transform followed by a decrease, as compared with the time response if M_2 was not present. This prediction is borne out in Fig. III.16b, which gives the derivatives (impulse responses) of the two curves in

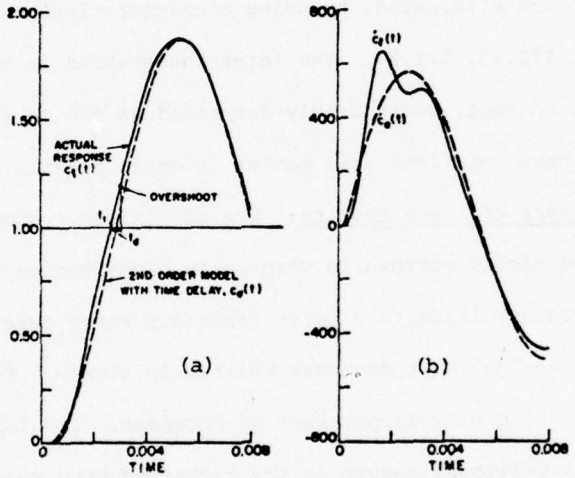

Figure III.16. The two significant phenomena of Part 2 of design.

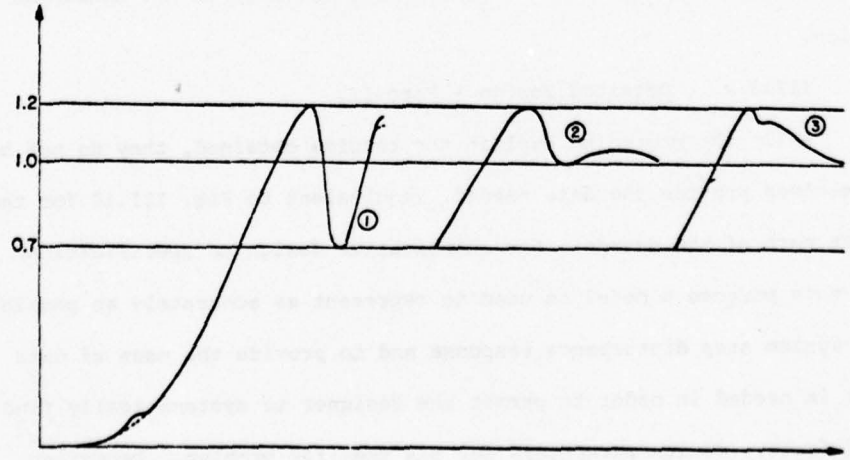

Figure III.17. Comparison of the three different designs system step responses at $k = 1000$.

Fig. III.16a. M_2 has a minor effect on the step responses in Fig. III.16a, but a major effect on their derivatives in Fig. III.16.b. The larger peaking in the impulse response (due to M_2), gives the undershoot observed in Fig. III.15 at k=1000. If one uses these impulse response curves together with Eq.(3.1), it is found that the nonlinear step response obtained is precisely as predicted by Eq.(3.1).

The above explanation suggests that the minor peak M_2 in Fig. III.14 should be eliminated, by using a characteristic such as L_2 or L_3 in Figs. III.13, III.14. The larger undershoot in the step response was thereby, in fact, considerably decreased as can be seen on Fig. III.17. We have gone into this matter in great detail, <u>because of the universal nature of these results</u>: Use of nonlinear compensation is justified and highly worthwhile when large high-frequency plant gain factor uncertainty leads to a large frequency range over which $|L(j\omega)|$ (in a linear design) must decrease relatively slowly. Nonlinear design permits a significantly larger rate of decrease. The loop characteristics have a universal nature in the high-frequency region, so it is important to thoroughly understand their properties in the nonlinear design.

III.3.e. <u>Detailed Design - Part II</u>.

While the preceding explain the results obtained, they do not by themselves provide the data needed, (equivalent to Fig. III.10 for the first part of the design), for quantitative design to specifications. For this purpose a model is used to represent as accurately as possible the system step disturbance response and to provide the mass of data that is needed in order to permit the designer to systematically find satisfactory design parameters for his specific problem. Depending

upon the nature (odd or even) of the excess of poles over zero e_L, use can then be made of:

$$(3.12)\quad L_A(s) = \begin{cases} \dfrac{(s+z)}{s^2(s^2+2\zeta_\ell\omega_\ell s+\omega_\ell^2)^{2n}} \quad \theta \quad \dfrac{\omega_\ell^{4n}}{z} & \text{if } e_L \text{ is odd} \\ \dfrac{(s+z)}{s^2(s+\omega_\ell)(s^2+2\zeta_\ell\omega_\ell s+\omega_\ell^2)^{2n}} \quad \theta \quad \dfrac{\omega_\ell^{4n+1}}{z} & \text{if } e_L \text{ is even.} \end{cases}$$

θ being such that $\theta = \omega_{cmax}^2$ where ω_{cmax} is the crossover frequency of the $L_{eq}(s)$ which corresponds to $k = k_{max}$.

In this 'part II' frequency range, it suffices to obtain a satisfactory design at $k = k_{max}$, corresponding to the zero db line shifted downward by 60 dbs (Fig. III.13, III.14). This is because the two phenomena previously noted have their maximum effects at k_{max}.

It is upto the designer to make sure that his actual $L_{eq}(s)$ (at $k = k_{max}$) approximates $L_A(s)$ quite closely for a decade or so on each side of the crossover frequency ω_{cmax}. If this is not so, the model $L_A(s)$ should be changed accordingly. Without loss of generality, following [H2] we select $e_L = 5$, i.e. $n = 2$. From Fig. III.13, $\theta = (\omega_{cmax})^2 \approx 32.10^4$. The design parameters are presented in Tables III.1, III.2. (1) The C_i parameter is related to the peaking in L, i.e. as i changes from 1 to 4, the nature of L changes in the manner in Fig. III.14 for L_j, j = 1 to 3. (2) G_m is the gain margin of L_i at $k = k_{max}$. (3) φ is the phase margin at the point at which Arg L_i begins to rapidly decrease. There are three data values given for each combination of the above parameters. These are (a) OV, being the first peak overshoot value as well as the second and third, when the latter two are also significant (b) UN, the first peak undershoot

Table III.1.

	C_1	C_2	C_3	C_4
	G_m = 10 dB, ϕ = 2.5°			
OV	40,77,90	30,44	29,32	27
UN	62,66,70	42	29	20
GF	0.39	0.68	1.04	1.6
	G_m = 12 dB, ϕ = 2.5°			
OV	23,48,50	25,33	23,24	24
UN	42,35	28	22	8
GF	0.65	1.07	1.55	2.2
	G_m = 14 dB, ϕ = 2.5°			
OV	26,42,38	26,27	24	18
UN	26	18	12.5	3.5
GF	1.06	1.80	3.17	9.20
	G_m = 10 dB, ϕ = 5°			
OV	28,64,79	35,57,58	31,38	30
UN	61,61,62	52	42	22
GF	0.68	0.72	1.02	2.00
	G_m = 12 dB, ϕ = 5°			
OV	18,43,46	22,37	27,28	21
UN	40	38	28	13
GF	1.07	1.16	1.60	4.80
	G_m = 14 dB, ϕ = 5°			
OV	26,40	21,28	21	20
UN	28	28	21	4
GF	1.67	2.00	2.92	12.3
	G_m = 10 dB, ϕ = 10°			
OV	15,39,44	27,36	26	
UN	43,34	50	20	
GF	2.12	1.63	4.61	
	G_m = 12 dB, ϕ = 10°			
OV	15,33,33	22,22	19	
UN	40	34	14	
GF	2.38	2.72	10.4	
	G_m = 14 dB, ϕ = 10°			
OV	20,29	17	13	
UN	37	30	10	
GF	5.01	4.74	28.8	

as well as the second and third when significant (c) GF, the normalized high frequency gain factor of $L_{eq}(j\omega)$. (Multiplication by θ gives the real gain.) The smaller GF , the more economical is the design.

It is necesssary to relate the design parameters of Table III.1 to design numbers, e.g. poles and zeros of L_A which correspond to any entry in Table III.1. This information is available from Table III.2 which relates the entries and parameters of Table III.1 to those of the loop transmission of (3.12).

For our design example let us assume that in addition to 20% overshoot, (design L_1), a maximum of 30% undershoot is tolerable, in the system step-disturbance response. Using Table III.1, a phase margin $\varphi = 2.5°$ is then first considered. A satisfactory design can be obtained with the combination C_4 and $G_m = 14$ db , however there is an overdesign with respect to undershoot specifications. At $\varphi = 5°$, it is seen that the combination C_3 with $G_m = 14$ db slightly violates the overshoot specification, but the undershoot is here too only 21% < 30% max. The last design is certainly more economic because its GF $=3.10^{16}$, compared to 9.10^{16} at $\varphi = 2.5°$. If $\varphi = 10°$, it is seen that combination C_3 for $G_m = 12$ db , is almost satisfactory. It corresponds (Table III.2) to the parameters $\zeta_\ell = .29$, $z = 1500$, $\omega_\ell^2 = 1.13\ 10^7$. By cut and try it is found that the design L_1 for which $\zeta_\ell = .29$, $z = 1750$, $\omega_\ell^2 = 1.15\ 10^7$ satisfies exactly the specifications, as shown on Fig. III.17, (curve 1).

If only a very small undershoot ($\simeq$0%) (design L_2) is tolerable, it can be found, following the same procedure, that the best design lies around combination C_4 , with $\varphi = 2.5°$ and $G_m = 14$ db , corresponding to

$\zeta_\ell = .50$, $\omega_\ell^2 = 2.4\ 10^7$ and $z = 2000$. By cut and try the design L_2 is then obtained with $\zeta_\ell = .53$, $\omega_\ell^2 = 2.25\ 10^7$, $z = 1750$ for which the step disturbance response satisfy 20% overshoot and 0% undershoot specifications, as can be seen in Fig. III.17. If we want an L_3 design for which the step disturbance response is similar to the one shown in Fig. III.17, the same procedure gives $\zeta_\ell = .65$, $\omega_\ell^2 = 2.5\ 10^7$, $z = 1750$.

The three different designs that were obtained (Fig. III.13, III.14) are:

$$L_i(s) = \frac{k(s+.905)(s+.92)(s+17.)(s+17.3)(s+26.1)(s+200)(s+1750)}{s(s+512)(s+5.28)(s+6.09)(s+23)(s+37.8)(s+50)(s+130)(s^2+2\zeta_\ell\omega_\ell s+\omega_\ell^2)^2}$$

with:

$k = 2.42\ 10^{13}$, $\omega_\ell^2 = 11.5\ 10^6$, $2\zeta_\ell\omega_\ell = 1950$ when $i = 1$

$k = 9.2\ 10^{13}$, $\omega_\ell^2 = 22.5\ 10^6$, $2\zeta_\ell\omega_\ell = 5000$ when $i = 2$

$k = 11.4\ 10^{13}$, $\omega_\ell^2 = 25.\ 10^6$, $2\zeta_\ell\omega_\ell = 6500$ when $i = 3$

The prefilter for all three designs is, not unexpectedly, the same as the one used in the linear time invariant design (see II.2 for details).

III.4. Design results.

The responses to command inputs for different plant parameter combinations are shown in Fig. III.18 for the nonlinear design. Not unexpectedly, these hardly differ from those obtained in the L.T.I. design (see [H2, S2]). Recalling II.2, let $F(s) = \frac{\alpha}{s+\alpha}$, $\alpha = 3$ rps as a crude approximation. Using a delayed second order approximation (Appendix A1) for the closed loop, we get (Fig. III.7):

$$C_\ell(s) = \frac{\omega_n^2\ e^{-st_d}}{s^2+2\zeta\omega_n s+\omega_n^2}\ \frac{\alpha}{s(s+\alpha)}$$ when the command is a unit step.

Table III.2.

	C_1	C_2	C_3	C_4
	G_m = 10 dB, ϕ =2.5°			
$z10^{-3}$	:4	3	2.5	2.0
$2^{\zeta_\ell - 7}$	:0.11	0.175	0.23	0.315
$\omega_\ell 10$	:0.7	0.8	0.9	1.0
	G_m = 12 dB, ϕ =2.5°			
$z10^{-3}$	:4	3	2.5	2
$2^{\zeta_\ell - 7}$	:0.125	0.195	0.255	0.398
$\omega_\ell 10$	:0.9	1.0	1.1	1.55
	G_m = 14 dB, ϕ =2.5°			
$z10^{-3}$	:4	3	2.5	2
$2^{\zeta_\ell - 7}$	:0.14	0.222	0.308	0.50
$\omega_\ell 10$	:1.75	1.3	1.57	2.4
	G_m = 10 dB, ϕ =5°			
$z10^{-3}$	:3	2.5	2.0	1.5
$2^{\zeta_\ell - 7}$	:0.12	0.165	0.23	0.37
$\omega_\ell 10$	:0.8	0.75	0.8	0.97
	G_m = 12 dB, ϕ =5°			
$z10^{-3}$	:3	2.5	2.0	1.5
$2^{\zeta_\ell - 7}$	:0.14	0.185	0.26	0.462
$\omega_\ell 10$	:1.0	0.95	1.0	1.5
	G_m = 14 dB, ϕ =5°			
$z10^{-3}$	:3.0	2.5	2.0	1.5
$2^{\zeta_\ell - 7}$	:0.155	0.21	0.3	0.59
$\omega_\ell 10$	:1.25	1.25	1.35	2.4
	G_m = 10 dB, ϕ = 10°			
$z10^{-3}$	:2.0	1.5	1.0	
$2^{\zeta_\ell - 7}$	:0.16	0.25	0.53	
$\omega_\ell 10$	:1.15	0.875	1.2	
	G_m = 12 dB, ϕ =10°			
$z10^{-3}$	:2.0	1.5	1.0	
$2^{\zeta_\ell - 7}$	:0.185	0.29	0.65	
$\omega_\ell 10$	:1.22	1.13	1.8	
	G_m = 14 dB, ϕ =10°			
$z10^{-3}$	:2.0	1.5	1.0	
$2^{\zeta_\ell - 7}$	:0.195	0.325	0.835	
$\omega_\ell 10$	:0.77	1.49	3.0	

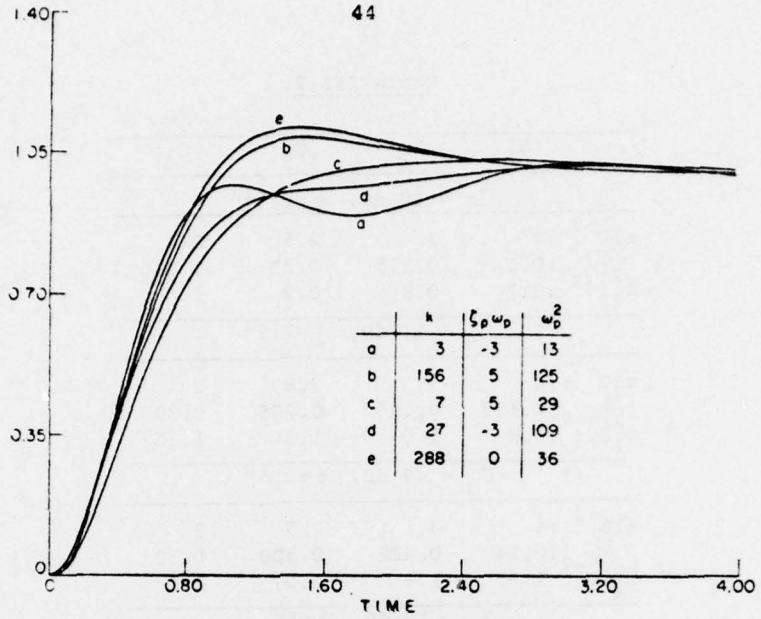

	k	$\zeta_p\omega_p$	ω_p^2
a	3	-3	13
b	156	5	125
c	7	5	29
d	27	-3	109
e	288	0	36

Figure III.18. Response to command step inputs.

Let $t \triangleq \text{TIME} - t_d$, then for $t > 0$,

$$C_\ell(t) = 1 - \frac{\omega_n^2}{\alpha^2 - 2\alpha\zeta\omega_n + \omega_n^2} e^{-\alpha t} + \frac{\alpha}{\sqrt{1-\zeta^2}} \frac{1}{\sqrt{\alpha^2 - 2\alpha\zeta\omega_n + \omega_n^2}} e^{-\zeta\omega_n t} \sin(\omega_n\sqrt{1-\zeta^2}\, t + \theta) \qquad (3.12a)$$

with θ such that $C_\ell(0) = 0$.

At gain factors $k \geq 50$ we have $\omega_n > 100$ rd/s (Fig. III.13) and $\zeta < .15$ (Appendix A1). As $\omega_n >> \alpha$,

$$C_\ell(t) \approx 1 - e^{-\alpha t} - \frac{\alpha}{\omega_n\sqrt{1-\zeta^2}} e^{-\zeta\omega_n t} \sin(\omega_n\sqrt{1-\zeta^2}\, t) \qquad (3.13)$$

because $\theta \approx \pi$ in this case, and for $0 < t < t_1$, the input to FORE is then:

$x(t) \approx \frac{\alpha}{\omega_n\sqrt{1-\zeta^2}} e^{-\zeta\omega_n t} \sin(\omega_n\sqrt{1-\zeta^2}\, t)$. Therefore, (1) $x(t)$ is very small and (2) the zero crossings are practically determined by the feedback loop, i.e., $T \approx \pi/\omega_n\sqrt{1-\zeta^2}$. Therefore, the first reset value is $x_1^* \approx \frac{\alpha}{\omega_n\sqrt{1-\zeta^2}} \int_0^T \sin(\omega_n\sqrt{1-\zeta^2}\, t)\, dt = \frac{2\alpha}{\omega_n^2(1-\zeta^2)}$ and (Fig. III.8

for $t_1 < t < t_2$,

$$C_T(t) = -x_1^* \dot{C}_\ell(t-t_1) = -\frac{2\alpha}{\omega_n\sqrt{1-\zeta^2}} \frac{1}{(1-\zeta^2)} e^{-\zeta\omega_n(t-t_1)} \sin(\omega_n\sqrt{1-\zeta^2}(t-t_1))$$

$$= \frac{2\alpha}{\omega_n(1-\zeta^2)^{3/2}} e^{-\zeta\omega_n(t-t_1)} \sin(\omega_n\sqrt{1-\zeta^2}t) \quad .$$

Therefore, the nonlinear system response is, for $t_1 < t < t_2$:

$C_{NL}(t) \approx 1-e^{-\alpha t} + \frac{\alpha}{\omega_n} \sin(\omega_n\sqrt{1-\zeta^2}t)$ (3.14) because ζ is very small. Noting now that $x_K^* \approx x_1^*$ for $K = 2,3,\ldots,$ it is seen that the nonlinear system response is $C_{NL}(t) \approx 1-e^{-\alpha t}$ for t not too small, i.e., when α/ω_n can be neglected in comparison of $1-e^{-\alpha t}$. For instance at $k = 1000$, $\omega_n \approx 600$ rps and $\alpha/\omega_n \approx 1/200$. Therefore when $t > .04$ seconds (compared to a settling time of approximately 1 second), $1-e^{-\alpha t} > .1 = 20\ \alpha/\omega_n$ and the sinusoidal component can be neglected. However for small t ($< .04$ seconds) this is not true and the nonlinear and linear system responses differ one from another. Fortunately, this cannot be noticed because all the quantities involved are then very small.

For intermediate values of the gain factor $(5 \leq k \leq 100)$ we have 30 rps $< \omega_n <$ 100 rps and $.5 < b/\omega_n < 1.66$ giving (Fig. III.5) at most a reset value of 30% of the reset value obtained with a C.I. in place of FORE, which can once more be neglected because here too $\omega_n >> \alpha$.

For small gain factors $(k < 5)$ the linear system is similar to the nonlinear one because $\omega_n <$ 30 rps and therefore $b/\omega_n > 2$ giving (Fig. III.5) a reset value which is very small ($< 5\%$) and can therefore be neglected.

Assume now that a command input is applied whose bandwidth is smaller than the bandwidth of the prefilter. At small gain factors giving $b/\omega_n > 2$ the reset value (< 5% of the C.I. reset (Fig.III.5)) can certainly be neglected. At large gain factors giving bandwidth of loop >> bandwidth of prefilter, we have by anology with (3.12a) and (3.13) $C_\ell(t) \approx$ command input + $A \sin(\omega_n\sqrt{1-\zeta^2}t + \vartheta)$ where the residue A is $\doteq 2 \left| \frac{F(j\omega_n)\ R(j\omega_n)}{2j\omega_n} \right|$. Therefore A is very small as before, and the arguments made previously are easily extended here.

At intermediate gain values, it might happen for some problems that the corresponding range ω_n is not big enough compared to the bandwidth of the prefilter, preventing us therefore from making general statements. However, for these problems (as in the present case) where ω_n >> bandwidth of the prefilter, even in the intermediate range of plant gain factor values, the previous assertions can be extended.

We can therefore conclude that the superposition theorem holds effectively, at all gain factors for command inputs, provided that the bandwidth of the command signal ≤ bandwidth of the prefilter. It is probably unlikely, in most cases, that the system will be subjected to command inputs whose bandwidth exceeds 3 times the bandwidth ω_f of the prefilter, (here $3\ \omega_f \approx 10$ rps) because the amplitude of the command signals at the output of the prefilter would then be very small (< 1/10 of the input command amplitude in the present case because (see II.2) $|F(j10)| \approx .1$) .

The step disturbance responses are shown on Fig. III.19.a & b at different plant parameter values for the L.T.I. design and in Fig. III. 20. a - c for all N.L. designs.

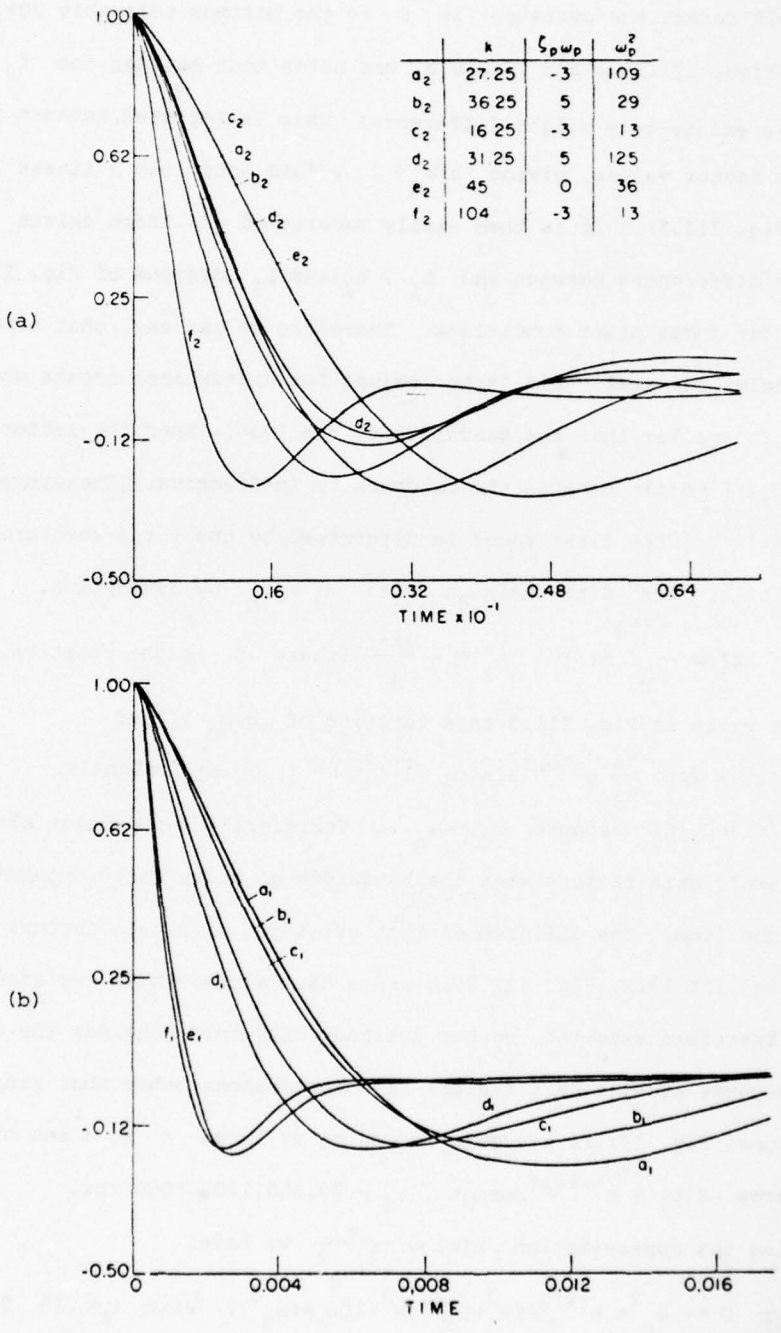

	k	$\zeta_p \omega_p$	ω_p^2
a_2	27.25	-3	109
b_2	36 25	5	29
c_2	16 25	-3	13
d_2	31 25	5	125
e_2	45	0	36
f_2	104	-3	13

Figure III.19. Response to step disturbance (linear design).

In all cases, the overshoot is $\leq$ to the maximum tolerable 20%. Comparing Figs. III.19.a and III.20.a, one notes that besides the f_2 case, there exists only slight differences. This is expected because for small gain factor values, giving $b/\omega_n > 2$, FORE acts like a linear element (Fig. III.5). It is then easily understood why there exists only minor differences between the L_1, L_2 and L_3 designs of Fig. III. 13 and 14 for those plant conditions. Therefore we can say, that superposition holds for small gain factor values for disturbance inputs whose bandwidth is smaller than the bandwidth of the loop. When the latter is untrue, $C_\ell(t) \approx d(t)$ because the feedback is ineffective. Therefore $x(t) \approx -d(t)$ and the first reset is determined by the first zero crossing of $d(t)$. Let $d(t) = A\sin\omega_d t$ with $\omega_d >> \omega_n$ by assumption. Therefore: $x_1^* \approx -\int_0^{\pi/\omega_d} d(\zeta)d\zeta \quad \eta \approx -\frac{2A\eta}{\omega_d}$ (where η is the reset value percentage given in Fig. III.5 as a function of b/ω_n), and $C_{NL}(t) \approx d(t) + 2A\eta \frac{\omega_n}{\omega_d} e^{-\zeta\omega_n t}\sin(\omega_n\sqrt{1-\zeta^2}t + \theta)$, or equivalently, $C_{NL}(t) \approx d(t) \approx C_\ell(t)$ because $\omega_d >> \omega_n$. Therefore superposition also holds at small gain factors when the bandwidth of disturbance >> bandwidth of the loop. The differences that exist for high gain factors between Fig. III.13.b, Fig. III.20.b and c have already been explained, and were therefore expected, so the designer need only consider the nonlinear response at high gain factors for disturbances other than steps. For instance, Fig. III.21 presents responses at large k to a set of disturbances $d(t) = e^{-.1\omega_d t}\cos\omega_d t$, ω_d = 30,300,1200,6000 rps.

Using the approximation $D(s) \approx \frac{s}{s^2+\omega_d^2}$ we have:
$Q(s) \triangleq \frac{L}{1+L} \quad D \approx -\omega_n^2 s\, e^{-st_d}/((s^2+\omega_d^2)(s^2+2\zeta\omega_n s+\omega_n^2))$ with $\zeta < .15$ for high gain factors as mentioned above. Therefore: ($t \triangleq$ TIME - t_d)

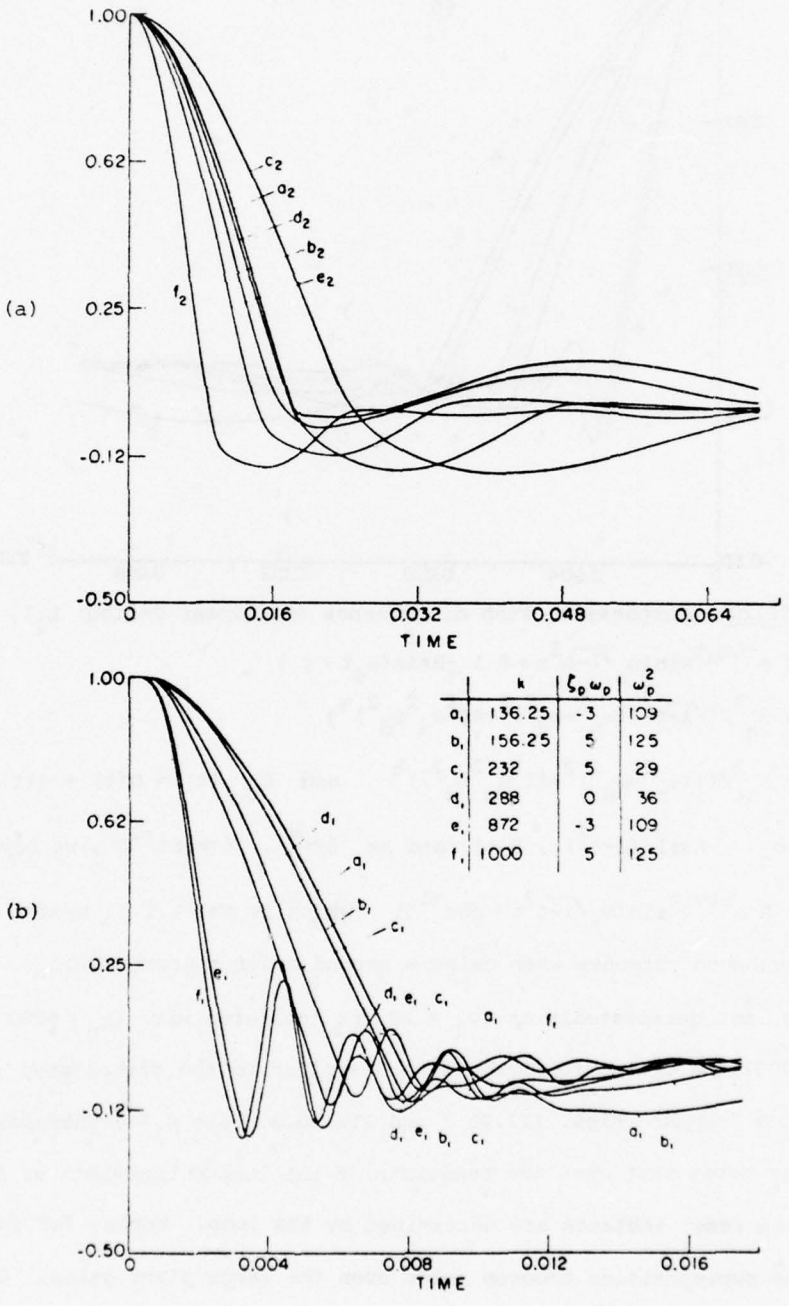

	k	$\zeta_p \omega_p$	ω_p^2
a_1	136.25	-3	109
b_1	156.25	5	125
c_1	232	5	29
d_1	288	0	36
e_1	872	-3	109
f_1	1000	5	125

Figure III.20. Response to step disturbance (nonlinear design L_1).

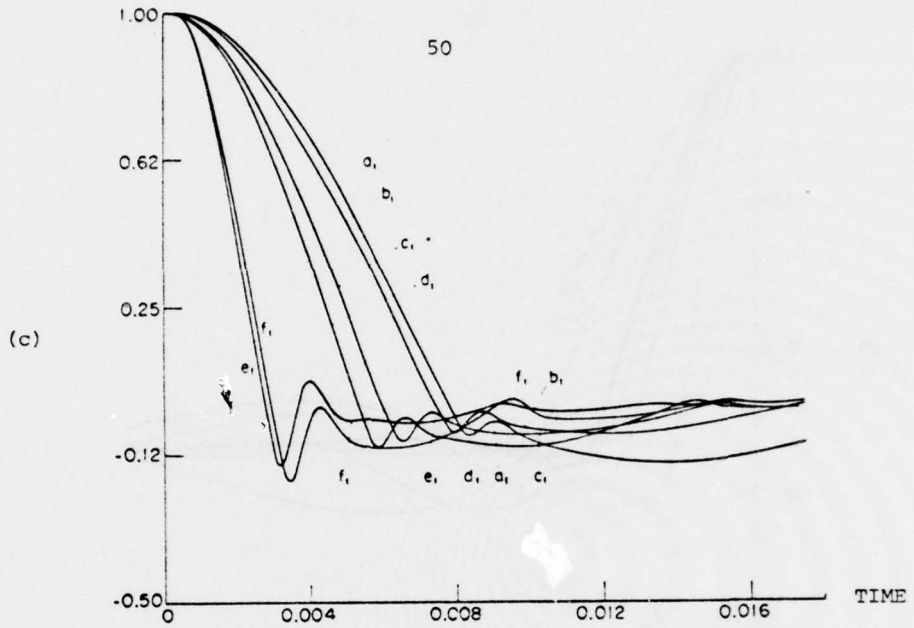

Figure III.20. Response to step disturbance (nonlinear design L_2).

$q(t) = +A\, e^{-\zeta\omega_n t}\sin(\omega_n\sqrt{1-\zeta^2}\,t + \theta) - B\sin(\omega_d t + \beta)$

with $A = \omega_n^2/(\sqrt{1-\zeta^2}((\omega_n^2-\omega_d^2)^2+4\zeta^2\omega_n^2\omega_d^2)^{\frac{1}{2}})$

$B = \omega_n^2/(((\omega_n^2-\omega_d^2)^2+4\zeta^2\omega_n^2\omega_d^2))^{\frac{1}{2}}$ and $C_{D,\ell}(t) = D(t) + q(t)$.

If $\omega_d << \omega_n$ $A \approx 1/(1-\zeta^2)$, $B \approx 1$ and as $\beta \approx \frac{\pi}{2}$, $\theta \approx \cos^{-1}\zeta$, we have:

$C_{D,\ell}(t) = A\, e^{-\zeta\omega_n t}\sin(\omega_n\sqrt{1-\zeta^2}\,t + \cos^{-1}\zeta)$ which is the L.T.I. system step disturbance response when using a second order approximation. Therefore, not unexpectedly at ω_d = 30 rps (compared with ω_n = 6000 rps at k = 1000) the system response is very similar to the system step disturbance (compare Figs. III.21.d and III.20.b, case f_1). Therefore the reader notes that when the bandwidth of the loop >> bandwidth of disturbance the reset instants are determined by the loop. Hence, for such inputs the superposition theorem holds even for large plant gains. Of course, the disturbance attenuation capability decreases as ω_d increases, as is seen in Fig. III.21.b - c. If ω_d = 6000 rps >> ω_n

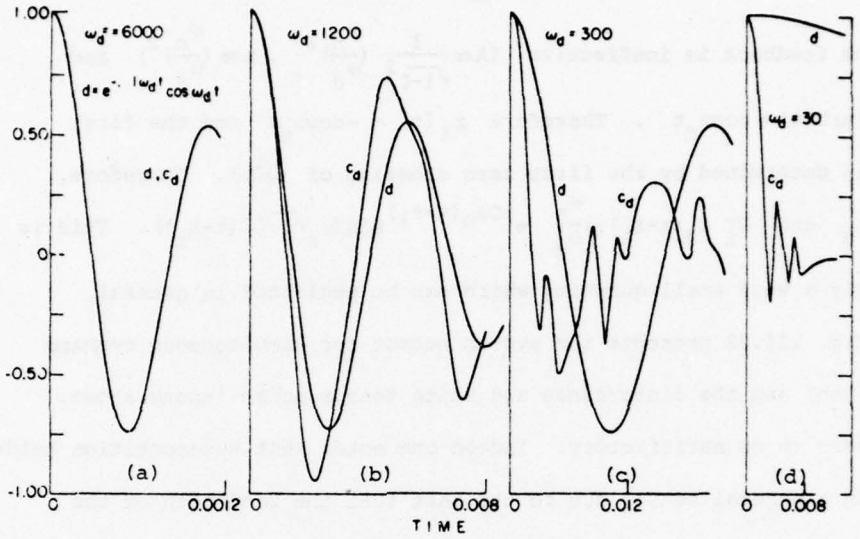

Figure III.21. Nonlinear design; response to $d(t)=\exp(-.1\omega_d t)\cos\omega_d t$ at $k = 10^3$.

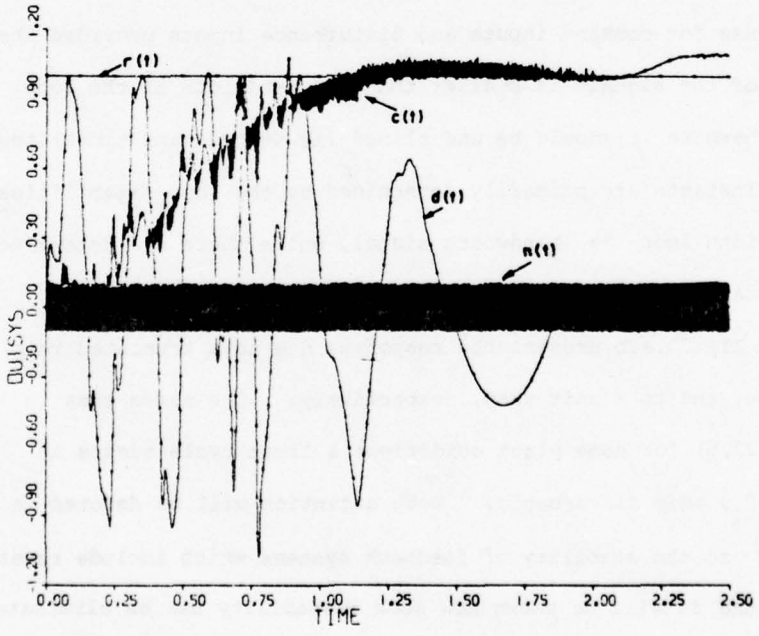

Figure III.22. Nonlinear design; response to simultaneous command, disturbances and sensor noise inputs at $k = 10^3$.

then the feedback is ineffective $(A \approx \frac{1}{\sqrt{1-\zeta^2}} (\frac{\omega_n}{\omega_d})^2$, $B \approx (\frac{\omega_n}{\omega_d})^2)$ and $C_{D,\ell}(t) \approx D(t) = \cos\omega_d t$. Therefore $x_\ell(t) = -\cos\omega_d t$ and the first reset is determined by the first zero crossing of $D(t)$. Therefore, $x_1^* \approx 2/\omega_d$ and $x_1^* \dot{C}_\ell(t-t_1) \approx \frac{\omega_n}{\omega_d} e^{-\zeta\omega_n(t-t_1)} \sin(\omega_n\sqrt{1-\zeta^2}(t-t_1))$. This is obviously a very small quantity which can be neglected in general.

Fig. III.22 presents the system output for simultaneous command (unit step) and the disturbance and white sensor noise inputs shown. It is seen to be satisfactory. Indeed one notes that superposition holds here, in a general sense, due to the fact that the bandwidth of the disturbance signal << bandwidth of the loop.

In summary we can say that the superposition theorem holds in a general sense for command inputs and disturbance inputs provided the bandwidth of the signals is smaller than the bandwidth of the loop.

Furthermore it should be underlined (as stated many times) that the reset instants are primarily determined by the loop capabilities when bandwidth loop >> bandwidth signal, while there are determined by the signal (command or disturbance) when the converse is true.

Fig. III.23.a,b present the responses due to a truncated ramp disturbance, and to a unit ramp, respectively. One notes that (Fig. III.23.b) for some plant conditions a limit cycle occurs in presence of a ramp disturbance. Much attention will be devoted in chapter IV to the stability of feedback systems which include reset elements, and it will be shown how such instability can be eliminated.

15 (a)

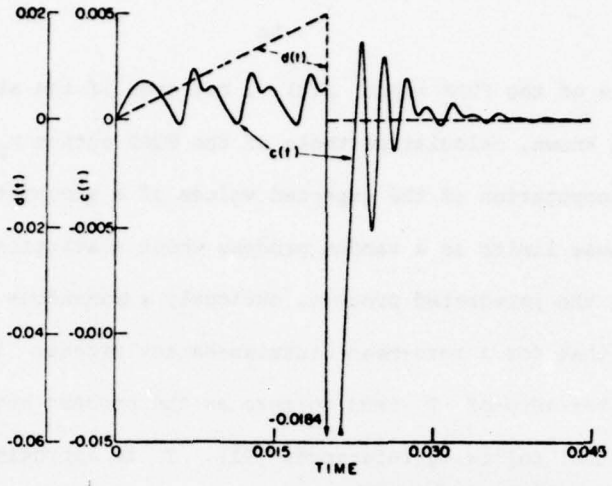

(b)

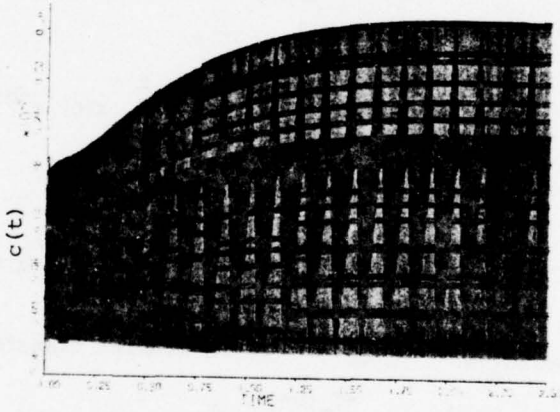

Figure III.23. Nonlinear design; response to a truncated ramp (a) disturbance and to a ramp disturbance (b) at $k = 10^3$.

III.5. Noise Response of FORE.

III.5a. Open Loop Characterization.

If in the input x to FORE, the forced component due to r(t) is large compared to a random component n and/or d in Fig. III.7 such that the zero crossings are primarily determined by the former, then FORE behaves as a linear element 1/(s+b) to the latter signal component. The case now considered is when a random stationary zero mean process is the only input to FORE, which implies that the interval of time T(t) between reset instants is also a stationary random process. In principle, the statistics of T(t) may be determined

from those of the FORE input $x(t)$, but even if the statistics of $T(t)$ are known, calculating those of the FORE output $y_f(t)$ would require computation of the expected values of a stochastic integral, one of whose limits is a random process whose statistics, in turn, depend on the integrated process, obviously a tremendous task. Using the fact that for a zero-mean Gaussian-Markov process $x(t)$, the mean and variance of T tend to zero as the process becomes more uncorrelated, following references [P1], T is approximated by its mean value T_m giving:

$$y_f(t) = \int_{t-T(t)}^{t} x(\zeta)\, e^{-b(t-\zeta)} d\zeta \approx \int_{t-T_m}^{t} x(\zeta)\, e^{-b(t-\zeta)} d\zeta \quad .$$

The cross-correlation of $x(t)$ and $y(t)$ is

$$\varphi_{yx}(\tau) = E\{y_f(t+\tau)x(t)\} = E\{ \int_{t+\tau-T_m}^{t+\tau} x(\zeta) e^{-b(t+\tau-\zeta)} x(t) d\zeta \}$$

$$= \int_0^{T_m} \phi_{xx}(p+\tau-T_m) e^{b(p-T_m)} dp \quad . \text{ Taking Fourier Transform gives [G1]}$$

$$\Phi_{yx}(\omega) = \Phi_{xx}(\omega) \frac{1}{b+j\omega} (1-e^{-T_m(b+j\omega)}) \triangleq \Phi_{xx}(\omega) N(\omega, T_m)$$

The normalized random-input describing function is therefore

$$N_n(\omega, T_m) = \frac{N(\omega, T_m)}{[1/(b+j\omega)]} = 1-e^{-T_m(b+j\omega)} \qquad (3.15)$$

so that $|N_n| > 1$ over some ω and <1 over others.

If the input x to FORE is a stationary white noise process of power spectrum $\Phi_{xx}(\omega) = \sigma_N^2$, then the root mean square value of the noise output y_f is given by:

$$(y_f)_{rms} = \left[\frac{1}{2\pi} \int_{-\infty}^{+\infty} |N(\omega, T_m)|^2 \sigma_N^2 d\omega \right]^{\frac{1}{2}}$$

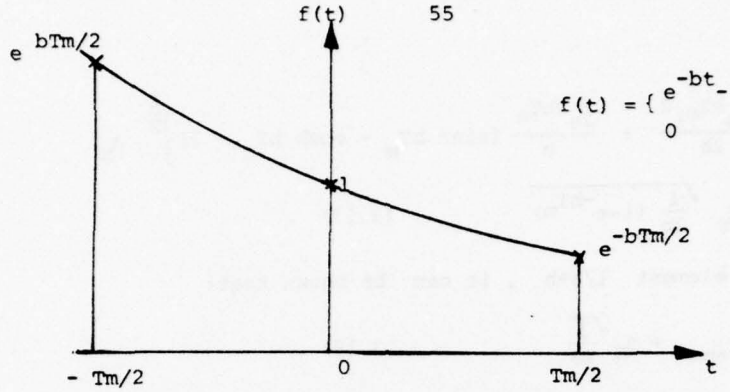

Figure III.24. Representation of the filter f(t) .

$$(y_f)_{rms} = \left[\frac{1}{2\pi} \int_{-\infty}^{+\infty} [(1+e^{-bT_m})^2 - 4\, e^{-bT_m} \cos^2 \frac{\omega T_m}{2}] \frac{1}{b^2+\omega^2}\, d\omega \right]^{\frac{1}{2}} \sigma_N$$

$$(y_f)_{rms} = \left[\frac{1}{2b} (1+e^{-bT_m})^2 - \frac{1}{2\pi} \int_{-\infty}^{+\infty} \frac{4}{b^2+\omega^2} e^{-bT_m} \cos^2 \frac{\omega T_m}{2}\, d\omega \right]^{\frac{1}{2}} \sigma_N \quad (3.16)$$

Let us consider the signal f(t) of Fig. III.24, we have

$$F(j\omega) = \frac{1}{s+b} (e^{(s+b)T_m/2} - e^{-(s+b)T_m/2}) = \frac{2}{s+b} \sinh(s+b) \frac{T_m}{2}$$

Using Paseval's relation: $\int_{-\infty}^{+\infty} f^2(t)dt = \frac{1}{2\pi} \int_{-\infty}^{+\infty} F(j\omega)\, F(-j\omega)d\omega$

$$= \frac{1}{2\pi} \int_{-\infty}^{+\infty} \frac{4}{\omega^2+b^2} \sinh(b-j\omega) \frac{T_m}{2} \sinh(b+j\omega) \frac{T_m}{2}\, d\omega$$

$$= \frac{1}{2\pi} \int_{-\infty}^{+\infty} \frac{4}{\omega^2+b^2} \left[\cosh^2 \frac{bT_m}{2} - \cos^2 \frac{\omega T_m}{2} \right] d\omega$$

$$= \frac{2}{b} \cosh \frac{bT_m}{2} - \frac{1}{2\pi} \int_{-\infty}^{+\infty} \frac{4a^2}{\omega^2+a^2} \cos^2 \frac{\omega T_m}{2}\, d\omega \quad (3.16a)$$

$$\text{But} \quad \int_{-\infty}^{+\infty} f^2(t)dt = \frac{e^{bT_m} - e^{-bT_m}}{2b} = \sinh \frac{bT_m}{b} \quad (3.16b)$$

Using (3.16a) and (3.16b) in (3.16) we get:

$$(y_f)_{rms} = \left[\frac{1}{2b} (1+e^{-bT_m})^2 + (\sinh bT_m - 2\cosh^2 \frac{bT_m}{2}) \frac{e^{-bT_m}}{b} \right] \sigma_N$$

and therefore:

$$(y_f)_{rms} = \left[\frac{(1+e^{-bT_m})^2}{2b} + \frac{2e^{-bT_m}}{b}(\sinh bT_m - \cosh bT_m - 1)\right]^{\frac{1}{2}} \sigma_N$$

$$\text{or} \quad (y_f)_{rms} = \sigma_N \sqrt{\frac{1}{2b}(1-e^{-bT_m})} \qquad (3.17)$$

For the linear element $1/s+b$, it can be shown that:

$$(y_{lin})_{rms} = \sigma_N \sqrt{\frac{1}{2b}} \quad . \qquad (3.18)$$

It can then be seen from Fig. III.25 that in this case the noise level at the output of FORE is always smaller than the noise level at the output of the linear element.

The theoretical results are in accordance with those obtained experimentally by controlling the interval between resets. It is noted that when $T_m b > 1$ by a factor of 3 or more, i.e. when the noise signal is relatively slow varying, then there is practically no difference between FORE and $1/s+b$. However, the difference becomes tremendous as $T_m b << 1$. Here too we can say that FORE can discriminate between fast-varying noise signals and slow-varying ones.

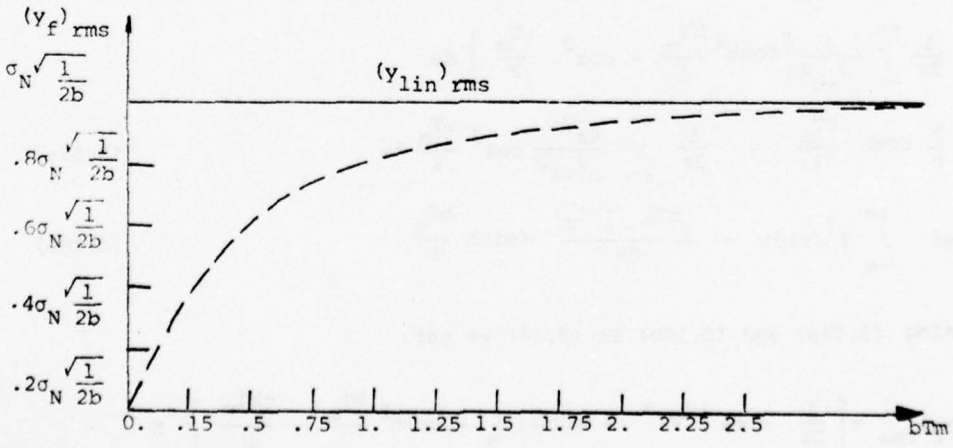

Figure III.25. R.M.S. values of the noise at the output of FORE & $1/s+b$ in the presence of white noise input.

III. 5b. Effect at the plant input (closed loop characterization).

The effect of white sensor noise, in the closed loop system, at the plant input Z is given by $\frac{\Phi_{zz}(\omega)}{\Phi_{nn}(\omega)} = \left|\frac{L/P}{1+L}\right|^2$ and the m.s. noise at z is $\sigma_z^2 = \int_{-\infty}^{\infty} \Phi_{zz}(\omega)\, \frac{d\omega}{2\pi}$, where the Φ are the power spectra. If $L = N_n(\omega, T_m) L_{eq}(s)$ of (3.15) is used, then at some T_m, the above becomes infinite, as shown in Fig. III.26. However, experimental determination of $\sigma_z^2(T_m)$ gave not unexpectedly finite results for all T_m, as shown in Fig. III.26. In this run T_m was controlled by having FORE reset determined externally at period T_m, rather than by the zero crossings of FORE.

When the actual nonlinear system was simulated, the experimental

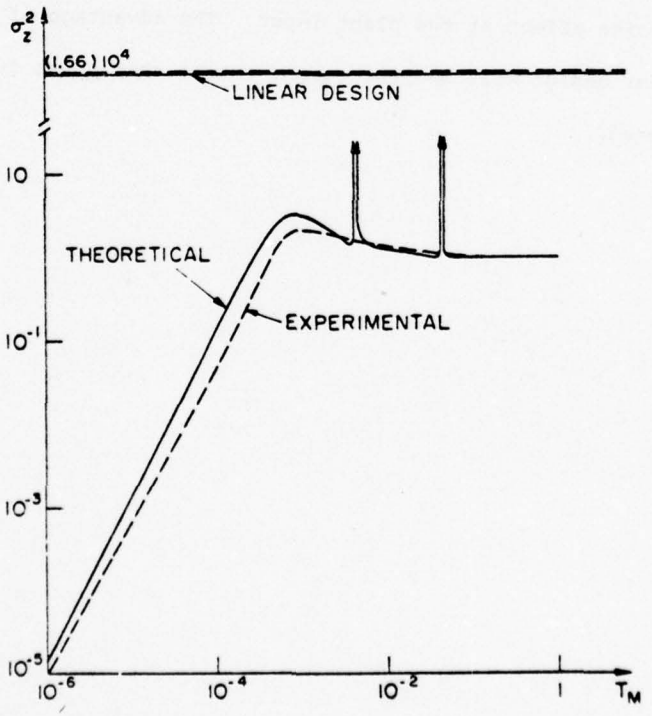

Figure III.26. Effect of sensor noise at plant input versus Tm at $k = 10^3$.

result was σ_z^2 (normalized) value of 0.37, corresponding to $T_m = (2.5)\ 10^{-4}$ sec. in Fig. III.26. The linear design of [H2] for the same problem resulted in σ_z^2 (normalized) = $(1.66)\ 10^4$, both theoretically and experimentally. Thus, the nonlinear design which achieves the same system output tolerances to command and disturbance inputs as the linear design, does so with rms sensor noise effect smaller by a factor of $\sqrt{0.37/(1.66)10^4} = .0047$. The improvement is very spectacular in this specific numerical example because of (1) the large uncertainty in the plant high-frequency gain factor k, which gave the nonlinear design a large freqency range in which to exploit its advantage of larger phase lag, and (2) the great difference between $|L|$ and $|P|$ in the high-frequency range, which leads to serious noise effect at the plant input. The advantage of nonlinear over linear design will be less to the extent that these two factors are lessened.

CHAPTER IV. STABILITY OF FEEDBACK SYSTEMS CONTAINING RESET ELEMENTS.

IV.1. Introduction.

General stability criteria are known for only a small class of nonlinear and time varying feedback systems. The circle criterion, for example, does not apply to the C.I., FORE or the more general reset elements. It was necessary therefore, to develop our own criteria for these elements.

In chapter III we implicitely restricted ourselves to stable open loop transfer function $L_{eq}(s)$ (Fig. IV.1.a) and will therefore derive sufficient conditions for Bounded Input Bounded Output stability of the nonlinear feedback system of Fig. IV.1.a. We will then investigate possible limit-cycles in the nonlinear feedback system of Fig IV.1.a. containing the element $(1/s+b)^*_\alpha$ whose output y is reset to zero whenever the input x equals the real value α ; $\alpha = 0$, $b \neq 0$ corresponding to FORE and $\alpha = 0$, $b = 0$ to C.I. Only stable limit-cycles with at most two reset instants per cycle will be considered. More general limit cycles can be considered, however todate, limit-cycles with more than 2 resets/cycle were never encountered experimentally.

Our primary objective will be to ensure stability when FORE is used, because of its usefulness, demonstrated in chapter III. In the following, intensive use of the z-transform is made with the usual notations $\cdot^*(s)$, $\cdot^*(\ )$, $z(\cdot)$. Note that x_K^* introduced in chapter III is a number. In this chapter, θ will denote the set of reset instants, i.e., $\theta = \{t_K \ni x(t_K) = \alpha\}$.

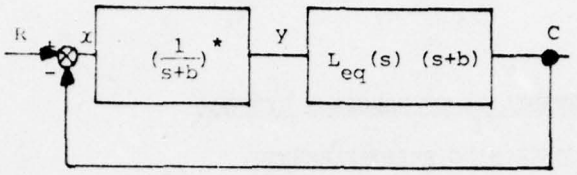

Figure IV.1.a. System Block Diagram.

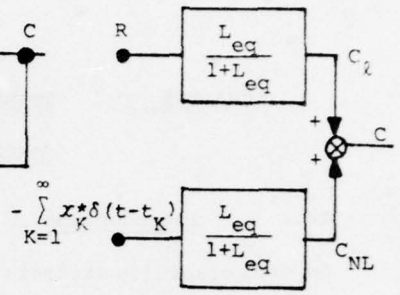

Figure IV.1.b. Equivalent representation.

IV.2. Bounded Input Bounded Output (B.I.B.O.) stability sufficient conditions for a class of nonlinear feedback systems.

Lemma 1: Consider the nonlinear feedback system of Fig. IV.1.a, where $L_{eq}(s)$ denotes the open loop transfer function of the L.T.I. system obtained in absence of resets. If the L.T.I. feedback system is asymptotically stable and if the sequence

$$\{|x_K^*| \triangleq \left| \int_{t_{K-1}}^{t_K} x(\zeta) e^{-b(t_K-\zeta)} d\zeta \right| ,\ t_{K-1}, t_K \in \theta\}$$ of the nonlinear system is bounded, then the nonlinear feedback system considered when resets occur is stable in the B.I.B.O. sense.

Proof: It was shown (equivalence of Fig. III.7 and III.8) that Fig. IV.1.a. is equivalent to Fig. IV.1.b.

Therefore $C(t) = C_\ell(t) + C_{NL}(t) = C_\ell(t) - \sum_{K=1}^{\infty} x_K^* C_\delta(t-t_K)$ (4.0),

where $C_\delta(t)$ denotes the L.T.I. system impulse response. By assumption the LTI system is asymptotically stable. So: $\forall t$, $\exists M_1, \alpha \in \mathbb{R}$ such that $|C_\delta(t)| \leq M_1 e^{-\alpha t}$ (A1) and (B.I.B.O. of the LTI design which follows from asymptotical stability) $\forall R$ such that $|R(t)| \leq M_r$ $\exists M$ such that $|C_\ell(t)| < M$ (A2) (see Fig. IV.1.b).

Let us first assume that the set θ of reset instants is finite, N.

Then, if $\mu \triangleq \sup_K |x_K^*|$ and using (A1) we have: for $t > t_N$

$$|C_{NL}(t)| = \left| \sum_{K=1}^{N} x_K^* \, C_\delta(t-t_K) \right| \leq \mu \sum_{K=1}^{N} |C_\delta(t-t_K)| \leq \mu \, N \, M_1 e^{-\alpha(t-t_N)} \quad .$$

Given $\varepsilon > 0$ arbitrarily small, $\exists\ t_\ell$ such that for $t > t_\ell$ $|C_{NL}(t)| < \varepsilon$ Using (4.0) and (A2), $|C(t)| \leq |C_\ell(t)| + |C_{NL}(t)| \leq M + \varepsilon$. Thus the lemma is proven if θ is finite.

Assume now that θ is infinite but countable. By assumption $\{|x_K^*|\}$ is bounded, so let $\mu \triangleq \sup_K |x_K^*|$. Let $\sigma_K \triangleq t_K - t_{K-1}$ with $t_K \in \theta$. $\forall K$, $0 < \sigma_K < \infty$, for if $\sigma_K = \infty$ for some K , θ would be finite, while if $\sigma_K = 0$ for some K , θ would not be countable. Therefore $\sigma \triangleq \inf_K \sigma_K > 0$. We have then:

$$|C_{NL}(t)| = \left| \sum_{K=1}^{\infty} x_K^* \, C_\delta(t-t_K) \right| \leq \mu \sum_{K=1}^{\infty} |C_\delta(t-t_K)|$$

$\forall t$, $\exists\ t_N$, $t_{N+1} \in \theta$ such that $t \in [t_N, t_{N+1}]$. Therefore $\forall K$, (using A1) $|C_\delta(t-t_K)| \leq M_1 e^{-\alpha(t-t_K)} = M_1 e^{-\alpha(t-t_N)} e^{-\alpha(t_N-t_K)}$.

However: $t_N - t_K = (t_N - t_{N-1}) + (t_{N-1} - t_{N-2}) + \ldots + (t_{K+1} - t_K) < (N-K)\,\sigma$

So: $|C_\delta(t-t_K)| \leq M_1 e^{-\alpha(t-t_N)} e^{-\alpha\sigma(N-K)}$. Therefore for $t_N < t < t_{N+1}$

$$|C_{NL}(t)| \leq \mu M_1 e^{-\alpha(t-t_N)} (1 + e^{-\alpha\sigma} + \ldots + e^{-\alpha(N-1)\sigma})$$

$$\leq \mu M_1 (1 + e^{-\alpha\sigma} + \ldots + e^{-\alpha(n-1)\sigma})$$

and as $N \to \infty$: $|C_{NL}(t)| \leq \mu M_1 (1 + e^{-\alpha\sigma} + e^{-2\alpha\sigma} + \ldots + e^{-K\alpha\sigma} + \ldots) = \dfrac{\mu M_1}{1 - e^{-\alpha\sigma}} < \infty$

Using then (4.0) and (A.2) $|C(t)| \leq M + \dfrac{\mu M_1}{1 - e^{-\alpha\sigma}} < \infty$ and B.I.B.O. Stability is therefore proven when θ is countable.

Assume now that θ is not countable. It means that there exists at least one instant $t_p \in \theta$ and that $t_p + \varepsilon \in \theta$ for arbitarily small $\varepsilon > 0$. In other terms, there exists at least one interval $\Omega_p \triangleq [t_p, t_p + \eta]$ $\eta > 0$, on which $x(t) \equiv 0$. By definition,

$$x_p^* = \int_{t_{p-1}}^{t_p} e^{-b(t_p - \zeta)} x(\zeta) \, d\zeta \quad \text{and therefore}$$

$x^*_{p+1} = \lim_{\varepsilon=0} \int_{t_p}^{t_p+\varepsilon} x(\zeta) e^{-b(t_p-\zeta)} d\zeta = 0$. The contribution to $C_{NL}(t)$ (Fig. IV.1.b) of the interval $]t_p, t_p+\eta]$ is therefore null and the contribution to $C_{NL}(t)$ of Q_p is therefore the same as a single reset occuring at time $t = t_p$. A new equivalent set $\hat{\theta}$ is then obtained by removing all the possible intervals Q_p from θ and by replacing them by the time instant t_p . Obviously $\hat{\theta}$ is countable if and only if $\{Q_p\}$ is countable. Given two intervals Q_s and Q_t we have: $Q_s \cap Q_t = \emptyset$ for all s , t and $\cup Q_i \subset \mathcal{R}$. Using the fact that between two real numbers there always exists a rational number, each Q_p is associated with one rational number. The rational numbers being countable, so is $\{Q_p\}$. The lemma being true for the countable set $\hat{\theta}$ we have proven the lemma for an uncountable set θ .

Lemma 1 rests on the assumption of a bounded sequence $\{|x_K^*|\}$. x_m^* and t_m are defined by the set of equations:

$$\begin{cases} x(t_m) = x_\ell(t_m) + \sum_{K=1}^{m-1} x_K^* \, C_\delta(t_m - t_k) = 0 \\ x_m^* = \int_{t_{m-1}}^{t_m} x_\ell(\zeta) e^{-b(t_m-\zeta)} d\zeta + \sum_{K=1}^{m-1} x_K^* \int_{t_{m-1}}^{t_m} e^{-b(t_m-\zeta)} C_\delta(\zeta - t_K) d\zeta \end{cases}$$

with $x_\ell(t) \triangleq R(t) - C_\ell(t)$. In absence of a rigorous proof we conjecture that $\{|x_K^*|\}$ is bounded if the LTI feedback system is asymptotically stable. It should be emphasized that once the above is rigorously established, fruitful results on stability will follow such as: a) generalization of lemma 1 to any reset element g* (defined in chapter V), because g* will be seen to be a finite combination of element $(1/s+b)^*$. b) asymptotic stability of the nonlinear feedback system.

IV.3. Investigation of limit cycles with one reset/cycle.

Sections IV.3,4 are exclusively devoted to such limit cycles, even when not explicitely so stated. Recalling (3.0a) the system of Fig, IV.2.a is described by:

$$y(t) = \int_{t_0}^{t} e^{-b(t-\zeta)} x(\zeta)d\zeta - \sum_{K=1}^{\infty} \left[\int_{t_{K-1}}^{t_K} e^{-b(t-\zeta)} x(\zeta)d\zeta \right] u(t-t_K) \quad (4.1)$$

with $t_K \in \theta = \{t_K : x(t_K) = \alpha\}$

Equivalently:

$$y(t) = \int_{t_0}^{t} e^{-b(t-\zeta)} x(\zeta)d\zeta - \sum_{k=1}^{\infty} \left[\int_{t_0}^{t_K} e^{-b(t-\zeta)} x(\zeta)d\zeta \right] u(t-t_K)$$

$$+ \sum_{K=1}^{\infty} \left[\int_{t_0}^{t_{K-1}} e^{-b(t-\zeta)} x(\zeta)d\zeta \right] u(t-t_K) \quad (4.2)$$

$$y(t) = \int_{t_0}^{t} e^{-b(t-\zeta)} x(\zeta)d\zeta - \sum_{K=1}^{\infty} \left[\int_{t_0}^{t_K} e^{-b(t-\zeta)} x(\zeta)d\zeta \right] \left[u(t-t_K) - u(t-t_{K+1}) \right] \quad (4.3)$$

$$y(t) = \int_{t_0}^{t} e^{-b(t-\zeta)} x(\zeta)d\zeta - \sum_{K=1}^{\infty} e^{-b(t-t_K)} \int_{t_0}^{t_K} e^{-b(t_K-\zeta)} x(\zeta)d\zeta \left[u(t-t_K) - u(t-t_{K+1}) \right] \quad (4.4)$$

Let $y_\ell(t_K) \triangleq \int_{t_0}^{t_K} e^{-b(t_K-\zeta)} x(\zeta)d\zeta$ (4.5a) , i.e., $y_\ell(t_K)$ is the output at $t = t_K$ of $(1/s+b)$ due to the input $x(t)$ (Fig. IV.2.b).

Therefore:

$$y(t) = y_\ell(t) - \sum_{K=1}^{\infty} e^{-b(t-t_K)} y_\ell(t_K) \left[u(t-t_K) - u(t-t_{K+1}) \right] \quad (4.5b)$$

Note that $y_\ell(t_K)\ [u(t-t_K) - u(t-t_{K+1})]$ can be considered as the output of a sampler followed by a zero order hold, with sampling times corresponding

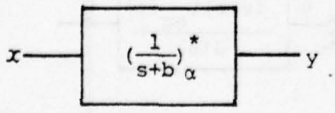

Figure IV.2.a. α - FORE.

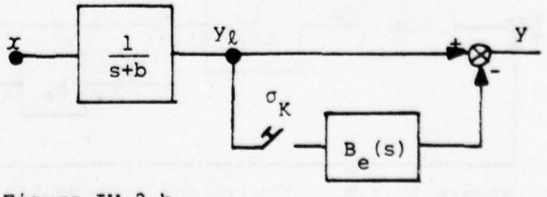

Figure IV.2.b.
Equivalent representation of an α - FORE.

to the reset-instants $t_K \in \theta$, when the input is $y_\ell(t)$, (Fig. IV.2.b). The output of the hold is then multiplied by $e^{-b(t-t_K)}$ which is the impulse response of $1/s+b$. Therefore by taking Laplace transform, we have:

$$B_e(s) \triangleq \mathcal{L}\left[[u(t-t_K) - u(t-t_{K+1})]\, e^{-b(t-t_K)} \right] = \left(B_0(s) * \frac{1}{s+b}\right)$$

where $B_0(s) = \dfrac{1-e^{-s\sigma_K}}{s}$, i.e., $B_0(s)$ is the Laplace transform of a zero order hold and $\sigma_K \triangleq t_K - t_{K-1}$.

Therefore: $$B_e(s) = \frac{1}{2\pi j} \int_{c-j\infty}^{c+j\infty} \frac{1-e^{-(s-\zeta)\sigma_K}}{s-\zeta} \cdot \frac{1}{\zeta+b}\, d\zeta \qquad (4.6)$$

and $$B_e(s) = \frac{1-e^{-(s+b)\sigma_K}}{s+b} \qquad (4.7)$$

Relation (4.5b) can therefore be considered as the sum of two signals as in Fig. IV.2.b, which is equivalent to Fig. IV.2.a from the input-output point of view.

If a limit cycle with one reset per cycle occurs, then as $t \to \infty$, $\sigma_K \to T$, a constant period. Therefore in the steady state, the nonlinear feedback system of Fig. IV.3.a becomes equivalent to the

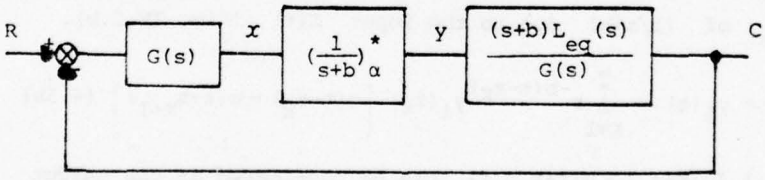

Figure IV.3.a. Feedback system containing an α - FORE.

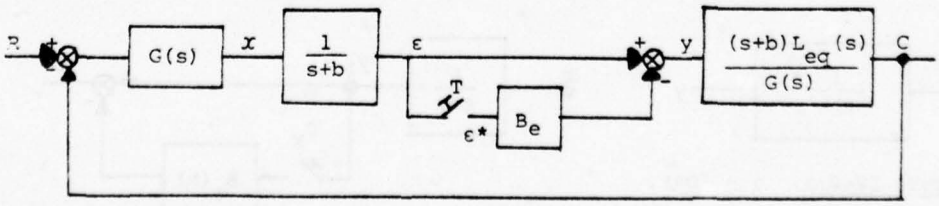

Figure IV.3.b. Equivalent representation when a limit cycle with one reset/cycle occurs.

linear sampled data feedback system shown in Fig. IV.3.b. The real number x_K^* was defined in chapter III as: $x_K^* \triangleq \int_{t_{K-1}}^{t_K} e^{-b(t_K-\zeta)} x(\zeta)d\zeta$.

Under the assumption of a limit cycle of period T ,

$x_K^* = \int_{(K-1)T}^{KT} e^{-b(KT-\zeta)} x(\zeta)d\zeta$ (4.8). Recalling the equivalent representation of Fig. III.6, x_K^* represents the strength of an impulse whose effect is the same as the reset. Therefore, if a limit cycle sustains, all the reset values are equal and:

$x_K^* = x_{K-1}^* = \ldots = x_1^* = \mu$ (4.9), where μ is independant of K .

What relation then exists between x_K^* and $\varepsilon(kT)$? We have:

$\varepsilon^*(z) \triangleq Z[\sum_{K=1}^{\infty} \varepsilon(kT)\ \delta(t-KT)]$ (4.10). However, from (4.5a) $\varepsilon(kT) = y_\ell(kT)$ by definition. Replacing (4.5a) in (4.10) gives:

$$\varepsilon^*(z) = Z\left[\sum_{K=1}^{\infty} \left[\int_0^{KT} e^{-b(KT-\zeta)} x(\zeta)d\zeta\right] \delta(t-KT)\right]$$

$$= Z\left[\sum_{K=1}^{\infty} \left[\int_0^{T} e^{-b(T-\zeta)} x(\zeta)d\zeta\ e^{-b(k-1)T} + \int_T^{2T} + \ldots \right.\right.$$

$$\left.\left. + \int_{\gamma T}^{(\gamma+1)T} e^{-b((\gamma+1)T-\zeta)} x(\zeta)d\zeta\ e^{-b(K-(\gamma+1))T} + \ldots + \int_{(K-1)T}^{KT} e^{-b(KT-\zeta)} x(\zeta)d\zeta\right]\delta(t-KT)\right]$$

(4.11). Using (4.9) in (4.11) gives:

$$\varepsilon^*(z) = Z\left[\sum_{K=1}^{\infty} \mu(1+e^{-bT}+\ldots+e^{-b(K-1)T})\ \delta(t-KT)\right] \qquad (4.12a)$$

$$= Z\left[\sum_{K=1}^{\infty} \sum_{m=1}^{K} \mu e^{-b(m-1)T}\ \delta(t-KT)\right] \qquad (4.12b) \text{ and: } \varepsilon^*(z) = \frac{\mu z}{(z-1)(z-e^{-bT})} \qquad (4.13)$$

Let us now consider the system of Fig. IV.3.b. We have:

$$(1+L_{eq}(s))\ \varepsilon(s) = R(s)G(s)\ \frac{1}{s+b} + B_e(s)\ L_{eq}(s)\ \varepsilon^*(s)$$

or equivalently:

$$\varepsilon(s) = \frac{R(s)G(s)}{(1+L_{eq}(s))(s+b)} + B_e(s)\ \frac{L_{eq}(s)}{1+L_{eq}(s)}\ \varepsilon^*(s) \qquad (4.14)$$

Taking the z-transform gives:

$$\varepsilon^*(s) = \left(\frac{RG}{(1+L_{eq})(s+b)}\right)^* + \left(B_e \frac{L_{eq}}{1+L_{eq}}\right)^* \varepsilon^*(s) \qquad (4.14a)\ .$$

As $B_e(s) = \frac{1-e^{-(s+b)T}}{s+b}$, $1 - \left(\frac{B_e L_{eq}}{1+L_{eq}}\right)^* = 1 - (1-z^{-1}e^{-bT}) \left(\frac{L_{eq}}{(s+b)(1+L_{eq})}\right)^*$

$= 1-(1-z^{-1}e^{-bT}) \left(\frac{1}{s+b} - \frac{1}{(1+L_{eq})(s+b)}\right)^* = (1-z^{-1}e^{-bT}) \left(\frac{1}{(1+L_{eq})(s+b)}\right)^*$

and (4.14a) becomes:

$$\varepsilon^*(s) = \frac{z}{z-e^{-bT}} \frac{\left(\frac{RG}{(1+L_{eq})(s+b)}\right)^*}{\left(\frac{1}{(1+L_{eq})(s+b)}\right)^*} \qquad (4.15)$$

$$\varepsilon^*(s) \triangleq \frac{z}{z-e^{-bT}} \Delta^*(s) \qquad (4.16)$$

with:

$$\Delta^*(s) \triangleq \frac{\left(\frac{RG}{(1+L_{eq})(s+b)}\right)^*}{\left(\frac{1}{(1+L_{eq})(s+b)}\right)^*} \qquad (4.17)$$

As $x(s) = (s+b)\,\varepsilon(s)$, (4.14) gives then:

$$x(s) = \frac{R(s)G(s)}{1+L_{eq}(s)} + B_e(s) \frac{L_{eq}(s)(s+b)}{1+Leq(s)} \varepsilon^*(s)$$

Taking the z-transform gives:

$$x^*(z) = \left(\frac{RG}{1+L_{eq}}\right)^* (z) + \Delta^*(z) \left(\frac{L_{eq}}{1+L_{eq}}\right)^* (z) \qquad (4.18)$$

Comparing (4.16) and (4.13) we can conclude that $\Delta^*(z)$ represents the train of impulses due to the resets, and therefore if a limit cycle exists, $\Delta^*(z) = f(z) + \frac{\mu z}{z-1}$ where $f(z)$ has all its poles strictly inside the unit circle, and equivalently at the steady state $\Delta^*(z) = \frac{\mu z}{z-1}$.

Conversely if, as $t \to \infty$, the reset values tend toward a constant $\mu \neq 0$ with periodicity T, i.e., $\Delta^*(z) \to \frac{\mu}{z-1}$ as $z \to 1$, and this occurs when the input x tends toward α with the same periodicity, i.e., $x^*(z) \to \frac{\alpha}{z-1}$ as $z \to 1$, then we can conclude to a sustained limit

cycle of period T . We have thus proven:

Theorem 2: A nonlinear feedback system which contains an element $\left(\frac{1}{s+b}\right)^*_\alpha$ whose output y is reset to zero whenever the input x crosses α , for a given α , sustains a limit cycle of period T with one reset per cycle if and only if there exists some finite nonzero T , $\mu \in \mathcal{R}$ such that in the neighborhood of $t=\infty$, we satisfy:

$$\text{I} \qquad \lim_{z=1} (z-1)\ \Delta^*(z) = \mu \tag{4.19a}$$

$$\text{II} \qquad \lim_{z=1} (z-1)\ x^*(z) = \alpha \tag{4.19b}$$

Qualitative statements about possible limit cycles can be made by inspection of (4.17). From (4.19a) a limit cycle exists if $\Delta^*(z) \to \frac{\mu}{z-1}$ as $z \to 1$. However, the number of poles at $z=1$ of $\Delta^*(z)$ is only related to the number of poles at $s=0$ of $\Delta^*(s)$, or in other words, to the excess e of poles at $s=0$ of $\left(\frac{RG}{(s+b)(1+L)}\right)^*$ over $\left(\frac{1}{(s+b)(1+L)}\right)^*$. If $e=0$ no limit cycle can sustain, while if $e=1$ a limit cycle is predicted. 4.19a and b give then the two unknowns μ , T which characterize the limit cycle. Furthermore, as can be seen from (4.17) the value of e is only a function of the number of poles at $s=0$ of R and number of poles at $s=0$ of L , under the assumption that G has no such pole. It is therefore very striking how for such a nonlinear feedback system the stability problem is related to the "type" of input R applied and "type" of L , where by "type" we mean the number of integrations. (Type "0" R corresponds to a signal R without integration, type "1" to one integration, etc...)

IV.4. Examples of applications of Theorem 2.

It will be assumed that $L_{eq}(s)$ has one integration. Therefore, in both cases $(b = 0\ ,\ b \neq 0)$, $\left(\frac{1}{(s+b)(1+L_{eq})}\right)^*$ (which is the denominator of $\Delta^*(s)$) has no pole at $z = 1$.

IV.4.a. Type "0" inputs.

In this case, $e = 0$ and theorem 2 predicts that no limit cycle can sustain.

IV.4.b. Type "1" inputs.

If $b \neq 0$, $\left(\frac{RG}{(s+b)(1+L_{eq})}\right)$ has no pole at $s = 0$, therefore $e = 0$ and theorem 2 predicts no limit cycle. However, if $b = 0$, then $e = 1$ and a limit cycle can be sustained.

In the latter, let $G = 1$, $L_{eq}(s) = \frac{\Lambda}{s(s+2\sigma)}$, $R = \frac{1}{s}$.

We have, from (4.17):

$$\Delta^*(s) = \frac{Z\left[\frac{1}{s}\ \frac{s+2\sigma}{s^2+2\sigma s+\Lambda}\right]}{Z\left[\frac{s+2\sigma}{s^2+2\sigma s+\Lambda}\right]}$$

Suppose that $\sigma^2 - \Delta < 0$ and let $\omega_0 \triangleq \sqrt{\Lambda-\sigma^2}$, then:

$$\Delta^*(s) = \frac{\frac{2\sigma}{\Lambda}\left[z\left(1-e^{-\sigma T}\cos\omega_0 T - e^{-\sigma T}\left(\sigma-\frac{\Lambda}{2\sigma}\right)\frac{\sin\omega_0 T}{\omega_0}\right)+e^{-2\sigma T}-e^{-\sigma T}\cos\omega_0 T+\left(\sigma-\frac{\Lambda}{2\sigma}\right)e^{-\sigma T}\frac{\sin\omega_0 T}{\omega_0}\right]}{(z-1)\left(z - e^{-\sigma T}\cos\omega_0 T + \frac{\sigma}{\omega_0}e^{-\sigma T}\sin\omega_0 T\right)}$$

and

$$x^*(s) = \frac{\left(z(z-e^{-\sigma T}\cos\omega_0 T + \frac{\sigma}{\omega_0}e^{-\sigma T}\sin\omega_0 T\right)}{z^2 - 2z\,e^{-\sigma T}\cos\omega_0 T + e^{-2\sigma T}} + \frac{z\,\frac{\Lambda}{\omega_0}e^{-\sigma T}\sin\omega_0 T\,\Delta^*(s)}{z^2-2z\,e^{-\sigma T}\cos\omega_0 T + e^{-2\sigma T}}$$

According to theorem 2, a limit cycle exists if and only if, $\exists\ T>0$, such that: [condition II]

$$\lim_{Z=1}(z-1)\,x^*(s) = \frac{2\sigma}{\omega_0}\ \frac{e^{-\sigma T}\sin\omega_0 T}{1-e^{-\sigma T}\cos\omega_0 T+\frac{\sigma}{\omega_0}e^{-\sigma T}\sin\omega_0 T} = \alpha$$

In the case of a C.I. $(\alpha = 0)$, it is easily found that:

$$\omega_0 T = \pi \quad \text{or} \quad T = \frac{\pi}{\omega_0} = \frac{\pi}{\sqrt{\Lambda - \sigma^2}}$$

$$\text{and} \quad \mu = \lim_{z=1} (z-1)\,\Delta^*(z) = \frac{1 - 2e^{-2\sigma T}\cos\omega_0 T + e^{-2\sigma T}}{1 - e^{-\sigma T}\cos\omega_0 T + \frac{\sigma}{\omega_0}\sin\omega_0 T} = 1 + e^{-\sigma T}$$

If $\sigma^2 - \Lambda > 0$, no reset occurs, and the system is stable if $\sigma > 0$, and unstable if $\sigma < 0$. The reader should note that if $\sigma > 0$, a reset occurs at $t = \infty$ and therefore a 'limit cycle' then occurs of period $T = \infty$. These limit cycles were not predicted by using the Dual input describing functions [G1]. As mentioned before, if $b \neq 0$, no limit cycle can sustain. Thus the regions of stability with respect to a step input can be compared in the σ - Λ plane on Fig. IV.4.a,b,c for the L.T.I., the C.I. and the FORE case respectively. This proves then that FORE is superior to the C.I. from the stability point of view (at least for type "1" inputs) as already stated many times in chapter III. Furthermore for the C.I. $(b = 0)$, the criterion suggests to introduce a zero at $s = 0$ in $G(s)$ in order to stabilize the nonlinear

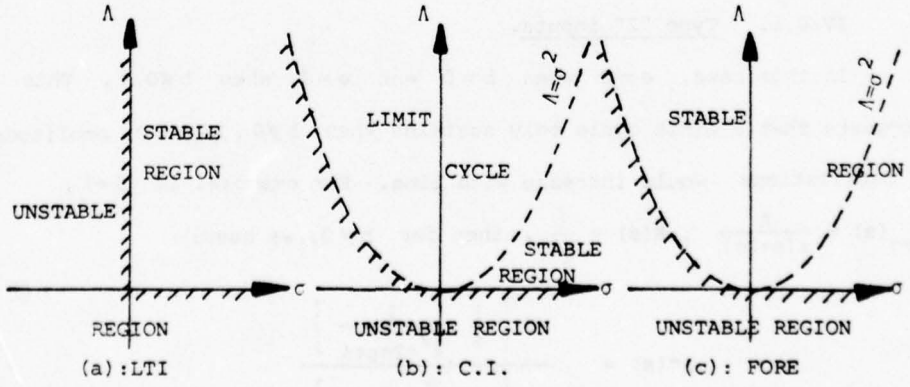

Figure IV.4. Comparison of the stability regions.

feedback system of Fig. IV.3.a. Another alternative is to introduce two poles at $s = 0$ in the open loop transfer function $L_{eq}(s)$. Those results can be physically easily understood. Indeed, consider a L.T.I. feedback system containing a linear integrator (L.I.) in its loop, whose input is x and output y. When a type "0" input R is applied to such a system, as $t \to \infty$, $R \to 0$, $x \to 0$ and $y \to 0$. If the L.I. is replaced by a C.I., one notes that the steady state ($x = 0$, $y = 0$) is compatible and thus no limit cycle can sustain. If now R is type "1", then as $t \to \infty$, $R \to k_r$, $x \to 0$ and $y \to k_y$ for the L.T.I. system. Unfortunately the steady state ($x = 0$, $y = k_y$) is impossible to sustain in the nonlinear mode with a C.I. in place of the L.I. and therefore a limit cycle occurs. (Note that this mode is compatible with FORE, thus explaining the difference from the stability point of view.) To place some derivative in G (fig. IV.3.a) as is suggested by the criterion implies to place another integration in the loop (because of the factor $1/G$) and therefore the state ($x = 0$, $y = 0$) for the C.I. becomes a compatible one and a limit cycle is therefore avoided.

IV.4.c. Type "2" inputs.

In this case, $e = 2$ when $b = 0$ and $e = 1$ when $b \neq 0$. This suggests that a limit cycle only sustains when $b \neq 0$. If $b = 0$, amplitude of oscillations would increase with time. For example, if $G = 1$, $L_{eq}(s) = \frac{\Lambda}{s(s+2\sigma)}$, $R(s) = \frac{1}{s^2}$, then for $b \neq 0$, we have:

$$\Delta^*(s) = \frac{Z\left[\frac{1}{s}\,\frac{1}{s^2+2\sigma s+\Lambda}\right]}{Z\left[\frac{s}{s^2+2\sigma s+\Lambda}\right]}$$

If $\sigma^2 - \Lambda < 0$ and using $\omega_0 = \sqrt{\Lambda - \sigma^2}$, we have:

$$\Delta^*(s) = \frac{z(1-e^{-\sigma T}\cos\omega_0 T - \frac{\sigma}{\omega_0} e^{-\sigma T}\sin\omega_0 T) + e^{-\sigma T}(e^{-\sigma T} - \cos\omega_0 T + \frac{\sigma}{\omega_0}\sin\omega_0 T)}{(z-1)(z - \frac{\sigma}{\omega_0} e^{-\sigma T}\sin\omega_0 T - e^{-\sigma T}\cos\omega_0 T)}$$

and:

$$x(z) = z\left[\frac{2\sigma/\Lambda}{s} - \frac{\frac{2\sigma}{\Lambda}s + \frac{4\sigma^2}{\Lambda} - 1}{s^2 + 2\sigma s + \Lambda}\right] + \delta(z)\,\frac{\Lambda z\, e^{-\sigma T}\sin\omega_0 T}{z^2 - 2ze^{-\sigma T}\cos\omega_0 T + e^{-2\sigma T}}$$

so, as $z \to 1$,

$$x(z) \to \frac{\frac{2\sigma}{\Lambda}(1 - e^{-\sigma T}\cos\omega_0 T - e^{-\sigma T}\frac{2\sigma^2 - \Lambda^2}{2\sigma\omega_0}\sin\omega_0 T)}{(z-1)(1 - e^{-\sigma T}\cos\omega_0 T - \frac{\zeta}{\sqrt{1-\zeta^2}} e^{-\sigma T}\sin\omega_0 T)}$$

and with $\sigma = \zeta\omega_N$, $\Lambda = \omega_N^2$ and $\phi = \cos^{-1}\zeta$ we know that a limit cycle exists if:

$$\exists\ T \text{ such that } \lim_{z=1}(z-1)x(z) = \frac{\frac{2\zeta}{\omega_N}\left(1 - e^{-\zeta\omega_N T}\,\frac{\sin(\omega_0 T + 2\phi}{\sin 2\phi}\right)}{1 - e^{-\zeta\omega_N T}\,\frac{\sin(\omega_0 T + \phi)}{\sin\phi}} = \alpha$$

Let $\alpha = 0$ (FORE) then we have to satisfy:

$$\sin 2\phi = e^{-\zeta\omega_N T}\sin(\omega_0 T + 2\phi) \quad \text{and} \quad \exists\ T \neq 0, \quad \text{if } -1 < \zeta \leq .19,$$

for which case a limit cycle exists. Region of stability with respect

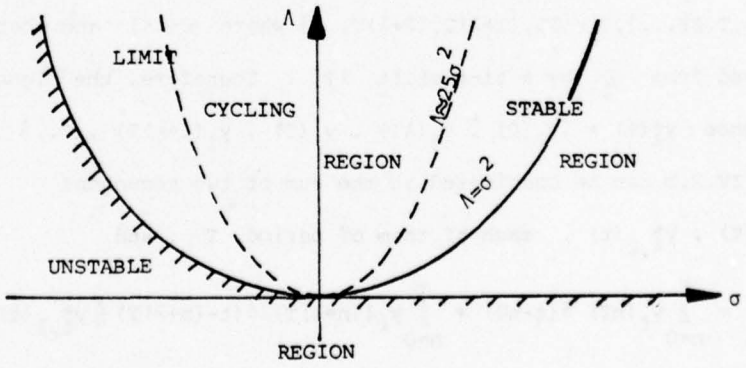

Figure IV.5. Stability regions of FORE with ramp inputs.

to a ramp input are then shown on Fig. IV.5 for the FORE. In order to overcome the unstability problem noted here, the criterion suggests here too, to place a zero at $s=0$ in the filter G. An element like $G = \frac{s}{s+\alpha}$ seems then to be reasonable in order to avoid possible limit cycles in the nonlinear ramp input response and more generally in the response to type "2" inputs. Indeed,

$$\Delta^*(s) = \frac{Z\left[\frac{1}{s+\alpha}\ \frac{1}{s^2+2\sigma s+\Lambda}\right]}{Z\left[\frac{s}{s^2+2\sigma s+\Lambda}\right]} \quad \text{and thus} \quad e=0 \ .$$

We should underline here that theorem 2 only predicts limit cycle with one reset/cycle. This type of cycle usually only occurs with ideal 2nd order systems. Therefore, if conditions I and II of theorem 2 are not satisfied, as it does usually for high order systems, one should investigate possible limit cycles with 2 resets/cycle which is the most commonly found experimentally.

IV.5. Investigation of limit cycles with two resets/cycle.

If a limit cycle of period T with two resets/cycle sustain, it means that the set of reset-instants is composed of two susbsets $\theta_1=\{0,T,2T,..\},\theta_2=\{\lambda T,(1+\lambda)T,(2+\lambda)T,..\}$ where $0<\lambda<1$ and where θ_2 is deduced from θ_1 by a time shift λT. Therefore, the signal sequence $y_\ell^*(t) = \{y_\ell(0)\ ,\ y_\ell(\lambda T)\ ,\ y_\ell(T)\ ,\ y_\ell(1+\lambda)T)\ ,....,\}$ of Fig. IV.2.b can be considered as the sum of two sequences $y^*_{\ell,1}(t)$, $y^*_{\ell,2}(t)$, each of them of period T , and

$$y_\ell^*(t) = \sum_{n=0}^{\infty} y_\ell(nT)\ \delta(t-nT) + \sum_{n=0}^{\infty} y_\ell((n+\lambda)T)\ \delta(t-(n+\lambda)T) \triangleq y^*_{\ell,1}(t) + y^*_{\ell,2}(t) \tag{4.20}$$

so:

$$y_\ell^*(z) = \sum_{n=0}^{\infty} y_\ell(nT)z^{-nT} + \sum_{n=0}^{\infty} y_\ell((n+\lambda)T)z^{-(n+\lambda)T} = y^*_{\ell,1}(z) + y^*_{\ell,2}(z) \tag{4.21}$$

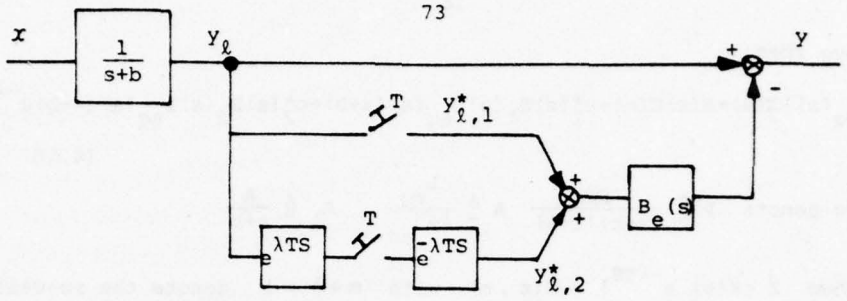

Figure IV.6. Equivalent representation of FORE when a limit cycle with two resets per cycle occurs.

Therefore Fig. IV.2.b is equivalent to Fig. IV.6, with

$B_e(s) = \frac{1-e^{-(s+b)\sigma_K}}{s+b}$ (recall 4.7) where $\sigma_K = t_K - t_{K-1}$. When such a limit cycle sustains, $\sigma_K \triangleq t_K - t_{K-1}$ has two distinct limits $\sigma_K^1 = (n+\lambda)T - nT = \lambda T$ (4.22) and $\sigma_K^2 = (n+1)T - (n+\lambda)T = (1-\lambda)T$ (4.23). Therefore (recall 4.7 and the definition of $y_\ell^*(t)$), $B_e(s) = B_1(s) = \frac{1-e^{-(s+b)\sigma_K^1}}{s+b}$ (4.24) when acting on the sequence $y_{\ell,1}^*(t)$ while $B_e(s) = B_2(s) = \frac{1-e^{-(s+b)\sigma_K^2}}{s+b}$ (4.25) when acting on $y_{\ell,2}^*(t)$. Therefore the nonlinear feedback system of Fig. IV.3.a becomes then equivalent to the linear sampled data feedback system shown on Fig. IV.7 from the input output point of view.

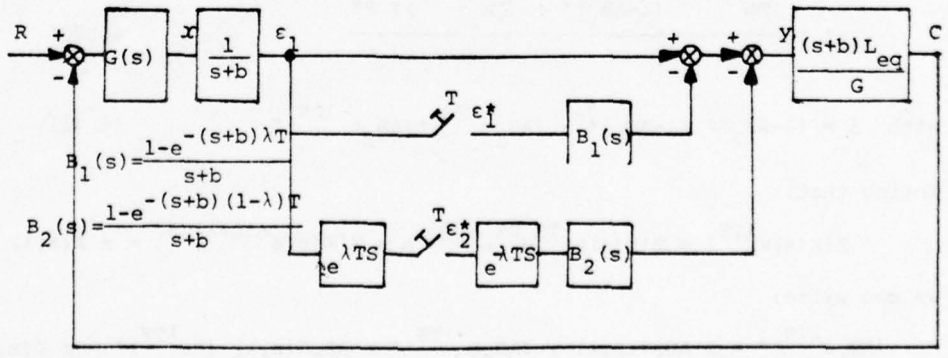

Figure IV.7. Equivalent representation of the nonlinear feedback when a limit cycle with two resets/cycle sustains.

We have then:

$$(1+L_{eq}(s))\mathcal{X}(s)=R(s)G(s)+\varepsilon_1^*(s)B_1(s)L_{eq}(s)(s+b)+\varepsilon_2^*(s)B_2(s)L_{eq}(s)(s+b)e^{-\lambda TS} \tag{4.26}$$

Let us denote $P \triangleq \frac{RG}{(s+b)(1+L)}$ $A \triangleq \frac{L_{eq}}{1+L_{eq}}$ $A_1 \triangleq \frac{A}{s+b}$

Let then $Z\,[K(s)\,e^{-\lambda TS}] = K(z,m)$ with $m+\lambda = 1$ denote the so-called modified Z-transform (see [L1], [J1], [S3]). (4.26) becomes:

$$\mathcal{X}(s) = (s+b)P + \varepsilon_1^*(s)B_1(s)A(s)(s+b) + \varepsilon_2^*(s)B_2(s)A(s)(s+b)e^{-\lambda TS} \tag{4.27}$$

and:

$$\varepsilon_1(s) = \frac{\mathcal{X}(s)}{s+b} = P + \varepsilon_1^*(s)B_1(s)A(s) + \varepsilon_2^*(s)B_2(s)A(s)e^{-\lambda TS} \tag{4.28a}$$

$$\varepsilon_2(s) = \varepsilon_1(s)e^{\lambda TS} = Pe^{\lambda TS} + \varepsilon_1^*(s)B_1(s)A(s)e^{\lambda TS} + \varepsilon_2^*(s)B_2(s)A(s) \tag{4.28b}$$

Therefore after taking the Z-transform:

$$\varepsilon_1^* = P^* + \varepsilon_1^*\,(B_1A)^* + (B_2Ae^{-\lambda TS})^*\,\varepsilon_2^*$$

$$\varepsilon_2^* = (Pe^{\lambda TS})^* + \varepsilon_1^*\,(B_1Ae^{\lambda TS})^* + (B_2A)^*$$

or equivalently:

$$\varepsilon_1^* = \frac{P^*(1-AB_2)^* + (AB_2e^{-\lambda TS})^*\,(Pe^{\lambda TS})^*}{\Delta} \tag{4.29}$$

$$\varepsilon_2^* = \frac{(Pe^{\lambda TS})^*\,(1-AB_1)^* + (AB_1e^{\lambda TS})^*\,P^*}{\Delta} \tag{4.30}$$

with $\Delta = (1-AB_2)^*\,(1-AB_1)^* - (AB_1e^{\lambda TS})^*(AB_2e^{-\lambda TS})^*$ (4.31)

Noting that:

$$Z[K(s)e^{\lambda TS}] = Z[K(s)e^{-TS}e^{TS}e^{\lambda TS}] = z\,Z[K(s)e^{-(1-\lambda)TS}] = z\,K(z,\lambda)\ ,$$

we can write:

$$(AB_1e^{\lambda TS})^* = z\,AB_1^*(z,\lambda)\ ,\ (AB_2e^{-\lambda TS})^* = AB_2^*(z,\lambda)\ (Pe^{\lambda TS})^* = z\,P(z,\lambda)$$

As: $AB_1^* = Z\left[A\,\frac{1-e^{-(s+b)\lambda T}}{s+b}\right] = A_1^*(z) - e^{-b\lambda T}A_1^*(z,m)$

$AB_2^* = Z\left[A\,\frac{1-e^{-(s+b)(1-\lambda)T}}{s+b}\right] = A_1^*(z) - e^{-mbT}A_1^*(z,\lambda)$

$AB_1^*(z,\lambda) = Z\left[A\,\frac{1-e^{-(s+b)\lambda T}}{s+b}\,e^{-(1-\lambda)ST}\right] = A_1^*(z,\lambda) - z^{-1}e^{-\lambda bT}A_1^*(z)$

$AB_2^*(z,m) = Z\left[A\,\frac{1-e^{-(s+b)mT}}{s+b}\,e^{-\lambda ST}\right] = A_1^*(z,m) - z^{-1}e^{-mbT}A_1^*(z)$

(4.29), (4.30) are rewritten as: $\varepsilon_1^*(z) =$

$$\frac{P(z)(1-A_1(z)+e^{-mbT}A_1(z,\lambda))+P(z,\lambda)(zA_1(z,m)-e^{-mbT}A_1(z))}{(1-A_1(z)+e^{-\lambda bT}A_1(z,m))(1-A_1(z)+e^{-mbT}A_1(z,\lambda))-(A_1(z,m)-z^{-1}e^{-mbT}A_1(z))(zA_1(z,\lambda)-e^{-\lambda bT}A_1(z))} \qquad (4.32)$$

$\varepsilon_2^*(z) =$

$$\frac{zP(z,\lambda)(1-A_1(z)+e^{-\lambda bT}A_1(z,m))+P(z)(zA_1(z,\lambda)-A_1(z)e^{-\lambda bT})}{(1-A_1(z)+e^{-\lambda bT}A_1(z,m))(1-A_1(z)+e^{-mbT}A_1(z,\lambda))-(A_1(z,m)-z^{-1}e^{-mbT}A_1(z))(zA_1(z,\lambda)-e^{-\lambda bT}A_1(z))} \qquad (4.33)$$

Taking the z-transform of (4.27) and using

$$(B_1A(s+b))^* = Z\left[A\,(1-e^{-\lambda T(s+b)})\right] = A(z) - A(z,m)e^{-\lambda bT}$$

$$(B_2A(s+b))^* = Z\left[A\,(1-e^{-mT(s+b)})\right] = A(z) - A(z,\lambda)e^{-mbT}$$

gives: (4.34a)

$$x(z) = ((s+b)P)^* + (A(z)-e^{-\lambda bT}A(z,m))\varepsilon_1(z) + (A(z,m)-z^{-1}e^{-mbT}A(z))\varepsilon_2(z)$$

and by taking the z-transform $(x(s)e^{\lambda TS})^*$ (4.34b)

$$x(z,\lambda) = ((s+b)P)^*(z,\lambda) + (A(z,\lambda)-e^{-\lambda Tb}A(z))\varepsilon_1(z) + (A(z)-e^{-mbT}A(z,\lambda))\varepsilon_2(z)\ .$$

If a limit cycle with two resets per cycle sustains, then the sequence of reset values $\{x_K^* \triangleq \int_{t_{K-1}}^{t_K} x(\zeta)e^{-b(t_k-\zeta)}d\zeta\}$ defined in chapter III is composed of two subsequences

$$\{x_1^* = x_3^* = \ldots = x_{2n+1}^* = \int_{nT}^{(n+\lambda)T} x(\zeta)e^{-b((n+\lambda)T-\zeta}d\zeta = \ldots = u_1\}$$

and:

$$x_2^* = x_4^* = \ldots = x_{2(n+1)}^* = \int_{(n+\lambda)T}^{(n+1)} x(\zeta) e^{-b((n+1)T-\zeta)} d\zeta = \ldots = \mu_2$$

with μ_1 and μ_2 independant of K .

Therefore, by anology with (4.10) to (4.13), at the steady state:

$$\varepsilon_1^*(z) = \frac{\mu_1 z}{(z-1)(z-e^{-bT})} \quad (4.35) \qquad \varepsilon_2^*(z) = \frac{\mu_2 z}{(z-1)(z-e^{-bT})} \quad (4.36)$$

Conversely, if it exists μ_1 , μ_2 , T such that, for the system of Fig. IV.7, (4.35) and (4.36) are satisfied, it implies that as $t \to \infty$, the reset values x_K^* have two distinct limits μ_1 , μ_2 and therefore a limit cycle of period T with two resets per cycle sustains.

Therefore we have proven:

Theorem 3: A nonlinear feedback system which contains the non-linear element $\left(\frac{1}{s+b}\right)_\alpha^*$, whose output y is reset to zero whenever the input x crosses α , for a given α , sustains a limit cycle of period T with two resets per cycle, if and only if, there exists finite nonzero T , μ_1 , $\mu_2 \in \mathbb{R}$ and $\lambda \in]0,1[$ such that in the neighbourhood of $t = \infty$ we have:

$$\begin{cases} \lim_{z=1} (z-1)(z-e^{-bT})\varepsilon_1(z) = \mu_1 & (4.37a) \\ \lim_{z=1} (z-1)(z-e^{-bT})\varepsilon_2(z) = \mu_2 & (4.37b) \end{cases}$$

$$\begin{cases} \lim_{z=1} (z-1)x(z) = \alpha & (4.38a) \\ \lim_{z=1} (z-1)x(z,\lambda) = \alpha & (4.38b) \end{cases}$$

The expressions involved here are more complicated than those of Theorem 2. It is however possible, here too, as shown below, to have a very good qualitative feeling as to when a limit cycle occurs, without necessarily solving algebraically (4.37) and (4.38) if one is

not interested in the precise value of T and λ .

As $A_1 = \frac{A}{s+b} = \frac{1}{s+b} \frac{L_{eq}(-b)}{1+L_{eq}(-b)} + \Sigma(s) = \frac{1}{s+b} + \Sigma(s)$ where

$\Sigma(s)$ denotes the remaining part of the fractional expansion of $A_1(s)$ and where it is implicitly assumed that $L_{eq}(s)$ has one pole at $s = -b$.

Then: $1-A_1(z) + e^{-\lambda bT} A_1(z,m) = 1 - \frac{z}{z-e^{-bT}} - \Sigma^*(z) + \frac{e^{-\lambda bT} e^{-mbT}}{z-e^{-bT}} + e^{-\lambda bT}\Sigma^*(z,m)$

$= e^{-\lambda bT}\, \Sigma^*(z,m) - \Sigma^*(z)$ (because $m+\lambda = 1$)

and $1-A_1(z) + e^{-mbT} A_1(z,\lambda) = e^{-mbT}\, \Sigma^*(z,\lambda) - \Sigma^*(z)$ (by anology)

$$A_1(z,m) - z^{-1} e^{-mbT} A_1(z) = \frac{e^{-mbT}}{z-e^{-bT}} + \Sigma^*(z,m) - \frac{z^{-1} e^{-mbT} z}{z-e^{-bT}} - z^{-1}\, \Sigma^*(z)$$

$$= \Sigma^*(z,m) - z^{-1}\, \Sigma^*(z)\, e^{-mbT}$$

and $zA_1(z,\lambda) - e^{-\lambda bT} A_1(z) = z\, \Sigma^*(z,\lambda) - \Sigma^*(z) e^{-\lambda bT}$

So in (4.32) and (4.33) the denominator

$$\Delta = (e^{-\lambda bT}\Sigma^*(z,m) - \Sigma^*(z))\ (e^{-mbT}\Sigma^*(z,\lambda) - \Sigma^*(z)) -$$

$$(\Sigma^*(z,m) - z^{-1}\Sigma^*(z)e^{-mbT})\ (z\Sigma^*(z,\lambda) - \Sigma^*(z)\ e^{-\lambda bT})$$

or $\Delta = (e^{-bT}-z)\ \Sigma^*(z,m)\Sigma^*(z,\lambda) + \Sigma^*(z)^2(1-z^{-1}e^{-bT})$

$$\Delta = (z-e^{-bT})\ (z^{-1}\Sigma^*(z)^2 - \Sigma^*(z,m)\ \Sigma^*(z,\lambda))$$

(4.32) and (4.33) are then written as:

$$\varepsilon_1^*(z) = \frac{P(z)(e^{-mbT}\ \Sigma^*(z,\lambda) - \Sigma^*(z)) + P(z,\lambda)(z\Sigma^*(z,m) - e^{-mbT}\Sigma^*(z))}{(z-e^{-bT})(z^{-1}\Sigma^*(z)^2 - \Sigma^*(z,m)\ \Sigma^*(z,\lambda))}$$

$$\triangleq \frac{\Delta_1^*(z)}{z-e^{-bT}} \qquad (4.39)$$

$$\varepsilon_2^*(z) = \frac{zP(z,\lambda)(e^{-\lambda bT}\Sigma^*(z,m) - \Sigma^*(z)) + P(z)(z\Sigma^*(z,\lambda) - e^{-\lambda bT}\Sigma^*(z))}{(z-e^{-bT})(z^{-1}\Sigma^*(z)^2 - \Sigma^*(z,m)\ \Sigma^*(z,\lambda))}$$

$$\stackrel{\Delta}{=} \frac{\Delta_2^*(z)}{(z-e^{-bT})} \qquad (4.40)$$

Two cases are now investigated.

a). $b = 0$ and, as it is implicitely assumed that $L_{eq}(s)$ has only one pole at $s = 0$, $\Sigma(s)$ has no pole at $s = 0$, and therefore all Σ^* have no pole at $z = 1$. As $\lim_{z=1} (e^{-mbT}\Sigma^*(z,\lambda) - \Sigma^*(z)) \neq 0$ (4.41)

$\lim_{z=1} (z\Sigma^*(z,m) - e^{-mbT}\Sigma^*(z)) \neq 0$ (4.42), $\lim_{z=1} (e^{-\lambda bT}\Sigma^*(z,m) - \Sigma^*(z)) \neq 0$ (4.43)

$\lim_{z=1} (z\Sigma^*(z,\lambda) - e^{-\lambda bT}\Sigma^*(z)) \neq 0$ (4.44) and $\lim_{z=1} (z^{-1}\Sigma^*(z)^2 - \Sigma^*(z,m)\Sigma^*(z,\lambda)) \neq 0$ (4.45), we conclude that the number of poles of Δ_1^*, Δ_2^* at $z = 1$ are exactly equal to the number of poles at $z = 1$ of $P(z)$ (which has the same poles as $P(z,\lambda)$).

b). $b \neq 0$ and then $\Sigma(s)$ has one pole at $s = 0$, whose residue is $1/b$. The inequalities (4.41 to 4.45) are here too satisfied. Furthermore, all terms Σ^* in the numeration of both ε_1^* and ε_2^* have one pole at $z = 1$ which is cancelled out by the one pole at $z = 1$ of $z^{-1}\Sigma^*(z)^2 - \Sigma^*(z,m)\,\Sigma^*(z,\lambda)$.

Indeed, one notes that the latter has no such term as $\frac{\gamma(z)}{(z-1)^2}$ with $\gamma(1) \neq 0$ because $\gamma(z) = z^{-1} \cdot \frac{z^2}{b^2} - \frac{1}{b^2} = \frac{z-1}{b^2}$ and therefore $\gamma(z)$ has one zero at $z = 1$, implying then that $z^{-1}\Sigma^*(z)^2 - \Sigma^*(z,\lambda)\,\Sigma^*(z,m)$ has only one pole at $z = 1$. Therefore we can conlcude here, too, that the number of poles at $z = 1$ of Λ_1^*, Δ_2^* is exactly equal to the number of poles at $z = 1$ of $P(z)$.

Therefore in all cases ($b = 0$, $b \neq 0$) condition I of Theorem 3 is satisfied if $P(s)$ has one pole at $s = 0$, implying then that a

limit cycle with two resets per cycle may sustain. The reader has certainly noted that $P(s)$ is exactly the same quantity than the numerator of $\Delta^*(s)$ in (4.17) [Theorem 2]. Therefore the qualitative discussion made in section IV.4 for Theorem 2 is easily extended here and it is seen that the occurence of a limit cycle is entirely determined by the number of integrations (type) of the system-input, while the limit cycle itself is mainly characterized by the loop transfer function $L_{eq}(s)$. If G has no zeros at $s = 0$, we can conclude then, that a nonlinear feedback system containing a C.I. sustains in general, a limit cycle with "type 1" inputs but such limit cycle does not occur when the C.I. is replaced by FORE. However a nonlinear feedback system containing FORE sustains a limit cycle, in general, with "type 2" inputs.

It remains to show that condition II of Theorem 3 is a consequence of condition I. This is now established.

Replacing (4.39), (4.40) in (4.34a) we get:

$$x(z) = ((s+b)P)^* + A(z)\left[\frac{P(z)(e^{-mbT}\Sigma^*(z,\lambda) - \Sigma^*(z)) + P(z,\lambda)(z\Sigma^*(z,m) - e^{-mbT}\Sigma^*(z)) - z^{-1}e^{-mbT}(zP(z,\lambda)(e^{-\lambda bT}\Sigma^*(z,m) - \Sigma^*(z)) + zP(z)(\Sigma^*(z,\lambda) - z^{-1}e^{-\lambda bT}\Sigma^*(z)))}{\Delta}\right]$$

$$+A(z,m)\left[\frac{zP(z,\lambda)[e^{-\lambda bT}\Sigma^*(z,m) - \Sigma^*(z)] + P(z)[z\Sigma^*(z,\lambda) - e^{-\lambda bT}\Sigma^*(z)] - e^{-\lambda bT}(P(z)[e^{-mbT}\Sigma^*(z,\lambda) - \Sigma^*(z)] + P(z,\lambda)[z\Sigma^*(z,m) - e^{-mbT}\Sigma^*(z)])}{\Delta}\right]$$

$$\text{or } x(z) = ((s+b)P)^* + \frac{A(z)(-P(z)\Sigma^*(z)z^{-1} + P(z,\lambda)\Sigma^*(z,m))(z-e^{-bT})}{(z^{-1}\Sigma^*(z)^2 - \Sigma^*(z,m)\Sigma^*(z,\lambda))(z-e^{-bT})}$$

$$+ A(z,m)\frac{(P(z)\Sigma^*(z,\lambda) - P(z,\lambda)\Sigma^*(z))(z-e^{-bT})}{(z^{-1}\Sigma^*(z)^2 - \Sigma^*(z,m)\Sigma^*(z,\lambda))(z-e^{-bT})} \qquad (4.46)$$

Equivalently from (4.34b) we have:

$$\chi(z,\lambda) = ((s+b)P)^*(z,\lambda) +$$

$$z^{-1}\,\frac{A(z)(P(z)\Sigma(z,\lambda) - P(z,\lambda)\Sigma(z)) + A(z,\lambda)(P(z,\lambda)\Sigma(z,m) - P(z)\Sigma(z))}{z^{-1}\Sigma(z)^2 - \Sigma(z,m)\Sigma(z,\lambda)} \tag{4.47}$$

Defining $\eta = \lim_{s=0}(sP(s))$ we have then:

$$\zeta(T,\lambda) \triangleq \lim_{z=1} \chi(z)\,(z-1) = \eta\,\frac{A^*(1)(\Sigma^*(1,m) - \Sigma^*(1)) + A^*(1,m)(\Sigma^*(1,\lambda) - \Sigma^*(1))}{\Sigma^*(1)^2 - \Sigma^*(1,m)\Sigma^*(1,\lambda)} \tag{4.48a}$$

$$\text{and } \lim_{z=1}\chi(z,\lambda)(z-1) = \eta\,\frac{A^*(1)(\Sigma^*(1,\lambda) - \Sigma^*(1)) + A^*(1,\lambda)(\Sigma^*(1,m) - \Sigma^*(1))}{\Sigma^*(1)^2 - \Sigma^*(1,m)\Sigma^*(1,\lambda)} \tag{4.48b}$$

$$= \zeta(T,1-\lambda) \quad \text{(by definition of } \zeta\text{)} \quad .$$

Recalling that condition I is satisfied if $P(s)$ has one pole at $s=0$, we conclude (in that case $\eta \neq 0$) that condition II of Theorem 3 is a consequence of condition I.

IV.6. Example of application of Theorem 3.

Let $L_{eq}(s) = \dfrac{2}{s(s+1)^2}$ and $G=1$. Consider $R(s) = \dfrac{1}{s}$.

Then $A(s) = \dfrac{2}{(s+2)(s^2+1)}$ and thus it can be seen that the L.T.I. system obtained is unstable (oscillatory). The corresponding system response is plotted on Fig. IV.9.

Suppose that $b=0$, $\alpha=0$ (C.I.) then:

$$P(s) = \frac{(s+1)^2}{s(s+2)(s^2+1)} \qquad \text{so } \eta = \lim_{s=0} sP(s) = \frac{1}{2}$$

$$A_1(s) = \frac{2}{s(s+2)(s^2+1)} = \frac{1}{s} + \Sigma(s) \quad \text{with} \quad \Sigma(s) = \frac{.2}{s+2} - \frac{.4(2s+1)}{s^2+1}$$

and thus:

$$\Sigma(z) = -\frac{.2z}{z-e^{-2T}} - .4\,\frac{2z(z-\cos T)+z\sin T}{z^2-2z\cos T+1}$$

$$\Sigma(z,\lambda) = -\frac{.2e^{-2\lambda T}}{z-e^{-2T}} - .4\,\frac{2(z\cos\lambda T-\cos mT)+z\sin\lambda T+\sin mT}{z^2-2z\cos T+1}$$

Besides:

$$A(z) = \frac{2}{5}\left(\frac{z}{z-e^{-2T}} - \frac{z(z-\cos T) - 2z\sin T}{z^2 - 2z\cos T + 1}\right)$$

$$A(z,m) = \frac{2}{5}\left(\frac{e^{-2mT}}{z-e^{-2T}} - \frac{(z\cos mT - \cos\lambda T) - 2(\sin mT + \sin\lambda T)}{z^2 - 2z\cos T + 1}\right)$$

$\zeta(T,\lambda)$ of (4.48a) and (4.48b) is then plotted on Fig. IV.8.a for different values of T and λ. (The reader should remember that $m \triangleq 1-\lambda$ so relations (4.48a) at $\lambda = .2$ say corresponds also to relation (4.48b) at $m = .8$).

Condition II of Theorem 3 implies that we should satisfy:

$\exists\ T,\lambda$ such that $\zeta(T,\lambda) = \zeta(T,1-\lambda) = 0$ (4.49)

From Fig. IV.8.a (4.49) is satisfied for: $3 < T < 5$ and $.1 < \lambda < .2$, and therefore this region is magnified on Fig. IV.8.b.

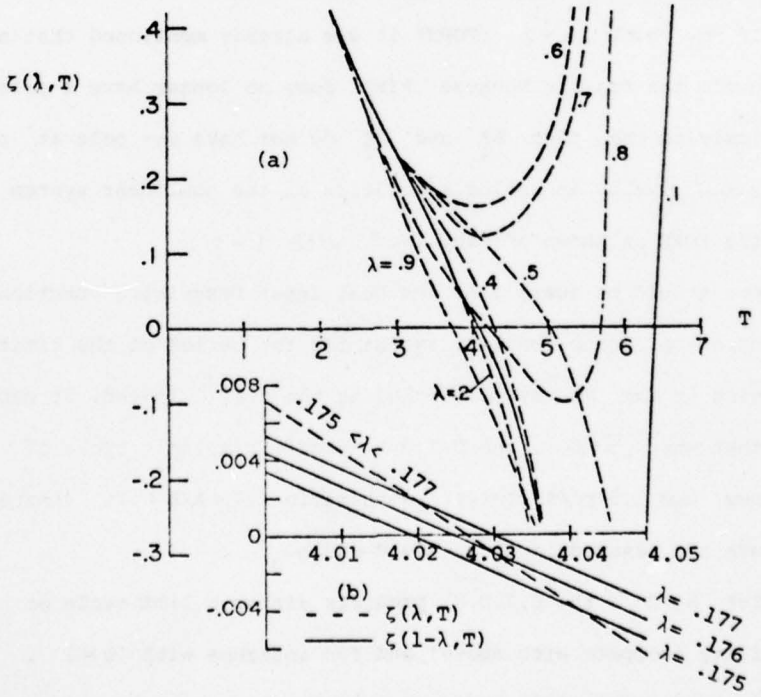

Figure IV.8. Plot of $\zeta(\lambda,T)$ versus T, for the characterization of a limit cycle with two resets per cycle.

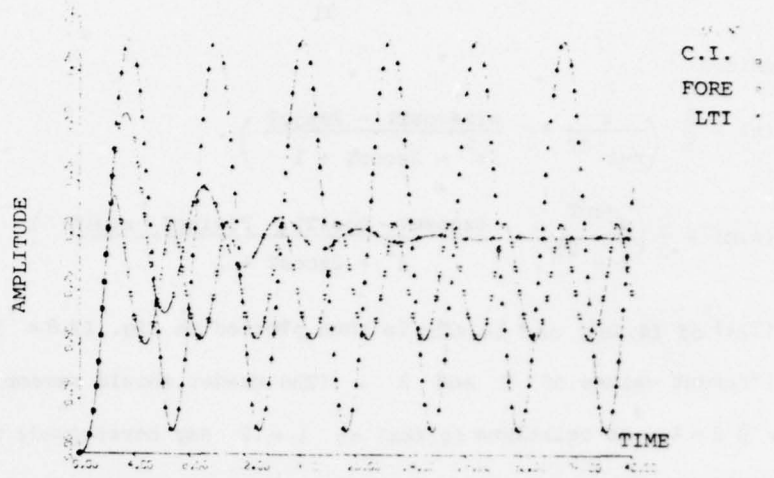

Figure IV.9. Comparison of the three system step responses.

Thus Theorem 3 predicts a limit cycle of period T such that $4.02 < T < 4.03$ with λ such that $.176 < \lambda < .177$. This is then confirmed by an analog simulation of the nonlinear system including a C.I. as shown on Fig. IV.9.

If now $b \neq 0$, $\alpha = 0$ (FORE) it was already mentioned that no limit cycle can sustain because $P(s)$ does no longer have a pole at $s = 0$ implying then that Δ_1^* and Δ_2^* do not have any pole at $z = 1$. This is confirmed by an anolog simulation of the nonlinear system including FORE as shown on Fig. IV.9, with $b = 1$.

One should be aware that the Dual Input Describing Functions [G2] give, here too, wrong results, except for the period of the limit cycle sustaining in the NL system including the C.I. Indeed, it can be shown that when $b = 0$, the D.I.D.F. predicts a limit cycle of frequency $\omega_0 \approx 1.5$ rd/s ($T \approx 4$s) with ratio $.7 < A/B < .75$ (instead of .5) where the assumed input is $x = B + A\sin\omega_0 t$.

For $b \neq 0$, the D.I.D.F. predicts either a limit cycle or instability (compare with above) and for instance with $b = 1$, a limit cycle is predicted, characterized by $1. < \omega_0 < 1.1$ and a ratio $.8 < A/B < .9$.

CHAPTER V. GENERALIZATIONS OF FORE.

V.1. Introduction.

The C.I. has been generalized into FORE. It is therefore natural to think about possible generalizations of FORE. One way is by resetting the output y whenever the input $x = \alpha \neq 0$. However, nothing is gained by doing this when both positive and negative command inputs are to be applied to the system. Resetting for $x = |a| \neq 0$ is conceivable but the performances for two input signals $x(t)$ and $k \cdot x(t)$, with k real $\neq 0$, would no longer be proportional with ratio k and this is certainly a big weakness if the objective is to guarantee T.D.S. of a linear type.

Another way to generalize, is to extend FORE to LLRE (Lead-Lag ...) $= \left(\frac{s+b}{s+a}\right)^*$, SORE (second-order ...) $= \left(\frac{1}{(s+b)(s+a)}\right)^*$, TORE (third-order ...) $= \left(\frac{1}{(s+a)(s+b)(s+c)}\right)^*$ etc..., and in a very general manner to $g(s)^*$, where $g(s)$ is any rational transfer function whose output y is reset whenever the input x is zero. (Fig. V.1)

V.2. First equivalent representation of g^*.

Let $\theta = \{t_K : x(t_K) = 0\}$ be the set of reset instants. Then:

$$y(t) = \int_0^t x(\zeta)g(t-\zeta)d\zeta - \sum_{K=1}^{\infty} \int_{t_{K-1}}^{t_K} x(\zeta)g(t-\zeta)d\zeta \; u(t-t_K)$$

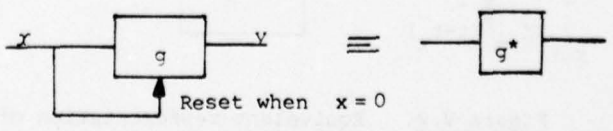

Figure V.1. General reset element (Equivalent notation).

Suppose we restrict G to elements with m real poles, so

$$g(t) = h_0\delta(t) + \sum_{i=1}^{m} A_i e^{-\alpha_i t}$$

Thus:

$$y(t) = \int_0^t x(\zeta)g(t-\zeta)d\zeta - \sum_{i=1}^{m} A_i \sum_{K=1}^{\infty} \int_{t_{K-1}}^{t_K} x(\zeta)e^{-\alpha_i(t_k-\zeta)}d\zeta \int_0^t e^{-\alpha_i(t-\tau)}\delta(\tau-t_K)d\tau$$

or if $x^*_{K,i} \triangleq \int_{t_{K-1}}^{t_K} e^{-\alpha_i(t_K-\zeta)}x(\zeta)d\zeta$ with $t_K \in \theta$

$$y(t) = \int_0^t x(\zeta)g(t-\zeta)d\zeta - \sum_{K=1}^{\infty}\sum_{i=1}^{m} A_i\, x^*_{K,i} \int_0^t e^{-\alpha_i(t-\tau)}\delta(\tau-t_K)d\tau \quad ,$$

leading to the equivalent representation shown on Fig. V.2.

If g^* is imbedded in the feedback system of Fig. V.3.a, it can be replaced by its equivalent representation of Fig. V.2. Therefore, by application of the superposition theorem to all the signals, the output $c(t)$ can be computed by using the equivalent representation

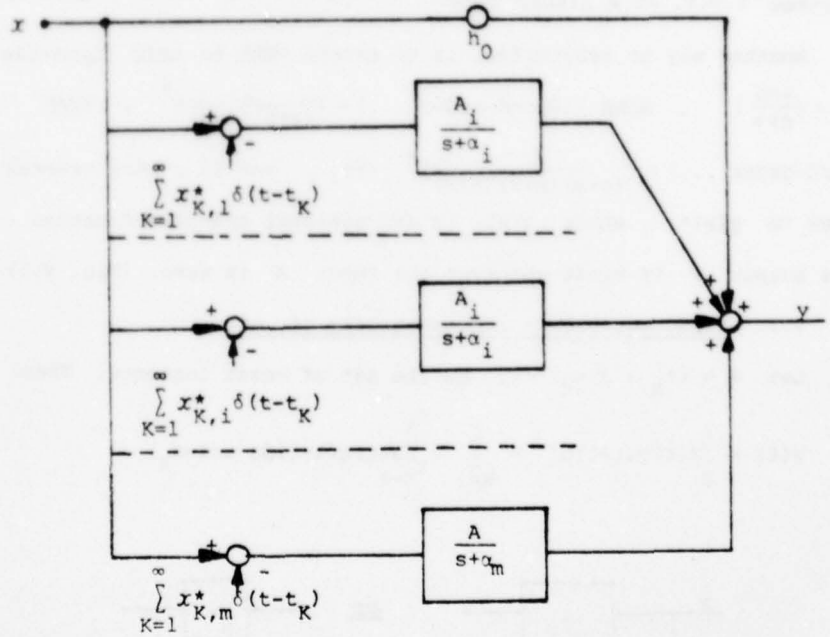

Figure V.2. Equivalent representation of g^* .

of Fig. V.3.b. Using such a representation it is possible to derive charts similar to Fig.III.10 for any specific g . If one is then to choose α_i , $i = 1,\ldots m$ such that $g(s)^* \simeq g(s)$ from the command input point of view, the design philosophy used with FORE can then be applied here too. This was used for instance with LLRE, but no improvement over FORE could be noticed.

V.3. Second equivalent representation: stability criterion.

If we restrict ourselves to elements $G(s)$ such that:

$$g(t) = \sum_{i=1}^{m} A_i e^{-\alpha_i t} \quad \text{then:}$$

$$y(t) = \int_{t_0}^{t} x(\zeta) g(t-\zeta)\, d\zeta - \sum_{K=1}^{N} \sum_{i=1}^{m} \int_{t_{K-1}}^{t_K} A_i e^{-\alpha_i (t-\zeta)} x(\zeta)\, d\zeta \; u(t-t_K) \qquad (5.0)$$

Using: $\int_{t_{K-1}}^{t_K} = \int_{0}^{t_K} - \int_{0}^{t_{K-1}}$ we have:

$$y(t) = \int_{t_0}^{t} x(\zeta) g(t-\zeta)\, d\zeta - \sum_{i=1}^{m} \sum_{K=1}^{N} e^{-\alpha_i (t-t_K)} \int_{0}^{t_K} A_i e^{-\alpha_i (t_K-\zeta)} x(\zeta)\, d\zeta$$

$$[u(t-t_K) - u(t-t_{K+1})] \qquad (5.1)$$

and therefore, by anology with the previous chapter, (section IV.3) the system of Fig. V.1 is equivalent to that of Fig. V.4, where

$\sigma_K \triangleq t_K - t_{K-1}$ and $B_i(s) = \dfrac{1-e^{-(s+\alpha_i)\sigma_K}}{s+\alpha_i}$. $\quad \vartheta_i = \sum_K x^*_{K,i}\, \delta(t-t_K)$

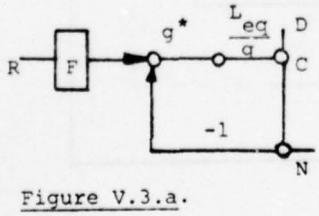

Figure V.3.a.

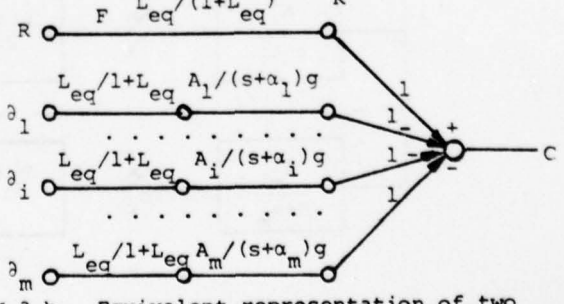

Figure V.3.b. Equivalent representation of two degree of freedom structure.

As before, this equivalent representation is very suitable for stability analysis. Let us now consider the closed loop nonlinear feedback system of Fig. V.3.a (with F=1) in which g(s)* is imbedded. If, as $t\to\infty$, a limit cycle with one reset per cycle sustains, it means that $\sigma_K \to T$ a constant number and therefore, using Fig. V.4, the N.L. feedback system of Fig. V.3.a becomes, at the steady state, equivalent to the purely linear sampled data system shown on Fig. V.5.

It can be easily seen that (4.10) can be generalized, giving:

$$\varepsilon_i^*(z) = \frac{\mu_i}{z-1} \quad \frac{z}{z-e^{-\alpha_i T}} \qquad (5.2) \quad \text{for} \quad i = 1, 2 \ldots m$$

where $\mu_i = \lim_{K\to\infty} x^*_{K,i} = \lim_{t_K\to\infty} \int_{t_{K-1}}^{t_K} e^{-\alpha_i(t_K-\zeta)} x(\zeta)d\zeta$. We can then write

$$\text{(Fig. V.5)} \quad x = \frac{R}{1+L} + \sum_{i=1}^{m} \varepsilon_i^* \frac{B_i}{g} \frac{L}{1+L} \qquad (5.3)$$

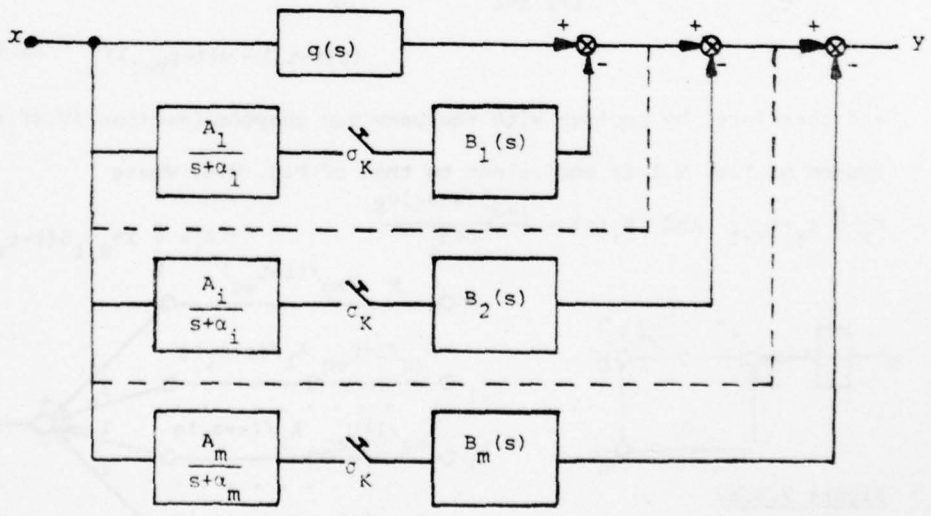

Figure V.4. Second equivalent representation of G* .

If $g_i \triangleq \frac{A_i}{s+\alpha_i}$, then $\varepsilon_\ell = xg_\ell = \frac{Rg_\ell}{1+L} + \sum_{i=1}^{m} \varepsilon_i^* \frac{B_i g_\ell}{g} \frac{L}{1+L}$

for $\ell = 1,2...m$. So:

$$(5.4)\quad \begin{bmatrix} 1-\left(\frac{B_1 g_1}{g}\frac{L}{1+L}\right)^* & -\left(\frac{B_2 g_1}{g}\frac{L}{1+L}\right)^* \cdots & -\left(\frac{B_m g_1}{g}\frac{L}{1+L}\right)^* \\ -\left(\frac{B_K g_1}{g}\frac{L}{1+L}\right)^* \cdots & 1-\left(\frac{B_K g_K}{g}\frac{L}{1+L}\right)^* \cdots & \\ -\left(\frac{B_m g_1}{g}\frac{L}{1+L}\right)^* \cdots & & 1-\left(\frac{B_m g_m}{g}\frac{L}{1+L}\right)^* \end{bmatrix} \begin{bmatrix} \varepsilon_1^* \\ \varepsilon_K^* \\ \varepsilon_m^* \end{bmatrix} = \begin{bmatrix} \left(\frac{Rg_1}{1+L}\right)^* \\ \left(\frac{Rg_K}{1+L}\right)^* \\ \left(\frac{Rg_m}{1+L}\right)^* \end{bmatrix}$$

and:

$$x^* = \left(\frac{R}{1+L}\right)^* + \sum_{i=1}^{m} \varepsilon_1^* \left(\frac{B_i}{g}\frac{L}{1+L}\right)^* \qquad (5.5)$$

If a limit cycle of period T with one reset/cycle exists, then $x^*_{K,i}$ has a constant value μ_i and in virtue of (5.2),

$\varepsilon_i^*(z) = \frac{\mu_i}{(z-1)} \frac{z}{z-e^{-\alpha_i T}}$ for $i = 1,2...m$. The converse is obvious.

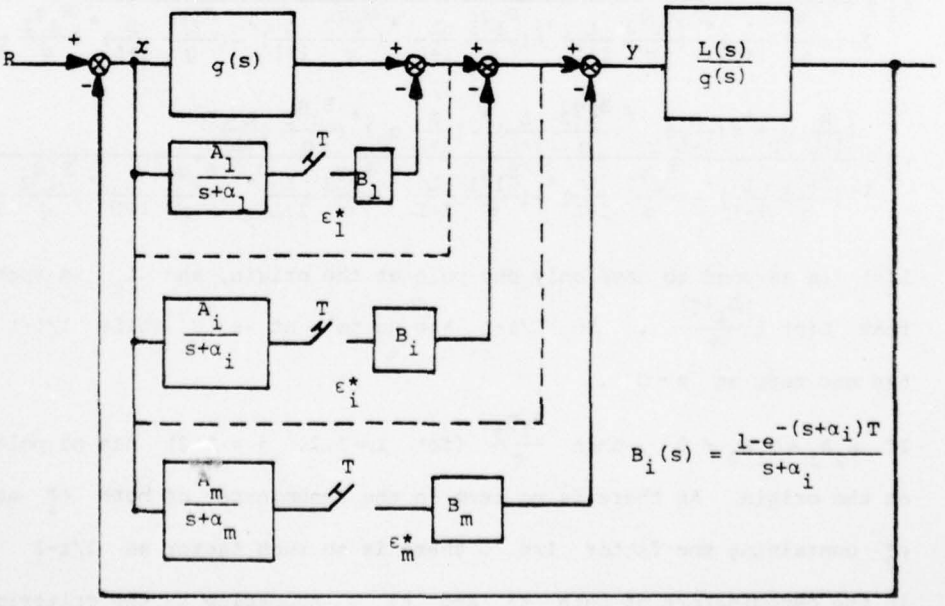

Figure V.5. Equivalent system when the nonlinear feedback system sustains a limit cycle with one reset/cycle.

By anology with Theorem 2 we can state:

If in the neighborhood of $t=\infty$, there exists, for the system of Fig. V.5, some finite nonzero numbers T, $\mu_1, \ldots \mu_m \in \mathcal{R}$ such that:

$$\text{I} \quad \lim_{z=1} (z-e^{-\alpha_i T})(z-1)\, \varepsilon_i^*(z) = \mu_i \quad \text{for } i = 1,2\ldots m \tag{5.6}$$

$$\text{II} \quad \lim_{z=1} (z-1)\, x^*(z) = 0 \tag{5.6a}$$

then a limit cycle with one reset/cycle exists.

V.4. Application: 'LL FORE'.

In general it is not necessary, as previously, to solve (5.6) and (5.6a) algebraically if one is less interested in the specific value of T than in the existence of a limit cycle.

This will now be illustrated by considering the simple example, $m=2$, i.e., $g(s) = \frac{A_1}{s+\alpha_1} + \frac{A_2}{s+\alpha_2} = g_1 + g_2$. (5.4) is used in order to get:

$$\varepsilon_1^* = \frac{(\frac{R}{1+L}\, g_1)^* + (\frac{R}{1+L}\, g_2)^* (\frac{B_2 g_1}{g}\, \frac{L}{1+L})^* - (\frac{R}{1+L}\, g_1)^* (\frac{B_2 g_2}{g}\, \frac{L}{1+L})^*}{1-(\frac{B_1 g_1}{g}\, \frac{L}{1+L})^* - (\frac{B_2 g_2}{g}\, \frac{L}{1+L})^* + (\frac{B_1 g_1}{g}\, \frac{L}{1+L})^* (\frac{B_2 g_2}{g}\, \frac{L}{1+L})^* - (\frac{B_2 g_1}{g}\, \frac{L}{1+L})^* (\frac{B_1 g_2}{g}\, \frac{L}{1+L})^*}$$

$$\varepsilon_2^* = \frac{(\frac{R}{1+L}\, g_2)^* + (\frac{R}{1+L} g_1)^* (\frac{B_1 g_2}{g}\, \frac{L}{1+L})^* - (\frac{R}{1+L}\, g_2)^* (\frac{B_1 g_1}{g}\, \frac{L}{1+L})^*}{1-(\frac{B_1 g_1}{g}\, \frac{L}{1+L})^* - (\frac{B_2 g_2}{g}\, \frac{L}{1+L})^* + (\frac{B_1 g_1}{g}\, \frac{L}{1+L})^* (\frac{B_2 g_2}{g}\, \frac{L}{1+L})^* - (\frac{B_2 g_1}{g}\, \frac{L}{1+L})^* (\frac{B_1 g_2}{g}\, \frac{L}{1+L})^*}$$

$L(s)$ is assumed to have only one pole at the origin, and L_1 is such that $L(s) \triangleq \frac{L_1(s)}{s}$. So $L/1+L$ has no pole at $s=0$ while $1/1+L$ has one zero at $s=0$.

If $\alpha_2 A_1 + \alpha_1 A_2 \neq 0$, then $\frac{B_1 g_j}{g}$ (for $i=1,2$, $j=1,2$) has no pole at the origin. As there is no term in the denominator of both ε_1^* and ε_2^* containing the factor $1/s$, there is no such factor as $1/z-1$ in the denominators of both ε_1^* and ε_2^*. According to the criterion

there exists a limit cycle if ε_1^* and ε_2^* contain the factor $1/z-1$, Therefore, this can only occur here if the numerators of both ε_1^* and ε_2^* contain such a factor, i.e. for "type 2" inputs R, and especially with ramp inputs. Indeed, $R/1+L$ has then a pole at the origin and the residue at $z=1$ of the number ε_i^* is $\frac{A_i}{\alpha_i L_1(0)}$ $(i=1,2)$ which is finite non zero.

The stability criterion then implicitely suggests the insertion of a zero at $s=0$ in G, i.e. to choose A_1, A_2, α_1, α_2 such that $A_1\alpha_2 + A_2\alpha_1 = 0$ (5.7) if one is to avoid limit cycles with "type 2" inputs. Indeed we have then:

$$\frac{B_1 g_1}{g}\frac{L}{1+L} = (1-z^{-1}e^{-\alpha_1 T})\left(\frac{A_1}{A_1+A_2}\frac{s+\alpha_2}{s}\,Q(s)\right), \text{ with } Q(s) \triangleq \frac{L(s)}{1+L(s)}$$

$$= (1-z^{-1}e^{-\alpha_1 T})\frac{A_1}{A_1+A_2}\left[\frac{\alpha_2 Q(0)}{s} + \Sigma_1(s)\right] \text{ (after fractional expansion).}$$

$$\frac{B_2 g_2}{g}\frac{L}{1+L} = (1-z^{-1}e^{-\alpha_2 T})\frac{A_2}{A_1+A_2}\left[\alpha_1\frac{Q(0)}{s} + \Sigma_2(s)\right]$$

$$\frac{B_2 g_1}{g}\frac{L}{1+L} = (1-z^{-1}e^{-\alpha_2 T})\frac{A_1}{A_1+A_2}\left[\alpha_2\frac{Q(0)}{s} + \Sigma_1(s)\right]$$

$$\frac{B_1 g_2}{g}\frac{L}{1+L} = (1-z^{-1}e^{-\alpha_1 T})\frac{A_1}{A_1+A_2}\left[\alpha_1\frac{Q(0)}{s} + \Sigma_2(s)\right]$$

The denominator of both ε_1^* and ε_2^* is then:

$$1-(1-z^{-1}e^{-\alpha_1 T})\frac{A_1}{A_1+A_2}\frac{\alpha_2 Q(0)}{1-z^{-1}} - (1-z^{-1}e^{-\alpha_2 T})\frac{A_2}{A_1+A_2}\frac{\alpha_1 Q(0)}{1-z^{-1}}$$

$$+ \frac{Q(0)\,(1-z^{-1}e^{-\alpha_1 T})(1-z^{-1}e^{-\alpha_2 T})}{(A_1+A_2)(1-z^{-1})}\Big(\Sigma_1(z)A_2\alpha_1 + \Sigma_2(z)A_1\alpha_2 - \Sigma_1(z)A_2\alpha_1 - \Sigma_2(z)A_1\alpha_2\Big)$$

$$+ \frac{(1-z^{-1}e^{-\alpha_1 T})(1-z^{-1}e^{-\alpha_2 T})A_1A_2\,Q(0)}{(A_1+A_2)\,(1-z^{-1})^2}(\alpha_1\alpha_2 - \alpha_1\alpha_2) + P(z)$$

AD-A046 012 COLORADO UNIV BOULDER SYSTEMS ENGINEERING LAB F/G 12/2
REDUCTION OF THE COST OF FEEDBACK IN SYSTEMS WITH LARGE PARAMET--ETC(U)
AUG 77 P ROSENBAUM, I HOROWITZ AFOSR-76-2946

UNCLASSIFIED AFOSR-TR-77-1224 NL

2 OF 3
AD
A046012

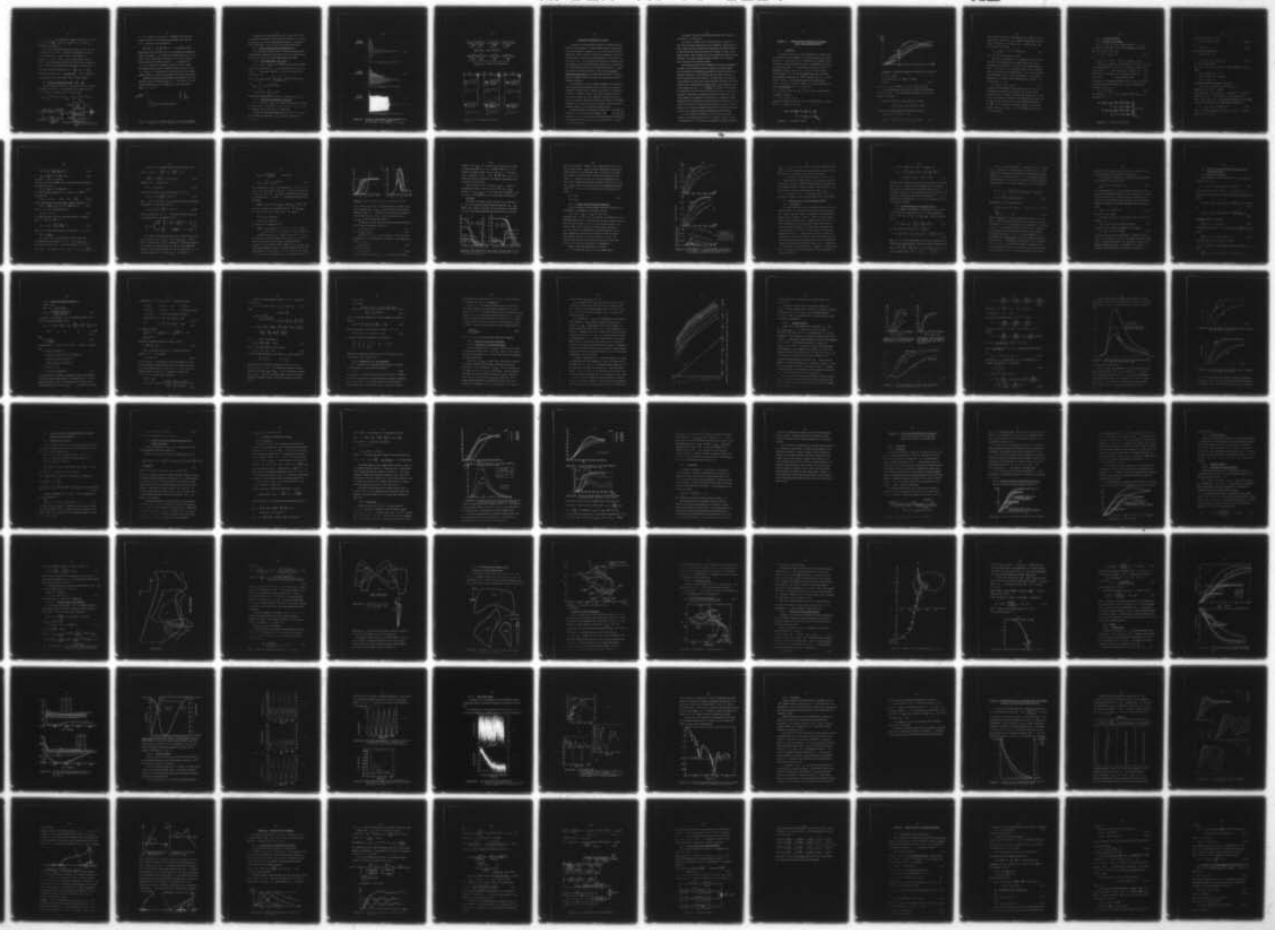

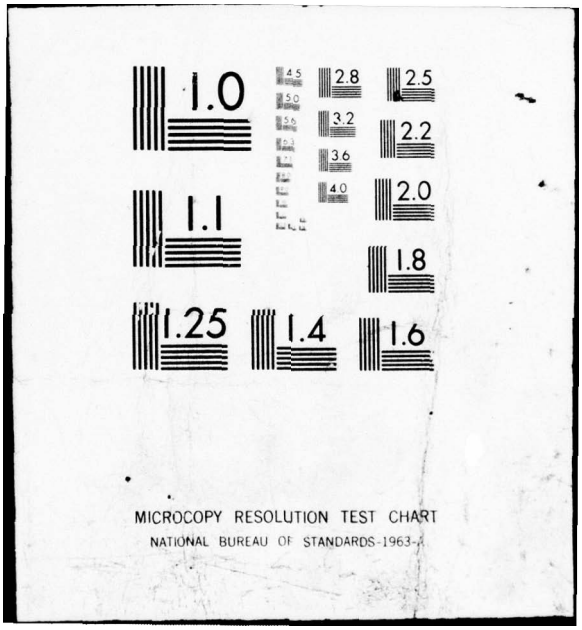
1.0
1.1
1.25
1.4
1.6
1.8
2.0
2.2
2.5
2.8
3.2
3.6
4.0
4.5
5.0
MICROCOPY RESOLUTION TEST CHART
NATIONAL BUREAU OF STANDARDS-1963-A

where $P(1) \neq \infty$. So the denominator contains now the factor $1/1-z^{-1}$ with a residue $\frac{Q(0)}{A_1+A_2}\ (A_1\alpha_2 e^{-\alpha_1 T} + \alpha_1 A_2 e^{-\alpha_2 T}) \neq 0$ because by assumption $A_1\alpha_2 + \alpha_1 A_2 = 0$.

It is easily seen that the numerators of both ε_1^* and ε_2^* have no such term as $1/(1-z^{-1})^2$. Therefore, the numerators of both ε_1^* and ε_2^* have at most, a term in $1/1-z^{-1}$ and therefore if $A_1\alpha_2 + \alpha_1 A_2 = 0$ both ε_1^* and ε_2^* do not contain such a factor as $1/1-z^{-1}$, preventing then the system from limit cycling in presence of "type 2" inputs, and in particular with ramp-inputs. Relation (5.7) is for instance satisfied by choosing $A_1 = -\frac{\alpha_1}{\alpha_2-\alpha_1}$ and $A_2 = \frac{\alpha_2}{\alpha_2-\alpha_1}$ leading to the element $G(s)^* = \left(\frac{s}{(s+\alpha_1)(s+\alpha_2)}\right)^*$ that is referred to as a Lead - Lag - and - First-Order - Reset - Element (LLFORE).

V.5. Synthesis procedure with LLFORE $\left(\frac{s}{s+\alpha}\ \ \frac{1}{s+b}\right)^*$

Using the results of section V.2 (Fig. V.3.a and b) the nonlinear feedback system of Fig. V.6.a is equivalent from the output signals point of view to the linear system of Fig. V.6.b with:

$$x^*_{K,1} \triangleq \int_{t_{K-1}}^{t_K} e^{-b(t-\zeta)} x(\zeta)\,d\zeta = x^*_{K_{FORE}} \qquad x^*_{K,2} = \int_{t_{K-1}}^{t_K} e^{-\alpha(t-\zeta)} x(\zeta)\,d\zeta$$

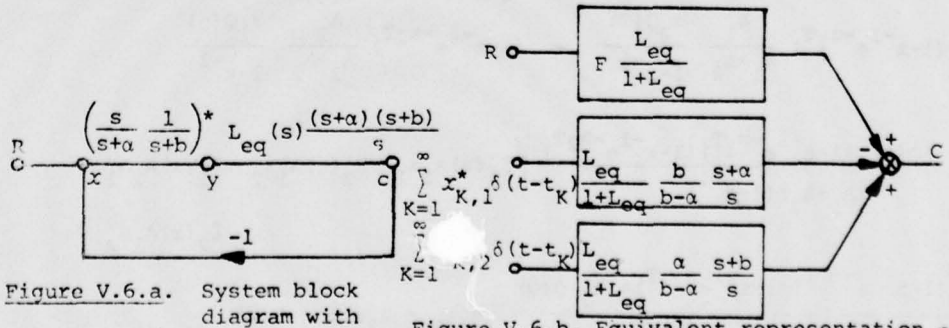

Figure V.6.a. System block diagram with LLFORE.

Figure V.6.b. Equivalent representation of a feedback system containing an LLFORE.

If α is so chosen as to satisfy $\alpha <<$ Bandwidth of the open loop transfer function for all possible plant parameter, then obviously $\alpha << b$, therefore we can consider that:

$$\frac{b}{b-\alpha}\ \frac{s+\alpha}{s} \approx 1 \quad \text{and} \quad \frac{\alpha}{b-\alpha}\ \frac{s+b}{s} \approx 0$$

and therefore LLFORE behaves practically like FORE. This is in accordance with experimental results: the design L_1 of chapter III was used and on Fig. V.7 it is shown, for the maximum plant gain factor, the non linear step disturbance response for different values of α. As expected, for $\alpha \lesssim 1$ rps. (compared to a bandwidth of 600 rps.) there is hardly any difference from the result obtained with FORE (see Fig. III.20.b (f 1)), while as α increases up to 10,000 rps., the nonlinear system response tends to be like the one obtained with a purely linear system.

Therefore the design procedure derived with FORE needs only to be completed here by a suitable choice of α. Since (Fig. III.13) the minimum bandwidth of $L_{eq}(s)$ is roughly 6 rps., one can choose for example α = .01 rps.

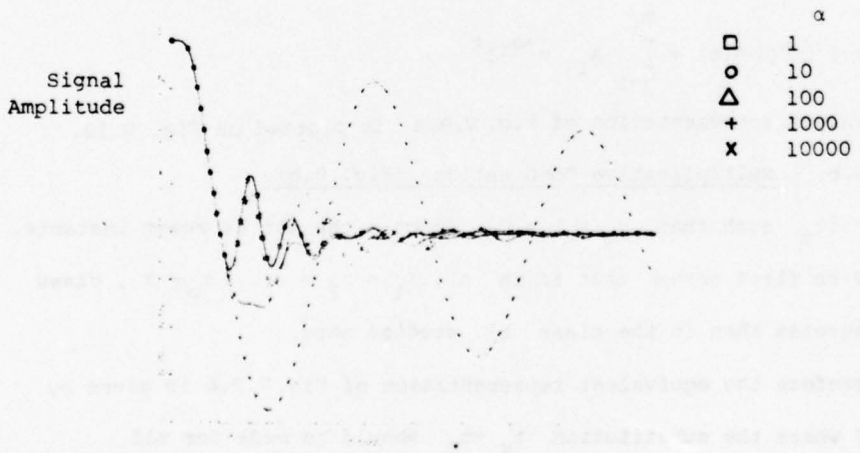

Figure V.7. System step disturbance response of the nonlinear feedback system at $k = 1000$ for different values of the parameter α.

As expected, one notes from Fig. V.8.a,b,c that no limit cycle is sustained in presence of a ramp input for all values of α , but it is seen that the transient gets bigger and bigger as α decreases, which is reminiscent of the limit cycle that existed with FORE.

V.6. Serial and multiplicative combination of G's.

It is worthwhile to mention that g* can itself be generalized by considering a system of the type shown on Fig. V.9.a or of the type shown on Fig. V.9.b, or any system which combines both types.

V.6.a. Serial Combination (Fig. V.9.a).

If $\tau_i = \{t_{K_i}$, $y_i(t_{K_i}) = 0\}$ denotes the set of reset instants associated with the input y_i , it is then obvious that $\tau_0 \subset \tau_1 \subset \tau_2 \ldots \subset \tau_{p-1}$. If we assume that each g_i has m_i real poles, then for $i = 1,2,\ldots p$.

$$y_i(t) = \int_0^t y_{i-1}(\zeta) g_i(t-\zeta)\, d\zeta - \sum_{j=1}^{m_i} A_{ij} \sum_{K_i=1}^{N} x^*_{K_i j} \int_0^t e^{-\alpha_{ij}(t-\zeta)} \delta(\zeta - t_{K_i})\, d\zeta$$

where

$$x^*_{K_i l} = \int_{t_{K_i - 1}}^{t_{K_i}} y_i(\zeta) e^{-\alpha_{ij}(t_{K_i} - \zeta)}\, d\zeta \ .$$

and

$$g_i(t) \triangleq h_{0i}\, \delta(t) + \sum_{j=1}^{m_i} A_{ij}\, e^{-\alpha_{ij} t}$$

The equivalent representation of Fig. V.9.a is plotted on Fig. V.10.

V.6.b. Multiplicative Combination (Fig. 9.b).

$\tau = \{t_K$ such that $y_0(t_K) = 0\}$ denotes the set of reset instants. It should be first noted that if in a), $\tau_1 = \tau_2 = \ldots = \tau_p = \tau$, class a) degenerates then in the class b) studied here.

Therefore the equivalent representation of Fig. V.9.b is given by Fig. V.10 where the substitution $t_{K_i} = t_K$ should be made for all $i = 1,2,\ldots p$.

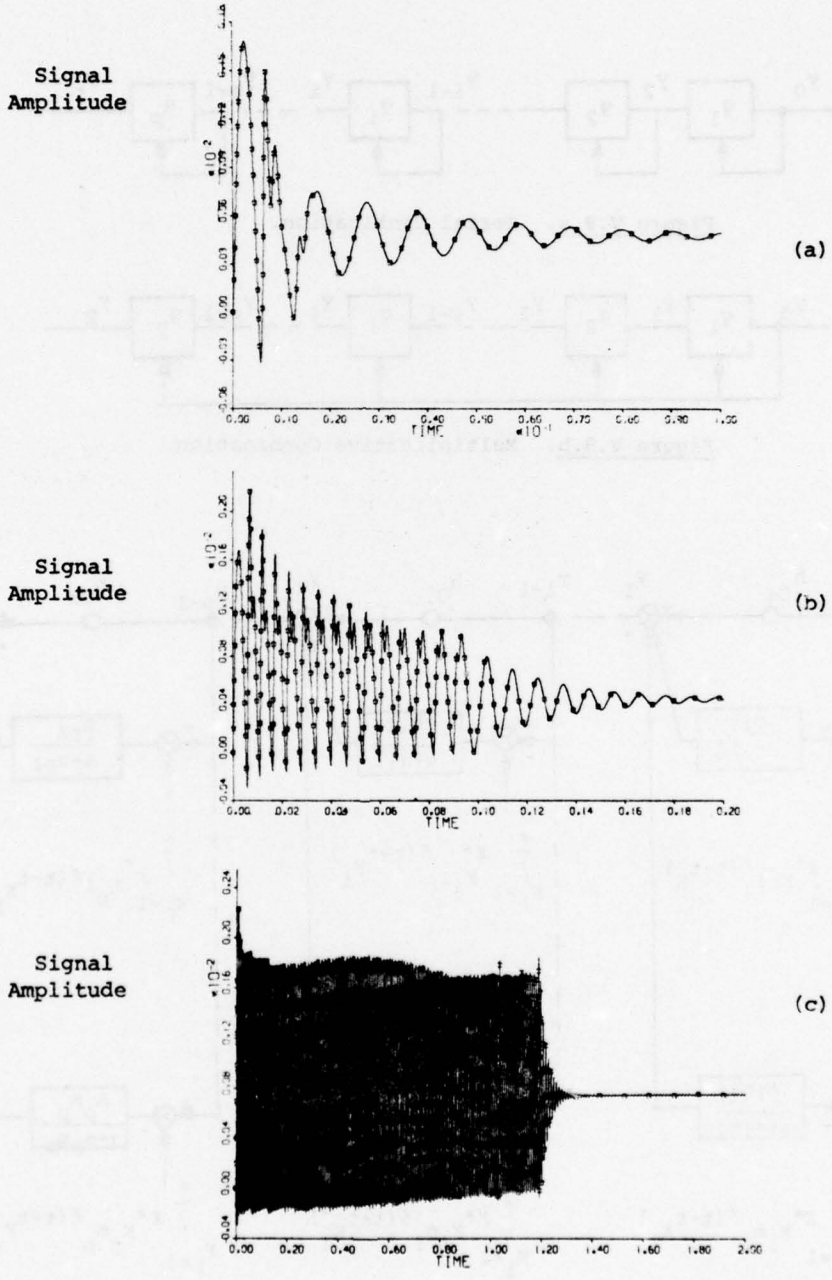

Figure V.8. Nonlinear system response to ramp disturbance for different values of the parameter α .
a) $\alpha = 100$ rps , b) $\alpha = 10$ rps , c) $\alpha = 1$ rps

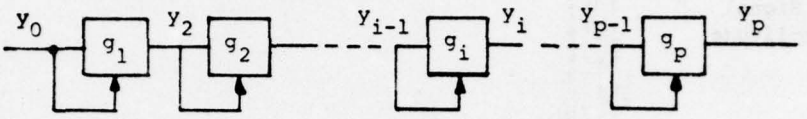

Figure V.9.a. Serial Combination.

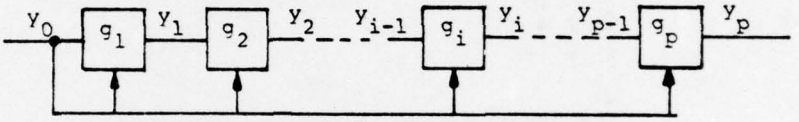

Figure V.9.b. Multiplicative Combination.

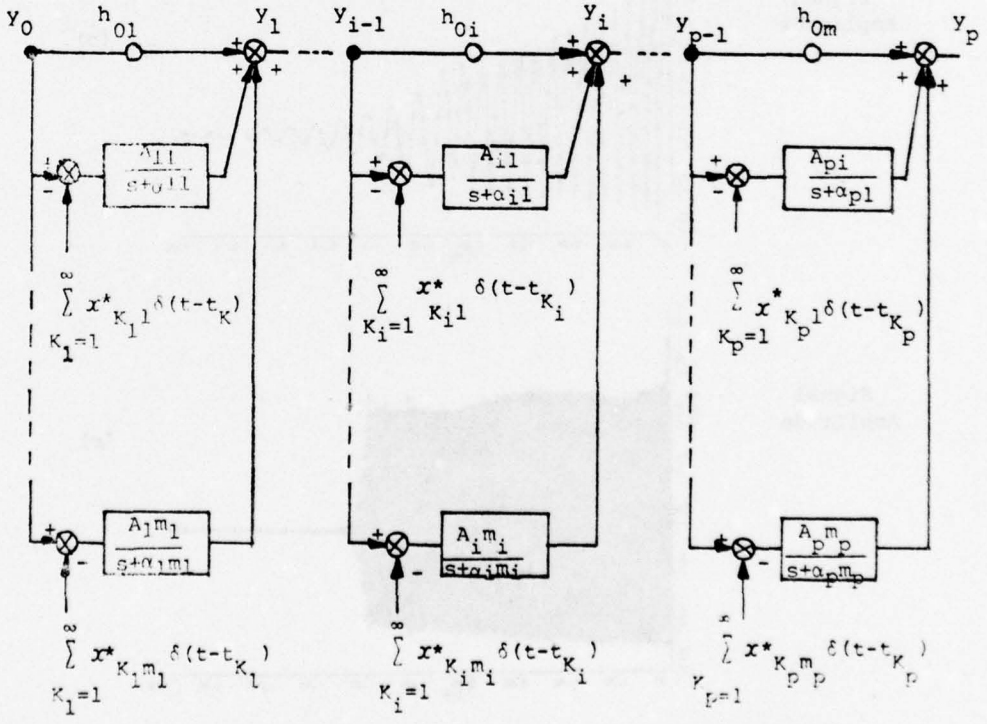

Figure V.10. Equivalent representation.

CONCLUSIONS TO CHAPTERS III , IV & V .

A systematic engineering design procedure for drastically reducing the 'cost of feedback' of linear feedback systems has been presented and illustrated in chapter III. It is clear that the nonlinear compensation (FORE) introduced is justified in problems of large parameter uncertainty, and that the design procedure is a general one for this problem class. The nonlinear design permits the attainment of the same command and disturbance performance tolerances as a linear design, but with significantly smaller loop transmission bandwidth. An important feature of the design procedure is that it permits design to quantitative specifications, a property generally lacking in present nonlinear feedback synthesis techniques, for systems with significant parameter uncertainty.

It is important to note the inherent assumption in that chapter, that the primary design problem is that of satisfying the response tolerances to command inputs. However, realistically, consideration is also given to disturbance inputs in the form of steps at the output, with assigned restrictions on the damping of the resulting output. Since the disturbance response is nonlinear (in contrast to the command response which is essentially linear), one cannot in general guarantee acceptable response to all possible disturbance inputs.

Therefore emphasis was then placed (chapter IV) on the stability problem for this class of nonlinear systems. Sufficient conditions were derived for B.I.B.O. stability and it was conjectured that the nonlinear system possesses B.I.B.O. stability, if the equivalent L.T.I. system is asymptotically stable.

Furthermore, necessary and sufficient conditions were derived for the existence of a limit cycle.

The results of chapters III & IV were then used in chapter V to derive the new element LLFORE which can be considered a generalization of FORE. Indeed, the latter improves the performances of FORE with respect to ramp disturbances (and more generally with respect to "type 2" disturbance inputs), without harming any of the quantitative benefits obtained with FORE. The design procedure derived in chapter III is therefore easily extended to this nonlinear element.

The philosophy and motivation prompting the nonlinear compensation, is based on linear frequency concepts, coupled with linear feedback design techniques for guaranteeing performance tolerances despite large parameter uncertainty. This philosophy has thus proven itself as at least one approach worthy of pursuing. One might search for other nonlinear elements with even greater phase advantages than FORE, over linear elements with the same magnitude characteristic. As an example the nonlinear element such that: $y = \begin{cases} + \int x(\zeta)d\zeta & \text{if } x\dot{x} > 0 \\ - \int x(\zeta)d\zeta & \text{if } x\dot{x} < 0 \end{cases}$ is a "0° phase lag integrator" from the describing function point of view. With FORE, the equivalent linear phase lag useable was shown to be almost 180°. Nonlinear elements can undoubtedly be found which in a describing function charaterization, would permit even greater phase lag. However, as with the 0° phase lag integrator, the more difficult challenge is to find a characterization of the nonlinear element useable for the useful system control signals, and so permitting design to quantitative specifications.

It will certainly be worthwhile in the future to extend this research to multivariable systems, once a rigorous synthesis procedure is available for L.T.I. multivariable systems with large plant ignorance.

CHAPTER VI. LINEAR TIME VARYING COMPENSATION OF FEEDBACK SYSTEMS WITH NONSTATIONARY INPUTS.

VI.1 Introduction

It was noted (section II.3) that the typical set of command inputs to a system can often be imbedded in the set of non-stationary processes. Therefore, it is expected that L.T.V. compensation in a feedback system will result in better performances than L.T.I. compensation, with respect to sensor noise effects. It is implied that the instant of input (R) application is known. Given (F,G) (Fig. VI.1), we get different output responses $c_i(t)$ for the same command input, due to different plant parameter combinations $P_i \in \mathcal{P}$, as shown in Fig. VI.2. At each instant of time t_0, the maximum spread is then characterized by $\Delta c(t_0)$ (Fig. VI.2). The L.T.V. networks F,G can be associated [S5] with L.T.V. operators f,g, i.e. (Fig. VI.1):

$v(t) = \int_0^t f(t,\zeta)\, r(\zeta)\, d\zeta$ and $x(t) = \int_0^t g(t,\zeta)\, e(\zeta)\, d\zeta$ can be written in the symbolic notations:

$$v = f \cdot r \quad \text{and} \quad x = g \cdot e \ .$$

Therefore, the effect of the noise $n(t)$ at the plant input x (assuming $R = 0$) is given by: (Fig. VI.1)

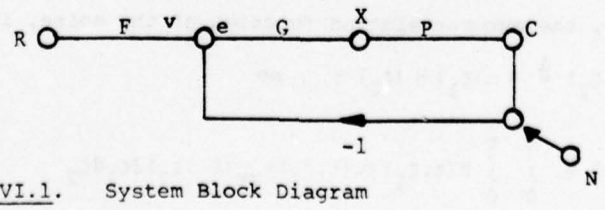

Figure VI.1. System Block Diagram

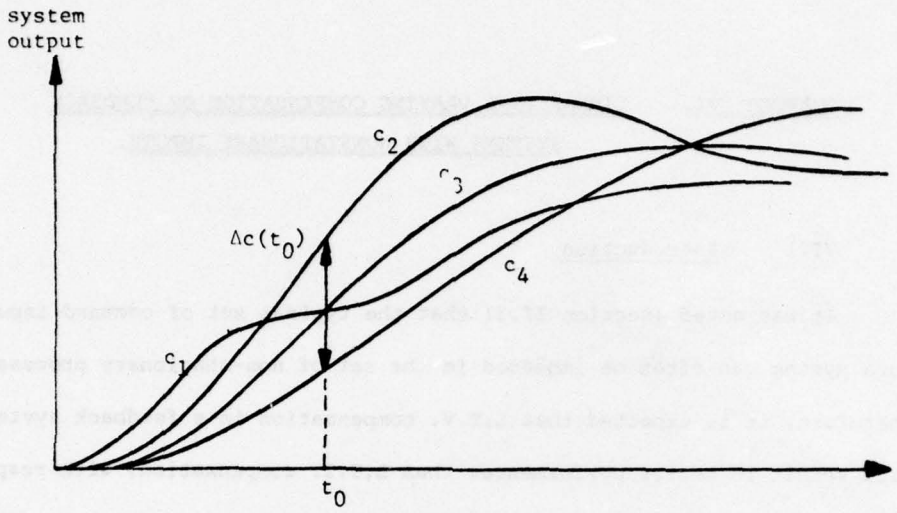

Figure VI.2. System Output Response for Different Plant Parameters

$$x_n = -g \cdot n \quad -g \cdot p \cdot x_n$$

$$x_n = -(1+g \cdot p)^{-1} \cdot g \cdot n \quad \text{if} \quad (1+g \cdot p)^{-1} \quad \text{exists.}$$

$$x_n \triangleq \theta \cdot n \qquad (6.1.a)$$

where θ is a L.T.V. operator, i.e. $x_n(t) = \int_0^t \theta(t,\zeta)\, n(\zeta) d\zeta$.

The mean square value of the noise at the plant input defined as $\sigma^2_{P.I.}(t) = \langle x_n(t)^2 \rangle$, where the bracket sign stands for the ensemble-average, is therefore:

$$\sigma^2_{P.I.}(t) = \left\langle \int_0^t \theta(t,\zeta_1)\, n(\zeta_1) d\zeta_1 \int_0^t \theta(t,\zeta_2)\, n(\zeta_2) d\zeta_2 \right\rangle$$

$$= \int_0^t \int_0^t \theta(t,\zeta_1)\, \theta(t,\zeta_2) \langle n(\zeta_1)\, n(\zeta_2) \rangle d\zeta_1 d\zeta_2 \quad .$$

By definition, the autocorrelation function of the noise, is

$$\gamma_{NN}(\zeta_1,\zeta_2) \triangleq \langle n(\zeta_1)\, n(\zeta_2) \rangle \quad , \text{ so}$$

$$\sigma^2_{P.I.}(t) = \int_0^t \int_0^t \theta(t,\zeta_1)\, \theta(t,\zeta_2) \gamma_{NN}(\zeta_1,\zeta_2) d\zeta_1 d\zeta_2 \qquad (6.1.b)$$

Using arguments analogous to those used for L.T.I. systems, it can be shown that the spread $\Delta c(t)$ is a conflicting factor with $\sigma^2_{P.I.}(t)$, namely, the bigger Δc the smaller $\sigma^2_{P.I.}$, and vice versa. The challenge then is to solve:

$$\forall t \quad \min_{(f,g)\ L.T.V.} \{\Delta c^2(t) + W^2(t)\sigma^2_{P.I.}(t)\} \tag{6.2}$$

with $W(t)$ some given weighting function.

Because of the complexity of P in general, solving (6.2) over the range of plant-uncertainty is a difficult task for which no techniques exist at present. Let $c_i(t)$ be the system response to input r when $P = P_i$. It is tempting in order to have a solvable problem, to pretend that the maximum range $\Delta c(t)$ in (6.2) consists of the differences $(c_1 - c_2)$ and this for <u>all t</u>, in the system response due to 2 'extreme' plant conditions $P_1(s)$ and $P_2(s)$, to the same input r, i.e.,

$$\forall t, \quad \Delta c(t)^2 = (c_1(t) - c_2(t))^2 \tag{6.3}.$$

In practice the extreme points of the spread $\Delta c(t)$ in Fig. VI.2 do not necessarily correspond to the outputs $(\forall t)$ for any 2 plant conditions chosen as 'extreme'. The weighting function $W(t)$ in (6.2) is then an extra degree of freedom, to help contend with the fact that the upper and lower bounds (Fig. VI.2) of the system responses for $P_i \in \mathcal{P}$, do not, in general, correspond for <u>all t</u>, to the two 'extreme' plants $P_1(s)$, $P_2(s)$, i.e. (6.3) usually does not hold in a realistic problem.

VI.2 An idealized problem.

VI.2.a Statement of the problem.

Let P(s) (Fig. VI.1) be a binary plant $\tilde{P} = \{P_1 \text{ or } P_2\}$. Following [H7] we show that $\Delta c^2(t)$ has a simple physical meaning. When $P = P_2$ we have (Fig. VI.1):

$$x_2 = g \cdot f \cdot r - g \cdot p_2 \cdot x_2 - g \cdot n \tag{6.4}$$

Let:

$x_2 \triangleq x_1 + \Delta x$ (6.4.a) $\quad x_1 \triangleq g \cdot f \cdot r - g \cdot p_1 \cdot x_1$ (6.4.b)

$\Delta c \triangleq c_2 - c_1$, $c_1 \triangleq p_1 \cdot x_1$ (6.4.c), giving $\Delta x = -g \cdot \Delta c - g \cdot n$ (6.4.d)

(6.4.a) and (6.4) give: $x_1 + \Delta x = g \cdot f \cdot r - g \cdot p_2 \cdot (x_1 + \Delta x) - g \cdot n$ (6.5)

Using (6.4.b): $\Delta x = -g \cdot (p_2 - p_1) \cdot x_1 - g \cdot p_2 \cdot \Delta x - g \cdot n$ (6.6)

and (6.4.d) in (6.6) gives: $g \cdot \Delta c = g \cdot (p_2 - p_1) \cdot x_1 + g \cdot p_2 \cdot \Delta x$ (6.7)

Using (6.4.c): $\Delta c = (p_2 - p_1) \cdot p_1^{-1} \cdot c_1 + p_2 \cdot \Delta x$ (6.8)

Therefore Fig. VI.1 becomes equivalent to Fig. VI.3 and $\Delta c(t)$ can be considered as the system response (when $P = P_2$) to the equivalent disturbance: (when $N = 0$)

$$d_2 = (p_2 - p_1) \cdot p_1^{-1} \cdot c_1 \tag{6.9}$$

(The subscript 2 in d is kept in order to recall that d_2 is associated with P_2).

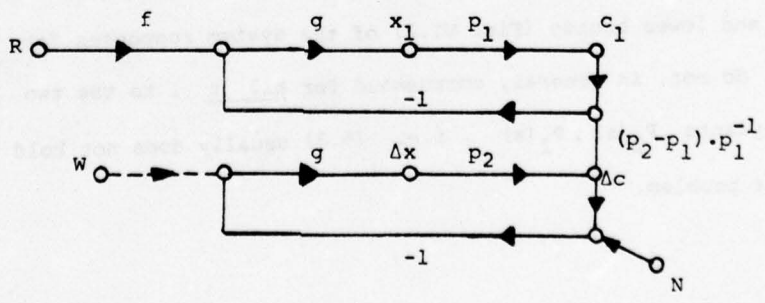

Figure VI.3. Equivalent Representation.

Using (6.4.d) and (6.9) in (6.8),

$$\Delta c = d_2 - p_2 \cdot g \cdot \Delta c - p_2 \cdot g \cdot n \qquad (6.9.a)$$

Let

$$\ell_2 \overset{\Delta}{=} p_2 \cdot g \qquad (6.9.b)$$

then (6.9.a) is rewritten as:

$$(1+\ell_2) \cdot \Delta c = d_2 - \ell_2 \cdot n$$

or

$$\Delta c = (1+\ell_2)^{-1} \cdot d_2 - (1+\ell_2)^{-1} \cdot \ell_2 \cdot n \qquad (6.9.c)$$

if $(1+\ell_2)$ has an inverse.

Let $d_2 \equiv 0$, then $\Delta c_n = -(1+\ell_2)^{-1} \cdot \ell_2 \cdot n$ which together with (6.4.d) gives:

$$\Delta x_n = g \cdot [(1+\ell_2)^{-1} \cdot \ell_2 - 1] \cdot n$$

$$\Delta x_n = g \cdot (1+\ell_2)^{-1} \cdot [\ell_2 - (1+\ell_2)] \cdot n$$

$$\Delta x_n = - g \cdot (1+\ell_2)^{-1} \cdot n$$

which can be rewritten, (recalling (6.9.b)), as:

$$\Delta x_n = - p_2^{-1} \cdot \ell_2 \cdot (1+\ell_2)^{-1} \cdot n = p_2^{-1} \cdot (1+\ell_2)^{-1} \cdot \ell_2 \cdot n$$

because ℓ_2 and $(1+\ell_2)^{-1}$ commute.

Note (6.9.b) that $- p_2^{-1} \cdot \ell_2 \cdot (1+\ell_2)^{-1} = -g \cdot (1+p_2 \cdot g)^{-1} = - (1+g \cdot p_2)^{-1} \cdot g$, so from (6.1.a), $\theta = - p_2^{-1} \cdot \ell_2 \cdot (1+\ell_2)^{-1}$ (6.9.d) when $P = P_2$.

Hence, for the plant $P = P_2$, the minimization problem of (6.2) becomes (under the above assumption of a binary plant) equivalent to:

$$\forall t \ , \ \underset{f,g}{\text{Min}} \ \{\Delta c(t)^2 + W^2(t) \sigma^2_{P.I.}(t)\} \qquad (6.10)$$

where $\Delta c(t)$ is the component due only to d_2 , and θ of (6.9.d) is used in (6.1.b) for $\sigma^2_{P.I.}$.

VI.2.b Derivation of the Optimum Filter.

Let $h_2(t,\tau)$ be the closed loop impulse response of the lower part of Fig. VI.3 when an impulse is applied at W at $t=\tau$, i.e.,

$$\Delta c_w = p_2 \cdot g \cdot w - p_2 \cdot g \cdot \Delta c_w \qquad \text{or} \qquad \Delta c_w = (1+\ell_2)^{-1} \cdot \ell_2 \cdot w$$

if $(1+\ell_2)^{-1}$ exists and therefore (by definition $\Delta c_w = h_2 \cdot w$)

$$h_2 = (1+\ell_2)^{-1} \cdot \ell_2 = \ell_2 \cdot (1+\ell_2)^{-1} \tag{6.11.a}$$

The effect of d_2 is given by letting $n=0$ in (6.9.c), so in (6.10)

$$\Delta c = + (1+\ell_2)^{-1} \cdot d_2 = - (1+\ell_2)^{-1}(1+\ell_2) \cdot d_2 + d_2 + (1+\ell_2)^{-1} \cdot d_2$$

$$= d_2 + (1+\ell_2)^{-1}[\,1 - (1+\ell_2)\,]d_2 = d_2 - (1+\ell_2)^{-1} \cdot \ell_2 \cdot d_2$$

$$= d_2 - h_2 \cdot d_2$$

i.e.,

$$\Delta c(t) = d_2(t) - \int_0^t h_2(t,\zeta) d_2(\zeta) d\zeta \quad . \tag{6.11.b}$$

By definition:

$$\Delta c(t)^2 = < (d_2(t) - \int_0^t h_2(t,\zeta) d_2(\zeta) d\zeta)^2 > \tag{6.12.a}$$

where the bracket indicates the ensemble-average over the set of command inputs $r_i(t)$. From (2.6)

$$\gamma_{DD}(t,\tau) \triangleq < d_2(t) d_2(\tau) > \cong \sum_{i=1}^{N} D_i(t) D_i(\tau) \triangleq \mathbb{D}_2(t) \cdot \mathbb{D}_2(\tau)^T \tag{6.12.b}$$

where $\mathbb{D}_2(\cdot)$ is an N-dimensional vector.

(6.12.a) is then

$$\Delta c(t)^2 = \gamma_{DD}(t,\tau) - 2 \int_0^t h_2(t,\zeta) \gamma_{DD}(\zeta,t) d\zeta +$$

$$+ \int_0^t \int_0^t h_2(t,\zeta_2) h_2(t,\zeta_1) \gamma_{DD}(\zeta_1,\zeta_2) d\zeta_1 d\zeta_2 \tag{6.12.c}$$

If the plant $P=k$, with $k \in [k_{min}, k_{max}]$ a pure gain factor and $W(t)=1$, then from (6.9.d, 6.11.a), $\theta = -\frac{1}{k_2}$. h_2 (6.12.d) and

using (6.12.c), (6.1.b) and (6.12.d), (6.10) becomes:

$$\forall t \ , \ \min_{h_2} \Bigg(\gamma_{DD}(t,t) - 2 \int_0^t h_2(t,\zeta)\gamma_{DD}(\zeta,t)d\zeta + \int_0^t \int_0^t h_2(t,\zeta_1)h_2(t,\zeta_2) \Big[\gamma_{DD}(\zeta_1,\zeta_2) + \frac{1}{k_2^2} \gamma_{NN}(\zeta_1,\zeta_2) \Big] d\zeta_1 d\zeta_2 \Bigg) \ . \qquad (6.13)$$

By using γ_{DD} instead of γ_{ID} in (2.5), we conclude that the optimum solution h_2 of (6.13) is the solution of the integral equation:

$$\forall \quad \tau \leq t \ , \ \int_0^t h_2(t,\zeta)\Big(\gamma_{DD}(\zeta,\tau) + \frac{1}{k_2^2} \gamma_{NN}(\zeta,\tau)\Big)d\zeta = \gamma_{DD}(t,\tau) \qquad (6.14)$$

We restrict ourselves, without loss of generality to white sensor noise of strength σ_N^2 , with resulting $\gamma_{NN}(\zeta,\tau) = \sigma_N^2 \, \delta(\zeta - \tau)$. Therefore (6.14) becomes:

$$\forall \quad t \geq \tau \ , \mu \, h_2(t,\tau) + \int_0^t h_2(t,\zeta) \mathbb{D}_2(\zeta) \, \mathbb{D}_2(\tau)^T d\zeta = \mathbb{D}_2(t) \, \mathbb{D}_2(\tau)^T \qquad (6.15)$$

with $\mu \triangleq \frac{\sigma_N^2}{k_2^2}$. (Note that $\mu \triangleq \frac{\sigma_N^2}{k_2^2} \ W(t)$ for $W(t) \neq 1$.)

(6.15) has a solution if:

$h_2(t,\tau) = \mathbb{G}(t) \cdot \mathbb{D}_2(\tau)^T u(t-\tau)$ where $\mathbb{G}$ is a N-dimensional vector, and the heaviside unit function $u(t-\tau) = \begin{cases} 0 & t < \tau \\ 1 & t \geq \tau \end{cases}$ is introduced to give a causal h_2 . (6.15) becomes:

$$t \geq \tau \ , \ \mu \, \mathbb{G}(t) \cdot \mathbb{D}_2(\tau)^T + \mathbb{G}(t) \int_0^t \mathbb{D}_2(\zeta)^T \mathbb{D}_2(\zeta) d\zeta \cdot \mathbb{D}_2(\tau)^T = \mathbb{D}_2(t) \mathbb{D}_2(\tau)^T \qquad (6.16)$$

(6.16) implies that:

$$\mathbb{G}(t) = \mathbb{D}_2(t) \Big[\mu \mathbb{1} + \int_0^t \mathbb{D}_2(\zeta)^T \mathbb{D}_2(\zeta) d\zeta \Big]^{-1} \qquad (6.17)$$

and if

$$\pi(t) \triangleq \left[\mu \mathbb{1} + \int_0^t \mathbb{D}_2(\zeta)^T \mathbb{D}_2(\zeta) d\zeta \right]^{-1} \tag{6.19}$$

$$h_2(t,\tau) = \mathbb{D}_2(t)\, \pi^{-1}(t) \cdot \mathbb{D}_2(\tau)^T u(t-\tau) \tag{6.18}$$

Note that π is an $N \times N$ matrix.

From (6.11.a) one gets (Appendix A 3.1) the open loop impulse response associated with $P = P_2$,

$$\ell_2(t,\tau) = \mathbb{D}_2(t)\, \pi^{-1}(\tau) \cdot \mathbb{D}_2(\tau)^T u(t-\tau) \tag{6.20}$$

The open loop impulse response $\ell(t-\tau)$ for any $P = k \in \mathbb{P}$ is (Appendix A3.2)

$$\ell(t,\tau) = \lambda\ \ell_2(t,\tau) \qquad (6.21) \qquad \text{with} \quad \lambda \triangleq \frac{k}{k_2} \tag{6.21.a}$$

and the corresponding closed loop impulse response (Appendix A 3.2):

$$h(t,\tau) = \lambda\, \mathbb{D}_2(t) \Lambda_1(t) \Lambda_1^{-1}(\tau) \pi^{-1}(\tau) \cdot \mathbb{D}_2(\tau)^T u(t-\tau) \tag{6.22}$$

where Λ_1 is a $N \times N$ matrix solution of:

$$\dot{\Lambda}_1 \Lambda_1^{-1} + \lambda\, \pi^{-1} \dot{\pi} = 0 \tag{6.23}$$

It is shown (Appendix A3.3) that the system response to a command input r , when $P = k \in \mathbb{P}$ is:

$$c(t) = c_1(t) \left(1 + \frac{k-k_1}{k_1} \left(\frac{\pi(0)}{\pi(t)} \right)^{\lambda} \right) \tag{6.24}$$

where $c_1(t)$ is the system response to the same input r at $P = k_1$.

VI.2.c Example.

Let $\{r(t)\}$ be a set of step command inputs of amplitude α , with average mean square value $\langle \alpha^2 \rangle = 1$; $P = k \in [k_{min}, k_{max}]$ is a real gain factor and $c_1(t)$ is the system response to $r(t) = u(t)$ when $P = k_1$. From (6.9), at $P = k_2$, and $r = \alpha\, u(t)$, $d_2 = \dfrac{(k_2-k_1)}{k_1} \alpha\, c_1$.

From (6.12.b), the autocorrelation function associated with

$$d_2(t) \text{ is } \gamma_{DD}(t,\tau) = < \frac{k_2-k_1}{k_1} \alpha\, c_1(t) \frac{k_2-k_1}{k_1} \alpha\, c_1(\tau) >$$

$$= \frac{k_2-k_1}{k_1} c_1(t) \frac{k_2-k_1}{k_1} c_1(\tau) \triangleq D_2(t) \cdot D_2(\tau) \quad . \tag{6.25}$$

Therefore $N = 1$, and from (6.19),

$$\pi(t) = \mu + \int_0^t D_2(\zeta)^2 d\zeta \quad . \tag{6.26}$$

From (6.22), the closed loop impulse response at $P = k$ is:

$$h(t,\tau) = \lambda\, D_2(t) \frac{\pi(\tau)^{\lambda-1}}{\pi(t)^{+\lambda}} D_2(\tau) u(t-\tau) \tag{6.27}$$

with $\lambda = k/k_2$ (from 6.21.a), and the system response to step command of amplitude α is given by (6.24), i.e.

$$c(t) = \alpha\, c_1(t) \left(1 + \frac{k-k_1}{k_1} \mu^{\lambda} \pi(t)^{-\lambda} \right) \tag{6.28}$$

noting in (6.26) that $\pi(0) = \mu$. The effect of white sensor noise at the plant input is (see Appendix A3.4):

$$\sigma^2_{P.I.}(t) = \begin{cases} \dfrac{D_2(t)^2}{2\lambda-1} \dfrac{\sigma_N^2}{k_2^2} \left(\dfrac{1}{\pi(t)} - \dfrac{\mu^{2\lambda-1}}{\pi(t)^{2\lambda}} \right) & \text{if } \lambda = \dfrac{k}{k_2} \neq \dfrac{1}{2} \\ D_2(t)^2 \dfrac{\sigma_N^2}{k_2^2} \dfrac{\ell n(\pi(t)/\mu)}{\pi(t)} & \text{if } \lambda = \dfrac{k}{k_2} = \dfrac{1}{2} \end{cases} \tag{6.29}$$

The reader has probably noted that, as yet, nothing has been said as how to select $P_1 = k_1$, $P_2 = k_2$, given $[k_{min}, k_{max}]$. This is one of the major issues if one is interested in a synthesis procedure. Let us assume in the meantime, that k_1 and k_2 have somehow been selected. Let the relative change $m(k, t_0)$ at a given time t_0 , in the system response at $P = k \in [k_{min}, k_{max}]$, be defined as:

$m(k,t_0) \triangleq \frac{c(t_0)-\alpha c_1(t_0)}{\alpha c_1(t_0)}$. Using (6.28),

$$m(k,t_0) = \frac{k-k_1}{k_1} \left(\frac{\mu}{\pi(t_0)} \right)^{k/k_2} \qquad (6.30)$$

As an illustration, $m(k,t_0)$ is plotted versus k, for $t_0 = .2,1.,\ldots,$ in Fig. VI.4.a for the case $k_1 = 100 > k_2 = 1$, and in Fig. VI.4.b for the case $k_1 = 1 < k_2 = 100$. The spread in the overall system response to a command input r, at time t_0, is obtained from these curves as follows:

$$\text{SPREAD} = c_1(t_0) * \left[(m(k,t_0))_{max} - (m(k,t_0))_{min} \right] \text{ where MAX}$$

and MIN are taken over all possible values of $k \in [k_{min},k_{max}]$. For instance in Fig. VI.4.a, when $k_{min} = .1$ and $k_{max} = 10.$,

$$[m(k,t_0)]_{max} = m(k_{max},t_0) ,$$

$$[m(k,t_0)]_{min} = m(k_{min},t_0) ,$$

and therefore it is easily seen that:

$$\text{SPREAD} = c_1(2.) * (.99-.24) = .72 * c_1(2.) \text{ at } t_0 = 2 \text{ seconds}$$

$$= c_1(9.) * (.76 - 0) = .76 * c_1(9.) \text{ at } t_0 = 9 \text{ seconds, etc.}$$

Consider the case $k_1 < k_2$, shown in Fig. VI.4.b. If $k_{min} < k_1$ then very poor results may be expected for $k_{min} < k < k_1$, since the settling time is seen to be very large. For the same reason, $k_1 < k_{min} < k_2$ is not a better choice. However, if $k_1 < k_2 < k_{min} < k_{max}$, then we get a reasonable spread in the system command responses, for large changes in $k \in [k_{min},k_{max}]$. If $k_2 = 1 < k_1 = 100$ are selected (Fig. VI.4.a) then, on the one hand $k_{min} \geq k_2$ should be satisfied, if

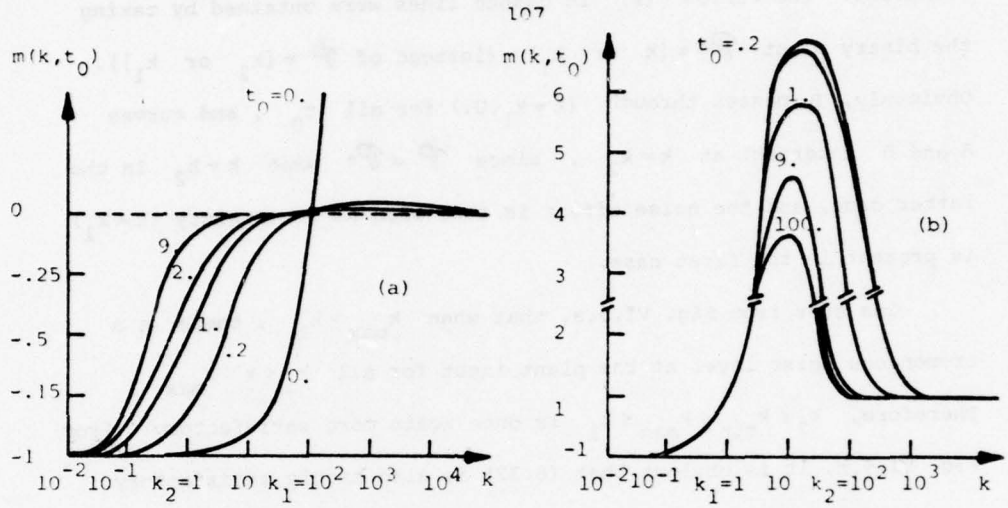

Figure VI.4 Plot of $m(k,t_0)$ for $k_1 > k_2$ (a) and $k_2 > k_1$ (b).

one is to avoid a long "tail" in the system response to command inputs, and on the other hand, $k_1 \leq k_{max}$ should be used to avoid tremendous overshoot at small t_0 . Note that all those results are independent of the nominal choice of $c_1(t_0)$, and of the actual values of k_{min}, k_{max} and are therefore very general.

To summarize, we have found that from the system command response point of view, two reasonable choices are:

$$k_1 < k_2 << k_{min} < k_{max} \tag{6.31}$$

or $$k_2 \leq k_{min} < k_{max} \leq k_1 \tag{6.32}$$

The curves $\sigma^2_{P.I.}(t_0,k)$ (curve A obtained by using (6.23)) are plotted versus k (see Appendix A3.4 for details), with parameter t_0 , in Fig. VI.5.a for

$$k_2 = 1 < k_1 = 100 \tag{6.33}$$

and in Fig. VI.5.b for

$$k_1 = 1 < k_2 = 100 \tag{6.34}$$

in order to evaluate choices for k_1 , k_2 from the noise response

viewpoint. The curves (B) in dashed lines were ontained by taking the binary plant $\mathcal{P}^* = [k \text{ or } k_1]$ (instead of $\tilde{\mathcal{P}} = [k_2 \text{ or } k_1]$). Obviously, B passes through $(k = k_1, 0.)$ for all t_0, and curves A and B intersect at $k = k_2$, since $\tilde{\mathcal{P}} = \mathcal{P}^*$ when $k = k_2$ in the latter case, and the noise effect is zero when no uncertainty $(k = k_1)$ is present in the first case.

One sees from Fig. VI.5.a, that when $k_{max} > k_1$, there is a tremendous noise level at the plant input for all $k_1 < k < k_{max}$. Therefore, $k_2 \leq k_{min} < k_{max} \leq k_1$ is once again more satisfactory. From Fig. VI.5.b, it is obvious that (6.32) is also highly satisfactory.

Discussion.

The choice (6.32) seems a better one than (6.31), especially if k_1 and k_2 are taken much smaller than the prescribed k_{min}, k_{max}. However, such a choice is very poor as far as stability is concerned, when higher order systems (obtained when dealing with more realistic

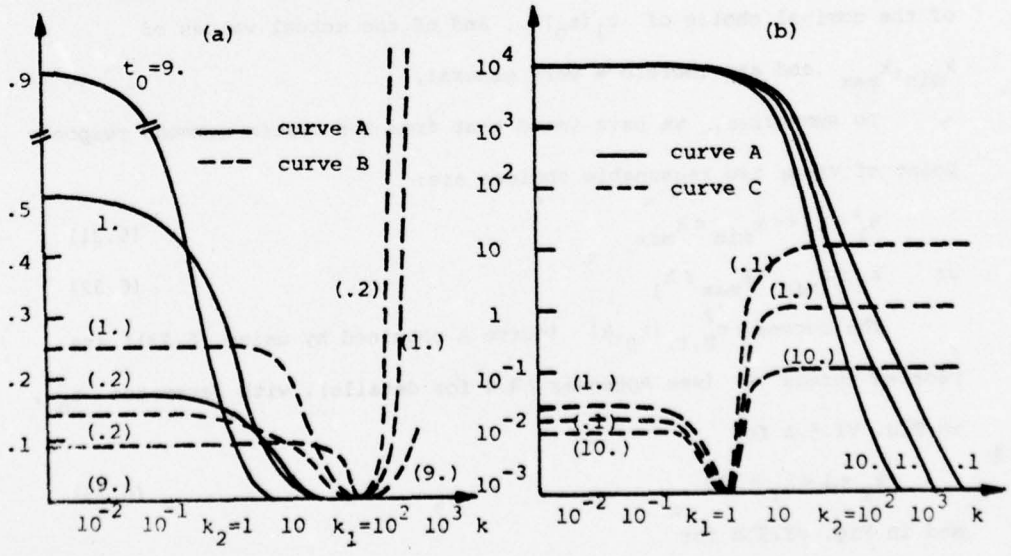

Figure VI.5 Mean square value of the noise at the plant input for different gain factor values of k and at different time instant t_0 when $k_1 > k_2$ (a) and $k_2 > k_1$ (b).

plants) are considered. Indeed, it will be shown (section VI.4.c) that for high order systems, k_{max}/k_2 should be made smaller than some real number, preventing (6.32) from being used. This result is not obvious here, because a first order system is stable for all values of gain factor k . Therefore, one has to use the other possibility (6.31) which is more compatible with stability problems. Noting (Fig. VI.4.a), that k_{min}/k_2 should be as large as possible to guarantee satisfactory spread (i.e., T.D.S.), we will therefore use for the remaining of this chapter:

$$\begin{cases} k_1 = k_{max} \\ k_2 \leq k_{min} \end{cases} \tag{6.35}$$

VI.2.d Results and Some Preliminary Conclusions.

We can now complete the above example (beginning of section VI.2.c). In addition to the assumptions already made, we take:

$c_1(t) = 1-e^{-t}$, $k_{min} = 1$, $k_{max} = 100$ and $w(t) = 1$.

Following (6.35), $k_1 = 100$, $k_2 = 1$ are selected. The design has thus been completed [Appendix A3.8.a for details], and the overall system responses to unit step input are shown on Fig. VI.6.a for different values of $P = k$. The mean square value of the noise at the plant input is shown in Fig. VI.6.c where it is compared with the results obtained in a L.T.I. design (Appendix A3.8.b) which acheives roughly the same time domain specifications (shown on Fig. VI.6.b) as the L.T.V. system. These results confirm that much may be gained in reduction of sensor noise effects at the plant input, by using L.T.V. compensation.

Several comments are appropriate at this stage:

α) It is seen that $\Delta c(t)$ of (6.2) is indeed equal to

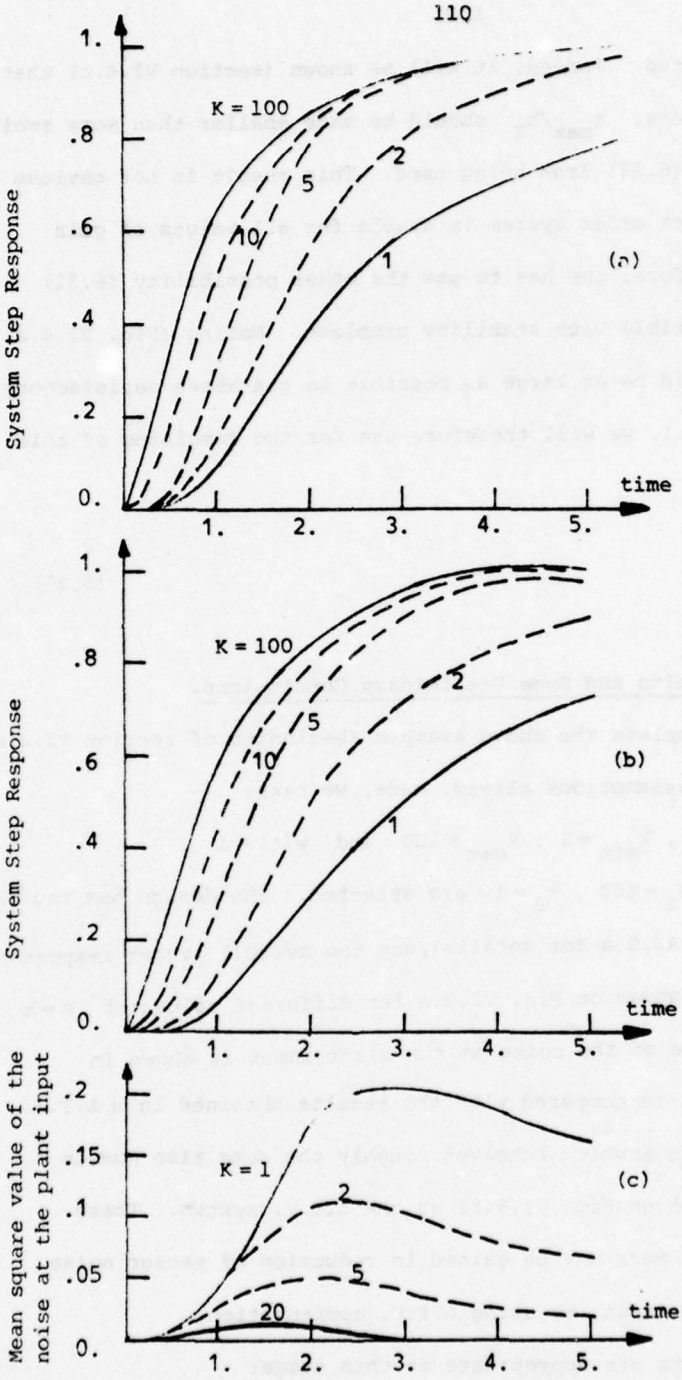

LTI design				
σ^2	.21	.11	.05	.015
k	1	2	5	20

Figure VI.6 System Response to a unit step command (a) LTV design, (b) LTI design. (c) Comparison of sensor noise rejection at the plant input between the LTI and LTV designs.

$c_{k_{max}}(t) - c_{k_{min}}(t)$, but this is true only for the simple first order system, and not in general for more realistic systems, even in the case where there is no uncertainty in the dynamics of the plant.

β) Note that (6.18) and (6.22) do not have $h(t,t) = 0$, $\forall k$, $\forall t$, implying that our optimum design is a first order one, which is of course not realistic. Therefore the above should be considered only as an academic excercise, giving us, however, insight as to how k_1 , k_2 should be chosen, given the uncertainty range $[k_{min}, k_{max}]$.

γ) Note that $h(t,\tau)$ is a stable design for $k \in]0, \infty[$, which will no longer be true (as already noted) in high order systems.

VI.3 Some Approaches to the More Realistic Problem.

VI.3.a Generalities.

It is noted that when the plant is a pure gain factor (as in the previous section), the minimization of the sensor noise (of strength σ_N^2) effect at the plant input, is equivalent to the minimization of sensor noise (of strength $\mu = \sigma_N^2/k^2$) effect at the plant output (which is also the system output). Therefore, the derivation in VI.2 can be considered as a direct extension of Wiener filter theory to linear nonstationary problems. As is well known, the derivation of the optimum filter in such cases, is always done on the closed loop impulse response $h(t,\tau)$, which does not explicitly feature the complexity of the plant and therefore a first order optimum solution is usually obtained (with white sensor noise), which is unsatisfactory if the excess of poles over zeros of the plant $e_p \geq 2$. (Indeed, as h is first order, so is the open loop ℓ , implying in the latter case that g possesses at least one derivative — which is impossible to implement precisely).

In L.T.I. systems, $P(s)$ and $G(s)$ commute, so:

$$\Phi_{P.I.}(\omega) = \frac{1}{2\pi}\int_{-\infty}^{+\infty} \left|\frac{G}{1+L}\right|^2 \Phi_{nn}(\omega)\,d\omega = \frac{1}{2\pi}\int_{-\infty}^{+\infty} \left|\frac{GP}{1+L}\right|^2 \left|\frac{\Phi_{nn}}{P}\right|^2 d\omega$$

$$= \frac{1}{2\pi}\int_{-\infty}^{+\infty} |H|^2\, \tilde{\Phi}_{nn}(\omega)\,d\omega \quad \text{with} \quad \tilde{\Phi} = \frac{\Phi_{nn}}{P} \tag{6.36}$$

This means that the mean square value of the noise effect at the plant-input $\Phi_{P.I.}(\omega)$ is equal to the mean square value, at the system output, due to a distorted sensor noise power spectrum $\Phi_{nn}/|P|^2$. It is therefore seen that H then emerges with the proper excess of poles over zeros, provided the sensor noise is distorted by P^{-1}. This reveals that the problem posed in (6.2) is a very realistic one, if it can be solved in general.

VI.3.b <u>The Problem Posed by the Solution of (6.2)</u>.

It is assumed in the remainder of this section, that the input r is deterministic, implying that $D_2(t)$ is also deterministic $(N = 1)$, and $P(s) = k/s$ with $k \in [k_{min}, k_{max}]$. Under such assumptions:

$$(6.1) \text{ becomes } \sigma^2_{P.I.} = \frac{\sigma_N^2}{k_2^2}\int_0^t \left[\frac{\partial h_2}{\partial t}(t,\zeta)\right]^2 d\zeta \tag{6.37}$$

and (6.2) becomes (using (6.12) and $\mu \triangleq \sigma_N^2/k_2^2$):

$$\forall t\,,\ \min_{h_2}\left[\left(D_2(t) - \int_0^t h_2(t,\zeta)D_2(\zeta)d\zeta\right)^2 + \mu\int_0^t \left[\frac{\partial h_2}{\partial t}(t,\zeta)\right]^2 d\zeta\right] \tag{6.38}$$

<u>Note</u>: If $P(s)$ is more complicated, then only the second part of the bracketed term would be modified, becoming in general a combination of terms in $\frac{\partial h_2}{\partial t}$, $\frac{\partial^2 h_2}{\partial t^2}$ ... $\frac{\partial^n h_2}{\partial t^n}$ where n is the order of the plant, plus some cross-product terms, $\frac{\partial h_2}{\partial t}\cdot h_2$, $\frac{\partial^2 h_2}{\partial t^2}\cdot h_2, \ldots, \frac{\partial^2 h_2}{\partial t^2}\cdot\frac{\partial h_2}{\partial t}$, ...

Using a variational argument, i.e., letting $h_2 = h_2^\circ + f$, where $h_2^\circ(t,\tau)$ represents the optimal solution of (6.38) and $f(t,\tau)$ is an arbitrary small impulse response belonging to the admissible class of solutions, i.e., satisfying $h(t,t) = 0$, it can be shown (the derivation omitted here, as the results are not used, but they are similar to those of Appendix A3.5), that the optimum $h_2(t,\tau)$ is the solution of:

$$\forall f \ , \ \forall t \ , \ t > \zeta_2 \ , \ \int_0^t \left(\left[\int_0^t h_2^\circ(t,\zeta)\gamma_{DD}(\zeta_1,\zeta_2)d\zeta - \gamma_{DD}(t,\zeta_2) \right] \right.$$

$$\left. f(t,\zeta_2) + \frac{\partial h_2^\circ}{\partial t}(t,\zeta_2)\ \frac{\partial f}{\partial t}(t,\zeta_2) \right) d\zeta_2 = 0 \qquad (6.39)$$

Mathematically, (6.40) is equivalent to:

$$\begin{cases} \int_0^t h_2^\circ(t,\zeta)\gamma_{DD}(\zeta,\tau)d\zeta = \gamma_{DD}(t,\tau) \quad , \ \forall t \ , \text{ for } \tau \leq t & (6.39.a) \\ \\ \dfrac{\partial h_2^\circ}{\partial t}(t,\tau) = 0 \qquad \forall t \geq \tau & (6.39.b) \end{cases}$$

which is unrealizable. This can be understood as follows. For $t = T$ with T fixed, the optimum solution exists and since (6.39.b) should be satisfied at $t = T$, the optimum solution is dependent on T . Therefore at $t = T' > T$, the optimum solution is a funtion of T' , and unless (6.39.a) happens to be satisfied (which can only occur by chance), this optimum solution for $t = T'$ is no longer optimum for $t = T$, and therefore there does not exist a solution to problem (6.38) and in general to (6.2). The reader may note that when $\partial h/\partial t$ is replaced by h in (6.38), i.e., when the noise effect is considered at the system-output (rather than at the plant input), then (6.2) has a unique solution (derived in VI.2). This may be surprising at first glance,

but note that in the latter case, (6.39.a) does not need to be satisfied, thus explaining the uniqueness of the solution.

One alternative, therefore, is to modify the original problem of (6.2) and solve: (for a given fixed T)

$$\underset{h_2}{\text{Min}} \int_0^T [\Delta c^2(t) + W(t)^2 \sigma^2_{\text{P.I.}}(t)]dt \tag{6.40}$$

It is shown (Appendix A 3.5) that (6.40) has a solution given by an Euler-Lagrange differential equation. Another alternative is to distort the noise characteristics in such a way that the resulting $h_2(t,\tau)$ will have the proper excess of poles over zeros. For this purpose, we introduce artificially an equivalent autocorrelation function of the noise:

$$\tilde{\gamma}_{NN}(t,\tau) = (-1)^e \sigma_N^2 \delta^e(t-\tau) \tag{6.41}$$

where $e \geq 1$ is an integer.

By analogy with the L.T.I. case (recall (6.36)), we then try to minimize:

$$\sigma^2_{\text{out}} = \int_0^t \int_0^t h_2(t,\zeta_1)h_2(t,\zeta_2)\tilde{\gamma}_{NN}(\zeta_1,\zeta_2)d\zeta_1 d\zeta_2 \tag{6.42}$$

in place of (6.1). Under this assumption, (6.2) becomes:

$$\forall t \quad , \underset{h}{\text{Min}} \{\Delta c^2(t) + W(t)^2 \sigma^2_{\text{out}}\} \tag{6.43}$$

which has a unique solution as shown below. It should be recalled that in L.T.V. systems, g and p do not commute and therefore $\sigma^2_{\text{out}} \neq \sigma^2_{\text{P.I.}}$. The weighting function $W(t)$ might then be used to try to partially compensate for this. The remainder of this chapter is devoted to a detailed discussion of the above two approaches.

VI.4 Solution to the Filter Problem by Distortion of the Noise Characteristics.

VI.4.a Statement of the Problem.

The minimization of (6.43) was solved in (2.5), giving for the optimum solution $h_2(t,\tau)$

$$t \geq \tau \quad \gamma_{DD}(t,\tau) = \int_0^t h_2(t,\zeta)[\gamma_{DD}(\zeta,\tau) + \tilde{\gamma}_{NN}(\zeta,\tau)]d\zeta \tag{6.44}$$

Using (6.41) and recalling (6.9) that $D_2 = (p_2 - p_1)\cdot p_1^{-1}\cdot c_1$ is deterministic because the input signals are assumed to be deterministic, we get:

$$D_2(t)D_2(\tau) = \int_0^t h_2(t,\zeta)D_2(\zeta)D_2(\tau)d\zeta + (-1)^e\sigma_N^2 W(t)\int_0^t h_2(t,\zeta)\delta^e(\zeta-\tau)d\zeta \tag{6.45}$$

or:

$$D_2(t)D_2(\tau) = \int_0^t h_2(t,\zeta)D_2(\zeta)D_2(\tau)d\zeta + (-1)^e\sigma_N^2 W(t)\frac{\partial^e}{\partial\tau^e}h_2(t,\tau) \tag{6.46}$$

A necessary condition is therefore:

$$\frac{\partial^e}{\partial\tau^e}h_2(t,\tau) = -\gamma(t)D_2(\tau)u(t-\tau) \tag{6.47}$$

Integrating with respect to τ, and requiring that $\left.\frac{\partial^{e-1}}{\partial\tau^{e-1}}h_2(t,\tau)\right|_{\tau=t} = 0$ we get:

$$\frac{\partial^{e-1}}{\partial\tau^{e-1}}h_2(t,\tau) = \gamma(t)\,[\,D_2^1(t) - D_2^1(\tau)\,]\,u(t-\tau) \tag{6.48}$$

where the notation $D_2^1(t) \triangleq \int_0^t D_2(\zeta)d\zeta$ is used.

Let $D_2^m(t) \triangleq \int_0^t D_2^{m-1}(\zeta)d\zeta$ and integrating (6.48) with respect to τ, gives:

$$\frac{\partial^{e-2}}{\partial\tau^{e-2}}h_2(t,\tau) = \gamma(t)\,[\,D_2^2(t) - D_2^2(\tau) - (t-\tau)D_2^1(t)\,]\,u(t-\tau) \quad .$$

After (e-2) more integrations with respect to τ, we have:

$$h_2(t,\tau) = \gamma(t)\Big[D_2^e(t) - D_2^e(\tau) - (t-\tau)D_2^{e-1}(t) + \frac{(t-\tau)^2}{2!}D_2^{e-2}(t) + \ldots + (-1)^{e-1}\frac{(t-\tau)^{e-1}}{(e-1)!}D_2^1(t)\Big]u(t-\tau) \triangleq \gamma(t)Q(t,\tau)u(t-\tau) \tag{6.49}$$

Inserting (6.49) into (6.45) gives:

$$\gamma(t) = D_2(t)/\left((-1)^{e-1}\sigma_N^2 W(t) + \int_0^t Q(t,\zeta)D_2(\zeta)d\zeta\right) \tag{6.49.a}$$

with

$$\int_0^t Q(t,\zeta)D_2(\zeta)d\zeta = \int_0^t\Big(D_2^e(t) - D_2^e(\zeta) - (t-\zeta)D_2^{e-1}(t) + \ldots + (-1)^{e-1}\frac{(t-\zeta)^{e-1}}{(e-1)!}D_2^1(t)\Big)D_2(\zeta)d\zeta \tag{6.49.b}$$

Integrating by parts,

$$\int_0^t (t-\zeta)D_2(\zeta)d\zeta = \Big[(t-\zeta)D_2^1(\zeta)\Big]_0^t + \int_0^t D_2^1(\zeta)d\zeta = D_2^2(t) \text{ because } D_2^1(0)=0$$

$$\int_0^t (t-\zeta)^2 D_2(\zeta)d\zeta = \Big[(t-\zeta)^2 D_2^1(\zeta)\Big]_0^t + \int_0^t (t-\zeta)D_2^1(\zeta)d\zeta = D_2^3(t)$$

$$- -$$

$$\int_0^t \frac{(t-\zeta)^{e-1}}{(e-1)!}D_2(\zeta)d\zeta = \quad - - - - - - - - - - = D_2^e(t)$$

Therefore (6.49.b) becomes:

$$\int_0^t Q(t,\zeta)D_2(\zeta)d\zeta = D_2^e(t)D_2^1(t) - \int_0^t D_2^e(\zeta)D_2(\zeta)d\zeta - D_2^{e-1}(t)D_2^2(t) + D_2^{e-2}(t)D_2^3(t) + \ldots + (-1)^k D_2^{e-k}(t)D_2^{k+1}(t) + \ldots + (-1)^{e-1}D_2^1(t)D_2^e(t) \tag{6.50}$$

Noting that:

$$
\begin{aligned}
-\int_0^t D_2^e(\zeta)D_2(\zeta)d\zeta &= -D_2^e(t)D_2^1(t) + \int_0^t D_2^{e-1}(\zeta)D_2^1(\zeta)d\zeta \\
&= -D_2^e(t)D_2^1(t) + D_2^{e-1}(t)D_2^2(t) - \int_0^t D_2^{e-2}(\zeta)D_2^2(\zeta)d\zeta \\
&\quad - \\
&= -D_2^e(t)D_2^1(t) + D_2^{e-1}(t)D_2^2(t) - D_2^{e-2}(t)D_2^3(t) + \ldots \\
&\quad + (-1)^{e-2}D_2^1(t)D_2^e(t) + (-1)^{e-1}\int_0^t D_2(\zeta)D_2^e(\zeta)d\zeta
\end{aligned}
\tag{6.51}
$$

(6.50) becomes:

$$
\int_0^t Q(t,\zeta)D_2(\zeta)d\zeta = (-1)^{e-1}\int_0^t D_2(\zeta)D_2^e(\zeta)d\zeta \tag{6.52}
$$

so finally:

$$
Y(t) = D_2(t) \Big/ \left((-1)^{e-1}\sigma_N^2 W(t) + (-1)^{e-1}\int_0^t D_2(\zeta)D_2^e(\zeta)d\zeta \right)
$$

and

$$
h_2(t,\tau) = \frac{(-1)^{e-1}D_2(t)\left[D_2^e(t) - D_2^e(\tau) - (t-\tau)D_2^{e-1}(t) + \frac{(t-\tau)^2}{2!}D_2^{e-2}(t) + \ldots + (-1)^{e-1}\frac{(t-\tau)^{e-1}}{(e-1)!}D_2^1(t)\right]}{\sigma_N^2 W(t) + \int_0^t D_2(\zeta)D_2^e(\zeta)d\zeta} u(t-\tau)
\tag{6.53}
$$

(6.53) holds for $e = 1,2,3\ldots$, and it can be checked that:

$$
h(t,t) = \frac{\partial h}{\partial t}(t,t) = \frac{\partial^2 h}{\partial t^2}(t,t) = \ldots = \frac{\partial^{e-1}}{\partial t^{e-1}}h(t,t) = 0 \quad ,
$$

implying that the system obtained is of order $e+1$ ($e+1$ poles and no zeros).

VI.4.b. Analysis for different values of e

VI.4.b.α e = 1

When e = 1 , (6.53) becomes

$$h_2(t,\tau) = \frac{D_2(t)[D_2^1(t) - D_2^1(\tau)]u(t-\tau)}{\sigma_N^2 W(t) + D_2^1(t)^2/2} \tag{6.54}$$

If $W(t)\sigma_N^2 = \mu$ is a constant, (6.54) is associated (Appendix A 3.6) with the Differential Equation (D.E.):

$$[h_2] : \ddot{y} + \left[2D_2^1 g - 3\frac{\dot{D}_2}{D_2}\right]\dot{y} + \left[D_2 g - 2\frac{D_2^1 \dot{D}_2}{D_2} g + 3\left(\frac{\dot{D}_2}{D_2}\right)^2 - \frac{\ddot{D}_2}{D_2}\right] y = D_2 g X$$

$$\triangleq \ddot{y} + \alpha_1 \dot{y} + \alpha_2 y = D_2 g X \tag{6.55}$$

where

$$g \triangleq \frac{D_2}{\mu + (D_2^1)^2/2} \tag{6.56}$$

Recalling that $h = \ell\cdot(1+\ell)^{-1}$ with $\ell \triangleq p\cdot g$, we have: $\ell = p\cdot p_2^{-1}\cdot \ell_2$ and:

$$h = p\cdot p_2^{-1}\cdot \ell_2 (1+p\cdot p_2^{-1}\cdot \ell_2)^{-1}$$

$$= p\cdot p_2^{-1}\cdot \ell_2 \cdot (1+\ell_2)^{-1} \ ((1+\ell_2)^{-1})^{-1}(1+p\cdot p_2^{-1}\cdot \ell_2)^{-1}$$

$$= p\cdot p_2^{-1}\cdot h_2 \cdot ((1+p\cdot p_2^{-1}\cdot \ell_2)(1+\ell_2)^{-1})^{-1}$$

$$= p\cdot p_2^{-1}\cdot h_2 \cdot ((1+\ell_2)^{-1} + p\cdot p_2^{-1}\cdot h_2)^{-1}$$

As $(1+\ell_2)^{-1} = 1 - h_2$

$$h = p\cdot p_2^{-1}\cdot h_2 \cdot (1+h_2(p\cdot p_2^{-1}-1))^{-1} \tag{6.57}$$

As we know from L.T.I. systems, the problem of sensor noise rejection at the plant input becomes crucial in the region where P(s) has its asymptotic behavior, $k/s^e p$, so we can restrict ourselves to gain factor uncertainty with $p\cdot p_2^{-1} = k/k_2 \triangleq \lambda$. The differential equation

associated with $h = \lambda h_2 \cdot (1+h_2(\lambda-1))^{-1}$ is obtained as follows:

$$[(\lambda-1)h_2] \quad : \ddot{y} + \alpha_1\dot{y} + \alpha_2 y = (\lambda-1)D_2 gX$$

$$[1+(\lambda-1)h_2] \quad : \ddot{y} + \alpha_1\dot{y} + \alpha_2 y = ((\lambda-1)D_2 g+\alpha_2)X+\alpha_1\dot{X}+\ddot{X}$$

$$[1+(\lambda-1)h_2]^{-1} \quad : \ddot{y} + \alpha_1\dot{y} + [\alpha_2+(\lambda-1)D_2 g]y = \ddot{X}+\alpha_1\dot{X}+\alpha_2 X$$

$$[h_2[1+(\lambda-1)h_2]^{-1}] : \ddot{y} + \alpha_1\dot{y} + [\alpha_2+(\lambda-1)D_2 g]y = D_2 gX \qquad (6.57.a)$$

$$[h] \quad : \ddot{y} + \alpha_1\dot{y} + [\alpha_2+(\lambda-1)D_2 g]y = D_2 gX \qquad (6.58)$$

In a practical problem:

$$\lim_{t=\infty} D_2(t) = K \ , \quad \lim_{t=\infty} \dot{D}_2(t) = 0 \ , \quad \lim_{t=\infty} \frac{D_2^1(t)}{t} = K \quad \text{and}$$

$$\lim_{t=\infty} g(t)\cdot Kt^2 = 2$$

Therefore the asymptotic behavior of the D.E. (6.58) is:

$$\ddot{y} + \frac{4\dot{y}}{t} + \frac{2\lambda}{t^2} y = \frac{2\lambda}{t^2} X \qquad (6.59)$$

This is a Cauchy-Euler type of D.E. Through the change of variable $t = e^u$, (6.59) becomes:

$$\ddot{y} + 3\dot{y} + 2\lambda y = 2\lambda X \qquad (6.60)$$

B.I.B.O. stability is guaranteed for (6.60) and therefore for (6.59). We can then apply a theorem by Cesari ([C5], p.38) which states that if (6.55) tends asymptotically to (6.59), as $t \to \infty$, and if (6.59) has bounded solutions, so has (6.55). Therefore, we conclude that $\forall\ \lambda > 0$, (6.55) secures B.I.B.O. stability.

VI.4.b.β $\underline{e=2}$

(6.53) gives: $$h_2(t,\tau) = \frac{D_2(t)\,[D_2^2(\tau) - D_2^2(t) + (t-\tau)D_2^1(t)]}{\sigma_N^2 W(t) + \int_0^t D_2(\zeta) D_2^2(\zeta)\, d\zeta}\, u(t-\tau) \qquad (6.61)$$

Following the same procedure as above $h(t,\tau)$ is associated with the D.E.:

$$[h] \quad : \quad \dddot{y} + \alpha_1(t)\ddot{y} + \alpha_2(t)\dot{y} + \alpha_3(t)y = \lambda D_2(t)g(t)X \tag{6.62}$$

with

$$g(t) \triangleq \frac{D_2(t)}{\sigma_N^2 + \int_0^t D_2(\zeta)D_2^2(\zeta)d\zeta}$$

$$\alpha_1 \triangleq 3D_2^1 g - 5\frac{\dot{D}_2}{D_2}$$

$$\alpha_2 \triangleq 3D_2^1 g - 7\frac{\dot{D}_2}{D_2}D_2^2 g - 4\frac{\ddot{D}_2}{D_2} + 12\left(\frac{\dot{D}_2}{D_2}\right)^2$$

$$\alpha_3 = \lambda D_2 g + 12(D_2^2 g)^3 - 6D_2^1 D_2^2 g^2 - \frac{\dot{D}_2}{D_2}(30(D_2^2 g)^2 - 3D_2^1 g) + 21D_2^2 g\left(\frac{\dot{D}_2}{D_2}\right)^2$$
$$- 12\left(\frac{\dot{D}_2}{D_2}\right)^3 - \left(\frac{\ddot{D}_2}{D_2}\right) + 3D_2^2 g\frac{\ddot{D}_2}{D_2} + 3\frac{\dot{D}_2}{D_2}\frac{\ddot{D}_2}{D_2} \quad .$$

As $t \to \infty$, (6.62) is equivalent to:

$$\dddot{y} + \frac{9}{t}\ddot{y} + \frac{18}{t^2}\dot{y} + \frac{6\lambda}{t^3}y = \frac{6\lambda}{t^3}X \tag{6.63}$$

Using $(t = e^u)$ this Cauchy-Euler D.E. becomes:

$$\dddot{y} + 6\ddot{y} + 11\dot{y} + 6\lambda y = 6\lambda X \tag{6.64}$$

(6.64) has bounded solutions, if all minors Δ_i (Routh criteria) of:

$$\Delta = \begin{vmatrix} 6 & 1 & 0 \\ 6\lambda & 11 & 6 \\ 0 & 0 & 6\lambda \end{vmatrix} > 0 \quad , \quad \text{i.e.} \begin{cases} \lambda > 0 \\ \lambda < 11 \end{cases}$$

Therefore, B.I.B.O. stability is secured for (6.62) if $0 < \lambda < 11$. This imples that $k \leq 11\,k_2$, and therefore if we have to cope with uncertainty such that $k_{max} > 11\,k_{min}$, B.I.B.O. stability is secured when $k_{min} < k_2$, which is a very poor choice, as far as the system response is concerned, (recall (6.35) and the discussion in section VI.2.c).

VI.4.b.γ $\underline{e = 3}$

(6.35) gives:

$$h_2(t,\tau) = \frac{D_2(t)\left[D_2^3(t) - D_2^3(\tau) - (t-\tau)D_2^2(t) + \frac{(t-\tau)^2}{2!} D_2^1(t)\right]}{\sigma_N^2 W(t) + \int_0^t D_2(\zeta) D_2^3(\zeta)\, d\zeta}\, u(t-\tau) \tag{6.65}$$

$h(t,\tau)$ is then associated with a D.E. whose asymptotical behavior is given by:

$$[h]: \; y^{[4]} + \frac{16}{t}\dddot{y} + \frac{12}{t^2}\ddot{y} + \frac{96}{t^3}\dot{y} + \frac{24\lambda}{t^4} y = \frac{24\lambda}{t^4} X \tag{6.66}$$

which is equivalent, after the change of variable $t = e^u$, to:

$$y^{[4]} + 10\, y^{[3]} + 35\, \ddot{y} + 50\, \dot{y} + 24\lambda y = 24\lambda X \tag{6.67}$$

A sufficient condition for stability is then given by:

$$\begin{vmatrix} 10 & 1 & 0 & 0 \\ 50 & 35 & 10 & 1 \\ 0 & 24\lambda & 50 & 35 \\ 0 & 0 & 0 & 24\lambda \end{vmatrix} > 0 \iff 0 < \lambda < \frac{25}{3}$$

Note that the uncertainty range one can cope with efficiently in such a case is only 25/3 (recall (6.35)).

VI.4.b.δ $\underline{\text{Analysis for } e > 3 \text{ and Conclusions}}$

As e increases, we can develop similar relations. To secure B.I.B.O. stability, one gets sufficient condition

$$0 < \lambda < \kappa \tag{6.68}$$

with $\lim_{e=\infty} \kappa = 1$. It becomes once more clear that stability is conflicting with the sensitivity of the system response to parameter uncertainty. Note that our filter is an "all pole" filter and a big improvement might be obtained by inserting proper "zeros". We have not pursued

this direction, since the filter is L.T.V., and it is rather difficult to introduce those zeros in a systematic way.

As for $e > 2$, the stability problem prevents us from coping with large uncertainty, the corresponding systems are not so useful. However, for $e = 1$, no stability problem occurs, and therefore the idea arises to use the "second order system" obtained with $e = 1$, and to doctor the "equivalent transfer function" by inserting a L.T.I. far-off zero-pole package in order to come out with the desired excess of poles over zeros. Without loss of generality, we used a package similar to:

$$\frac{K(s+z)}{(s^2+2\zeta_p\omega_p s+\omega_p^2)^n} \tag{6.69}$$

where n, z, ζ_p, ω_p are to be suitably chosen by the designer.

VI.4.c. Synthesis for Large Gain Uncertainty.

VI.4.c.α Philosophy of the Synthesis Procedure

Let the uncertainty range, $[k_{min}, k_{max}]$ and the T.D.S. be given. It is found experimentally that if $k_1 = k_{max}$ (recall (6.35)) is used, then the nominal response $c_1(t)$ is best chosen close to the prescribed time domain upper bound.

Using (6.35) $k_2 = k_{min}$ is first chosen. This leads, in general, to the slowest possible response signal, which may or may not be satisfactory. If not satisfactory, $k_2 < k_{min}$ (6.35) is adjusted until the response signal for $k = k_{min}$ is satisfactory. This can be understood physically from the fact that specifying a larger uncertainty range $[k_2, k_1]$ than the actual $[k_{min}, k_{max}]$ means that $\ell(t,\tau)$ handles a bigger burden due to uncertainty, which then leads to an increase in its "Bandwidth" and thus a smaller spread $\Delta c(t)$ for the

considered range $[k_{min}, k_{max}] \subset [k_2, k_1]$.

As a consequence, the sensor noise effect at the plant input is increased, but there is still preserved a certain improvement over L.T.I. design, as seen from the examples below. Note that the factor $W(t)$ in (6.1) can also be used; however this is, in general, only efficient at small t .

In a general sense $k = k_{min}$ does correspond to the lower Time Domain Bound but $k = k_{max}$ does not correspond to the upper one, because as $k \to k_{max}$, corresponding signals have the tendency to oscillate around the nominal signal $c_1(t)$ (see for example Fig. VI.8 and VI.10). Therefore, if one is to acheive T.D.S. this can certainly be done by cut and try, i.e., once k_2 has been selected, to correct the nominal signal $c_1(t)$ in order to satisfy those T.D.S. and then derive a new k_2 to satisfy the lower bound and so on. The above 'cut and try' is always inevitable whenever a 'trade-off' optimization criterion is used as the basis of design, whereas the primary specifications are in the form of performance bounds. We are at least finding a systematic cut and try procedure.

In order to determine the L.T.I. pole zeros package, the concept of "frozen-time open loop transmission" is used. This means that for each fixed time t_0 , the L.T.V. differential equation becomes a L.T.I. one and thus one can define the associated L.T.I. open loop transfer function $\Lambda(s,t_0)$ (Fig. VI.7). We are aware of the fact that L.T.V. system can be unstable although each of its associated $\Lambda(s,t_0)$ leads to a stable design, which means that the tool used here is certainly not a very accurate one. However, it turns out that this concepts can be applied successfully here and therefore we did not investigate more

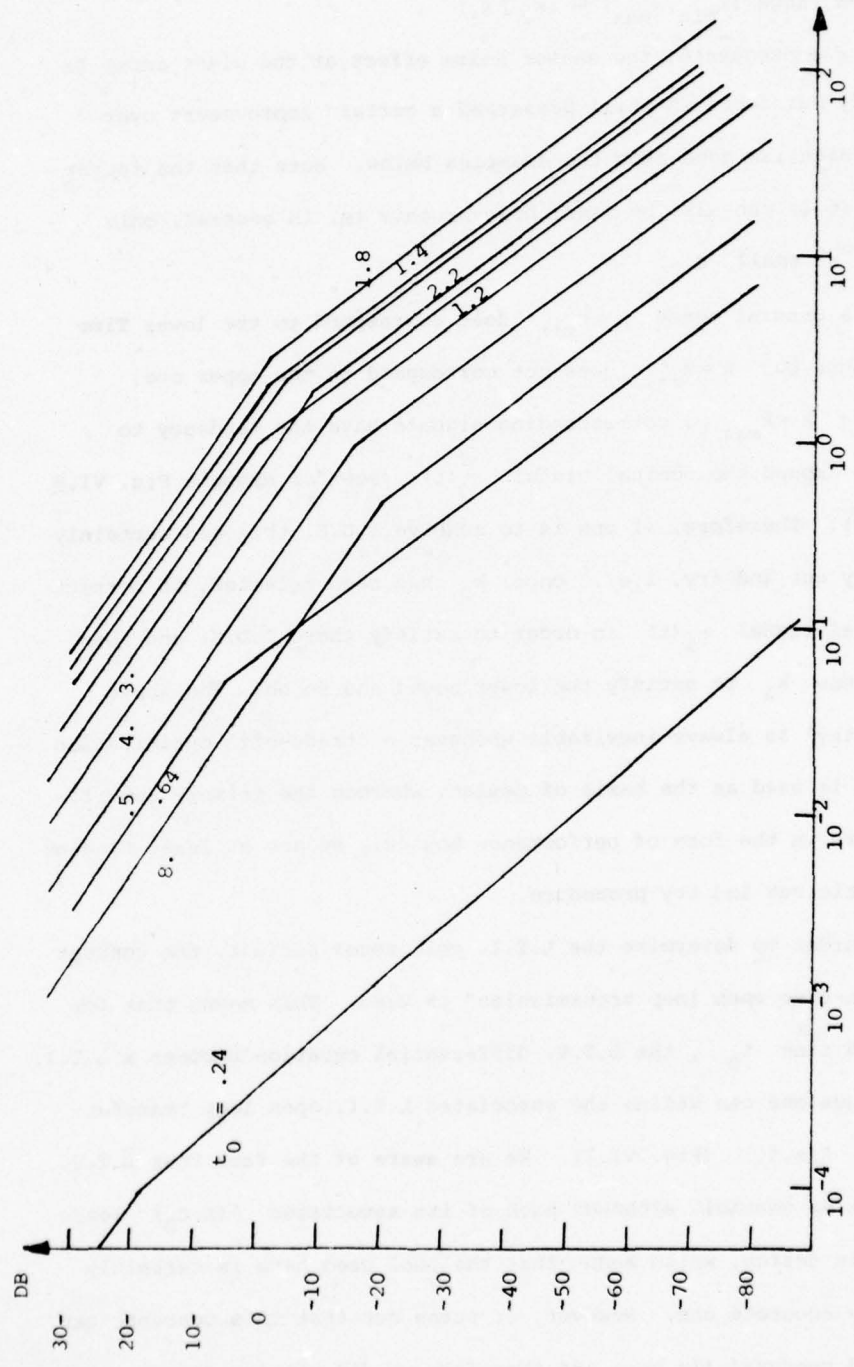

Figure VI.7 Bode Plot of the "frozen time open loop transmission" for different time t_0 .

accurate methods like the application of the EPLTI concept (see chapter VII).

The package is chosen to give a very small contribution to $\Lambda(s,t_0)$ in the low frequency range. Therefore, it suffices to consider the worst case, i.e., the $\Lambda_M(s,t_0)$ with the biggest bandwidth (Fig. VI.7). Thus it is conceivable that a 'time-varying far-off pole zero package' may be better.

VI.4.c.β Example and Results.

Assume a set of step command inputs of amplitude α_i, with $\langle\alpha_i^2\rangle$ Average over $i = 1$, and let the T.D.S. be as shown in Fig. VI.8.c. The plant $P(s) = k/s$ is considered with $k \in [1,100]$. Furthermore, it is assumed that the strength of the white sensor noise is $\sigma_N^2 = 1$. Following the above procedure, the nominal system response $c_1(t) = (1-e^{-t})^2$ is selected and paired with $k_1 = k_{max} = 100$. $k_2 = k_{min} = 1$ and $W(t) = 1$ are then first chosen. The corresponding system response to a step command are then shown in Fig. VI.8.a for different values of the gain factor, and it is seen that the T.D.S. are not satisfied. The sensitivity of the system response to plant uncertainty can be decreased by decreasing $W(t)$, giving then less emphasis to the noise performances. For instance with $W(t) = .01$ (Fig. VI.8.b) over-design is acheived. By cut and try $W(t) = .1$ is found satisfactory and the system response to a step command are then shown in Fig. VI.8.c for different values of the gain factor k.

Note that the plant is first order, therefore a far off zero pole package is not needed in the present case since the closed loop transmission, described by (6.58) with all terms in $\dot{D}/D$ and $\ddot{D}/D$ dropped, is second order, i.e.,

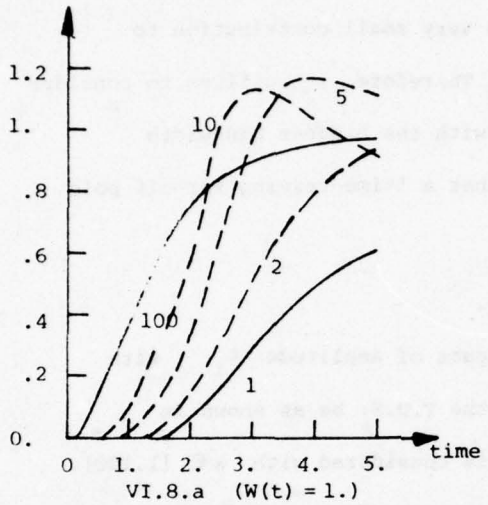

VI.8.a (W(t) = 1.)

Figure VI.8.a LTV system response to a command input for different plant gain factors when W(t) = 1. [P(s) = k/s].

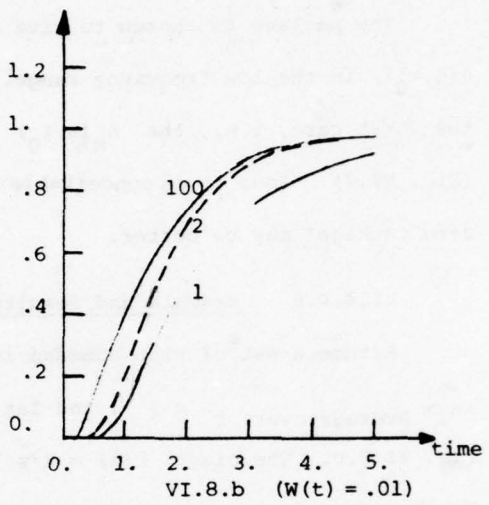

VI.8.b (W(t) = .01)

Figure VI.8.b LTV system response to a command input for different plant gain factors when W(t) = .01 [P(s) = k/s].

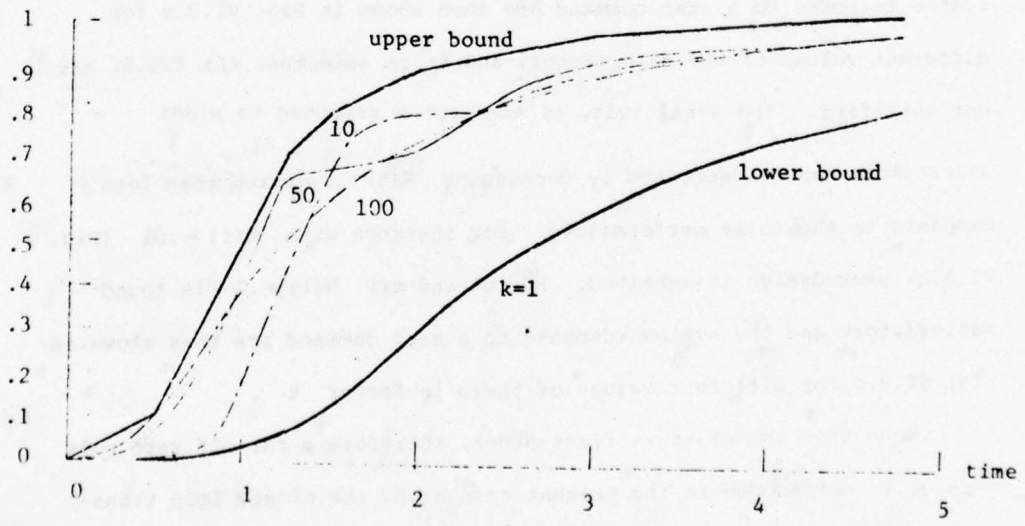

Figure VI.8.c LTV system response to a command input for different plant gain factors when W(t) = .1 [P(s) = k/s] .

$$[h] \quad : \quad \ddot{y} + \frac{2D_2^1 D_2}{\mu+(D_2^1)^2/2}\,\dot{y} + \left[\frac{\lambda(D_2)^2}{\mu+(D_2^1)^2/2} - \frac{2D_2^1\dot{D}_2}{\mu+(D_2^1)^2/2} \right] y = \frac{\lambda(D_2)^2}{\mu+(D_2^1)^2/2}\,X \tag{6.69.a}$$

where here: $D_2(t) = \frac{k_2-k_1}{k_1}\, c_1(t)$, $D_2^1(t) = \int_0^t D_2(\zeta)\,d\zeta$,

$\mu = W(t)\sigma_N^2/k_2^2 = .1$ and $\lambda = k/k_2$.

From (6.69.a) and recalling that $\ell = h(1-h)^{-1}$, we get:

$$[\ell] \quad : \quad \ddot{y} + \frac{2D_2^1 D_2}{\mu+(D_2^1)^2/2}\,\dot{y} - \frac{2D_2^1\dot{D}_2}{\mu+(D_2^1)^2/2}\,y = \frac{(D_2)^2}{\mu+(D_2^1)^2/2}\,X$$

The plant is $[p]: \dot{y} = kx$, so $[p^{-1}] : ky = \dot{x}$ and as $g = p^{-1}\cdot\ell$ we have:

$$[g] \quad : \quad \ddot{y} + \frac{2D_2^1 D_2}{\mu+(D_2^1)^2/2}\,\dot{y} - \frac{2D_2^1\dot{D}_2}{\mu+(D_2^1)^2/2}\,y = \frac{1}{k_2}\,\frac{\lambda(D_2)^2}{\mu+(D_2^1)^2/2}\,\dot{X} \tag{6.69.b}$$

As $c_1(s) = \frac{6}{s(s+1)(s+2)(s+3)}$ we have: ($c_1 \triangleq t_1$ r)

$T_1(s) = \frac{6}{(s+1)(s+2)(s+3)}$ and $T_1(s)$ is therefore associated with the D.E.

$$[t_1] : \quad \dddot{y} + 6\ddot{y} + 11\dot{y} + 6y = 6X \tag{6.69.c}$$

By definition, h_1 (obtained with $k = k_1$) is associated with t_1 , *therefore, the prefilter* f is such that:

$$\text{or} \quad \begin{matrix} h_1 \cdot f \triangleq t_1 \\ f = h_1^{-1}\cdot t_1 \end{matrix} \tag{6.69.d}$$

Using (6.69.a) and (6.69.c) we get:

$$[f] \quad : \quad \frac{k_1}{k_2}\,\frac{(D_2)^2}{\mu+(D_2^1)^2/2}\,[\dddot{y} + 6\ddot{y} + 11\dot{y} + 6y] = 6\left[\ddot{x} + \frac{2D_2^1 D_2}{\mu+(D_2^1)^2/2}\,\dot{x} + x\left(\frac{k_1}{k_2}\,\frac{(D_2)^2}{\mu+(D_2^1)^2/2} - \frac{2D_2^1\dot{D}_2}{\mu+(D_2^1)^2/2} \right) \right] \tag{6.69.e}$$

The mean square values of the sensor noise effect at the plant-input are shown on Fig. VI.9 for different plant conditions. The results are also given for the L.T.I. design [Appendix A3.8.b] which achieves the

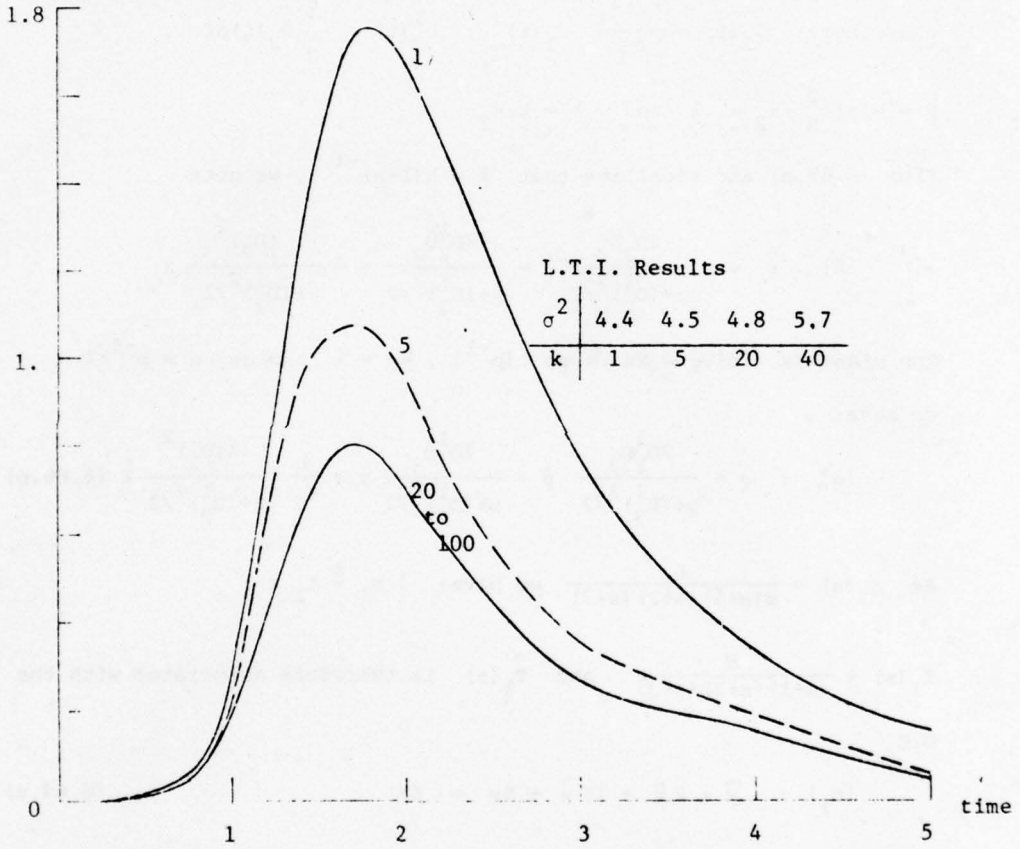

Figure VI.9 Mean square value of the Noise at the Plant Input for the L.T.V. and L.T.I. design (P(s) = k/s). .

same T.D.S. shown in Fig. VI.8.b.

There is clearly a big improvement in the noise level at the plant input. Note that $\sigma^2_{P.I.}(t) \to 0$ as $t \to \infty$ and for $t \to 0$. This can be understood from the fact that as $t \to \infty$, the L.T.V. network behaves like an open circuit and as $t \approx 0$ the signal $e(t)$ (Fig. VI.1) which is fed into G is very small and slow-varying, so a large bandwidth for G is not required. It is very interesting to note that

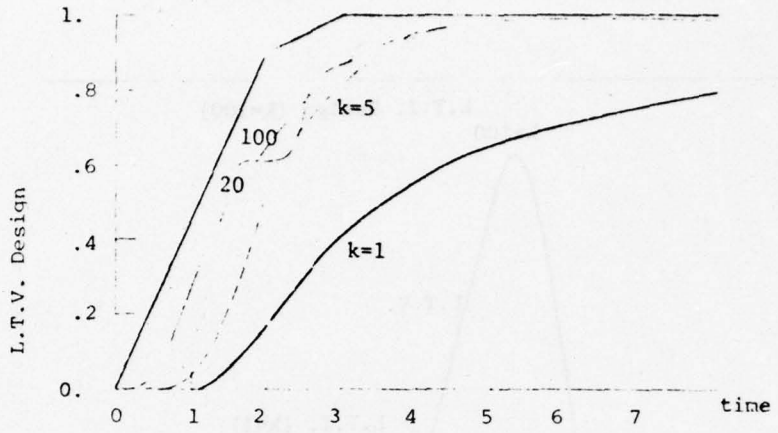

Figure VI.10 LTV system response to step command inputs for different plant gain values $(P(s) = k/s^2)$.

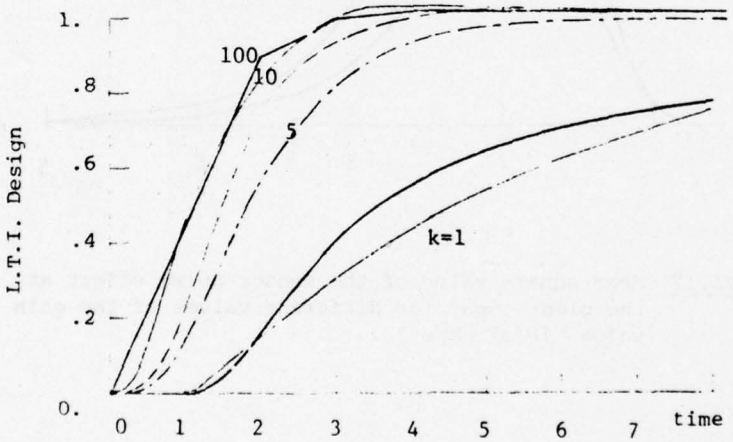

Figure VI.11 LTI system response to step command inputs for different plant gain values $(P(s) = k/s^2)$.

(Fig. VI.7) the bandwidth of our system has a maximum, leading to an extremum in the noise level, both occuring roughly at the same time as the maximum of $\frac{dc}{dt}$. The trade-off between noise level and bandwidth

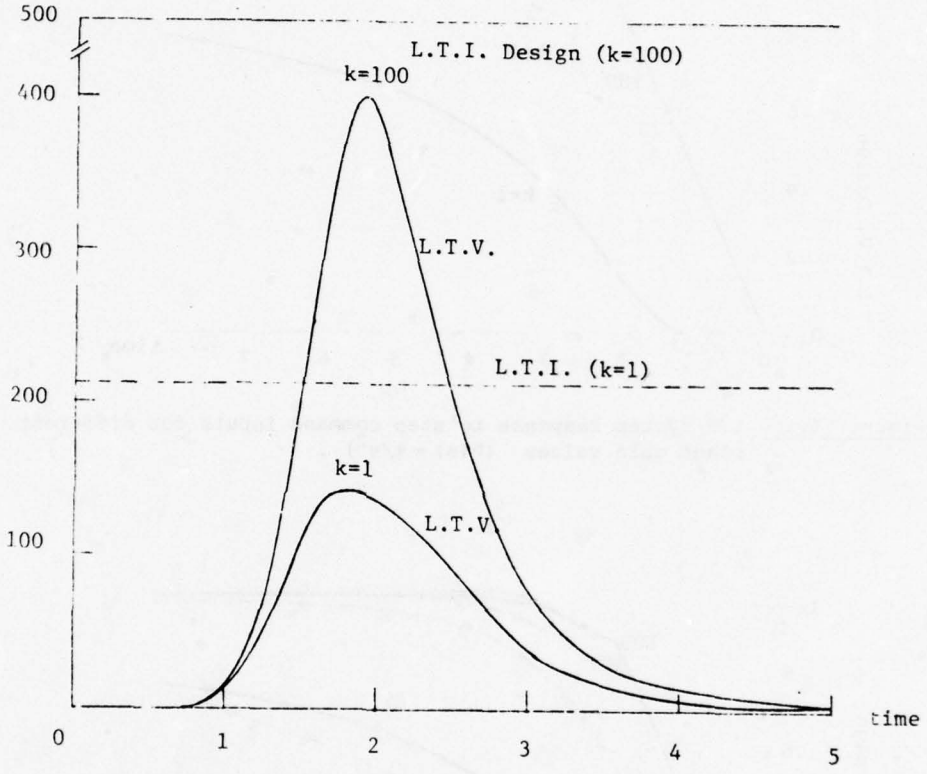

Figure VI.12 Mean square value of the sensor noise effect at the plant input for different values of the gain value $[P(s) = k/s^2]$.

of a system needed to handle fast varying signals is once more very clear.

Let us now consider the plant $P(s) = k/s^2$ with $k \in [1, 100]$

with the same set of command inputs as before. The T.D.S. are shown on Fig. VI.10 for this case. The nominal output $c_1(t) = (1-e^{-t})^3$ is once more selected and associated with $k = k_1 = k_{max} = 100$. Using the above procedure, $k_2 = k_{min} = 1$ is taken, and by cut and try $W(t) = .1$ is found satisfactory for the T.D.S. to be matched. However, as the plant is second order, we need here a far-off pole-zero package in order to be able to realize the compensation G . $n = 1$ is selected in (6.69) and the package used is: $\frac{\omega_p^2}{z} \frac{(s+z)}{(s^2+2\zeta_p\omega_p s+\omega_p^2)}$. The addition of such a package should not affect too much the signal responses obtained with the "second order system". Therefore, we took as a criterion, a phase lag of at most 5° at the maximum crossover frequency $\omega_{c_{max}} = 20$ rps. (Fig. VI.7) in the family of $\Lambda(s,t_0)$ depicted on that figure. The 'best' package is then found to be the one for which $z = 70$ rps. $\zeta_p = .4$, $\omega_p = .75 \times z$. In a similar way to the previous example (equations 6.69.a-e) the D.E. for f and g can be obtained; this step is skipped here to avoid lengthy derivations. System output responses are plotted in Fig. VI.10 for different plant conditions. Using then the T.D.S. shown on Fig. VI.10, a L.T.I. system was designed, for which the system responses to command are shown in Fig. VI.11. For both designs, the mean square value of the sensor's noise at the plant input is plotted in Fig. VI.12 for the two extreme cases. Improvement is seen for all $k \in [1 , 100]$.

VI.5 Solution to the filter problem by means of the Euler-Lagrange differential equation.

VI.5.a Statement of the problem.

It was explained in section VI.3.a, that the minimization problem of (6.2) has no solution and might be replaced by that given in (6.40), which has a solution (Appendix A3.5).

Let $P(s) = \frac{k}{s+\alpha}$ with uncertainty in both α and in k .

Let $P_1 = k_1/(s+\alpha_1)$ be paired with output signal $c_1(t)$.

For $P_2 = k_2/(s+\alpha_2)$ we want to:

$$\underset{h_2}{\text{Min}} \int_0^T \left[\left(D(t) - \int_0^t h_2(t,\zeta)D(\zeta)d\zeta\right)^2 W(t) + \sigma^2_{P.I.}(t) \right] dt \qquad (6.70)$$

where $\sigma^2_{P.I.}(t)$ is defined in (6.1), with (6.1a)

$\theta(t,\zeta) = \frac{1}{k_2}\left(\frac{\partial}{\partial t} h_2(t,\zeta) + \alpha_2 h_2(t,\zeta)\right)$ and $\gamma_{NN}(\zeta_1,\zeta_2) = \sigma_N^2 \delta(\zeta_1-\zeta_2)$

(6.70) becomes $\left(\mu \triangleq \frac{\sigma_N^2}{k_2^2}\right)$

$$\underset{h_2}{\text{Min}} \int_0^T \left[\left(D(t) - \int_0^t h_2(t,\zeta)D(\zeta)d\zeta\right)^2 W(t) + \mu \int_0^t \left[\frac{\partial}{\partial t} h_2(t,\zeta) + \alpha_2 h_2(t,\zeta)\right]^2 d\zeta \right] dt \qquad (6.71)$$

As shown in Appendix A3.5, if $\alpha_2 = 0$, (6.71) is equivalent to the Euler-Lagrange D.E.

$$\frac{\partial^2 h_2}{\partial t^2}(t,\tau) + D(\tau)\left[D(t) - \int_0^t h_2(t,\zeta)d\zeta\right] = 0 \quad . \qquad (6.72)$$

No closed form solution exists, in general, and (6.72) must be solved by numerical methods. This is certainly a direction to pursue in some future research, but as we want to avoid numerical methods, we assume $h_2(t,\tau)$ has the form:

$$h_2(t,\tau) = A(t)(\theta(t) - \theta(\tau))u(t-\tau) \tag{6.73}$$

where $A(t)$ is unknown and $\theta(t)$ is given.

VI.5.b Solution to the filter problem and outline of the synthesis procedure.

As shown in Appendix A3.7, when (6.73) is inserted into (6.70), the Euler-Lagrange differential equation is:

$$\ddot{A}\left(t\theta^2(t) - 2\theta(t)\theta_1(t) + \int_0^t \theta^2(\zeta)d\zeta \right) + 2\dot{A}\dot{\theta}(t)\left(t\theta(t) - \theta_1(t) \right)$$

$$+ A\left(\ddot{\theta}(t)(t\theta(t) - \theta_1(t)) - \alpha_2^2\left(t\theta^2(t) - 2\theta(t)\theta_1(t) + \int_0^t \theta^2(\zeta)d\zeta \right) - \frac{W(t)}{\mu} J^2(t) \right)$$

$$= - \frac{D(t)W(t)J(t)}{\mu} \tag{6.74}$$

where $J(t) = \int_0^t (\theta(t) - \theta(\zeta))D(\zeta)d\zeta$ and $\theta_1(t) \triangleq \int_0^t \theta(\zeta)d\zeta$

(6.74) is a singular differential equation which has in general at least one unstable solution, because the coefficient in A is always negative, while those in $\ddot{A}$ and $\dot{A}$ are both positive. To extract the stable solution involves here too, numerical methods, which we want to avoid. However, it seems that by a proper choice of $A(0)$ and $\dot{A}(0)$, we can obtain quasi-stable solutions of (6.74), that is, solutions which can be considered as stable over some finite interval $[0,T]$, big enough for our purposes.

The synthesis procedure is then very similar to that described in section VI.4.d.α. $c_1(t)$ is chosen to lie within the prescribed T.D.S., close to the upper bound and is paired with P_1 corresponding to the highest gain value $k = k_{max}$. We then try first $k_1 = k_{max}$, $k_2 = k_{min}$. As before, a cut and try procedure is then used to find k_2 and $W(t)$ such that the output signals corresponding to

$k \in [k_{min}, k_{max}]$ lie within the T.D.S.

VI.5.c Examples of application and results.

VI.5.c.α P(s) = k/s

The plant $P(s) = k/s$ with uncertainty in the gain factor $k \in [1,100]$ is considered here. This example was already considered in section VI.4.d.β. The T.D.S. shown on Fig. VI.13 are to be satisfied for system step command inputs. The nominal output response to a unit step command is taken as $c_1(t) = (1-e^{-t})^3$ and is paired with $k = k_1 = k_{max} = 100$. $k_2 = k_{min} = 1$ is then selected, $\theta(t)$ in (6.73) is taken as $\theta(t) = D_1(t)$, $(\dot{\theta}(t) = D(t))$, where: $D(t) = \frac{k_2 - k_1}{k_1} c_1(t)$, and it is assumed that $\sigma_N^2 = 1$, implying that $\mu = \sigma_N^2/k_2^2 = 1$. In a manner similar to the procedure described in VI.4.d.β. $W(t) = 1$ is first chosen and by cut and try, $W(t) = .1$ is found to be satisfactory. Therefore the 'optimum' system (under the present assumption) is obtained from (6.73) as $h_2(t,\tau) = A(t)(D_1(t) - D_1(\tau))u(t-\tau)$ with $A(t)$ the solution of: (recall 6.74)

$$\left(tD_1^2(t) - 2D_1(t)D_2(t) + \int_0^t D_1^2(\zeta)d\zeta\right) + 2\dot{A}D(t)\left(tD_1(t) - D_2(t)\right)$$

$$+ A\left(\dot{D}(t)(tD_1(t) - D_2(t)) - .1\,\frac{D_1^4(t)}{4}\right) = -.1\,\frac{D(t)D_1^4(t)}{4}$$

Using Appendix (A3.6), the differential equation associated with h_2 is:

$$[h_2]: \quad \ddot{y} - \dot{y}\left(2\frac{\dot{A}}{A} - \frac{\dot{D}}{D}\right) + y\left[2\left(\frac{\dot{A}}{A}\right)^2 + \frac{\dot{A}}{A}\frac{\dot{D}}{D} - \frac{\ddot{A}}{A}\right] = ADX$$

and therefore $(\ell_2 = h_2(1-h_2)^{-1})$

$$[\ell_2]: \quad \ddot{y} - \dot{y}\left(2\frac{\dot{A}}{A} - \frac{\dot{D}}{D}\right) + y\left[2\left(\frac{\dot{A}}{A}\right)^2 + \frac{\dot{A}}{A}\frac{\dot{D}}{D} - \frac{\ddot{A}}{A} - AD\right] = ADX$$

so $g = p_2^{-1} \cdot \ell_2$ is associated with the differential equation:

$$[g]: \quad \ddot{y} - \dot{y}\left(2\frac{\dot{A}}{A} - \frac{\dot{D}}{D}\right) + y\left(2\left(\frac{\dot{A}}{A}\right)^2 + \frac{\dot{A}}{A}\frac{\dot{D}}{D} - \frac{\ddot{A}}{A} - AD\right) = \frac{AD}{k_2}\dot{X} \quad .$$

The prefilter f is obtained by satisfying

$$\ell_1 \cdot (1+\ell_1)^{-1} \cdot f = t_1$$

or:

$$f = (1+\ell_1) \cdot \ell_1^{-1} \cdot t_1 = (1+\ell_1^{-1}) \cdot t_1$$

where t_1 is the specified overall transfer function associated with $P = P_1$, i.e., $T_1(s) = \frac{C_1(s)}{R(s)} \quad \frac{8}{(s+1)(s+2)(s+4)}$ in the present case.

The system response to step command inputs are shown on Fig. VI.13 for different plant gain factors. It should be noted, as stated above, that all these solutions are "unstable" at infinite t, but can be regarded as "stable" over some finite interval of time. This is not inconvenient if one has to satisfy T.D.S. over a finite interval $[0,T]$, as is often the case with L.T.V. designs (recall that L.T.V. designs do not give identical results for $[0,T]$ and $[a, T+a]$).

The effect of white sensor noise (of power spectrum $\sigma_N^2 = 1.$) is shown on Fig. VI.14 for different plant gain factors, and is compared with the results given by a L.T.I. network which achieves the same T.D.S.

VI.5.c.β $\underline{P(s) = k/s+\alpha}$

Consider the plant $P(s) = k/(s+\alpha)$ with uncertainty in $\alpha \in [.1 , 1.]$ and with no uncertainty in the gain factor. Let us select $k_2 = 1.2$, $k_2 = 1.$, and assume that $c_1(t) = (1-e^{-t})^3$ is paired with $P_1(s) = k_1/s+1$. Let $\sigma_N^2 = 1$ and let the T.D.S. to step command inputs be as shown in Fig. VI.15. Once more, by cut and try, $W(t) = .1$,

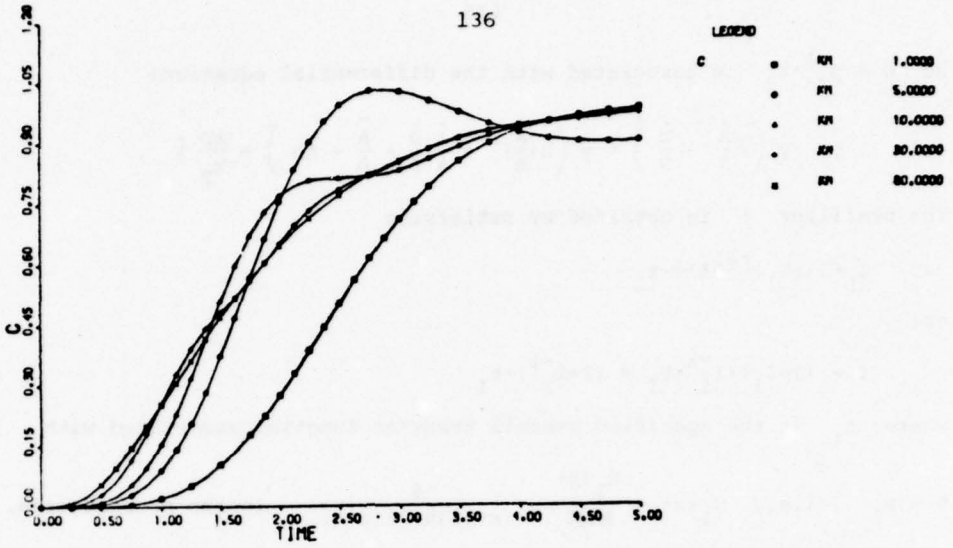

Figure VI.13 LTV system response to a step input command for different plant gain values.

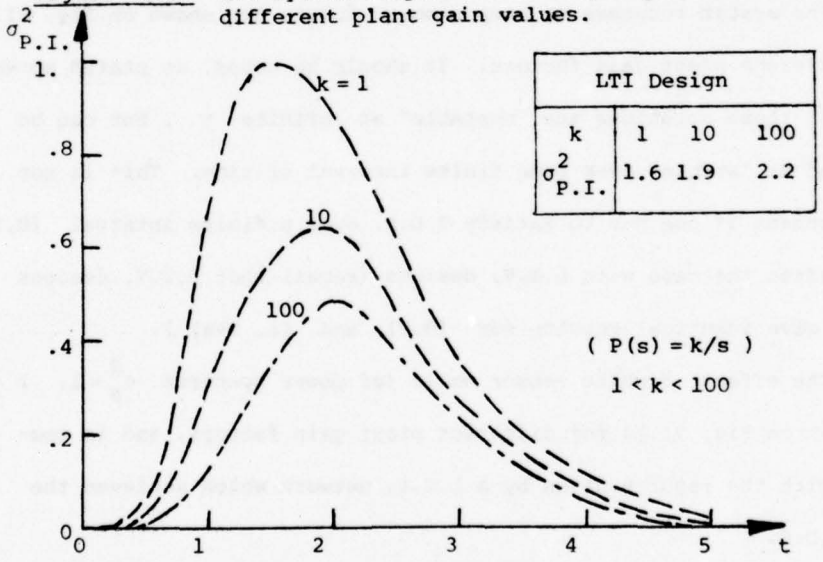

LTI Design			
k	1	10	100
$\sigma^2_{P.I.}$	1.6	1.9	2.2

Figure VI.14 Mean square value of the noise at the plant input due to white sensor noise for the LTV and LTI design.

is found satisfactory giving, for different values of α, the responses to a step command shown in Fig. VI.15; g and f can be obtained as in the above section. (The details are therefore skipped here.)

It should be underlined that our synthesis technique cannot cope with large uncertainty in both the gain factor k and the pole α. (Note that this was also true with the first approach.)

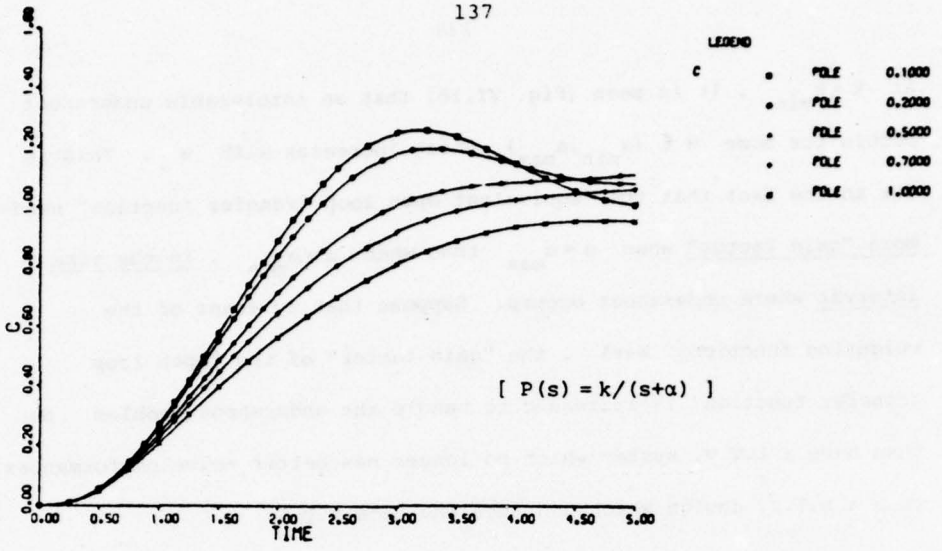

Figure VI.15 LTV system response to a step input command for different values of the pole α .

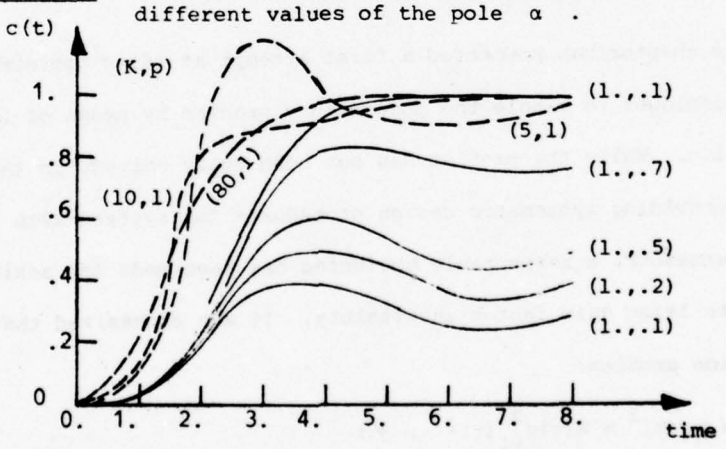

Figure VI.16 Typical LTV system response to step command inpute for different plant conditions. $P(s) = k/(s+p)$.

This is due to the fact that our optimum design is very sensitive, because it is "tuned" to the two extreme cases, $P_1(s) = \frac{k_{max}}{s+\alpha_{max}}$ and $P_2(s) = \frac{k_{min}}{s+\alpha_{min}}$ (interchange of α_{max} and α_{min} does not help). This means that both approaches give correct system responses [Fig. VI.16] for the gain factor values $k \in [k_{min}, k_{max}]$ when $\alpha = \alpha_{min}$. However,

at $k = k_{min}$, it is seen [Fig. VI.16] that an intolerable undershoot occurs for some $\alpha \in (\alpha_{min}, \alpha_{max})$ which increases with α . This is due to the fact that the "equivalent open loop transfer function" needs more "gain factor" when $\alpha = \alpha_{max}$ than when $\alpha = \alpha_{min}$, in the time interval where undershoot occurs. Suppose that by means of the weighting functions $W(t)$, the "gain factor" of the "open loop transfer function" is increased to handle the undershoot problem. We then have a L.T.V. system which no longer has better noise performances than a L.T.I. design which achieves the same T.D.S.

VI.6. Conclusions

This chapter has presented a first attempt at using optimum filter techniques to handle the uncertainty problem by means of LTV compensation. While the problem has not been fully solved, in the sense of providing systematic design procedures for systems with large plant uncertainty, a respectable beginning has been made for achieving TDS despite large gain factor uncertainty. It was emphasized that the minimization problem:

$$\underset{h_2}{\text{Min}} \left(\Delta c(t)^2 + W(t)\sigma_{pI}^2(t) \right) \quad , \forall t$$

had no analytical solution for realistic plants (of order $n \geq 1$).

Two alternatives were then presented, leading to realistic solutions with substantial improvements over LTI design in terms of sensor noise rejection at the plant input. We can conclude that this chapter gave us a better understanding of the achievements and the limitations that can be expected from LTV networks, when used to cope with the uncertainty problems. Considerable work has yet to be done

to arrive at a comprehensive synthesis theory for large and general plant uncertainty. A possible direction is try numerical methods, inasmuch it was noted that no closed form solution can in general be expected.

It is seen that the improvements were much more spectacular with N.L. compensations (recall FORE), as might have been expected. One price paid is obviously in terms of stability, since the stability problem is usually more difficult in non-linear systems than in LTV systems. Also, one must design for specific input classes in non-linear systems and must carefully check for the system response to the occasional signal belonging to other classes. While, here, we also tailor the design to a specific class of inputs, one can much more easily determine its response to other input classes. However, it should be mentioned that a significant restriction of LTV systems is that one must know precisely when a specific input (of a certain class) begins in time.

CHAPTER VII. NONLINEAR FEEDBACK SYNTHESIS FOR SYSTEMS WITH LARGE PLANT IGNORANCE FOR PRESCRIBED TIME DOMAIN SPECIFICATIONS OF A "NONLINEAR TYPE".

VII.1. Introduction.

VII.1.a Generalities.

It was shown in chapter II (section 4) that some classes of N.L.T.V. plant W can be characterized by a set $P^{\alpha}[s]$, denoted as the EPLTI, which is associated with the system input $i^{\alpha}(t)$ and defined over a set of acceptable system output $C^{\alpha}[t]$. This equivalent characterization of the plant (that was proven by application of Schauder's fixed point theorem) lends itself very easily to quantitative specifications and is therefore a powerful tool in the synthesis of nonlinear feedback systems. This technique has been applied successfully to the quantitative synthesis of feedback systems that included L.T.V. or static nonlinear uncertain plants. This chapter presents the first application of the EPLTI set concept to dynamic nonlinearities.

The synthesis technique for L.T.I. plants that was reviewed in chapter II (section 1) implicitely assumes T.D.S. of a linear "type", i.e., if r_i denotes a command input applied to the system of Fig. VII.1

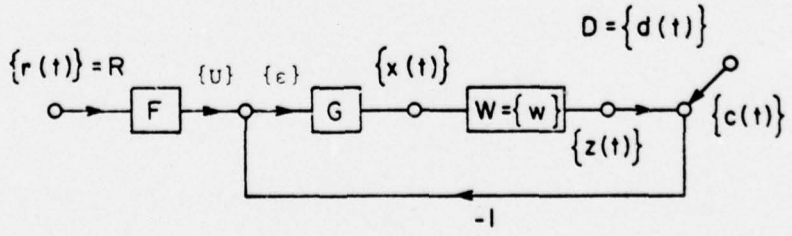

Figure VII.1. Feedback structure with nonlinear uncertain plant set W .

and c_i its corresponding output, then: $\forall r_1 = \lambda r_2 \Leftrightarrow c_1(t) = \lambda c_2(t)$ (7.1). However, it is conceivable that the T.D.S. are of a different nature, i.e., linear time varying (L.T.V.), nonlinear time invariant (N.L.) or nonlinear time varying (N.L.T.V.).

α). T.D.S. of a "L.T.V. type" means that the T.D.S. on the system impulse response are different for different instant of application of the impulse. This problem has been discussed elsewhere [H8], [H6].

β). T.D.S. of a "nonlinear type" means for example that the specifications are different for different signal amplitudes or the T.D.S. for a ramp input are not necessarily the integral of those for a step, or more generally given $(T.D.S.)_i$ for r_i and $r_j = g*r_i$, then $(T.D.S.)_j \neq g*(T.D.S.)_i$. This problem is considered here.

γ). T.D.S. of a "nonlinear time varying type" combines α) and β). The solution to this problem is therefore a combination of the solutions to α) and β).

VII.1.b Nonlinear time domain specifications (N.L.T.D.S.).

Fig. VII.2 shows the acceptable response tolerances for a

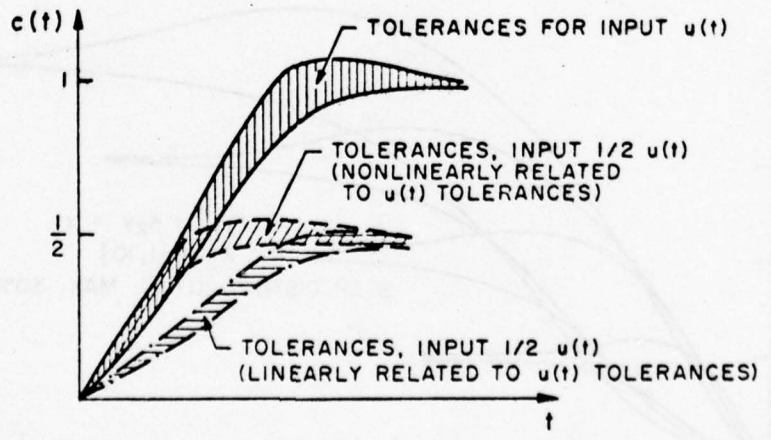

Figure VII.2. "Linear" and "nonlinear" tolerances on step response.

unit step response $r(t) = u(t)$. In a linear system, those for $r(t) = .5u(t)$ are one half of the former, as shown. In a nonlinear system they may be as shown in Fig. VII.2, of the kind usually associated with time optimal response. It is conceivable, for example, that one might want the unit ramp response to differ significantly from the integral of the unit step response, which is impossible in a linear system. One should note at this point that there is considerable ambiguity with N.L.T.D.S. so defined. Indeed, with L.T.I. system the response specifications are the same when the command input jumps from 0 to 1 , 1 to 2 or from 5.2 to 6.2 .

This is, however, no longer true for N.L.T.D.S. and therefore all the specifications that will be considered here are relative to the reference $r = 0$. Obviously, one can also incorporate other references than zero by adding some other contraints which then increase the complexity of the problem.

It is shown that it is possible to achieve N.L.T.D.S. of the type of Fig. VII.3, by using a L.T.I. compensation G(s) (Fig. VII.1) and a

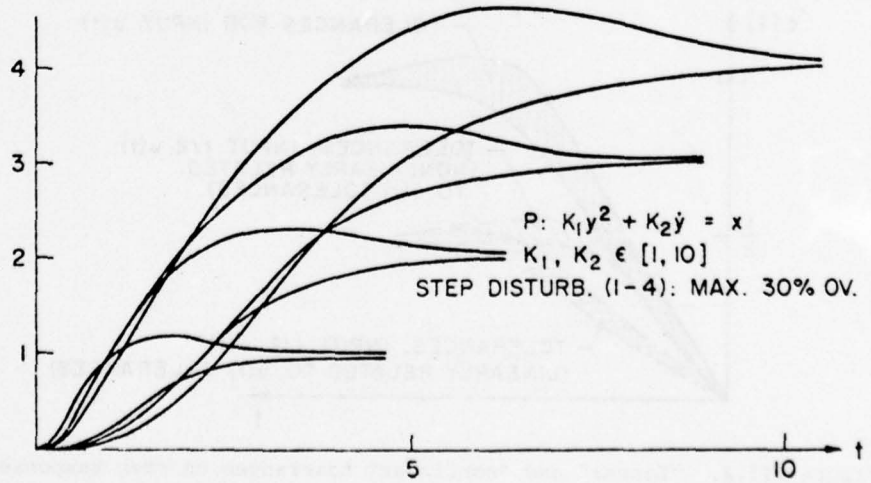

Figure VII.3. Problem statement.

nonlinear prefilter F .

VII.1.c Nonlinear prefilter.

The problem raised by the synthesis of such a nonlinear prefilter F introduces us to the research area of "open loop nonlinear synthesis", for which only primitive solutions exist up to now. The problem is: given a finite set of input signals $R = \{r\}$, design F such that to each input r_i there corresponds a specified output $u_i(t)$ (Fig. VII.1). One obvious necessary condition for the existence of such an F is that: if $r_i(t) \equiv r_j(t)$ for $t \in [0,t_1]$ then $u_i(t) \equiv u_j(t)$ for the same interval.

VII.2. Synthesis procedure.

VII.2.a Philosophy of the design procedure.

Following section II.4, the α - EPLTI transfer function set associated with input $i^\alpha(t) \in I$ over the admissible output set $C^\alpha[t]$ and the nonlinear plant set W , is

$P^\alpha[s] = \{P^\alpha_{i_\nu}(s)\ ,\ z^\alpha_\nu \in Z^\alpha[t]\ ,\ w_i \in W\}$, which is well defined for all frequencies $\omega \in \Omega = [0,\infty[$. It was shown [H2] that frequency domain specifications suffice to guarantee T.D.S., therefore the synthesis technique uses frequency domain concepts.

In the frequency domain, there is associated with each system input $i^\alpha(t) \in I$ a set $Q(\omega)$ of permissible equivalent overall transfer function $T^\alpha(j\omega)$ [see [S2]]. The synthesis technique for L.T.I. systems that was discussed in chapter II (section 1) can now be applied and Equations (2.1) and (2.2) are rewritten here as

$$\forall \omega \in \Omega \qquad \sup_i \Delta \ln \left| \frac{G(j\omega)\ P_i^\alpha(j\omega)}{1+G(j\omega)P_i^\alpha(j\omega)} \right| \leq \Delta \ln |T_\alpha(j\omega)| \qquad (7.2)$$

where i ranges over all possible plant parameters, and α over all possible command inputs.

Satisfaction of (7.2) at some frequency ω_ℓ, leads to a bound $B_\alpha(\omega_\ell)$ on the compensation $G(j\omega)$, due to the input $i^\alpha(t)$. This is repeated for each system input $i^\alpha(t) \in I$, leading at each ω_ℓ to N bounds $B_\alpha(\omega_\ell)$ (Fig. VII.4). $G(j\omega)$ should satisfy all these N bounds and therefore the final bound $B(\omega_\ell)$ (in dashed lines in Fig. VII.4) on $G(j\omega)$ is such that:

$$B(\omega_\ell) = \bigcup_\alpha \sup_\theta B_\alpha(\omega_\ell) \quad \text{with} \quad \theta = G(j\omega_\ell) \qquad (7.3).$$

This is conceptually done at each $\omega_\ell \in \Omega$, and one then obtains the optimum L.T.I. $G(s)$ in the same manner as in [H2], i.e., as the one which lies exactly on its bound at each $\omega_\ell \in \Omega$.

Once $G(s)$ is determined, the set $\{u\}$ (Fig. VII.1) which is to be paired with $\{r\}$ can then be obtained. The nonlinear prefilter F must produce $u_i(t) \in \{u\}$ when the input is $r_i(t) \in \{r\}$. Some primitive solutions are given in [H1] and in Appendix A2.

VII.2.b Details of the design procedure.

These are best understood through an example.

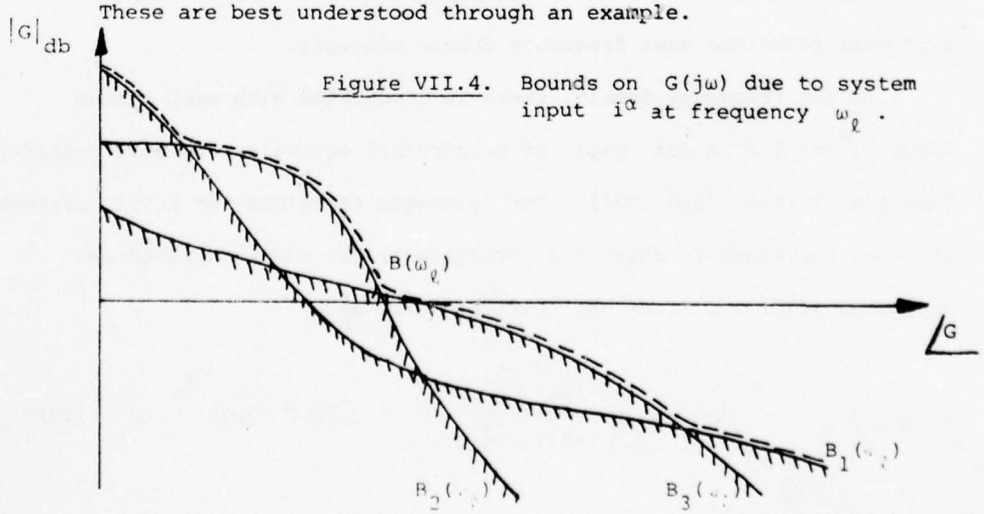

Figure VII.4. Bounds on $G(j\omega)$ due to system input i^α at frequency ω_ℓ.

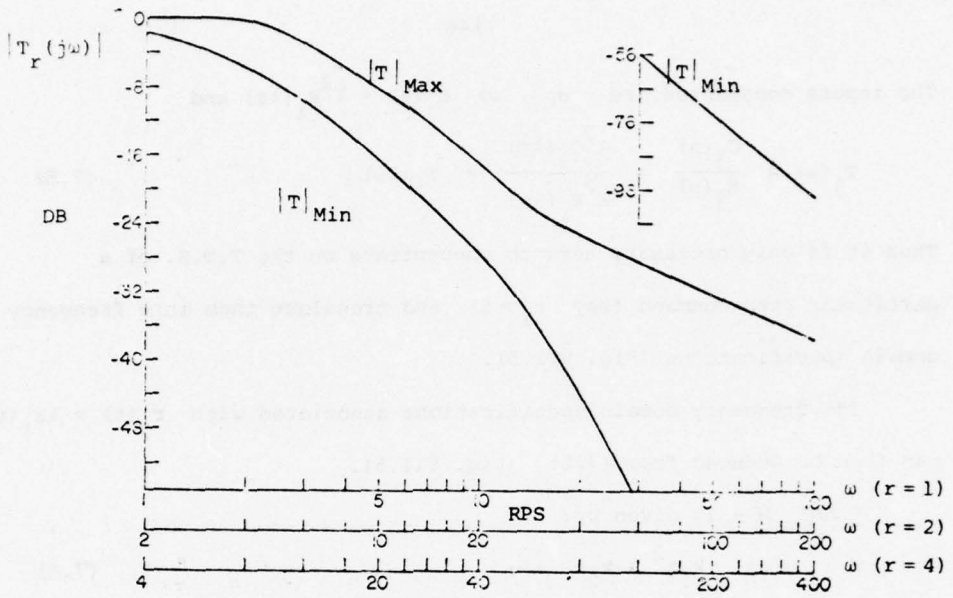

Figure VII.5. Frequency domain specifications due to command inputs.

VII.2.b.α Specifications.

SET OF SYSTEM INPUTS It consists of:

1) Step inputs $ru(t)$, $|r| \in [1,4]$ for which we want to achieve the N.L.T.D.S. given below.

2) 0 - 4 step disturbances for which the maximum tolerable overshoot in the system response is to be 30 percent.

Therefore we will take here: $I \triangleq \{i^{\alpha}(t) , \alpha = 1,\ldots,12\} = \{r = \pm 1 , \pm 2 , \pm 4 , d = \pm 1 , \pm 2 , \pm 4\}$ and expect that specifications will also be met for intermediate values. If the latter turns out untrue, then the design specifications would be enlarged to include those system inputs for which the specifications are violated.

N.L.T.D.S. They are shown on Fig. VII.3 for step commands. Those are chosen such that, given the tolerances on $C_i(t)$, those on $C_j(t)$ associated with input $r_j(t) = \lambda r_i(t)$ have quite closely the property $C_j(\lambda t) = \lambda C_i(t)$. Consequently:

$$C_j(s) = \int_0^{\infty} C_j(u)e^{-us}du = \lambda \int_0^{\infty} C_i(\tfrac{u}{\lambda})e^{-us}du = \lambda^2 \int_0^{\infty} C_i(\sigma)e^{-\sigma\lambda s}d\sigma = \lambda^2 C_i(\lambda s) \quad (7.4)$$

The inputs considered are steps, so $R_j(s) = \lambda^2 R_i(\lambda s)$ and

$$T_j(s) \triangleq \frac{C_j(s)}{R_j(s)} = \frac{\lambda^2 C_i(\lambda s)}{\lambda^2 R_i(\lambda s)} = T_i(\lambda s) \qquad (7.5)$$

Thus it is only necessary here to concentrate on the T.D.S. of a particular step command (say $r_i = 1$) and translate them into frequency domain specifications (Fig. VII.5).

The frequency domain specifications associated with $r_j(t) = \lambda r_i(t)$ can then be deduced from (7.5), (Fig. VII.5,

PLANT W - is given by:

$$W : \; u \to z \quad k_1 z^2 + k_2 \dot{z} = u \qquad (7.6)$$

with uncertainty k_1 , $k_2 \in [1,10]$ independently.

VII.2.b.β Characterization of the EPLTI set.

The acceptable system output $C_r(t)$ is represented here by a second order system step response, in order to obtain an analytic expression for $P^{\alpha}[s]$. For step inputs of amplitude r ,

$$C_r(t) = r\left(1 - \frac{e^{-\zeta_n \omega_n t}}{\sqrt{1-\zeta_n^2}} \sin\left(\omega_n \sqrt{1-\zeta_n^2}\, t + \cos^{-1}\zeta_n\right)\right)$$

Our T.D.S. translate into:

$$.2 < \zeta_n \omega_n < 4. \quad \text{and} \quad .5 < \omega_n \sqrt{1-\zeta_n^2} < 2 \; . \qquad (7.7)$$

If $\omega_0 \triangleq \omega_n \sqrt{1-\zeta_n^2}$, then:

$$C_r^2(t) = r^2\left(1 + \frac{1}{2(1-\zeta_n^2)} e^{-2\zeta_n\omega_n t} + \frac{1-2\zeta_n^2}{2(1-\zeta_n^2)} e^{-2\zeta_n\omega_n t}\cos 2\omega_0 t - 2e^{-\zeta_n\omega_n t}\left(\cos\omega_0 t + \frac{\zeta_n}{\sqrt{1-\zeta_n^2}}\sin\omega_0 t\right) + \frac{\zeta_n}{\sqrt{1-\zeta_n^2}} e^{-\zeta_n\omega_n t}\sin 2\omega_0 t\right) \qquad (7.8)$$

and $\mathcal{L}[C_r^2(t)] \triangleq C_r^2(s) = \dfrac{r^2 2\omega_n^4 (3s+4\zeta_n\omega_n)}{s(s+2\zeta_n\omega_n)(s^2+2\zeta_n\omega_n s+\omega_n^2)(s^2+4\zeta_n\omega_n s+4\omega_n^2)}$

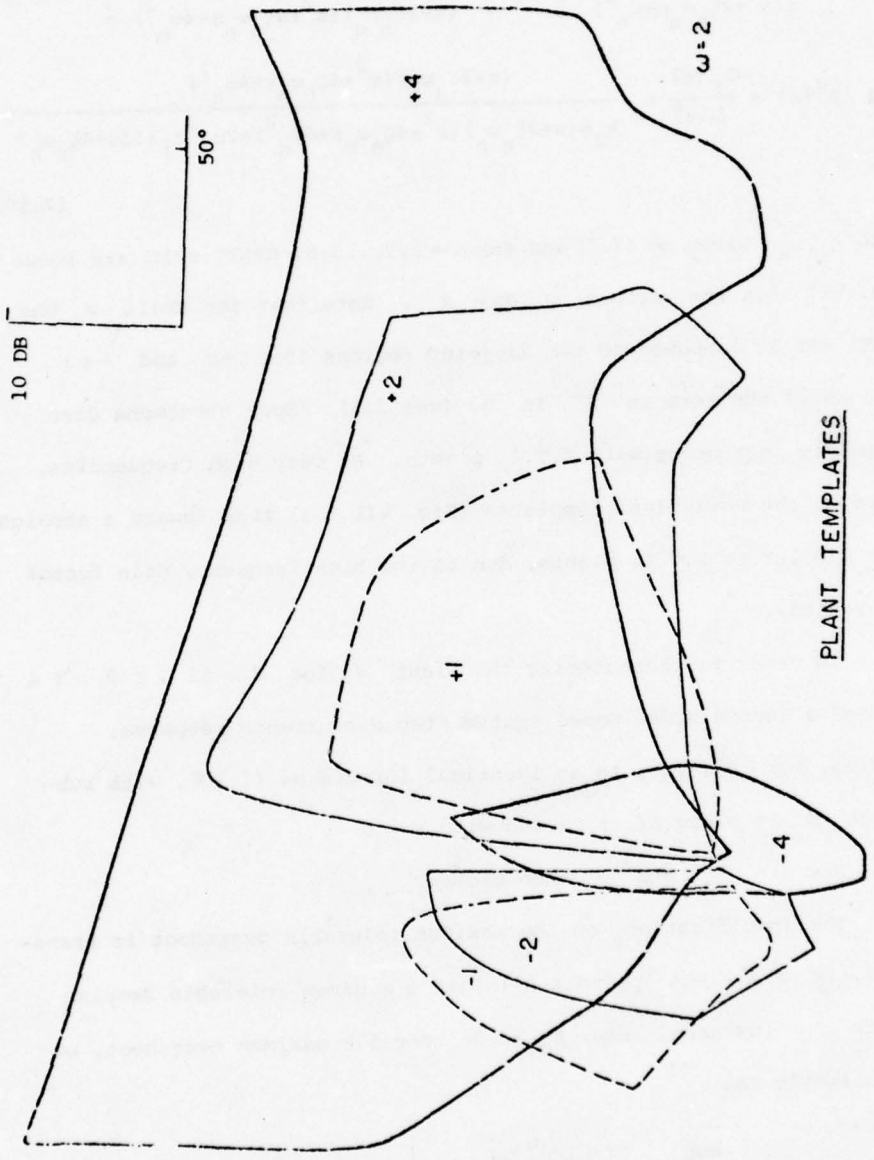

Figure VII.6.a.

Using (7.6)

$$u(s) = \frac{r\omega_n^2}{s(s^2+2\zeta_n\omega_n s+\omega_n^2)} \left[k_2 s + \frac{r2\omega_n^2 k_1(3s+4\zeta_n\omega_n)}{(s+2\zeta_n\omega_n)(s^2+4\zeta_n\omega_n s+4\omega_n^2)} \right] \quad (7.9)$$

$$\text{and } P^{\alpha}[s] = \frac{C_r(s)}{U(s)} = \frac{(s+2\zeta_n\omega_n)(s^2+4\zeta_n\omega_n s+4\omega_n^2)}{k_2 s(s+2\zeta_n\omega_n)(s^2+4\zeta_n\omega_n s+4\omega_n^2)+2\omega_n^2 k_1 r(3s+4\zeta_n\omega_n)} \quad (7.10)$$

with ζ_n, ω_n given by (7.7) and for $\alpha = 1,2,..5,6$. EPLTI sets are shown in Fig. VII 6.a for various ω and α. Note that for small ω the EPLTI set is composed of two disjoint regions (for $+r$ and $-r$) because of the term in z^2 in W (see 7.6). Such phenomena does obviously not occur with L.T.I. plants. At very high frequencies, however, the equivalent templates (Fig. VII.6.a) tend toward a straight line similar to L.T.I. plants, due to the high frequency gain factor uncertainty.

In order to characterize the plant W for $d = \pm 1, \pm 2, \pm 4$ we used a second order model system step disturbance response, leading, for $P^{\alpha}[s]$, to an identical formula as (7.10), with subscript d in place of r, and with $r = -d$.

How are ζ_d and ω_d then chosen?

The specification on the maximum tolerable overshoot is translated, as usual (see Appendix A1) into a minimum tolerable damping value. For instance, here $\zeta_d \geq .36$ for 30% maximum overshoot, or equivalently to:

$$\sup_i \left| \frac{G(j\omega)P_i^{\alpha}(j\omega)}{1+G(j\omega)P_i^{\alpha}(j\omega)} \right| \leq 3.4 \text{ db} \quad (7.11)$$

where i ranges over all possible plants and $\alpha = 7,8...,12$.

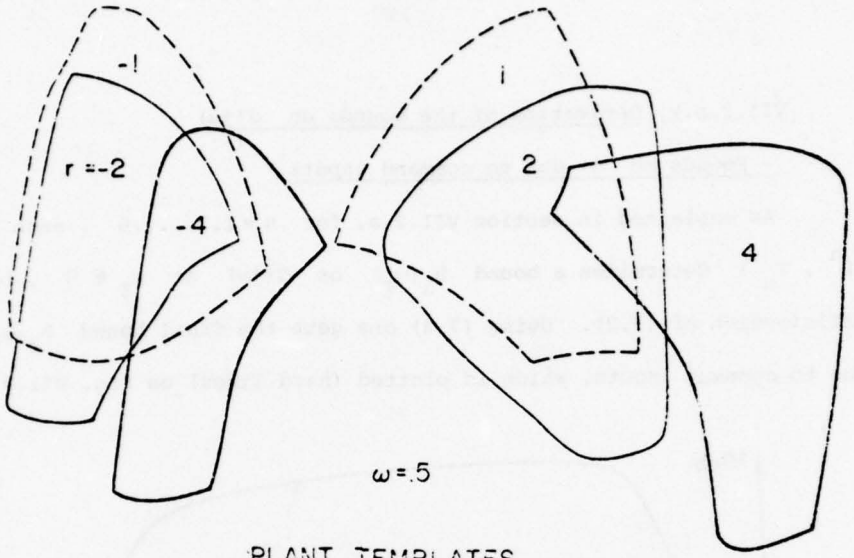

PLANT TEMPLATES

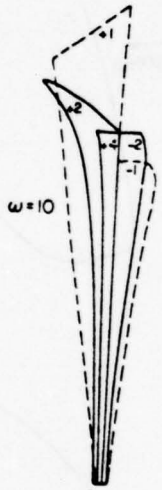

Figure VII.6.a. Templates at $\omega = .5, 2, 10$ rps. due to step command inputs $r = \pm 1 , \pm 2 , \pm 4$.

Unfortunately, ω_d cannot be known beforehand, leading to an unavoidable cut and try procedure that will be discussed later.

This specific problem is easier, in the above sense, if there are specific bounds on the disturbance response, for a class of input disturbances, when disturbance attenuation imposes a bigger feedback burden than satisfying command response specifications.

VII.2.b.γ Derivation of the bounds on $G(j\omega)$.

- Bounds on G due to command inputs.

As explained in section VII.2.a, for $\alpha = 1,2,\ldots,6$, each (P^{α}, T_{α}) determines a bound $B_{\alpha}(\omega_{\ell})$ on $G(j\omega)$ at $\omega_{\ell} \in \Omega$, by satisfaction of (7.2). Using (7.3) one gets the final bound $B_{c}(\omega_{\ell})$ due to command inputs, which is plotted (hard lines) on Fig. VII.7 for

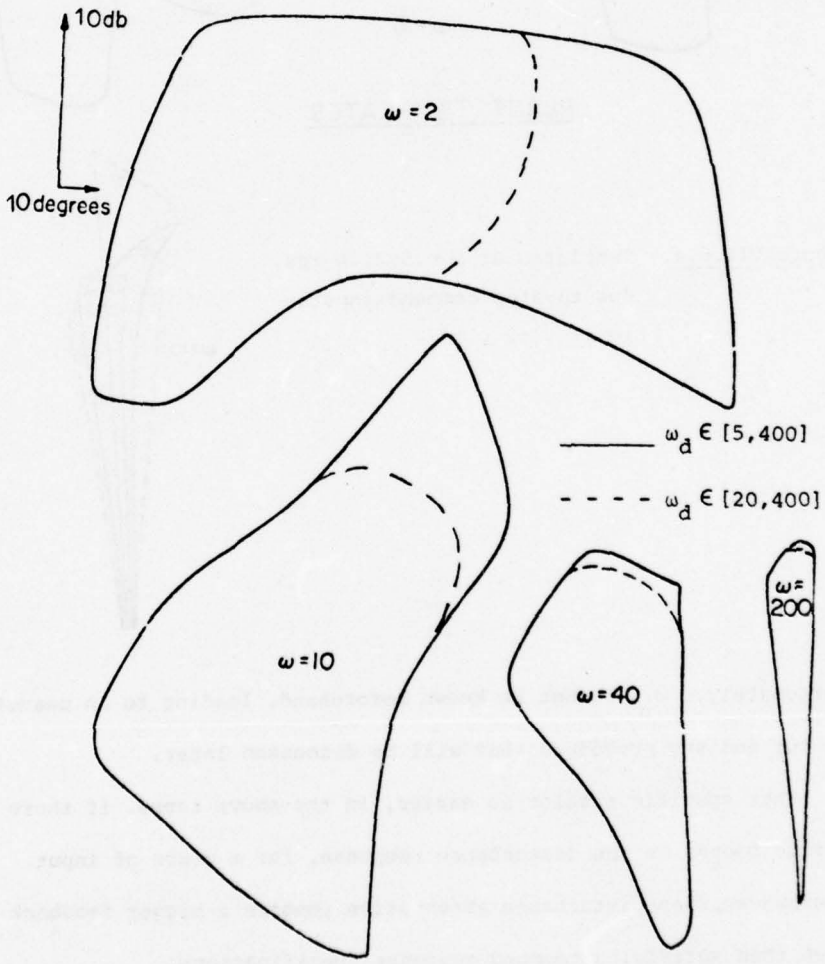

Figure VII.6.b. Templates at $\omega = 2.,10.,40.,200$ rps. due to step disturbances $|d| \in [0,4]$.

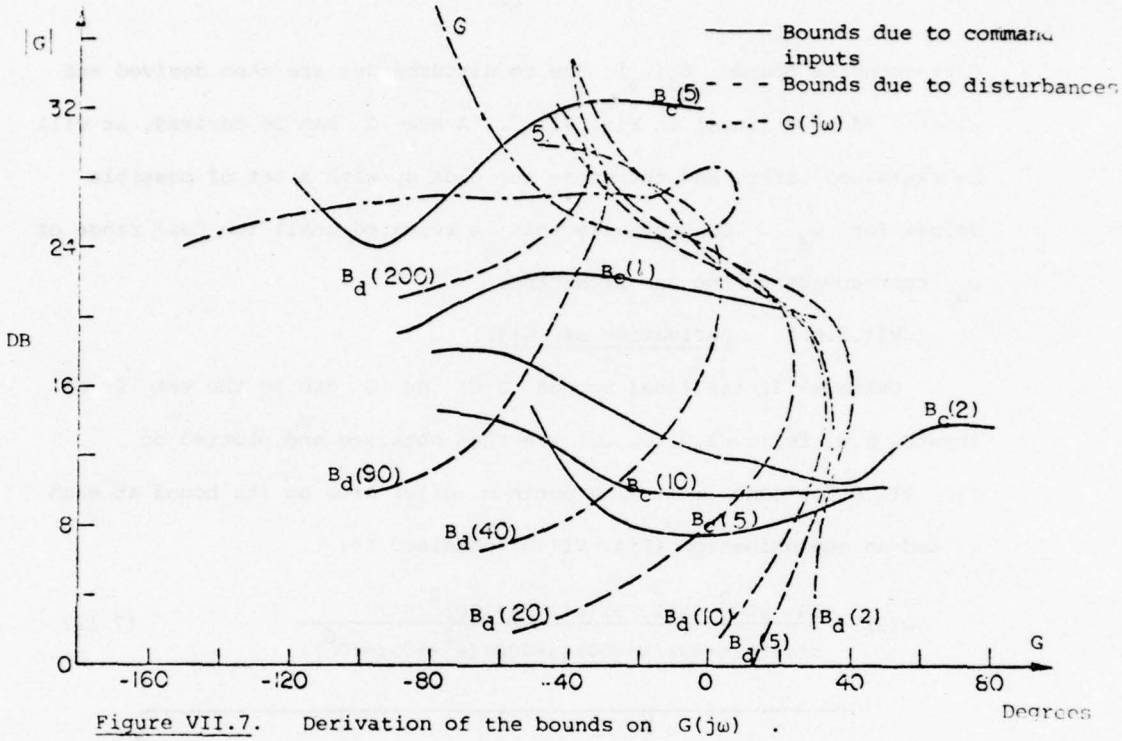

Figure VII.7. Derivation of the bounds on $G(j\omega)$.

some frequencies.

- Bounds on G due to disturbances.

If one is to derive $G(s)$ that satisfies the bounds on G due to command inputs only, one ends up with a final design for which the cross-over frequency of the equivalent open loop transfer function $\omega_c \in [4,80]$. Therefore for such a design, one guesses that $\omega_{d_{min}} \approx 4$ rps and $\omega_{d_{max}} \approx 80$ rps for the disturbance response approximation. It is obvious that those values represent approximate minimum bounds for both $\omega_{d_{min}}$ and $\omega_{d_{max}}$, because any $G(j\omega)$ which will also take care of the additional disturbance specifications can only be more conservative, and therefore ω_d can only be bigger. So, one guesses some range for ω_d [say (5,400)] and derives corresponding templates $P^{\alpha}[s]$ for $\alpha = 7,8,\ldots,12$ which are plotted on Fig. VII.6.b for some ω .

Corresponding bounds $B_d(\omega_\ell)$ due to disturbances are then derived and plotted (dotted lines) in Fig. VII.7. A new G can be derived, as will be explained later, and therefore one ends up with a set of possible values for ω_d . Conceptually this is repeated until the real range of ω_d corresponds to the one predicted.

VII.2.b.δ Derivation of $G(j\omega)$.

Using (7.3), the final bounds $B(\omega)$ on G due to the set I of inputs, (i.e. for $\alpha = 1,2,\ldots,12$) are then obtained and plotted on Fig. VII.8 for some ω . The optimum $G(j\omega)$ lies on its bound at each ω and an approximation (Fig. VII.8) obtained is:

$$G(s) = \frac{14.\ 10^{10}\ (s+1.25)(s+2)(s+120)^2}{s(s+5)(s+60)(s+300)(s+400)(s^2+800s+10^6)} \qquad (7.12)$$

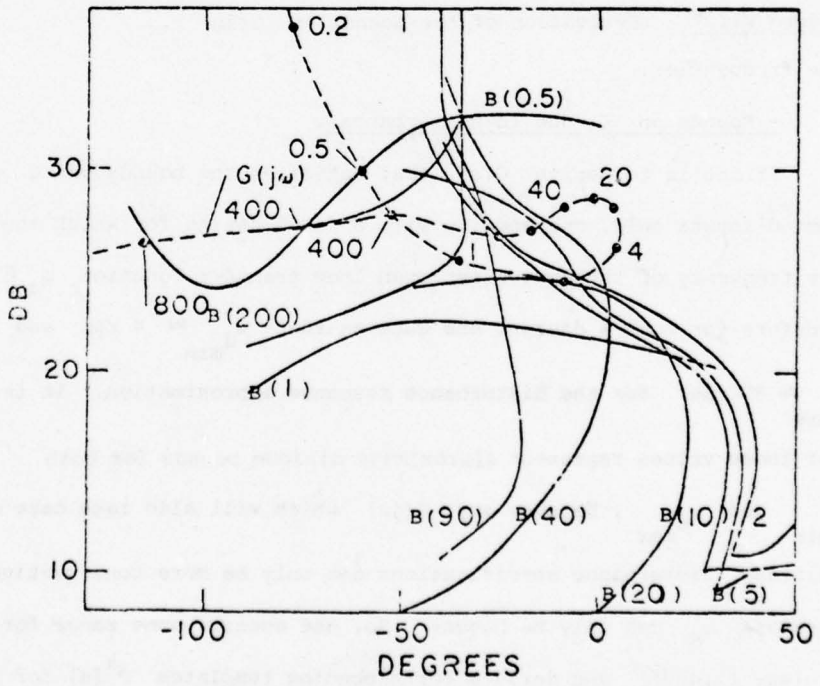

Figure VII.8. Final bounds on G and derivation of G .

for an excess of 3 poles over zeros.

The equivalent open loop transfer functions corresponding to the nominal plant K1=1 , K2=1 are then plotted on Fig. VII.9 for the values r = 1,2,4 of the command step inputs. We have (Fig. VII.9) $\omega_d \approx [20, 400]$ which is within the predicted range [5,400], implying some overdesign, and therefore one should begin again the design with a new prediction, say [10,400]. However, in the present example, removing the points corresponding to $\omega_d \in [5,20]$ leads to new templates (Fig. VII.6.b in dashed lines) which, in turn, leave the final bounds $B(\omega)$ unchanged. Therefore $G(j\omega)$ derived previously remains unchanged too, and the final design is given by (7.12).

Note that at high frequency all three loop transfer functions (Fig. VII.9) are identical. This is due to the fact that $P^{\alpha}[s]$ is independent of r at high frequency, as seen from (7.10).

VII.2.b.ε Derivation of the nonlinear prefilter.

Conceptually, one can derive 3 different prefilters corresponding to the 3 different linear time invariant designs that were obtained. The method presented in [H1] and in [A2] can then be used to actually build the nonlinear prefilter.

However, the relation (7.5) in T suggests that one can use a similar relation for F , namely:

$$F_j(s) = F_i(\lambda s) \quad \text{with} \quad \lambda \quad \text{such that:} \quad r_j(t) = \lambda r_i(t) \tag{7.13}$$

Indeed in a typical L.T.I. design, $L(j\omega)$ copes with plant uncertainty; therefore, at least for high gain factors, $L/1+L \doteq 1$ from the command input point of view, and therefore $T(s) \doteq F(s)$. If the reference is taken as the unit step, then (7.13) is rewritten as:

$$F_r(s) = F_1(rs) \tag{7.14}$$

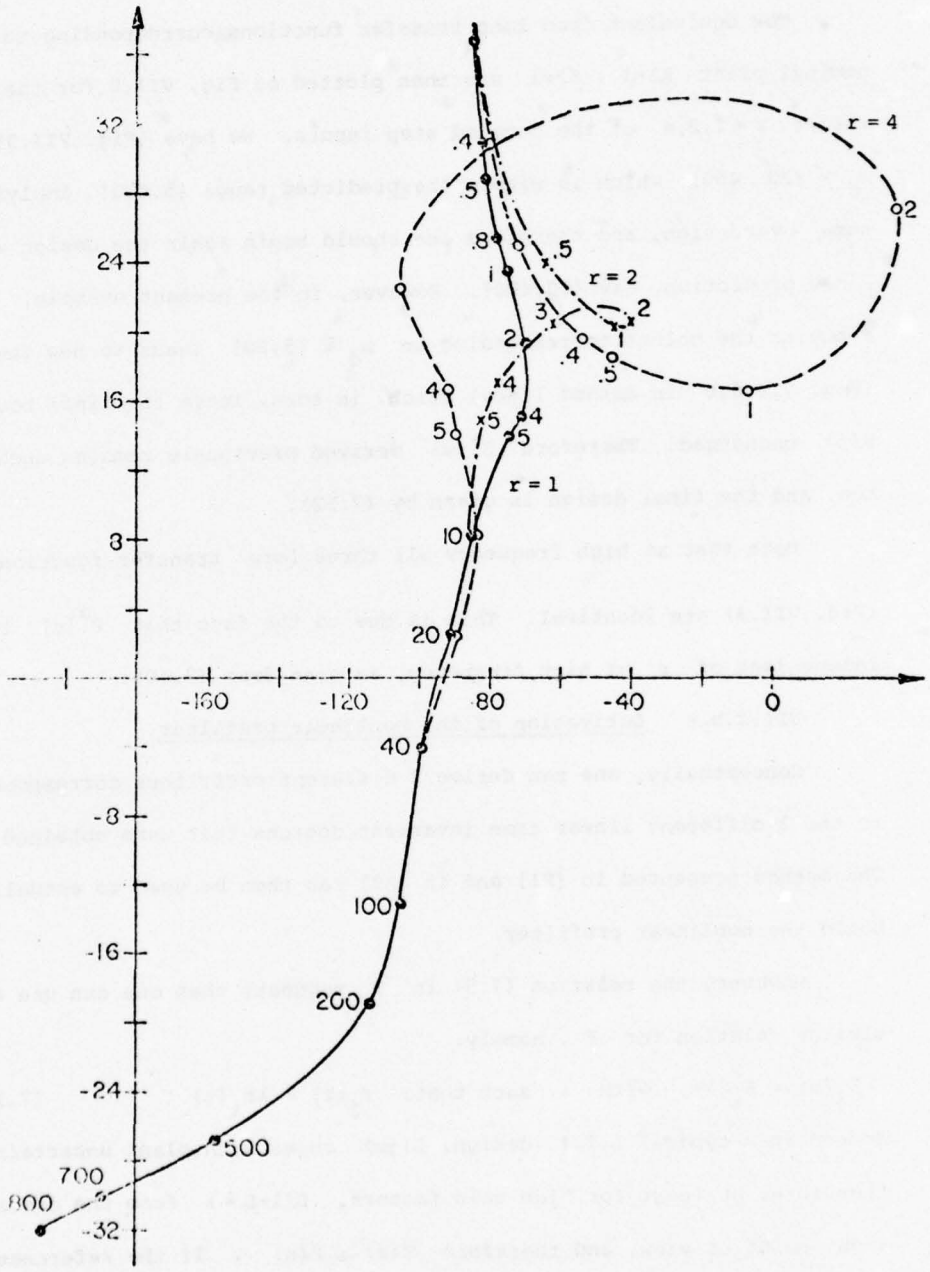

Figure VII.9. Nominal open loop transfer function for r = 1,2,4 .

Such a nonlinear prefilter F contains L.T.I. networks with time constants proportionnal to input magnitudes. In an analog computer realization, this is done by letting $|r|$ control the potentiometers and it has the great advantage of avoiding interpolation.

Following [H2] the prefilters $\mathcal{F}_1(s)$, $\mathcal{F}_2(s)$, $\mathcal{F}_4(s)$ are then derived for the three different command inputs considered. In order to derive $F_1(s)$, we normalize all three $\mathcal{F}_i$, $i = 1,2,3$ by using (7.14), i.e.,

$\mathcal{F}_{1,N}(s) \triangleq \mathcal{F}_1(s)$, $\mathcal{F}_{2,N}(s) \triangleq \mathcal{F}_2(\frac{s}{2})$ and $\mathcal{F}_{4,N}(s) \triangleq \mathcal{F}_4(\frac{s}{4})$. These are plotted on Fig. VII.10.

Recall from chapter II (section 1) that $\mathcal{F}_i(s)$ is obtained by:

$$\inf_j \left| \mathcal{F}_r(s) \frac{G(s)P_j^{\alpha}(s)}{1+G(s)P_j^{\alpha}(s)} \right| = \text{Min } T_r(s) \qquad (7.15)$$

where j ranges over all possible plants and $r = 1,2,4$.

(7.15) is then rewritten as:

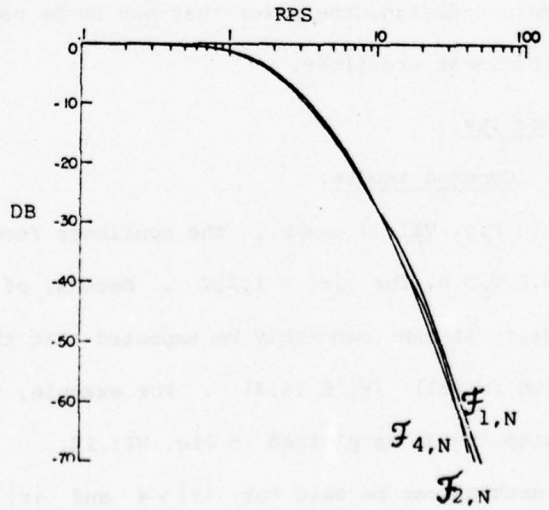

Figure VII.10. Normalized needed prefilters $\mathcal{F}_{r,N}(s)$, $r = 1,2,4$.

$$\inf_j \left| \mathcal{F}_{r,N}(rs) \; \frac{G(s)P_j^{\alpha}(s)}{1+G(s)P_j^{\alpha}(s)} \right| = \text{Min} \; T_1(rs) \qquad (7.16)$$

Taking into account that the inequality sign $>$ in place of $=$ in (7.16) implies overdesign, $F_1(s)$ is thus chosen as to satisfy:

$$F_1(s) = \min_r \mathcal{F}_{r,N}(s) \quad (7.17) \quad \text{for} \quad r = 1,2,4 \; .$$

It is found:

$$F_1(s) = \frac{6.25 \times 60}{(s+60)(s^2+4.75s+6.25)} \qquad (7.18)$$

which is plotted in Fig. VII.10.

One needs now to check that for all ω, and for $r = 1,2,4$

$$\sup_j \left| F_r(s) \; \frac{G(s)P_j^{\alpha}(s)}{1+G(s)P_j^{\alpha}(s)} \right| \leq \text{Max} \; T_r(s) \qquad (7.19)$$

when j ranges over all possible plants, which, in the present case, is easily satisfied. If this were untrue, i.e., if $\exists$ some frequency range Ω_α on which (7.19) is violated for some r, then one must use a smaller tolerable variation $\Delta T_r(j\omega)$ over that range and modify the design accordingly. This procedure is certainly convergent, but may lead to some overdesign, the price that has to be paid in return for such a simple nonlinear prefilter.

VII.3. Results.

VII.3.a. Command inputs.

As shown in Fig. VII.11.a.& b., the nonlinear feedback system satisfies the N.L.T.D.S. for $|r| = 1,2,4$. Because of the smoothness of the nonlinearity it can reasonably be expected that the N.L.T.D.S. will be satisfied for all $|r| \in [1,4]$. For example, the system response to a step $r = 3$ is plotted in Fig. VII.12.

However, nothing can be said for $|r| > 4$ and $|r| < 1$. The

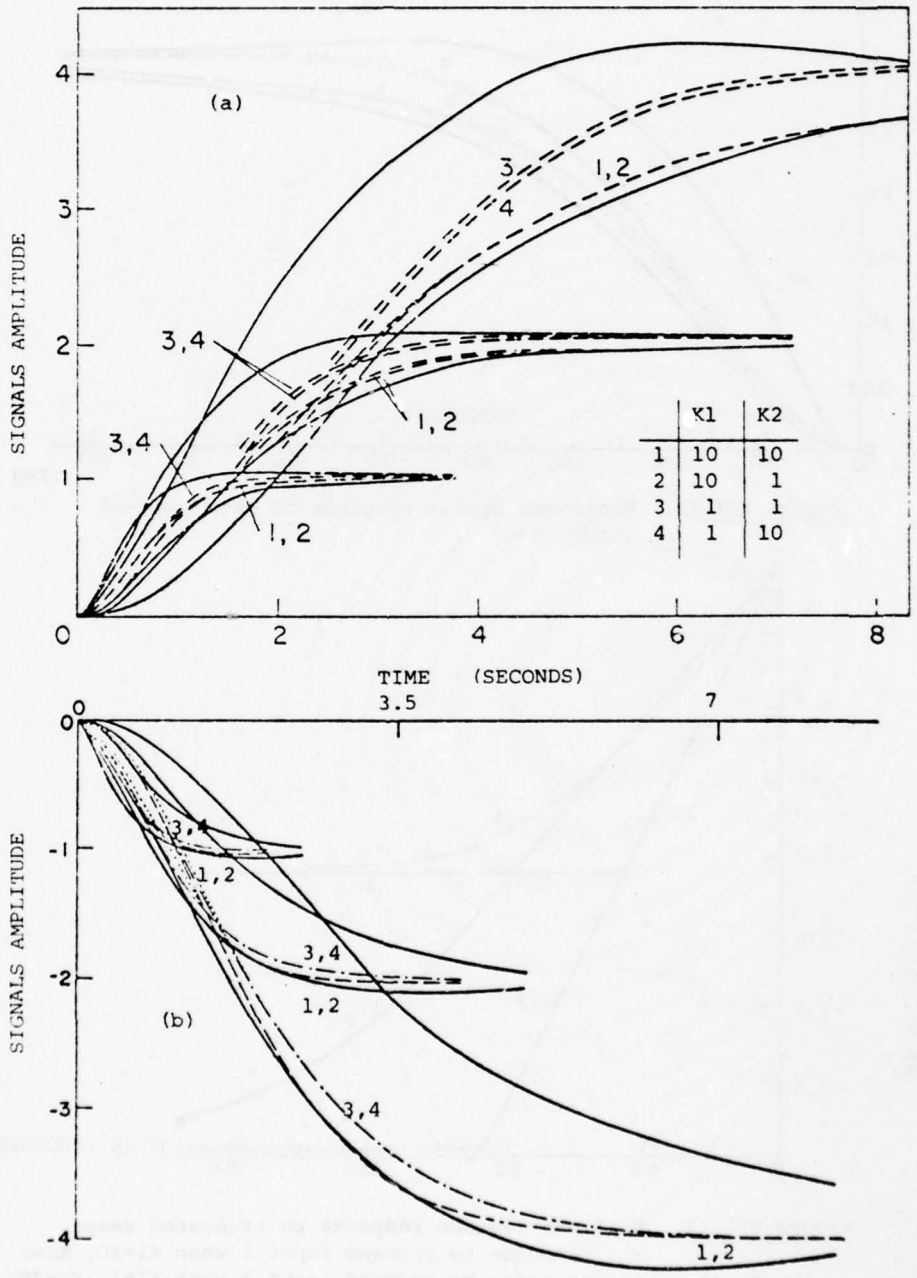

Figure VII.11. Nonlinear system responses to step command inputs $|r| = 1,2,4$. (a) positive commands (b) negative commands.

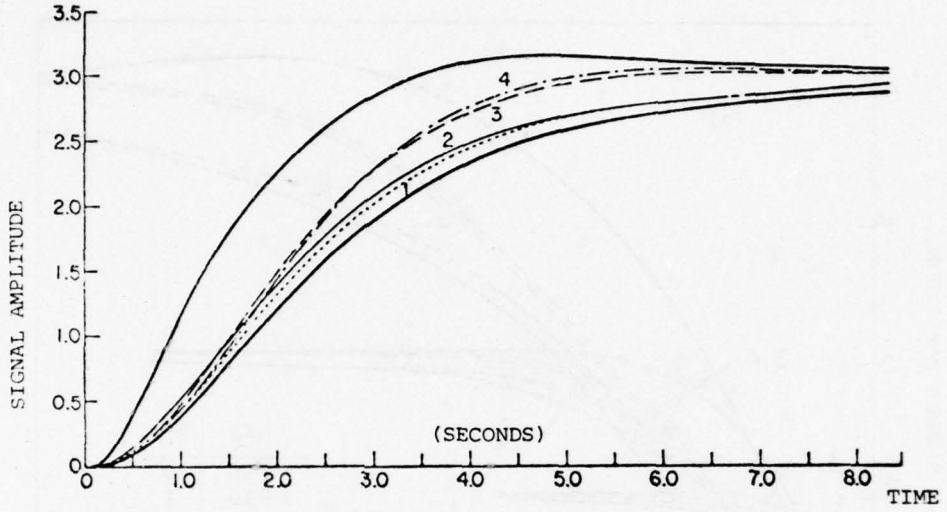

Figure VII.12. Nonlinear system response to step command input r = 3 .

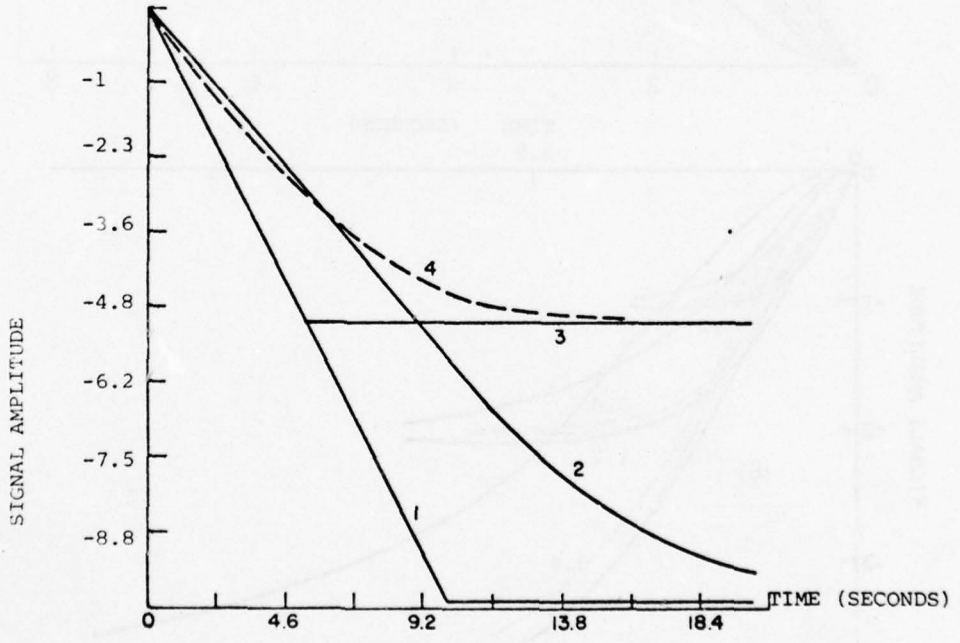

Figure VII.13. Nonlinear system response to truncated ramps.
2 : response to command input 1 when K1=10, K2=1
4 : response to command input 3 when K1=1, K2=10.

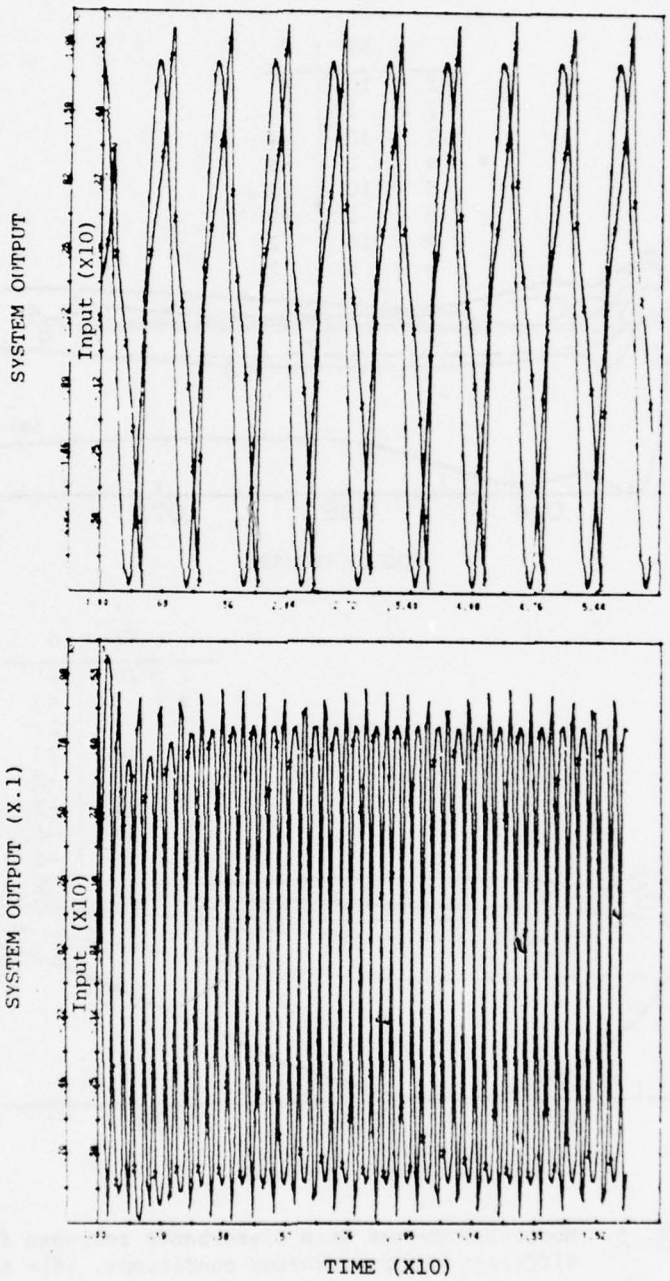

Figure VII.14. Nonlinear system response to sinusoidal commands. $A\sin\omega_0 t$. (1 is input, 2 is output). a) $\omega_0 = 1$ rps b) $\omega_0 = 10$ rps. In both cases A = 5, K1 = 1, K2 = 1.

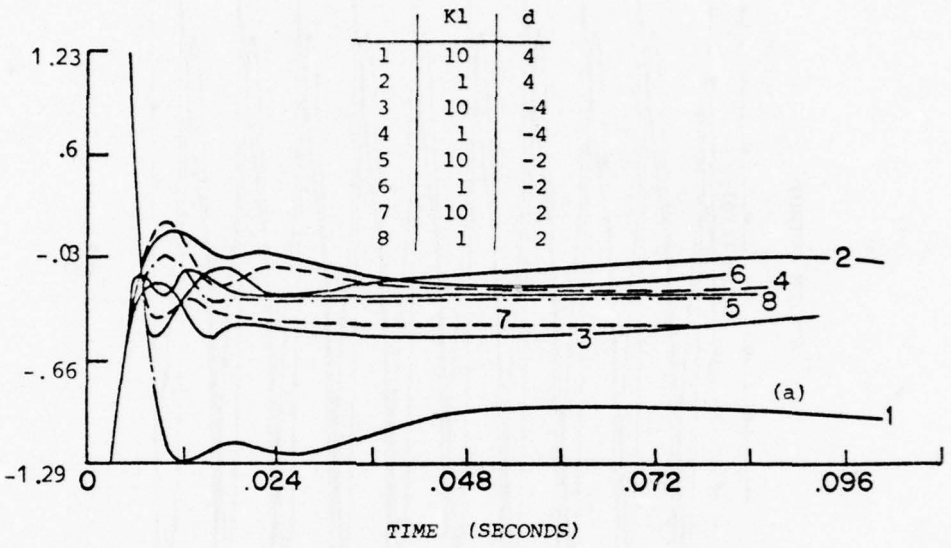

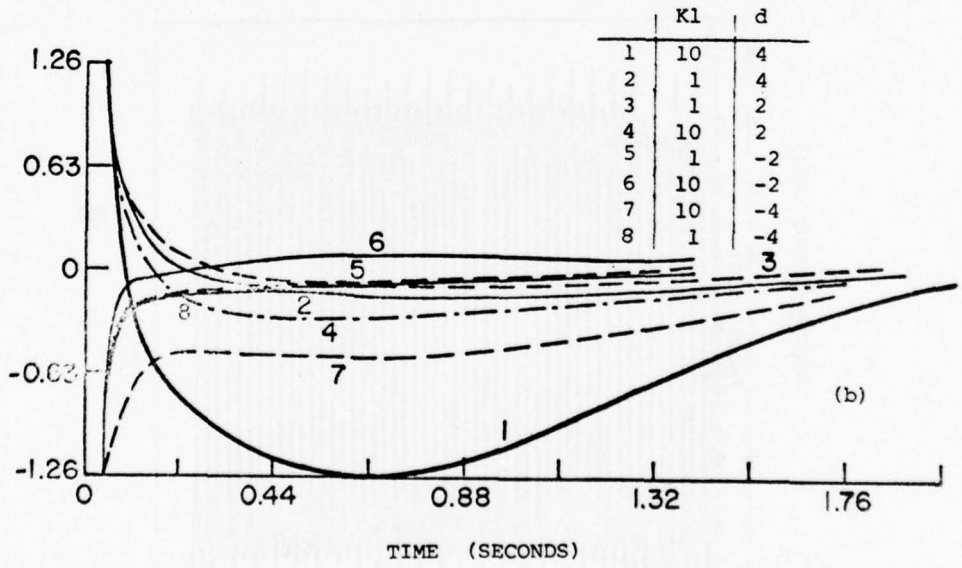

Figure VII.15. Nonlinear system step disturbance response for different plant parameter conditions. $|d| = 4$.
(a) K2 = 1
(b) K2 = 10 .

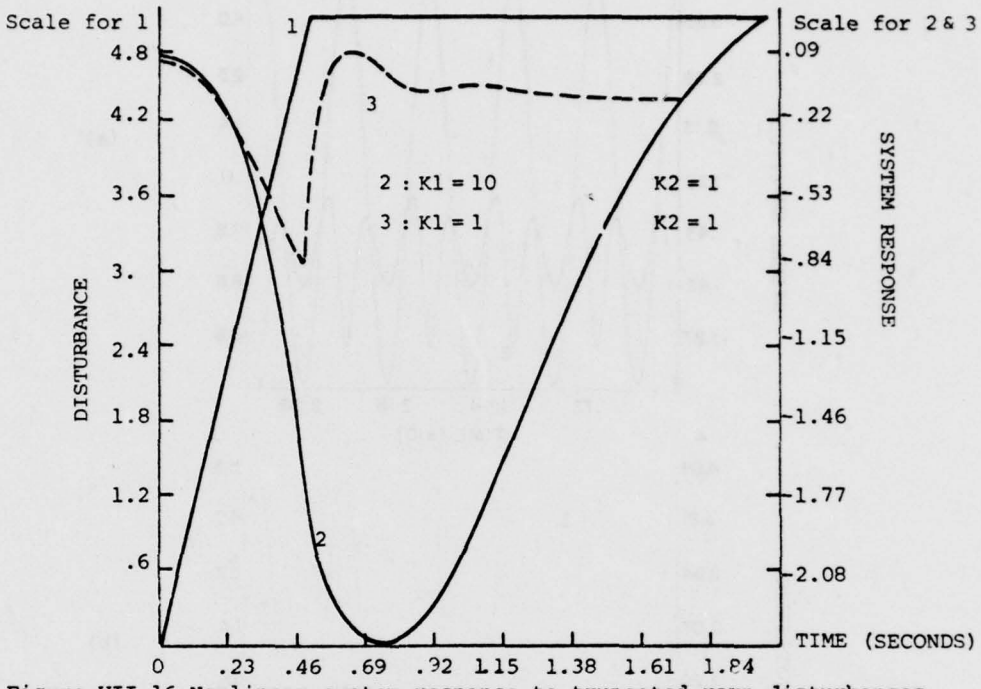

Figure VII.16. Nonlinear system response to truncated ramp disturbances.

system response to truncated ramp and sinusoidal command inputs are shown in Fig. VII.13 and VII.14. a & b respectively. They are seen to be quite reasonable, although the amplitude of the sine wave for example, varies between - 5 and + 5.

VII.3.b. Disturbance inputs.

From Fig. VII.15. a and b it can be seen that the specifications of 30% maximum overshoot for the step disturbance responses, is satisfied over the range of plant uncertainty.

For step disturbance greater than 6 , however, the system becomes unstable for some plant parameter values. This result is expected because the resulting equivalent linear plant representation predicted instability for the design used.

Fig. VII.16 and VII.17.a to d present the system responses to

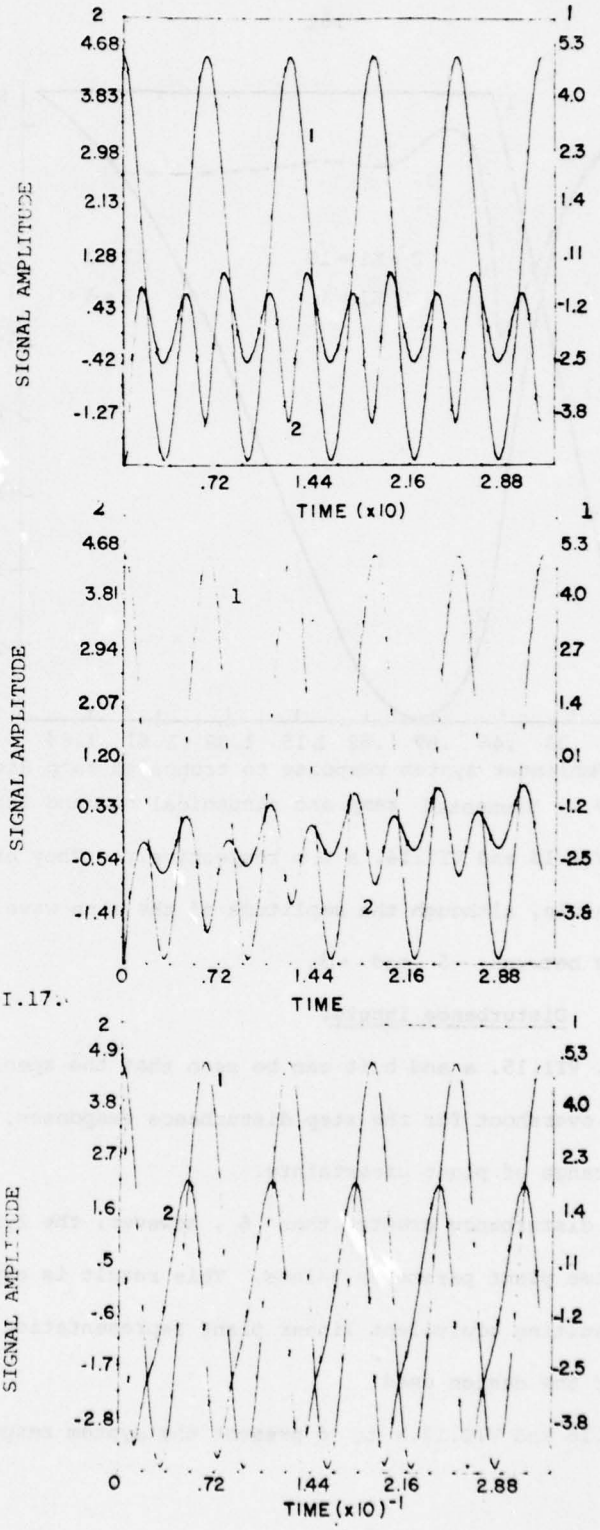

Figure VII.17.

truncated ramp and sinusoidal disturbances respectively. They are seen to be reasonable, although the amplitude of the input signal varies between -5 and $+5$. (Recall that the design was guaranteed for step disturbances $d \in [-4, 4]$).

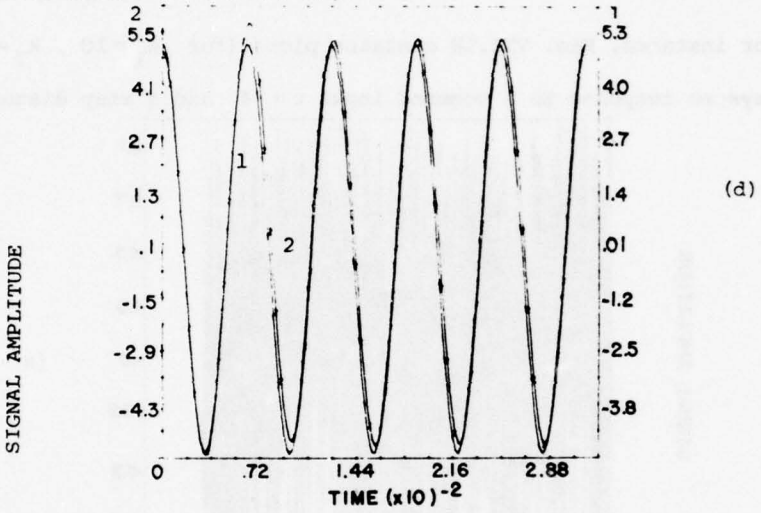

Figure VII.17. Nonlinear system response to a sinusoidal disturbance $d = 5\sin\omega_0 t$ for $k1 = 10$, $k2 = 1$. (a) $\omega_0 = 1$ rps, (b) $\omega_0 = 10$ rps, (c) $\omega_0 = 100$ rps, (d) $\omega_0 = 1000$ rps.

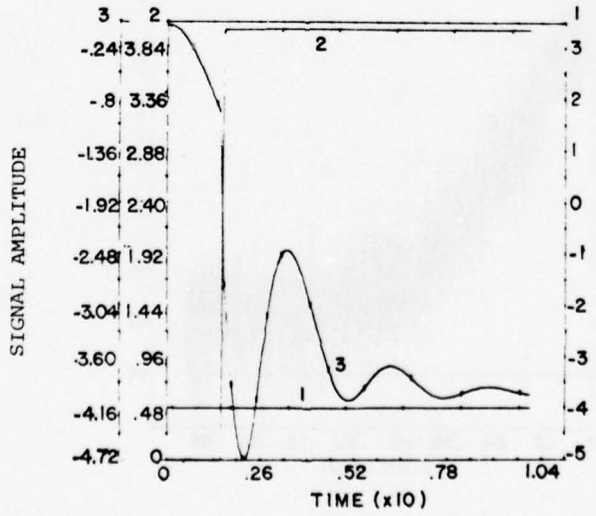

Figure VII.18. Nonlinear system response (3) to a combination of a step command (1) and step disturbance (2) for the plant condition $K1 = 10$, $K2 = 1$.

VII.3.c. Other system inputs.

A combination of a step command and a step disturbance leads to satisfactory results, although the superposition theorem does not hold here.

For instance, Fig. VII.18 contains plots (for $k_1 = 10$, $k_2 = 1$) of the system response to a command input $r = -4$ and a step disturbance

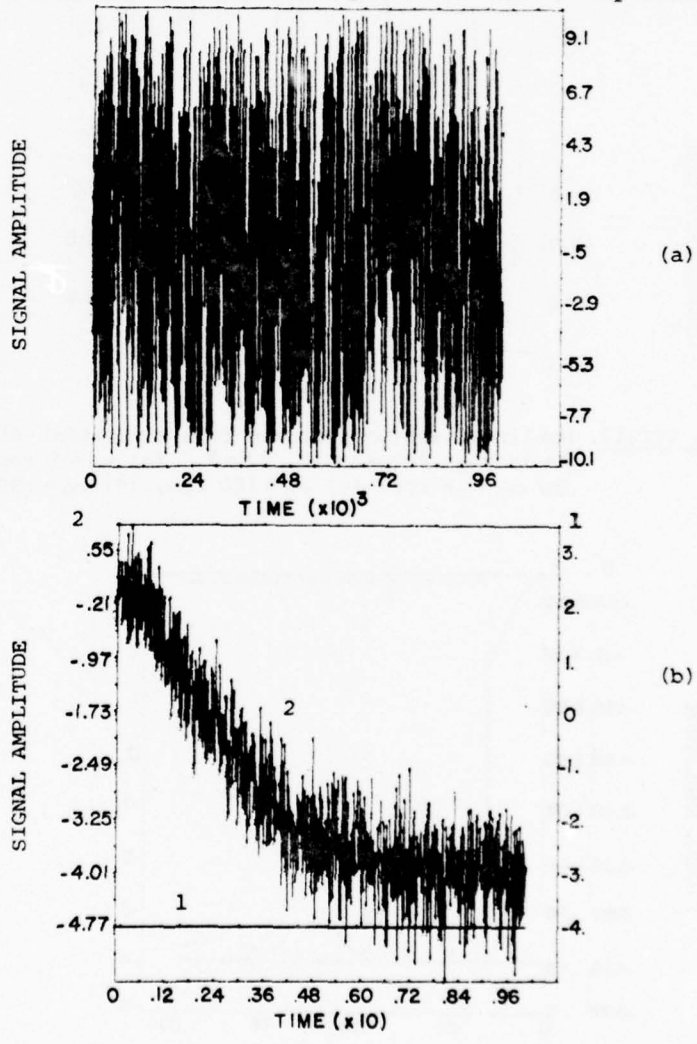

Figure VII.19. (a) white sensor noise (system input).
(b) nonlinear system response (2) for K1 = 10 , K2 = 1 to a step command (1) r = -4 in presence of (a).

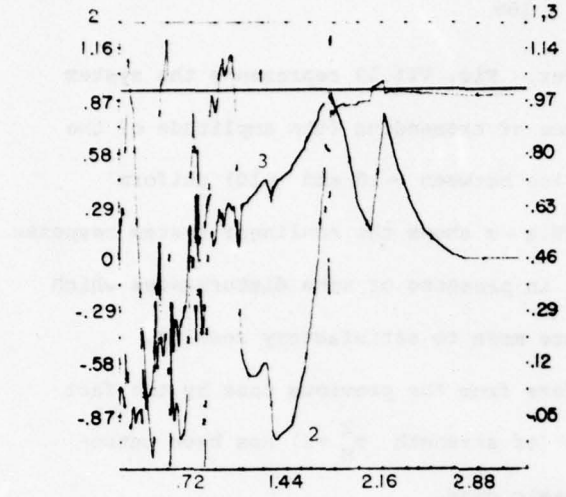

(c)

(a)

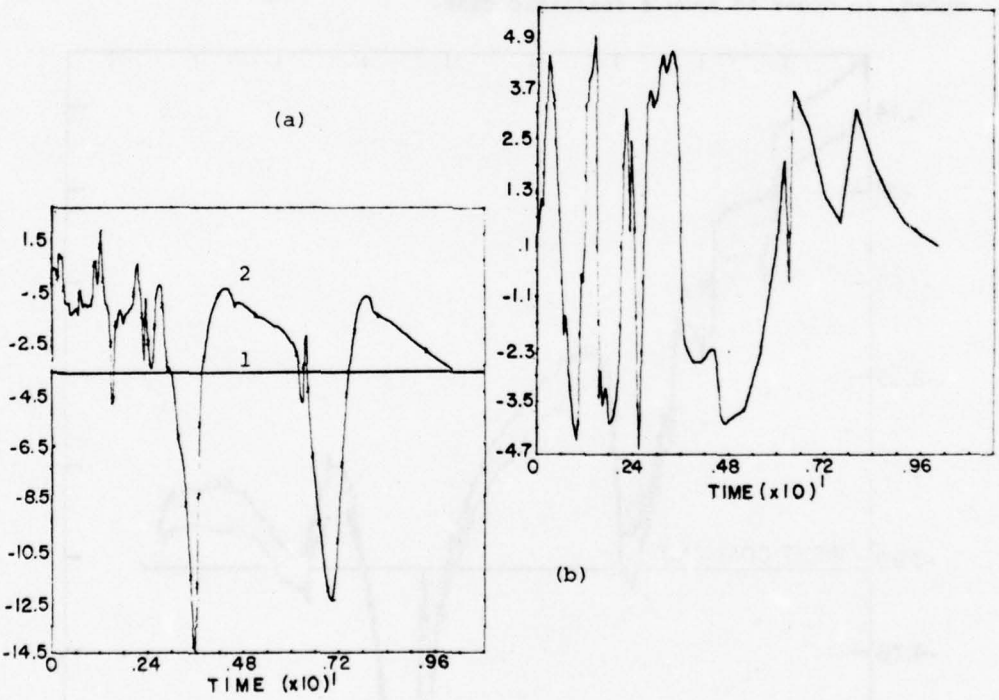

(b)

Figure VII.20. (a) Disturbance input
(b) Nonlinear system response (2) for K1 = 1, K2 = 10 to a step command r = -4 in presence of (a)
(c) Nonlinear system response (3) for K1 = 10, K2 = 1 to a step command r = 1 (1) and the disturbance (2).

d = +4 occuring 1.5 seconds later. Fig. VII.19 represents the system command step response in presence of tremendous (the amplitude of the noise input (Fig. VII.19.a) varies between - 10 and + 10) uniform white sensor noise. Fig. VII.20.a - c shows the nonlinear system response to a step input command r = -4 in presence of some disturbances which varies on [-4 , +4] leading once more to satisfactory results.

Finally, Fig. VII.21 differs from the previous case by the fact that uniform white sensor noise (of strength $\sigma_N^2 = 1$) has been introduced, in order to show a realistic case.

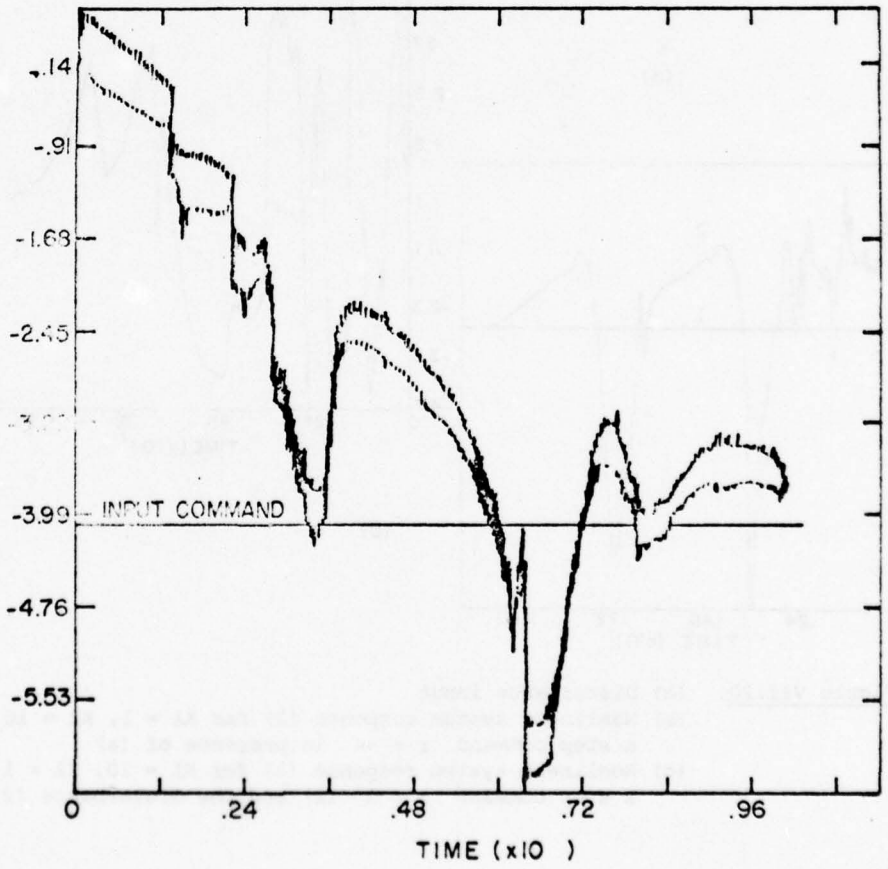

Figure VII.21. Nonlinear system response for K1 = 1, K2 = 10 to a command r = -4 in presence of disturbance and sensor noise.

VII.4. Conclusions.

The EPLTI concept was used successfully in the design of a nonlinear feedback system to achieve N.L.T.D.S. It was shown that a L.T.I. compensation G and a nonlinear prefilter F handle this nonlinear problem and achieve quantitative specifications both on the command and on the disturbance signals.

Nonlinear specification on the disturbance was not emphasized here but this could easily be handled by our design technique. Applications of the synthesis procedure to L.T.I. plants is straightforward, leading to the synthesis of L.T.I. loops with nonlinear prefilters, to achieve N.L.T.D.S.

The problem of a nonlinear prefilter has widely opened and supplied considerable motivation in the research area of nonlinear open loop synthesis. Some primitive solutions are presented in Appendix A2 , where it is shown, when possible, (i.e., for a large class of problems), how to use the same relationship on the set $\{F^{\alpha}\}$ that characterizes the set of $\{T^{\alpha}\}$, where T^{α} is a representative nominal T from the set of acceptable transfer functions for r^{α} . This approcah has the advantage of simplicity in both the derivation and implementation of F , although it might sometimes lead to some overdesign, a price that may have to be paid.

In our design, a L.T.I. G(s) was used which also accounts for the simplicity of the design procedure. This obviously leads to overdesign in the bandwidth of the effective L.T.I. open loop transfer function for some inputs. Certainly a nonlinear G would be much better in this senseand this should definitely be one research direction to pursue. Such a nonlinear G should present a different "transfer

function" for each command input and disturbance considered.

In such a case, let $\{\varepsilon\}_{\alpha_1}$ be the set of inputs to G when $i^{\alpha_1} = r^1$. There is a set because of the set W , i.e. each w in W gives a different z . It is necessary that the nonlinear G acts like $G^{\alpha_1}(s)$ a <u>fixed</u> transfer function to the <u>set</u> $\{\varepsilon\}_{\alpha_1}$, like $G^{\alpha_2}(s)$ to the <u>set</u> $\{\varepsilon\}_{\alpha_2}$, etc.

If disturbances are also to be considered, then the problem becomes even more difficult.

Therefore, one should be aware that if the problem of a nonlinear prefilter is a tough one, the problem of a nonlinear G is definitely a very difficult one for which even primitive solutions do no exist.

APPENDIX A1: CHARACTERIZATION OF A L.T.I. FEEDBACK SYSTEM STEP RESPONSE BY MEANS OF A SECOND ORDER MODEL WITH TIME-DELAY.

A justification is presented here for the use in chapters III & VII of a delayed second order model $T_A(s) = \frac{\omega_n^2 e^{-t_d s}}{s^2+2\zeta\omega_n s+\omega_n^2}$ as a means of predicting the overshoot in the L.T.I. system step response. Since mathematical equivalence can obviously not be made, some examples will be considered. We will show that if $T_A(s)$ is used, the predicted overshoot is the same as that obtained experimentally. Using Equation (3.1a) and (3.1b), Fig. A1.1 is first derived which gives the well known relations that exist between the damping factor ζ, the overshoot and the peaking in $|T_A(j\omega)|$ of a delayed second order system.

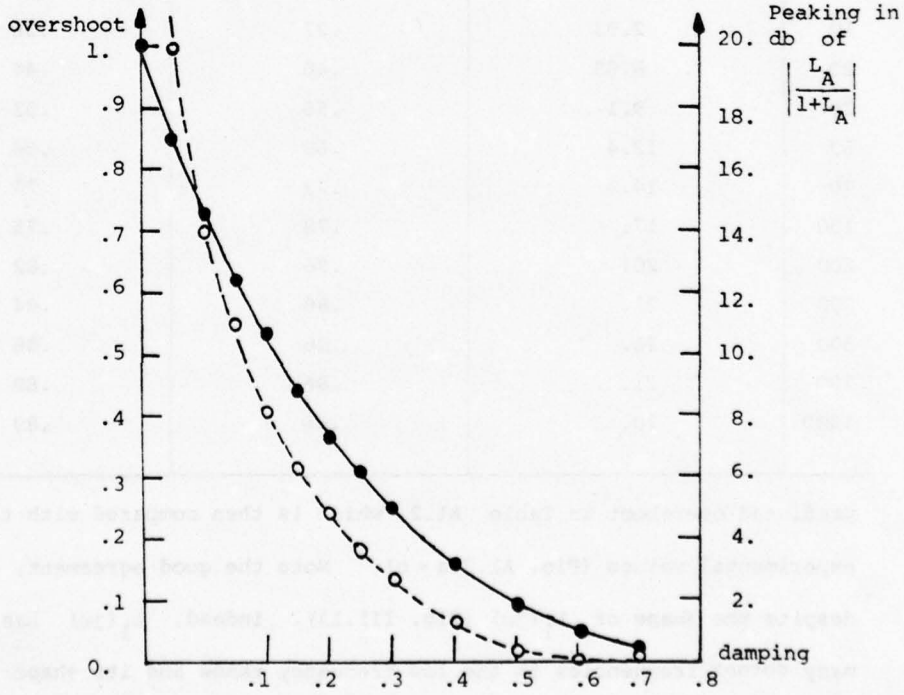

Figure A1.1 Overshoot in the step response and peaking of $|L/1+L|$ versus damping for a second order system.

Consider the high order open loop transfer function $L_1(s)$ (7 zeros - 12 poles) used in chapter III, Fig. III.13, corresponding to minimum gain factor $k = 1$. As k increases from 1 to $k_{max} = 1000$, the corresponding $L_{1,k}(s)$ is obtained by shifting the 0 db line in Fig. III.13 by the amount - 20 log k . Table A1.2 gives the peaking of $\left|L_{1,k}/1+L_{1,k}\right|_{db}$ versus k . Fig. A1.1 is then used to give the

TABLE A1.2

k	peaking in $\left\|\frac{L_{1,k}}{1+L_{1,k}}\right\|$	predicted overshoot	actual overshoot
1	0.	-	-
2	0.	-	-
3	0.	-	-
5	.3	.09	.09
7	1.35	.17	.17
10	2.93	.27	.26
20	6.63	.46	.44
30	9.1	.56	.53
50	12.4	.68	.64
70	14.6	.73	.70
100	17.	.78	.75
200	20.	.86	.82
300	21.	.86	.84
500	21.	.86	.86
700	21.	.86	.88
1000	20.	.86	.89

predicted overshoot in Table A1.2, which is then compared with the experimental values (Fig. A1.3.a - c). Note the good agreement, despite the shape of $L_1(j\omega)$ (Fig. III.13). Indeed, $L_1(j\omega)$ has many corner frequencies in the low frequency range and its shape in the high frequence range ($\omega > 600$ rps) is far from resembling a second

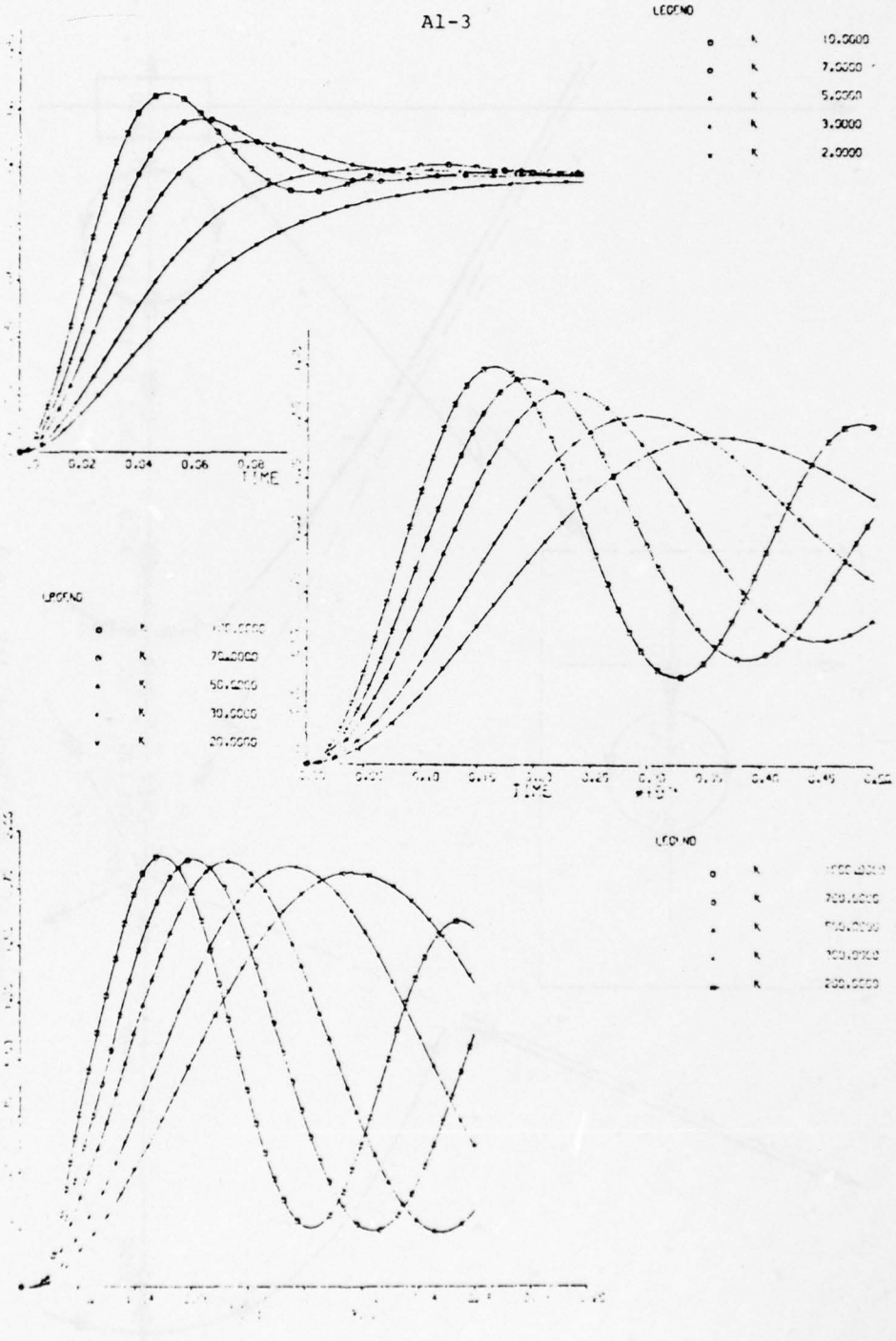

Figure A1.3a-c LTI system response to a unit step as the gain factor increases from 1 to 1000.

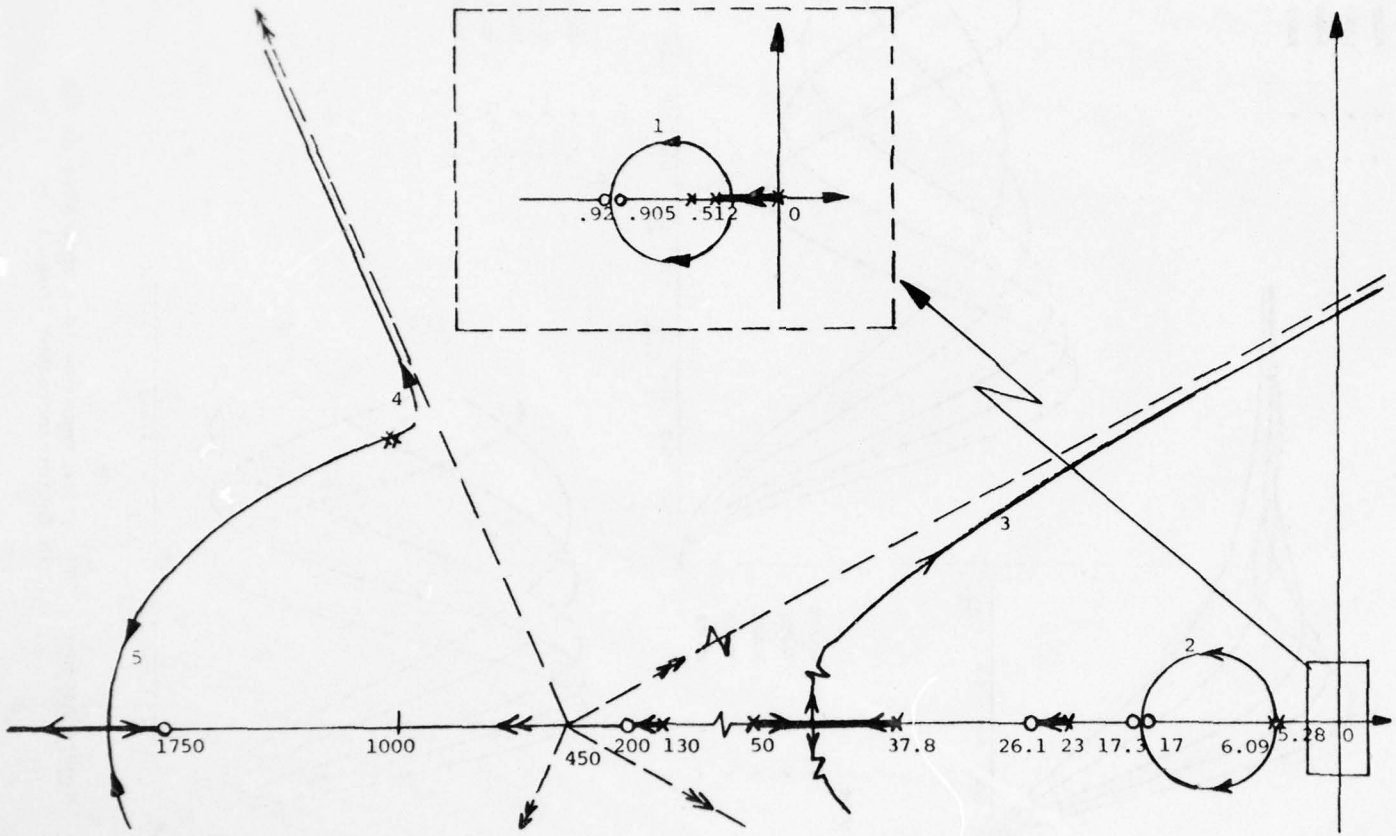

Figure A1.4 Root loci of $1+L_{1,k} = 0$

order system. Despite those two facts, it is seen that the prediction, as far as the step response overshoot is concerned, is good.

This can be understood by considering the root locus of $1+L_{1,k}$, as k varies, which is plotted on Fig. A1.4. At small k, the dominant pair of closed loop poles are located on arc 2 (the poles of arc 1 are very close to the zeros, even at $k=1$, so their effect can be neglected, while those of arc 3 are far, relative to those on arc 2). The pair located on arc 3 becomes dominant at intermediate and high gain values of k, the poles of arc 2 being then very close to the zeros. The effect of the two far-off pole pairs on arcs 4 and 5 can be neglected, (see [H7]). Therefore a second order model for $T(s)$ can be used here and this will remain true in general for systems with large uncertainty, because of the universal character of the resulting optimal loop functions ([H2], [S2]) for plants with large high frequency gain factor uncertainty, to which this work is devoted. Note that it is implicitely assumed that the two following cases do not appear, as

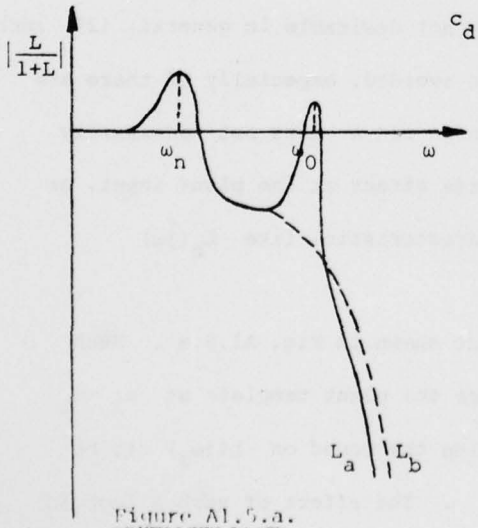

Figure A1.5.a.
Examples of open loop transfer functions.

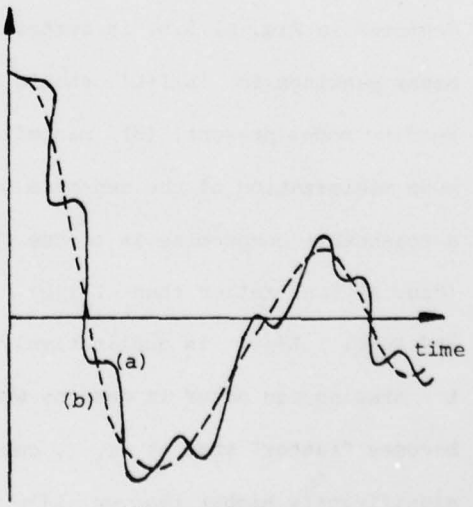

Figure A1.5.b.
Corresponding system responses c_d to a step disturbance.

discussed below.

1st case: $|L/L+1|$ qualitatively as shown (see L_a) in Fig. A1.5.a implying the system step disturbance response $c_d(t)$ of Fig. A1.5.b. In such a case it is obvious that the overshoot cannot be characterized by the above formula. Note that for such a system we would have a root locus for $1 + L$ qualitatively as shown on Fig. A1.5.c. Such a phenomena

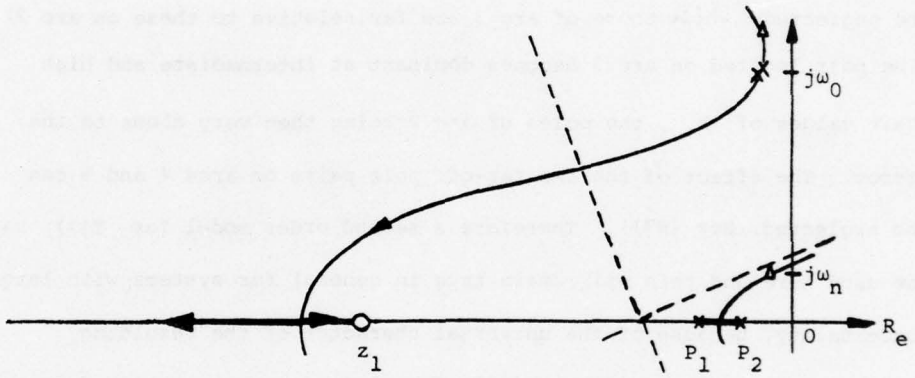

Figure A1.5.c. Root locus of $1 + L_{1,k}(s)$.

can occur at $k = k_{max}$, if the designer takes a very small damping factor in his far-off pole-zero package [S2] in order to descrease $|L|$ very fast. Suffice it to say that (1) the L.T.I. system response depicted in Fig. A1.5.b. is certainly not desirable in general, (2) such minor peakings in $|L/1+L|$ should be avoided, especially if there are bending modes present, (3) minimization of k does not necessarily mean minimization of the sensor's noise effect at the plant input, so a reasonable compromise is to use characteristics like $L_b(j\omega)$ (Fig. A1.5.a) rather than $L_a(j\omega)$.

2nd case: $L(j\omega)$ is qualitatively as shown in Fig. A1.6.a . Such L - shaping can occur in designs where the plant template at $\omega_2 > \omega_1$ becomes "fatter" than at ω_1 , causing the bound on $L(j\omega_2)$ to be significantly higher than on $L(j\omega_1)$. The effect of such a loop in

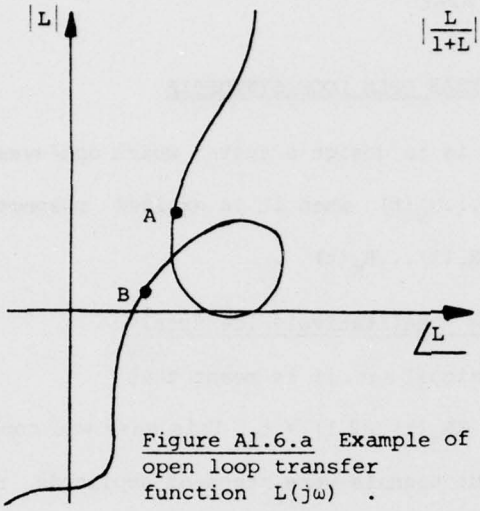

Figure A1.6.a Example of open loop transfer function $L(j\omega)$.

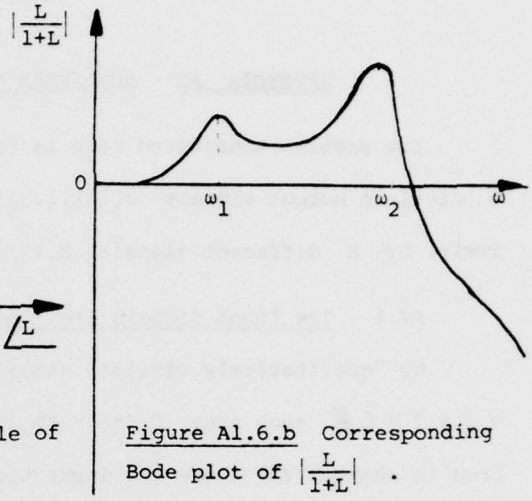

Figure A1.6.b Corresponding Bode plot of $\left|\frac{L}{1+L}\right|$.

Fig. A1.6.a gives rise to two peaks in $|L/1+L|$ as shown in Fig. A1.6.b, and is usually achieved by a pair of complex zeros and complex poles in $L(j\omega)$ as shown in Fig. A1.6.c. It should be recalled that such phenomena is less likely at high frequency because $P(s) \to k/s^e$. Therefore at such frequencies, at least, the poles of $L/1+L$ on arc 1 are practically cancelled out by the complex zeros of L , and therefore the complex pair lying on the arc 2 can be considered as dominant and a second order approximation is then legitimated. In those cases where, at low frequencies, the loop A - B prevents the designer to use a second order approximation, a more complex model must be derived unless overdesign can be tolerated.

Figure A1.6.c Root locus of $1+L_{1,k}$

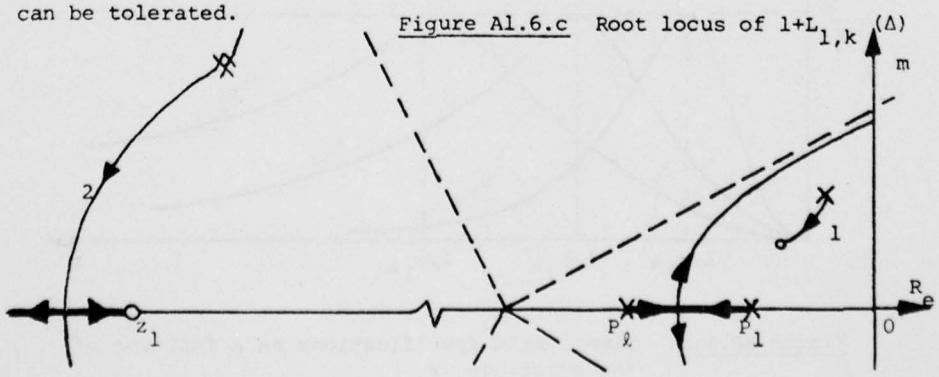

APPENDIX A2: NONLINEAR OPEN LOOP SYNTHESIS

The problem considered here is to design a system which achieves N distinct output signals $u_1(t)...u_N(t)$ when it is excited respectively, by N different signals $R_1(t)...R_N(t)$.

A2.1 The Input signals are "qualitatively identical".

By "qualitatively similar" signal set, it is meant that : $\forall\, i,j \;\exists\; K \in \mathbb{R}$ such that $R_i(t) = KR_j(t)$ (A2.1), $\forall$ t . This case was considered in chapter VII where the input signals were steps of amplitude r . Because some empirical formula $u_r(t) = ru_1(t/r)$ could then be found on the output signals, there existed a very simple prefilter whose transfer function had the simple expression:

$F_r(s) = F_1(rs)$ with $F_1(s) \triangleq \dfrac{U_1(s)}{R_1(s)}$ and $R_1(s) = \dfrac{1}{S}$. This concept will now be extended.

As another example, assume that the set of inputs consists of impulse $R_i(t) = r_i\delta(t-\tau)$, $r_i \in R$, which are to produce the set of outputs shown on Fig. A2.1.a where $\forall\, r_i$ the maximum value is γ occuring at

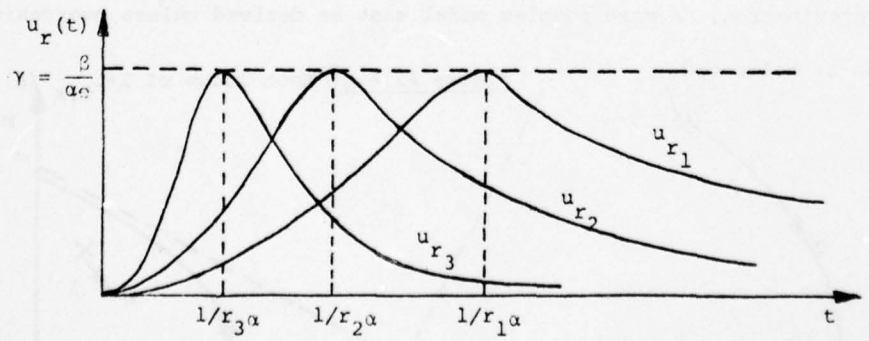

Figure A2.1.a. Time domain specifications as a function of the amplitude r_i .

a time t_0 inversely proportional to the amplitude of the input signal.

Suppose that: $u_r(t) = \beta r t\, e^{-r\alpha t}$ (A2.2.a), for which $t_0 = \frac{1}{r\alpha}$ and $\gamma = \frac{\beta}{\alpha e}$. Therefore $U_r(s) = \frac{r\beta}{(s+r\alpha)^2}$ and as $R(s) = r$ we have: $F_r(s) = \frac{\beta}{(s+r\alpha)^2}$ (A2.2.b).

More generally, if $u_r(t) = g(r)t\, e^{-f(r)t}$ then $F_r(s) = \frac{g(r)/r}{(s+f(r))^2}$.

This transfer function is easily implemented (Fig. A2.1.b) on an anolog computer, the amplitude r being obtained in this case, by integrating the input, i.e., $r = \int_0^t R(\zeta)d\zeta$.

As a third illustration, let the set $\{u\}$ of desired outputs in response to step-inputs be as shown on Fig. A2.2.a.

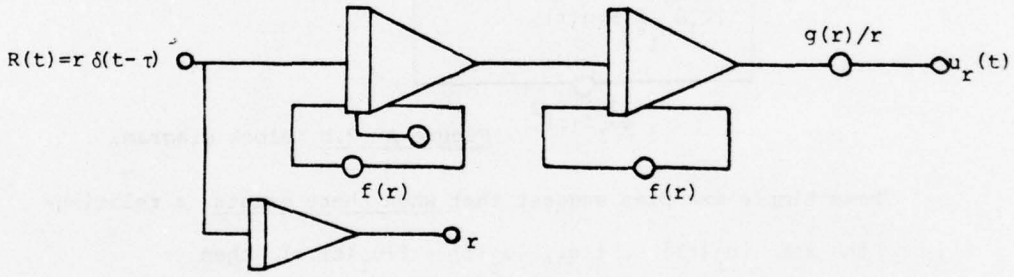

Figure A2.1.b Block diagram.

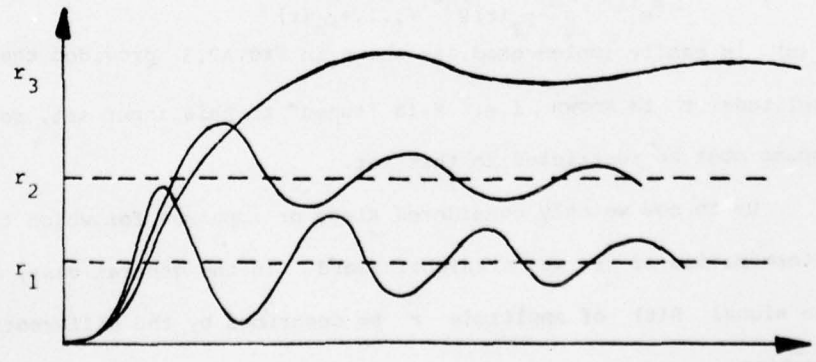

Figure A2.2.a. Time domain specifications as a function of the amplitude r_i.

Say,

$$u_1(t,\zeta_i,\omega_{n_1}) = 1 - \frac{e^{-\zeta_1\omega_{n_1}t}}{\sqrt{1-\zeta_1^2}} \sin(\omega_{n_1}\sqrt{1-\zeta_1^2}t \cos^{-1}\zeta_1) \quad \text{(A2.3.a)} \quad \text{and}$$

$u_r(t,\zeta_r,\omega_{n_r}) = u_1(t,\zeta_1 g(r),\omega_{n_1} f(r))$ .Therefore:

$$F_r(s) = \frac{\omega_{n_r}^2}{s^2+2\zeta_r\omega_{n_r}s+\omega_{n_r}^2} = \frac{\omega_{n_1}^2 f(r)^2}{s^2+2\zeta_1\omega_{n_1}f(r)g(r)s+\omega_{n_1}^2 f(r)^2} \quad \text{(A2.3.b)}$$

which is also easily implemented as shown in Fig. A2.2.b

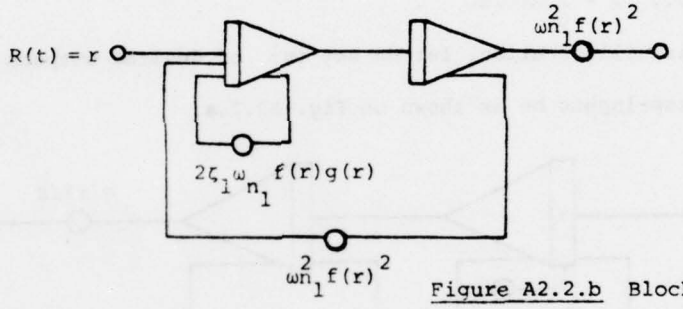

Figure A2.2.b Block diagram.

These simple examples suggest that <u>when there exists</u> a relationship on the set $\{u_r(t)\}$, i.e., $u_r(t) = f(u_1(t),r)$ then $F_r(s) = \mathcal{F}[F_1(s),r]$ which can be written in the general form:

$$F_r(s) = \frac{p_n(r)}{z_m(r)} \frac{s^m+z_1(r)s^{m-1}+,\ldots,+z_m(r)}{s^n+p_1(r)s^{n-1}+,\ldots+p_n(r)} \quad \text{(A2.4)}$$

$F_r(s)$ is easily implemented, as shown in Fig.A2.3 provided the amplitude r is known , i.e. F is "tuned" to this input set, so the inputs must be restricted to this set.

Up to now we only considered steps or impulses for which the determination of r was straightforward. In the general case, let the signal R(t) of amplitude r be described by the differential equation:

$$\frac{d^p}{dt^p} R(t) + \alpha_1 \frac{d^{p-1}}{dt^{p-1}} R(t) + ,\ldots,+ \alpha_p R(t) = r(\delta^q(t) + \beta_1 \delta^{q-1}(t) + ,\ldots,+\beta_q \delta(t))$$

$$\text{with} \quad p > q \quad . \qquad \text{(A2.5)}$$

Integrating (A2.5) p times gives:

$$R(t) + \alpha_1 \int_0^t R(\zeta)d\zeta + \ \ldots \ + \alpha_p \underbrace{\int\int \ldots \int}_{p \text{ times}} R(\zeta)d\zeta = r(t^{p-q-1} + \beta_1 t^{p-q} + \ \ldots \ + \beta_q t^{p-1})$$

$$\triangleq r\varphi(t) \quad . \qquad \text{(A2.6)}$$

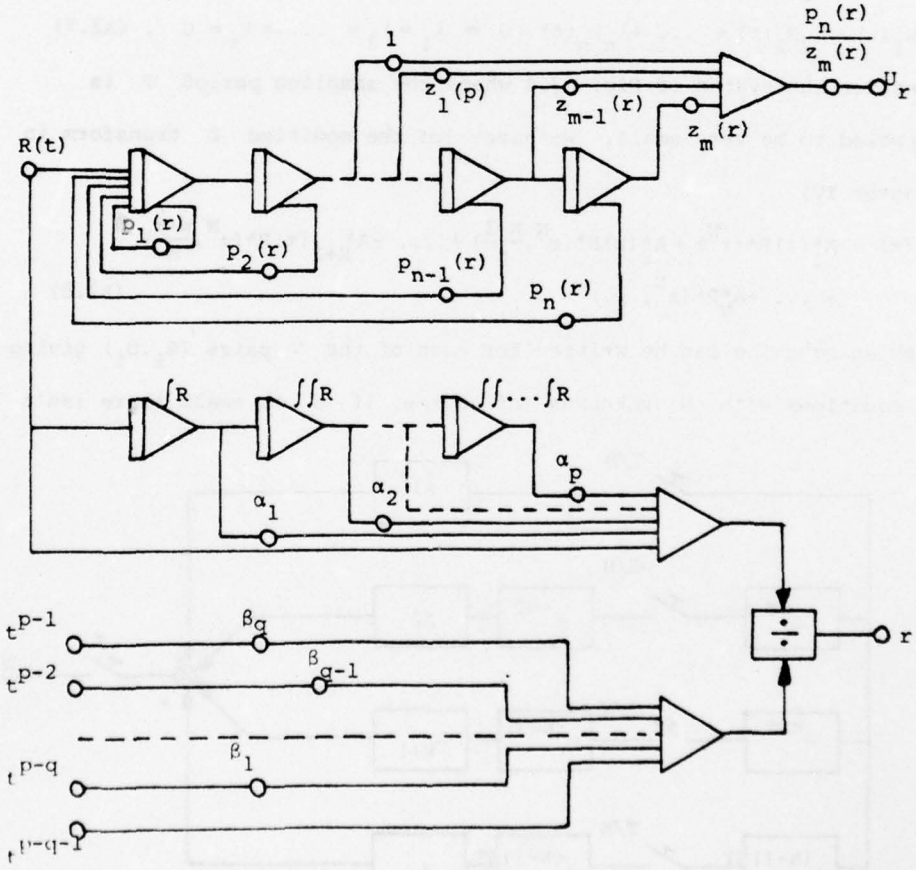

Figure A2.3 Block diagram for the Nonlinear prefilter.

The left-hand side of (A2.6) is easily obtained, as it only involves integrations of the input signals, and so is $\Phi(t)$ too. Therefore $\forall\, t > 0$, r can be estimated and its value is then used to compute all $z_i(r)$, $p_i(r)$ of (A2.4). It is important to recall that the above is restricted to 'qualitatively similar' input sets.

A2.2 The input signals are linearly independent.

Here, consider the more general case of n independent input signals $R_1, \ldots, R_n$, i.e.,

$$\lambda_1 R_1(t) + \lambda_2 R_2(t) + \ldots + \lambda_n R_n(t) = 0 \Leftrightarrow \lambda_1 = \lambda_2 = \ldots = \lambda_r = 0 \quad . \quad \text{(A2.7)}$$

Consider the system of Fig. A2.4 where the sampling period T is supposed to be very small. We have: [cf the modified Z transform in chapter IV]

$$U^*(z) = A_1^*(z)R^*(z^N) + A_2^*(z)R^*(z^N, \tfrac{N-1}{N}) + \ldots + A_{K+1}^*(z)R^*(z^N, \tfrac{N-K}{N}) + \ldots + A_N^* R^*(z^N, \tfrac{1}{N}) \quad . \quad \text{(A2.8)}$$

Such an equation can be written for each of the N pairs (R_i, U_i) giving N equations with N unknowns (of course, if N is small there isn't

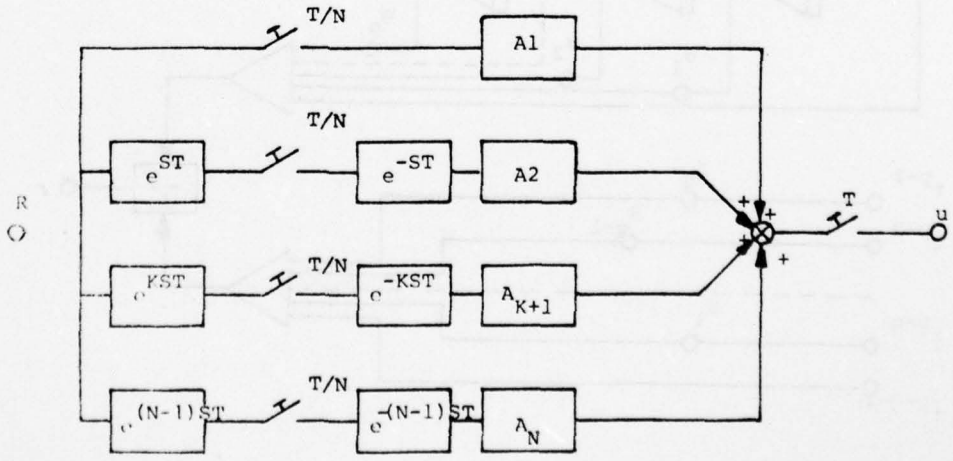

Figure A2.4. System configuration.

enough flexibility for good matching - but one can use $(N+M)$ terms and choose M of these arbitrarily to suit the approximation, solving for the remaining N).

$$\begin{bmatrix} R_1(z^N) & R_1(z^N,\frac{N-1}{N}) & \cdots & R_1(z^N,\frac{N-K}{N}) & \cdots & R_1(z^N,\frac{1}{N}) \\ R_2(z^N) & R_2(z^N,\frac{N-1}{N}) & \cdots & R_2(z^N,\frac{N-K}{N}) & \cdots & R_2(z^N,\frac{1}{N}) \\ \vdots & \vdots & & \vdots & & \vdots \\ R_K(z^N) & R_K(z^N,\frac{N-1}{N}) & \cdots & R_K(z^N,\frac{N-K}{N}) & \cdots & R_K(z^N,\frac{1}{N}) \\ \vdots & \vdots & & \vdots & & \vdots \\ R_N(z^N) & R_N(z^N,\frac{N-1}{N}) & \cdots & R_K(z^N,\frac{N-K}{N}) & \cdots & R_N(z^N,\frac{1}{N}) \end{bmatrix} \begin{bmatrix} A_1(z) \\ A_2(z) \\ \vdots \\ A_{K+1}(z) \\ \vdots \\ A_N(z) \end{bmatrix} = \begin{bmatrix} U_1(z) \\ U_2(z) \\ \vdots \\ U_K(z) \\ \vdots \\ U_N(z) \end{bmatrix} \quad \text{(A2.9)}$$

Using (A2.7) the rows are independent and (A2.9) has a unique solution which then solves the problem for the case considered.

APPENDIX A3: DETAILS OF THE L.T.V. SYNTHESIS PROCEDURES

A3.1 Derivation of $\ell_2(t,\tau)$ from $h_2(t,\tau)$

In any realistic L.T.V. system, the closed loop impulse response $h_2(t,\tau)$ is the solution of a linear differential equation of order N with variable coefficients, where the input x to be considered is a unit impulse occuring at $t = \tau$. This implies [S5] that

$$h_2(t,\tau) \triangleq A(t)\cdot B(\tau)^T u(t-\tau) \tag{A3.1}$$

with $A(\cdot)$ and $B(\cdot)$ two N-dimensional vectors. By anology with L.T.I. systems, if $h_2(t,\tau)$ is of order N, so is the open loop impulse response $\ell_2(t,\tau)$, and therefore

$$\ell_2(t,\tau) \triangleq \alpha(t)\cdot\beta(\tau)^T u(t-\tau) \tag{A3.2}$$

with $\alpha(\cdot)$ and $\beta(\cdot)$ two N-dimensional vectors.

ℓ_2 and h_2 are related through (6.11), i.e.,

$$\int_0^t (\ell_2(t,\zeta) + \delta(t-\zeta))h_2(\zeta,\tau)d\zeta = \ell_2(t,\tau) \tag{A3.3}$$

Noting that $\tau < \zeta < t$ due to the causality of h_2 and ℓ_2, and using (A3.1), (A3.2) in (A3.3) gives:

$$\tau < t \quad A(t)\cdot B(\tau)^T + \alpha(t) \int_\tau^t \beta(\zeta)^T A(\zeta)d\zeta B(\tau)^T = \alpha(t)\cdot\beta(\tau)^T \tag{A3.4}$$

Let

$$\Lambda(t) = \int_0^t \beta(\zeta)^T A(\zeta)d\zeta \quad \text{an } N\times N \text{ array} . \tag{A3.5}$$

Then (A3.4) becomes: $[\Lambda(t) + \alpha(t)\Lambda(t)]\cdot B(\tau)^T = \alpha(t)\cdot[\beta(\tau)^T + \Lambda(\tau)B(\tau)^T]$ and identifying terms in t and in τ gives:

$$\begin{cases} \alpha(t) = \Lambda(t)[1-\Lambda(t)]^{-1} & \text{(A3.6a)} \\ \beta(t) = B(t)[1-\Lambda(t)]^T & \text{(A3.6b)} \end{cases}$$

Using (A3.6b) in (A3.5) and differentiating with respect to time gives:

$$\dot{\Lambda}(t) = [1-\Lambda(t)]B(t)^T A(t) \qquad (A3.7)$$

A particular solution is $\tilde{\Lambda}(t) = 1$.

In section VI.2.b it was found that

$h_2(t,\tau) = D_2(t)\pi^{-1}(t)\cdot D_2(\tau)^T u(t-\tau)$ with $\pi(t) \triangleq \mathbb{1}\mu + \int_0^t D_2(\zeta)^T D_2(\zeta)d\zeta$

(recall 6.19) so, from (A3.1), $A(t) \triangleq D_2(t)\pi^{-1}(t)$ and $B(t) \triangleq D_2(t)$.

The homogenous part of (A3.7) becomes:

$$\dot{\Lambda}(t) + \Lambda(t)[D_2(t)^T D_2(t)\pi^{-1}(t)] = \dot{\Lambda}(t) + \Lambda(t)\dot{\pi}(t)\pi^{-1}(t) = 0$$

which implies that the homogenous solution is:

$\Lambda_0(t) = \mathbb{K}\cdot\pi^{-1}(t)$ where $\mathbb{K}$ is a non-singular matrix ,

independent of time. Therefore, (A3.7) gives $\Lambda(t) = \mathbb{1} + \mathbb{K}\pi^{-1}(t)$

and replacing in (A3.6):

$$\begin{cases} \alpha(t) = A(t)(-\mathbb{K}\pi^{-1}(t))^{-1} \\ \beta(t) = B(t)(-\mathbb{K}\pi^{-1}(t))^T \end{cases}$$

Therefore from A3.2, A3.1,

$$\ell_2(t,\tau) = D_2(t)\pi^{-1}(t)(-\pi(t)\mathbb{K}^{-1})(-\mathbb{K}\pi^{-1}(\tau))D_2(\tau)^T u(t-\tau)$$

$$= D_2(t)\pi^{-1}(\tau)\cdot D_2(\tau)^T u(t-\tau) \qquad (A3.8)$$

A3.2 Derivation of $h(t,\tau)$ from $\ell(t,\tau)$

Let

$$h(t,\tau) \triangleq A_1(t)\cdot B_1(\tau)^T u(t-\tau) \qquad (A3.9)$$

and

$$\ell(t,\tau) \triangleq \alpha_1(t)\cdot\beta_1(\tau)^T u(t-\tau) \qquad (A3.10)$$

where in the present case A_1 and B_1 are the unknowns, while α_1 , β_1 are given. (A3.3) to (A3.6a & b) can then be rederived with

subscript 1 .

Therefore, (A3.6a) and (A3.6b) are rewritten as:

$$\begin{cases} A_1(t) = \alpha_1(t)[\mathbb{1} - \Lambda(t)] & \text{(A3.11a)} \\ B_1(t)^T = [\mathbb{1} - \Lambda(t)]^{-1}\beta_1(t)^T & \text{(A3.11b)} \end{cases}$$

and (A3.5) becomes $\Lambda(t) \triangleq \int_0^t \beta_1(\zeta)^T A_1(\zeta)d\zeta = \int_0^t \beta_1(\zeta)^T\alpha_1(\zeta)[\mathbb{1} - \Lambda(\zeta)]\,d\zeta$

or by differentiating:

$$\dot{\Lambda}(t) = \beta_1(t)^T\alpha_1(t)[\mathbb{1} - \Lambda(t)] \qquad \text{(A3.12a)}$$

A particular solution is $\tilde{\Lambda}(t) = \mathbb{1}$.

The open loop impulse response $\ell(t,\tau)$ associated with $p \in \mathcal{P}$ is (Eq. 6.9.b) $\ell = p \cdot p_2^{-1} \cdot \ell_2 = \frac{k}{k_2} \cdot \ell_2$ at $p = k$. So $\ell(t,\tau) = \lambda\ell_2(t,\tau) = \lambda D_2(t) \cdot \pi(\tau)^{-1} \cdot D_2(\tau)^T u(t-\tau)$ by using (A3.8) and defining $\lambda \triangleq k/k_2$. By identification with (A3.10), $\alpha_1(t) \triangleq \lambda D_2(t)$ and $\beta_1(t)^T = \pi(t)^{-1}D_2(t)^T$ and therefore the homogenous part of (A3,12a) becomes:

$$\begin{aligned} \dot{\Lambda}(t) + \beta_1(t)^T\alpha_1(t)\Lambda(t) &= \dot{\Lambda}(t) + \lambda\pi(t)^{-1}D_2(t)^T D_2(t)\Lambda(t) \\ &= \dot{\Lambda}(t) + \lambda\pi(t)^{-1}\dot{\pi}(t)\Lambda(t) = 0 \end{aligned} \qquad \text{(A3.12b)}$$

from (6.19).

(A3.12b) has no closed-form solution, in general, so let $\Lambda_1(t)$ denote the solution to (A3.12b). Then: $\Lambda(t) = \mathbb{1} + \Lambda_1(t)\,\mathbb{K}$ where $\mathbb{K}$ is a nonsingular matrix. From (A3.11a & b) and using the above definitions of α_1 and β_1 ,

$$\begin{cases} \Lambda_1(t) = \lambda D_2(t)\ (-\Lambda_1(t)\,\mathbb{K}) \\ B_1(t)^T = -\,\mathbb{K}^{-1}\Lambda_1(t)^{-1}\,\pi(t)^{-1}D_2(t)^T \end{cases} .$$

Hence, from (A3.9), the closed loop impulse response associated with

$p \in \mathcal{P}$ is:

$$h(t,\tau) = \lambda D_2(t)(-\Lambda_1(t)\mathcal{K})(-\mathcal{K}^{-1}\Lambda_1(\tau)^{-1})\pi(\tau)^{-1}D_2(\tau)^T u(t-\tau)$$

$$= \lambda D_2(t)\Lambda_1(t)\Lambda_1(\tau)^{-1}\pi(\tau)^{-1}D_2(\tau)^T u(t-\tau) \qquad \text{(A3.13)}$$

where Λ_1 is such that:

$$\dot{\Lambda}_1(t) = -\lambda\pi^{-1}(t)\dot{\pi}(t)\Lambda_1(t) \qquad \text{(A3.13a)}$$

In the special case where the input R is deterministic, or when $D_2(t)$ is a one dimensional vector $\pi(t)$ becomes a number and so is $\Lambda_1(t)$ (instead of a matrix). Then the solution to (A3.13a) is $\Lambda_1(t) = +\pi(t)^{-\lambda}$ and (A3.13) becomes, in this special case:

$$h(t,\tau) = \lambda D_2(t)D_2(\tau)\frac{\pi(\tau)^{\lambda-1}}{\pi(t)^{\lambda}}\, u(t-\tau) \qquad \text{(A3.13b)}$$

A3.3 Derivation of the system response c(t) associated with $p = k$.

Let $c(t)$ be the system response to a command r, when $p = k$. From Fig. VI.3,

$$c(t) = c_1(t) + \Delta c(t) \qquad \text{(A3.14)}$$

For the sake of simplicity, let $N = 1$; this imples that the closed loop impulse response of the bottom part of Fig. VI.3 is given by (A3.13b). Under the above assumption, (Fig. VI.3):

$$\Delta c(t) = D(t) - \int_0^t h(t,\zeta)D(\zeta)d\zeta \qquad \text{(A3.15)}$$

with $D(t) = \frac{k-k_1}{k_1}c_1(t)$ (A3.15a)

(recalling the definition of D from (6.9)).

Replacing (A3.13b) in (A3.15) gives:

$$\Delta c(t) = D(t) - \frac{D_2(t)}{\pi(t)^{\lambda}}\int_0^t \lambda D_2(\zeta)\pi(\zeta)^{\lambda-1}D(\zeta)d\zeta \qquad \text{(A3.16)}$$

where $D_2 = \frac{k_2-k_1}{k_1}c_1(t)$.

AD-A046 012 COLORADO UNIV BOULDER SYSTEMS ENGINEERING LAB F/G 12/2
REDUCTION OF THE COST OF FEEDBACK IN SYSTEMS WITH LARGE PARAMET--ETC(U)
AUG 77 P ROSENBAUM, I HOROWITZ AFOSR-76-2946

UNCLASSIFIED AFOSR-TR-77-1224 NL

3 OF 3
AD
A046012

END
DATE FILMED
11-77
DDC

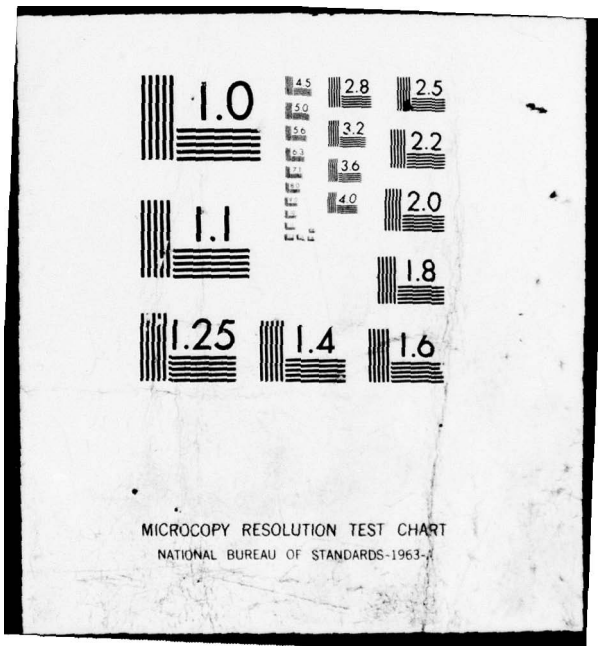
1.0
1.1
1.25
1.4
1.6
1.8
2.0
2.2
2.5
2.8
3.2
3.6
4.0
4.5
5.0
5.6
MICROCOPY RESOLUTION TEST CHART
NATIONAL BUREAU OF STANDARDS-1963-A

(A3.16) can be rewritten as:

$$\Delta c(t) = D(t) - \frac{D(t)}{\pi(t)^{\lambda}} \int_0^t \lambda \pi(\zeta)^{\lambda-1} D_2(\zeta)^2 d\zeta \qquad \text{(A3.17)}$$

Recalling (6.19) we have $D_2(\zeta)^2 = \dot{\pi}(\zeta)$ so

$$\Delta c(t) = D(t) - D(t)\left[\left(\frac{\pi(\zeta)}{\pi(t)}\right)^{\lambda}\right]_{\zeta=0}^{\zeta=t} = D(t)\left(\frac{\pi(0)}{\pi(t)}\right)^{\lambda} \qquad \text{(A3.18)}$$

Using (A3.15a), (A3.14) becomes

$$c(t) = c_1(t) + \frac{k-k_1}{k_1} c_1(t)\left(\frac{\pi(0)}{\pi(t)}\right)^{\lambda} .$$

So:

$$c(t) = c_1(t)\left[1 + \frac{k-k_1}{k_1}\left(\frac{\pi(0)}{\pi(t)}\right)^{\lambda}\right] \qquad \text{(A3.19)}$$

A3.4 Effect of white noise at plant input.

Under the above assumption that $N = 1$, we can use (6.1.b) and (6.12.d) to obtain the mean square value of the noise at the plant input when $P = P_2$, namely:

$$\sigma^2_{P.I.} = \frac{1}{k_2^2} \int_0^t \int_0^t h_2(t,\zeta_1) h_2(t,\zeta_2) \gamma_{NN}(\zeta_1,\zeta_2) d\zeta_1 d\zeta_2 \qquad \text{(A3.20)}$$

By anology with (6.12.d),

$$\theta = -\frac{1}{k} \cdot h \qquad \text{(A3.21)}$$

when the plant is any $P = k \in \mathbb{P}$, associated with the closed loop impulse response h of (A3.13b). Therefore, the mean square value of the noise at the plant input, becomes in this case: (from (6.1.b) and (A3.21))

$$\sigma^2_{P.I.} = \frac{1}{k^2} \int_0^t \int_0^t h(t,\zeta_1) h(t,\zeta_2) \gamma_{NN}(\zeta_1,\zeta_2) d\zeta_1 d\zeta_2 \qquad \text{(A3.22)}$$

Let the sensor noise be a white stationary process of strength σ_N^2 , i.e., $\gamma_{NN}(\zeta_1,\zeta_2) = \sigma_N^2 \delta(\zeta_1-\zeta_2)$ so (A3.22) becomes:

$$\sigma^2_{P.I.} = \frac{\sigma_N^2}{k^2} \int_0^t h(t,\zeta)^2 d\zeta \quad . \quad \text{Using (A3.13b),}$$

$$\sigma^2_{P.I.} = \frac{\sigma_N^2}{k^2} \lambda^2 \int_0^t D_2(t)^2 D_2(\zeta)^2 \frac{\pi(\zeta)^{2\lambda-2}}{\pi(t)^{2\lambda}} d\zeta$$

or

$$\sigma^2_{P.I.} = \frac{\sigma_N^2}{k_2^2} \frac{D_2(t)^2}{\pi(t)^{2\lambda}} \int_0^t \pi(\zeta)^{2\lambda-2} \dot{\pi}(\zeta) d\zeta \quad , \text{ because (6.19) } \dot{\pi}(t) = D_2(t)^2$$

and (6.21a) $\lambda = k/k_2$.

Finally:

$$\sigma^2_{P.I.}(t) = \begin{cases} \frac{\sigma_N^2}{k_2^2} \frac{D_2(t)^2}{2\lambda-1} \left[\frac{1}{\pi(t)} - \frac{\pi(0)^{2\lambda-1}}{\pi(t)^{2\lambda}} \right] & \text{if } \lambda \neq \frac{1}{2} \\ \frac{\sigma_N^2}{k_2^2} \frac{D_2(t)^2}{\pi(t)} \ell n\left(\frac{\pi(t)}{\pi(0)}\right) & \text{if } \lambda = \frac{1}{2} \end{cases} \qquad \text{(A3.23)}$$

As $\lambda = k/k_2$, for any $t = t_0$, $\sigma^2_{P.I.}(t_0)$ is a function of k .

Let $\mu \triangleq 2\lambda$, then for $\lambda \neq \frac{1}{2}$, i.e. $u \neq 1$,

$$\sigma^2_{P.I.}(t) = \frac{\sigma_N^2}{k_2^2} D_2(t)^2 \frac{1}{u-1} \left(\frac{1}{\pi(t)} - \frac{\pi(0)^{u-1}}{\pi(t)^u} \right)$$

Therefore,

$$\frac{\partial \sigma^2_{P.I.}}{\partial k} = \frac{2}{k_2} \frac{\partial \sigma^2_{P.I.}}{\partial u} = \frac{2}{k_2} \frac{\sigma_N^2}{k_2^2} D_2(t)^2 \frac{dJ(u)}{du}$$

where

$J(u) \triangleq \frac{1}{u-1} \left(\frac{1}{\pi(t)} - \frac{\pi(0)^{u-1}}{\pi(t)^u} \right)$, all derivatives being taken at fixed t_0 .

$$\frac{dJ}{du} = \frac{1}{(u-1)^2} \left[\frac{\pi(0)^{u-1}}{\pi(t_0)^u} - \frac{1}{\pi(t_0)} - \frac{(u-1)}{\pi(0)} \left(\frac{\pi(0)}{\pi(t_0)}\right)^u \ell n \left(\frac{\pi(0)}{\pi(t_0)}\right) \right] \qquad \text{(A3.23a)}$$

which can be written as:

$$\frac{dJ}{du} = \frac{1}{(u-1)^2} \frac{\pi(0)^{u-1}}{\pi(t_0)^u} \left[1 - \left(\frac{\pi(t_0)}{\pi(0)}\right)^{u-1} + \ell n\left(\frac{\pi(t_0)}{\pi(0)}\right)^{u-1} \right]$$

Since $\pi(t_0) \triangleq \pi(0) + \int_0^{t_0} D_2(\zeta)^2 d\zeta$ (recall 6.19), we have $x = \frac{\pi(t_0)}{\pi(0)} \geq 1$.

Noting that $1 - x^{u-1} + \log x^{u-1} < 0$ for all $x > 0$, we conclude that $\frac{dJ}{du} < 0$ for all u and therefore $\frac{\partial \sigma^2_{P.I.}}{\partial k} < 0$ for all k, which imples that $\sigma^2_{P.I.}(t_0,k)$ is a decreasing function of k for given t_0.

Note that as $u \to 1$, (i.e., $\lambda \to \frac{1}{2}$) then $u = 1+\varepsilon$ (with ε positive or negative), and

$$\frac{dJ}{du} = \frac{1}{\varepsilon^2} \frac{\pi(0)^{\varepsilon}}{\pi(t_0)^{1+\varepsilon}} [\, 1 - X^{\varepsilon} + \varepsilon \log X \,]$$

$$= \frac{1}{\varepsilon^2} \frac{\pi(0)^{\varepsilon}}{\pi(t_0)^{1+\varepsilon}} [\, 1 - (1+\varepsilon \ell nx + \varepsilon^2 (\ell nx)^2) + \varepsilon \ell nX \,]$$

$$= \frac{\pi(0)^{\varepsilon} (\ell nx)^2}{\pi(t_0)^{1+\varepsilon}} \quad \text{after using a serie expansion.}$$

$$\left(\frac{dJ}{du}\right)_{u=1} = \frac{1}{\pi(t_0)} \left[\ell n\left(\frac{\pi(t_0)}{\pi(0)}\right) \right]^2 \text{, which proves that } \sigma^2_{P.I.}$$

and $\frac{\partial \sigma^2_{P.I.}}{\partial k}$ are both continuous at $\lambda = \frac{1}{2}$ $(k = \frac{k_2}{2})$.

This explains the shape of curves A in Figs. VI.5.a & b.

A3.5 Solution to a certain filter problem.

The problem in (6.40) is to find $h_2(t,\tau)$ such that:

$$\underset{h_2}{\text{Min}} \int_0^{\tau} (\Delta c^2(t) + W(t)\sigma^2_{P.I.}(t))dt \quad , \text{ i.e., if we take } P = \frac{k}{s}$$

$$\underset{h_2}{\text{Min}} \int_0^{T} \left((D_2(t) - \int_0^t h_2(t,\zeta) D_2(\zeta) d\zeta)^2 + \mu \int_0^t \frac{\partial h_2}{\partial t}(t,\zeta)^2 d\zeta \right) dt \quad \text{(A3.24)}$$

with $\mu = \dfrac{\sigma_N^2 W(t)}{k_2^2}$ ($W(t)$ is assumed constant).

Let us use a variational argument, i.e., $h_2^1 = h_{2,0} + f$, with f an arbitrary function satisfying $f(t,t) = 0$.

$$I = \int_0^T \left[(D_2(t) - \int_0^t (h_{2,0}(t,\zeta) + f(t,\zeta) D_2(\zeta) d\zeta)^2 + \right.$$

$$\left. \mu \int_0^t \left[\frac{\partial h_{2,0}}{\partial t}(t,\zeta) + \frac{\partial f}{\partial t}(t,\zeta) \right]^2 d\zeta \right] dt \triangleq I_0 + \delta I \quad \text{with}$$

$$\delta I = -2 \int_0^T \left[(D_2(t) - \int_0^t h_{2,0}(t,\zeta) D_2(\zeta) d\zeta) \int_0^t f(t,\zeta) D_2(\zeta) d\zeta + \right.$$

$$\left. + 2\mu \int_0^t \frac{\partial h_{2,0}}{\partial t}(t,\zeta) \frac{\partial f}{\partial t}(t,\zeta) d\zeta \right] dt + 0(f^2) \quad \text{where} \quad 0(f^2)$$

indicates a positive function of $f(t,\zeta)$, which is zero when $f = 0$.

A necessary condition for an optimum is therefore that $\delta I = 0$

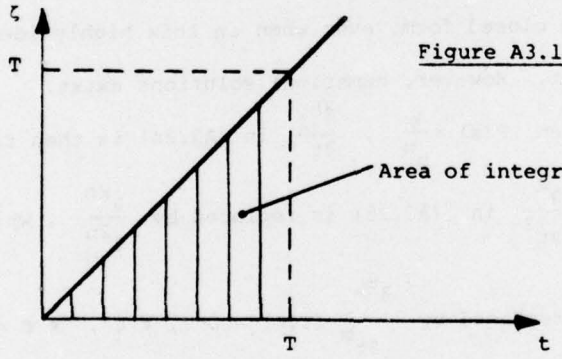

Figure A3.1

We can write:

$$J = \int_0^T dt \int_0^t \frac{\partial h_{2,0}}{\partial t}(t,\zeta) \frac{\partial f}{\partial t}(t,\zeta) d\zeta = \int_0^T d\zeta \int_\zeta^T \frac{\partial h_{2,0}}{\partial t}(t,\zeta) \frac{\partial f}{\partial t}(t,\zeta) dt$$

by permuting the order of integration. Integrating by parts,

$$J = \int_0^T d\zeta \left[\frac{\partial h_{2,0}}{\partial t}(t,\zeta) f(t,\zeta) \right]_{t=\zeta}^{t=T} - \int_0^T d\zeta \int_\zeta^T \frac{\partial^2 h_{2,0}}{\partial t^2}(t,\zeta) f(t,\zeta) dt$$

$$= \int_0^T \frac{\partial h_{2,0}}{\partial t}(T,\zeta) f(T,\zeta) d\zeta - \int_0^T dt \int_0^t \frac{\partial^2 h_{2,0}}{\partial t^2}(t,\zeta) f(t,\zeta) d\zeta \ .$$

So,

$$\delta I = -2\left[\int_0^T dt \int_0^t \left[(D_2(t) - \int_0^t h_{2,0}(t,\zeta)D_2(\zeta)d\zeta)D_2(\zeta) + \mu \frac{\partial^2 h_{2,0}}{\partial t^2}(t,\zeta)\right] f(t,\zeta)d\zeta \right] + 2\mu \int_0^T \frac{\partial h_{2,0}}{\partial t}(T,\zeta) f(\tau,\zeta)d\zeta$$

As $\delta I = 0$, it implies that the optimal solution is given by:

$$\begin{cases} \mu \dfrac{\partial^2 h_2(t,\tau)}{\partial t^2} + \left[D_2(t) - \displaystyle\int_0^t h_2(t,\zeta)D_2 d\zeta\right] D_2(\tau) = 0 \quad \forall\, t > \tau \\ h_2(t,t) = 0 \quad , \quad \forall\, t \\ \dfrac{\partial h_2}{\partial t}(T,\zeta) = 0 \quad , \quad \forall\, \zeta \end{cases} \tag{A3.25}$$

This proves that when $P(s) = \frac{k}{s}$, a solution to (6.40) exists. This solution is not in closed form, even when in this highly idealized case of $D_2(\zeta)$ constant. However, numerical solutions exist.

Note that when $P(s) = \frac{k}{s^n}$, $\frac{\partial h_2}{\partial t}$ in (A3.24) is then replaced by $\frac{\partial^n}{\partial t^n} h_2(t,\zeta)$ and $\frac{\partial^2}{\partial t^2}$ in (A3.25) is replaced by $\frac{\partial^{2n}}{\partial^{2n}}$, while $\frac{\partial h_2}{\partial t}(T,\zeta) = 0$ is replaced by $\frac{\partial^m h_2}{\partial t^m}(T,\zeta) = 0$, $\forall\, \zeta$, $\forall\, m = 1,2,\ldots,n$.

A3.6 Obtention of the differential equation, knowing $h_2(t,\tau)$

Let (6.54)

$$h_2(t,\tau) = \frac{D_2(t)[D_2^1(t) - D_2^1(\tau)]}{\sigma_N^2 W(t) + D_2^1(t)^2/2} u(t-\tau) \triangleq q(t)[D_2^1(t) - D_2^1(\tau)]u(t-\tau)$$

$$\dot{h}_2(t,\tau) = \frac{\dot{q}}{q} h_2(t,\tau) + q(t)D_2(t)u(t-\tau) \quad , \text{ from (6.48)}$$

$$\ddot{h}_2(t,\tau) = \left(\frac{\dot{q}}{q}\right)' h_2(t,\tau) + \frac{\dot{q}}{q}\dot{h}_2(t,\tau) + (qD_2)'u(t-\tau) + qD_2\delta(t-\tau) \quad .$$

Let $y(t) = h_2(t,\tau_0)$, $x(t) = \delta(t-\tau_0)$, and we get:

$$\ddot{y} = (\frac{\dot{g}}{g})' y + \frac{\dot{g}}{g}\dot{y} + \frac{(gD_2)'}{gD_2}(\dot{y} - \frac{\dot{g}}{g} y) + gD_2 x$$

so the D.E. is:

$$\ddot{y} + \dot{y}\left(-\frac{\dot{D}_2}{D_2} - 2\frac{\dot{g}}{g}\right) + y\left(2(\frac{\dot{g}}{g})^2 + \frac{\dot{g}}{g}\frac{\dot{D}_2}{D_2} - \frac{\ddot{g}}{g}\right) = gD_2 x$$

As

$$\frac{\dot{g}}{g} = \frac{\dot{D}_2}{D_2} - D_2^1 g \quad \text{and} \quad \frac{\ddot{g}}{g} = (\frac{\dot{D}_2}{D_2})' - D_2 g + (\frac{\dot{g}}{g})\left(\frac{\dot{D}_2}{D_2} - 2gD_2^1\right)$$

$$- \frac{\dot{D}_2}{D_2} - 2\frac{\dot{g}}{g} = 2D_2^1 g - 3\frac{\dot{D}_2}{D_2} \quad \text{and}$$

$$2(\frac{\dot{g}}{g})^2 + (\frac{\dot{g}}{g})\frac{\dot{D}_2}{D_2} - \frac{\ddot{g}}{g} = 2\left((\frac{\dot{D}_2}{D_2})^2 + (D_2^1 g)^2 - 2\frac{\dot{D}_2}{D_2} D_2^1 g\right) + (\frac{\dot{D}_2}{D_2})^2 - \frac{\dot{D}_2}{D_2} D_2^1 g$$

$$- (\frac{\dot{D}_2}{D_2})' + D_2 g - \left(\frac{\dot{D}_2}{D_2} - 2gD_2^1\right)\left(\frac{\dot{D}_2}{D_2} - D_2^1 g\right)$$

$$= D_2 g - 2\frac{\dot{D}_2}{D_2} D_2^1 g - \frac{\ddot{D}_2}{D_2} + 3(\frac{\dot{D}_2}{D_2})^2$$

and therefore $h_2(t,\tau)$ is associated with the D.E.:

$$\ddot{y} + \dot{y}\left(2D_2^1 g - 3\frac{\dot{D}_2}{D_2}\right) + y\left(D_2 g - 2\frac{\dot{D}_2}{D_2} D_2^1 g - \frac{\ddot{D}_2}{D_2} + 3(\frac{\dot{D}_2}{D_2})^2\right) = gD_2 x \qquad \text{(A3.26)}$$

A3.7 Derivation of the Euler-Lagrange Equation for a special case.

We want to

$$\min_{h_2} \int_0^T \left[\left(D_2(t) - \int_0^t h_2(t,\zeta) D_2(\zeta)\, d\zeta\right)^2 W(t) + u\int_0^t \left[\frac{\partial}{\partial t} h_2(t,\zeta) + \alpha_2 h_2(t,\zeta)\right]^2 d\zeta\right] dt$$

when $h_2(t,\zeta) = A(t)(\theta(t) - \theta(\zeta))u(t-\zeta)$, with $\theta(t)$ given.

The second term is rewritten as:

$$I_1 = u\int_0^t \left[\frac{\partial}{\partial t} h_2(t,\zeta)^2 + 2\alpha_2 h_2(t,\zeta)\frac{\partial}{\partial t} h_2(t,\zeta) + \alpha_2^2 h_2(t,\zeta)^2\right] d\zeta$$

$$= \mu \int_0^t \Big[\dot{A}(t)^2(\theta(t)-\theta(\zeta))^2 + A(t)^2\dot{\theta}(t)^2 + 2A(t)\dot{A}(t)\dot{\theta}(t)(\theta(t)-\theta(\zeta)) + \alpha_2^2 A(t)^2(\theta(t)-\theta(\zeta))^2$$

$$+ 2\alpha_2 A(t)\dot{A}(t)(\theta(t)-\theta(\zeta))^2 + 2\alpha_2 A(t)^2\dot{\theta}(t)(\theta(t)-\theta(\zeta)) \Big] d\zeta \qquad \text{(A3.27)}$$

Let $\psi(t) \triangleq \int_0^t (\theta(t)-\theta(\zeta))^2 d\zeta$, $\eta(t) = \int_0^t (\theta(t)-\theta(\zeta))d\zeta$

So $I_1 = \mu\left(\dot{A}^2\psi + A^2 t\dot{\theta}^2 + 2A\dot{A}\dot{\theta}\eta + \alpha_2^2 A^2\psi + 2\alpha_2 A\dot{A}\psi + 2\alpha_2 A^2\dot{\theta}\eta \right)$

Let $J(t) = \int_0^t (\theta(t)-\theta(\zeta))D_2(\zeta)d\zeta$, then (A3.27) is:

$$\underset{A}{\text{Min}} \int_0^T \Big[(D_2(t) - A(t)J(t))^2 W(t) + I_1(t) \Big] dt = \underset{A}{\text{Min}} \int_0^T F(t)dt \ .$$

The Euler equation is then derived as:

$$\frac{\partial F}{\partial A} = \frac{d}{dt}\left(\frac{\partial F}{\partial \dot{A}} \right) \qquad \text{(A3.28)}$$

which is:

$$J[D_2 - AJ]W + \mu(At\dot{\theta}^2 + \dot{A}\dot{\theta}\eta + \alpha_2^2\dot{A}\psi + \alpha_2\dot{A}\Psi + 2\alpha_2 A\dot{\theta}\eta]$$

$$= \mu \frac{d}{dt}[\dot{A}\psi + A\dot{\theta}\eta + \alpha_2 A\psi]$$

$$= \mu\left(\ddot{A}\psi + \dot{A}\dot{\psi} + \dot{A}(\dot{\theta}\eta + \alpha_2\psi) + A(\ddot{\theta}\eta + \dot{\theta}\dot{\eta} + \alpha_2\dot{\psi}) \right) \qquad \text{(A3.29)}$$

(A3.29) is rewritten as:

$$\ddot{A}\psi + \dot{A}(\dot{\psi} + \dot{\theta}\eta + \alpha_2\psi - \alpha_2\psi - \dot{\theta}\eta) + A(\ddot{\theta}\eta + \dot{\theta}\dot{\eta} + \alpha_2\dot{\psi} - 2\alpha_2\dot{\theta}\eta - \alpha_2^2\psi - t\dot{\theta}^2 - J^2\frac{W}{\mu})$$

$$= - D_2 \frac{JW}{\mu}$$

After simplifications: ($\dot{\eta} = \dot{\theta}t$, $\dot{\psi} = 2\dot{\theta}\eta$)

$$\ddot{A}\psi + \dot{A}\dot{\psi} + A(\ddot{\theta}\eta - \alpha_2^2\psi - \frac{J^2W}{\mu}) = - \frac{D_2 JW}{\mu} \qquad \text{or:} \quad \theta_1(t) = \int_0^t \theta(\zeta)d\zeta$$

$$\ddot{A}(t\theta^2 - 2\theta_1 + \varphi) + 2\dot{A}\dot{\theta}(t\theta - \theta_1) + A(\ddot{\theta}(t\theta - \theta_1) - \alpha_2^2(t\theta^2 - 2\theta\theta_1 + \varphi)$$

$$- \frac{W}{\mu}\left(\int_0^t (\theta(t) - \theta(\zeta))D_2(\zeta)d\zeta \right)^2 = \frac{D_2 W}{\mu} \ .$$

A3.8 Design details for both the LTV and LTI systems.

A3.8.a LTV system

The L.T.V. closed loop impulse response $h_2(t,\tau)$ of (6.27) is associated with the differential equation:

$$[h_2]: \quad \dot{y} + \left(\frac{\dot{\pi}}{\pi} - \frac{\dot{D}_2}{D_2}\right) y = D_2^2/\pi X \quad \text{where} \quad \pi(t) = \mu + \int_0^t D_2(\zeta)^2 d\zeta$$

Therefore the open-loop impulse response $\ell_2 = h_2(1-h_2)^{-1}$ is characterized by:

$$[\ell_2]: \quad \dot{y} + \left(\frac{\dot{\pi}}{\pi} - \frac{\dot{D}_2}{D_2} - \frac{D_2^2}{\pi}\right) y = D_2^2/\pi X$$

so $g = P_2^{-1} \cdot \ell_2 = \ell_2/k_2$

and:

$$[g]: \quad \dot{y} + \left(\frac{\dot{\pi}}{\pi} - \frac{\dot{D}_2}{D_2} - \frac{D_2^2}{\pi}\right) y = \frac{D_2^2}{\pi k_2} X \quad .$$

The overall transfer function t_1 is such that $T_1(s) \triangleq \frac{C_1(s)}{R(s)} \quad \frac{-1}{s+1}$,

for $c_1(t) = 1-e^{-t}$;

$$[t_1]: \quad \dot{y} + y = X$$

since the prefilter f should satisfy: $t_1 \triangleq h_1 \cdot f$ it follows that $f = h_1^{-1} \cdot t_1$.

Hence,

$$[\ell_1]: \quad \dot{y} + \left(\frac{\dot{\pi}}{\pi} - \frac{\dot{D}_2}{D_2} - \frac{D_2^2}{\pi}\right) y = \frac{k_1}{k_2} \frac{D_2^2}{\pi} X$$

$$[h_1]: \quad \dot{y} + \left(\frac{\dot{\pi}}{\pi} - \frac{\dot{D}_2}{D_2} + \left(\frac{k_1}{k_2} - 1\right) \frac{D_2^2}{\pi}\right) y = \frac{k_1}{k_2} \frac{D_2^2}{\pi} X$$

$$[f]: \quad \dot{y} + y = \frac{k_2}{k_1} \frac{\pi}{D_2^2} \left(\dot{X} + X \left(\frac{\dot{\pi}}{\pi} - \frac{\dot{D}_2}{D_2} + \left(\frac{k_1}{k_2} - 1\right) \frac{D_2^2}{\pi}\right)\right)$$

A3.8.b LTI Systems

A two degree of freedom structure (Fig. A3.2) is considered.

The LTI system roughly achieves (as seen in Fig. VI.6.b), for $P = k \in [1,100]$, the T.D.S. shown in Fig. VI.6.a for the LTV design. The LTI synthesis procedure given in [S2, H2] is used with

$$G(s) = \frac{5.69\ 10^6 (s+8.)(s+1.57)(s^2+2.34s+1.6)}{(s^2+1.65+1.1)(s^2+4s+8)(s^2+60s+5500.)(s^2+63s+6000.)}$$

$$F(s) = \frac{3396.(s+1.5)(s+1.7)(s+4.67)}{(s+.36)(s+226.)(s^2+1.32s+.67)(s^2+4s+8)}$$

If the plant $P = k/s$ with $k \in [1,100]$ is considered and the T.D.S. are those depicted in Fig. VI.8.c, following [S2, H2], it is found that

$$G(s) = \frac{11.43\ 10^6 (s+.6)(s+15.4)(s^2+1.5s+.72)}{(s+.8)(s+34.)(s^2+2.3s+1.8)(s^2+63.s+6600)(s^2+67s+7400.)}$$

$$F(s) = \frac{290.(s+.55)(s+1.43)}{(s^2+s+1.5)(s+1)^2(s+31.)}$$

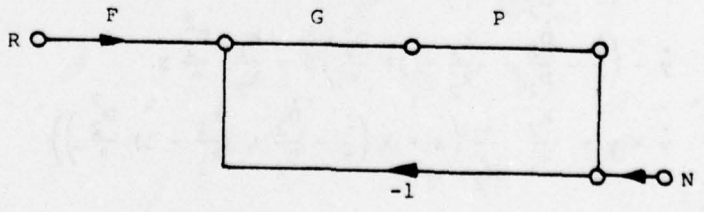

Figure A3.2 Two degree freedom structure

REFERENCES

[B1] BODE, H.W., Network Analysis and Feedback Amplifier Design. Van Nostrand, N.Y., (1945).

[B2] BOOTON, R.C., An Optimization theory for time-varying linear systems with nonstationary statistical inputs. Proc. IRE, p. 977, 981, 1952.

[C1] CLEGG, J.C., A Nonlinear integrator for servomechanisms, Trans. A.I.E.E. Part II, Appl. Ind., 1958

[C2] CHESNUT, H., Obstacles to progress in Non-linear control. Trans. IRE, AC-5, p. 59, 1958.

[C3] COURANT, R. and HILBERT, D., Methods of Mathematical Physics. Interscience Publishers, N.Y., 1966.

[C4] COCHRAN, J., Analysis of Linear Integral Equation. MacGraw-Hill, 1972.

[C5] CESARI, L., Asymptotic Behaviour and Stability Problems in Ordinary Differential Equations. Springer-Verlag, Berlin, 1959.

[D1] DAVENPORT, W. and ROOT, W., Random signal and Noise. MacGraw-Hill, 1958.

[E1] EMELYANOV, S., ULANOV, G., VIKTOROVA, V. and AGAFONOV, V., Synthesis of a variable structure system for automatic control of thickness of hot-rolled metal. Remote & Control, p. 262, 1970.

[F1] FLEISHER, P., Design of passive adaptive linear feedback systems with varying plants. Trans. IRE, AC-7, 1962.

[G1] GIBSON, J., Nonlinear Automatic Control. McGraw-Hill, 1963.

[G2] GELB. A. and VANDER VELDE, W., Multiple-input describing functions and nonlinear system design. McGraw-Hill, 1968.

[G3] GANTMACHER, F., Application of the theory of matrics. Inter-

science Publishers, 1959.

[H1] HOROWITZ, I., Synthesis of feedback systems with non-linear time varying uncertain plants to satify quantitative performance specifications. Proc. I.E.E.E., Vol. 64, No. 1, p. 123-130, 1976.

[H2] HOROWITZ, I. and SIDI, M., Synthesis of feedback systems with large plant ignorance for prescribed time domain tolerances. Int. J. Control, Vol. 16, p. 287, 1976.

[H3] HOROWITZ, I., Optimum loop transfer function in single loop minimum phase feedback systems. Int. J. Control, Vol. 18, p. 97, 1973.

[H4] HOROWITZ, I. and KRISHNAN, K., Synthesis of nonlinear feedback system with significant plant ignorance for prescribed system tolerances. Int. J. Control, Vol. 19, p. 689, 1974.

[H5] HOROWITZ, I. and ROSENBAUM, P., Non-linear design for cost of feedback reduction in systems with large parameter uncertainty. Int. J. Control, Vol. 21, p. 977, 1975.

[H6] HOROWITZ, I., ROSENBAUM, P., SIDI, M. and WU, M., A synthesis theory for non-linear systems with plant uncertainty. 6th Triennial World Congress IFAC. Part IC, 37.2, 1975.

[H7] HOROWITZ, I., Synthesis of feedback systems. Academic Press, 1963.

[H8] HOROWITZ, I., A synthesis theory for linear time varying feedback systems with plant uncertainty. Trans. I.E.E.E., AC-20, p. 454, August 1975.

[H9] HOROWITZ, I. and SIDI, M., Optimum Synthesis of non-minimum phase feedback systems with plant uncertainty. Int. J. Control. To appear.

[H10] HOLZMANN, E.G., Non-linearity in process systems. Trans. IRE, AC-5, p. 63-64, 1958.

[J1] JURY, E., Theory and application of the z-transofrm method. Wiley & Sons, N.Y., 1964.

[K1] KHABAROV, V.S., Optimal control of variable structure systems.

Remote & Control, p. 1603-1609, 1970.

[K2] KAILATH, T., A view of three decades of linear filtering theory. Trans. I.E.E.E., IT-20, p. 146, March 1974.

[K3] KAPLAN, W., Operational methods for linear systems. Wesley, 1962.

[L1] LINDORFF, D., Theory of sampled data control systems. Wiley & Sons, 1965.

[L2] LANIN, J. and BATTIN, R., Random processes in automatic control. McGraw-Hill, 1956.

[M1] MIRA, C., Etude des Systèms Asservis non-linéaires. Toulouse University, 1968.

[P1] PAPOULIS, A., Probability, random variables and stochastic processes. McGraw-Hill, N.Y., 1965.

[S1] SHINBROT, M., A generalization of a method for the solution of the integral equation arising in optimization of T.V.L.S. with non-stationary inputs. Trans. IRE, IT-3, 1957.

[S2] SIDI, M., Synthesis of linear feedback systems for prescribed time domain tolerances. Weizmann Institute Thesis, 1973.

[S3] SEVELY, Y., Asservissements echantillonnées linéaires. Toulouse University, 1968.

[S4] SCHWARTZ, L., Mathematics for the Physical Science. Wesley, 1966.

[S5] SOLODOV, A., Linear Automatic control systems with varying parameters.

[S6] STUBBERUD, A., Analysis and synthesis of linear time varying systems. University of California Press, 1964.

[U1] UTKIN, V., Equations of the slipping regime in discontinuous synthesis I. Remote & Contol, p. 1157, 1972.

[U1] UTKIN, V., Equations of the slipping regime in discontinuous synthesis II. Remote & Control, p. 211, 1972.

[W1] WIENER, N., The Extrapolation, Interpolation & Smoothing of Stationary Time Series", Wiley, N.Y., 1948.

REPORT DOCUMENTATION PAGE

READ INSTRUCTIONS BEFORE COMPLETING FORM

1. REPORT NUMBER: AFOSR-TR- 77 - 1224	2. GOVT ACCESSION NO.
3. RECIPIENT'S CATALOG NUMBER	
4. TITLE (and Subtitle): REDUCTION OF THE COST OF FEEDBACK IN SYSTEMS WITH LARGE PARAMETER UNCERTAINTIES	5. TYPE OF REPORT & PERIOD COVERED: Interim
	6. PERFORMING ORG. REPORT NUMBER
7. AUTHOR(s): Patrick Rosenbaum, Isaac Horowitz	8. CONTRACT OR GRANT NUMBER(s): AFOSR 76-2946
9. PERFORMING ORGANIZATION NAME AND ADDRESS: University of Colorado, Department of Electrical Engineering, Boulder, Colorado 80309	10. PROGRAM ELEMENT, PROJECT, TASK AREA & WORK UNIT NUMBERS: 61102F, 2304/A1
11. CONTROLLING OFFICE NAME AND ADDRESS: Air Force Office of Scientific Research/NM, Bolling AFB DC 20332	12. REPORT DATE: 1 Aug 77
	13. NUMBER OF PAGES: 200
14. MONITORING AGENCY NAME & ADDRESS (if different from Controlling Office)	15. SECURITY CLASS. (of this report): UNCLASSIFIED
	15a. DECLASSIFICATION/DOWNGRADING SCHEDULE

16. DISTRIBUTION STATEMENT (of this Report)

Approved for public release; distribution unlimited.

17. DISTRIBUTION STATEMENT (of the abstract entered in Block 20, if different from Report)

18. SUPPLEMENTARY NOTES

19. KEY WORDS (Continue on reverse side if necessary and identify by block number)

20. ABSTRACT (Continue on reverse side if necessary and identify by block number)

This work deals with the synthesis of feedback systems to achieve specified performance tolerances, despite large uncertainty in a constrained part of the system, denoted as the 'plant'. Part of this work deals with linear time-invariant (lti) plants where the 'cost of feedback', if lti compensation is used, is primarily in the bandwidth of → next page

DD FORM 1 JAN 73 1473 EDITION OF 1 NOV 65 IS OBSOLETE

UNCLASSIFIED

SECURITY CLASSIFICATION OF THIS PAGE (When Data Entered)

20. ABSTRACT (Continued)

the feedback loop being much larger than that of the system as a whole - making the system very sensitive to sensor noise. Here, the objective is to reduce the loop bandwidth by means of non-lti compensation. The result is a very significant reduction in loop bandwidth and with it, system sensitivity to sensor noise.

Another method of non-lti synthesis is by means of linear time-varying compensation, applicable to a certain problem class. The solution is not in general available analytically, but is found for certain cases and exhibits in these reduced 'cost of feedback'.

The plant can be nonlinear with large uncertainty giving a set of nonlinear plants W . The concept is use of a lti set P which is precisely equivalent to W providing the output is, in both cases, a member of an acceptable output set A .